

August 2019

Dissection of Floral Organ Development and Sterility in Sorghum Bicolor

Ashley R. Smith
University of Wisconsin-Milwaukee

Follow this and additional works at: <https://dc.uwm.edu/etd>



Part of the [Genetics Commons](#), [Molecular Biology Commons](#), and the [Plant Sciences Commons](#)

Recommended Citation

Smith, Ashley R., "Dissection of Floral Organ Development and Sterility in Sorghum Bicolor" (2019).
Theses and Dissertations. 2258.
<https://dc.uwm.edu/etd/2258>

This Dissertation is brought to you for free and open access by UWM Digital Commons. It has been accepted for inclusion in Theses and Dissertations by an authorized administrator of UWM Digital Commons. For more information, please contact open-access@uwm.edu.

DISSECTION OF FLORAL ORGAN DEVELOPMENT AND STERILITY IN *SORGHUM*
BICOLOR

by

Ashley R. Smith

A Dissertation Submitted in
Partial Fulfillment of the
Requirements for the Degree of
Doctor of Philosophy
in Biological Sciences

at

The University of Wisconsin-Milwaukee

August 2019

ABSTRACT

DISSECTION OF FLORAL ORGAN DEVELOPMENT AND STERILITY IN *SORGHUM BICOLOR*

by

Ashley Rae Smith

The University of Wisconsin-Milwaukee, 2019
Under the Supervision of Dazhong Zhao, PhD

Sorghum bicolor is a drought resistant cereal grain commonly grown for use in food, feed, fiber, and fuel production. Due to its versatility and modest sized genome it is poised to become an increasingly important research organism within the C4 plants. Sorghum produces spikelet pairs with one fertile sessile spikelet and one to two sterile pedicellate spikelets. One major area of interest in sorghum production is maximizing seed yield. While the importance of the grain is obvious there are several large gaps in the study of sorghum that prevent researchers and growers from maximum productivity. The first gap is that limited study has looked at the effects of heat stress on early anther development, the effects of varied heat stress durations and the effects of heat stress at 42°C on seed yield. Another key gap in sorghum study is the lack of a complete floral developmental series from primordia to anthesis. Building on this idea, no study has determined why over half of the spikelets produced in sorghum are sterile at maturity. The final gap is in the study of male fertility and anther development. Prior to this study a complete anther series from origin to dehiscence was not available, no male sterile mutants were fully characterized, and few sorghum mutants made available for hybrid breeding efforts. We demonstrated that heat stress applied at booting stage, where spikelets are only surrounded by a bulged leaf sheath, had devastating effects on yield.

Specifically, loss of male fertility resulted in loss of grain yield. In addition, limited effects were observed on vegetative development. Additionally, a complete floral developmental series was formed, which highlighted key developmental stages that were targeted for RNA-seq study. Transcriptomic analysis demonstrated altered expression of TEOSINTE BRANCHED 1, CYCLOIDEA, PCF1 transcription factor genes, MADS-box genes and phytohormone genes which are hypothesized to result in pedicellate sterility. Finally, a complete anther developmental series was constructed for the WT and *ms8* mutant and initial characterization of *Sbtdr* mutant development was completed. This work identified two important candidates for hybrid breeding efforts in sorghum. Overall these efforts provide important resources to fill developmental knowledge gaps in sorghum and further seed yield improvement research. From this work specific pathways have been identified for future study that could vastly improve seed yield.

© Copyright by Ashley Rae Smith, 2019
All Rights Reserved

To
Aaron, Moe, and Millie for all their love,
and to my parents for always supporting my dreams

TABLE OF CONTENTS

Chapter 1	1
Introduction	1
1.1 Origins and uses of <i>Sorghum bicolor</i>	1
1.2 Heat stress resistance	4
1.3 Floral anatomy and development in <i>S. bicolor</i>	8
1.4 Sterility in other cereal grains	11
1.5 Anther development	12
1.6 Male sterility and breeding systems	13
1.7 Significance of research	16
1.8 Thesis Statement	21
Chapter 2	23
The wide-ranging effects of heat stress on floral fertility and vegetative growth in <i>Sorghum bicolor</i>	23
2.1 Abstract	23
2.2 Introduction	24
2.3 Materials and Methods	27
2.3.1 Growing conditions and heat stress treatment	27
2.3.2 Sample collection and Alexander pollen staining	28
2.3.3 Pollen germination	28
2.3.4 Data collection and statistical analysis	28
2.4 Results	29
2.4.1 Heat stress has limited effects on the vegetative development of <i>S. bicolor</i> .	29
2.4.2 Long-term heat stress beginning at PMCs stage causes male sterility in <i>S. bicolor</i>	30
2.4.3 Heat stress at pollen stage abolished male fertility and promotes tiller formation at the plant apex in <i>S. bicolor</i>	30
2.5 Discussion	32
2.5.1 Significant agricultural impacts of heat stress on sorghum	32
2.5.2 Potential mechanism for altered tillering in heat-stressed sorghum	33
2.5.3 Heat stress severely impacts male fertility and seed yield in sorghum.....	35
Chapter 3	46

Spikelet development in <i>Sorghum bicolor</i> and the genetic basis for pedicellate floret sterility	46
3.1 Abstract.....	46
3.2 Introduction	48
3.3 Materials and Methods.....	53
3.3.1 Sorghum lines and growing conditions.....	53
3.3.2 Sample preparation and scanning electron microscopy.....	54
3.3.3 RNA-seq library preparation.....	55
3.3.4 RNA-seq data analysis.....	56
3.4 Results	57
3.4.1 <i>S. bicolor</i> spikelets display uniform development prior to the formation of reproductive floral organs.....	57
3.4.2 WT pedicellate spikelet development lags behind the sessile spikelet.....	58
3.4.3 <i>msd1</i> pedicellate development overcomes the developmental lag	61
3.4.4 Male sterile mutant <i>msa1</i> fails to develop stamens while producing numerous carpels	61
3.4.5 RNA-seq reveals differential expression of many key cell cycle, development, phytohormones, and TCP transcription factor genes between sessile and pedicellate spikelets	63
3.4.6 A group of master regulators, the TCP factor genes, are differentially expressed in sterile spikelets with limited effects on cell cycle gene expression ...	65
3.4.7 MADS-box genes play a role in establishing and maintaining the development of sessile spikelets	66
3.4.8 Expression of genes involved in JA biosynthesis, response, signaling, and transport is altered in sterile pedicellate spikelets	67
3.4.9 Auxin, gibberellic acid, and brassinosteroid genes do not strongly affect pedicellate fertility.....	69
3.5 Discussion	70
3.5.1 Development between sessile and pedicellate spikelets is distinctive	70
3.5.2 The pedicellate spikelet developmental lag and sterility are likely connected to TCP factor gene expression.....	73
3.5.3 Altered MADS-box gene expression is crucial for establishing and maintaining the developmental lag and sterility of the pedicellate spikelet.....	76
3.5.4 JA signaling is strongly correlated with pedicellate spikelet sterility	80
3.5.5 No clear connection is detected between the TCP factors and other phytohormones	83

3.5.6 The proposed pathway for controlling pedicellate spikelet sterility	85
Chapter 4.....	115
Functional identification of <i>MS8</i> and <i>SbTDR</i> genes in tapetal cell differentiation and degeneration in <i>Sorghum bicolor</i>.....	115
4.1 Abstract.....	115
4.2 Introduction	116
4.3 Materials and Methods.....	120
4.3.1 Sorghum lines and growing conditions.....	120
4.3.2 Alexander staining.....	120
4.3.3 Female fertility testing	120
4.3.4 Sample preparation, semi-thin sectioning, and imaging.....	121
4.3.5 Sequencing verification of <i>ms8</i> and <i>Sbtdr</i> mutations	122
4.3.6 Semi-quantitative RT-PCR	123
4.4 Results	123
4.4.1 Vegetative development, non-male floral organs, and female fertility are normal in the <i>ms8</i> mutant.....	123
4.4.2 The <i>ms8</i> mutant displays abnormal anther development after PMCs stage leading to the ultimate collapse of the anther lobes.	124
4.4.3 The <i>ms8</i> phenotype is attributed to mutations in Sb04g030850, and normally expressed in the sorghum spikelet and anthers from PMCs to microspore stage.	127
4.4.4 <i>Sbtdr</i> mutant plants display normal vegetative development with a similar anther sterility phenotype to <i>ms8</i>	128
4.4.5 The <i>Sbtdr</i> mutant phenotype is attributed to a mutation in Sb04g001650 which is expressed in anthers from PMCs through early pollen stage.	129
4.5 Discussion	130
4.5.1 Anther development in Sorghum is similar to other cereal grains.	130
4.5.2 Anther development in <i>ms8</i> and <i>Sbtdr</i> show obvious defects in tapetal cell development and differentiation.	131
4.5.3 Sorghum MS8 and SbTDR have similar functions to orthologs in rice	132
4.5.4 Use of <i>ms8</i> and <i>Sbtdr</i> in hybrid breeding	134
Chapter 5.....	148
Summary	148
5.1 Summary of key findings.....	148
5.2 Future work on sorghum heat stress	150

5.3 Future work to manipulate pedicellate spikelet sterility	151
5.4 Future work to use the <i>ms8</i> and <i>Sbtdr</i> mutants in 2-line breeding systems .	152
5.5 Concluding remarks.....	153
References.....	154
Curriculum Vitae.....	169

LIST OF FIGURES

Figure 1.1. Flower and floret structures in <i>Arabidopsis</i> and maize with corresponding ABCE models.....	19
Figure 1.2. Positioning of fertile and sterile maize and sorghum spikelets at maturity..	20
Figure 2.1. Comparison of control and heat-stressed (HS) plants beginning at the PMCs stage	37
Figure 2.2 Effects of heat stress applied beginning at the PMCs stage on plant height tiller formation.....	38
Figure 2.3. Effects of heat stress on seed count and weight	39
Figure 2.4. Pollen viability examined via Alexander staining in control and 12-day heat-stressed plants starting at PMCs stage.....	41
Figure 2.5. Similar total grain yield per plant in control and 3-day heat-stressed plants at the booting stage.....	43
Figure 2.6. Pollen fertility in control and 3-day heat-stressed plants	44
Figure 3.1. Early sorghum floral developmental stages 1-5 prior to the developmental lag of the pedicellate spikelet	87
Figure 3.2. Middle sorghum floral developmental stages 6-10 and the onset of the developmental lag of the pedicellate spikelet.....	89

Figure 3.3. Late sorghum floral developmental stages 11-13 and degeneration of the pedicellate spikelet.....	90
Figure 3.4. SEM micrographs of anther sections from spikelet pairs at stage 9 and 11.	91
Figure 3.5. <i>Sorghum bicolor</i> spikelet structure and floral comparisons to other cereal grains	93
Figure 3.6. Comparisons between WT and <i>msa1</i> floral organs.....	95
Figure 3.7. Differentially expressed genes across WT and <i>msd1</i> sessile and pedicellate spikelets.....	97
Figure 3.8. Key <i>SbTCP</i> transcription factor genes are differentially expressed.....	98
Figure 3.9. Differentially expressed cell cycle genes.....	99
Figure 3.10. Differentially expressed MADS-box genes	101
Figure 3.11. Differentially expressed genes involved in jasmonic acid, biosynthesis, response, signaling, and transport genes	102
Figure 3.12. Differentially expressed <i>SbIAA</i> genes. Few genes have differential expression of IAA genes.	103
Figure 3.13. Differentially expressed genes involved in gibberellic acid biosynthesis, inactivation, regulation and signal transduction.....	104

Figure 3.14. Differentially expressed genes involved in brassinosteroid biosynthesis, perception, and negative signal response.....	105
Figure 4.1. WT and <i>ms8</i> spikelet comparisons and evaluation of female and male fertility.....	136
Figure 4.2. Successive anther development in WT and <i>ms8</i>	138
Figure 4.3. SEM micrographs of WT and <i>ms8</i> anther sections demonstrating normal PMCs development in <i>ms8</i>	139
Figure 4.4. Sb04g030850 (Sobic.004G270900 locus) gene and mutation sites in <i>ms8</i> mutants	140
Figure 4.5. The <i>MS8</i> gene is expressed in flowers and anthers from PMCs to microspores stage.....	141
Figure 4.6. <i>Sbtdr</i> mutant plants display normal vegetative development but abnormal anthers.....	143
Figure 4.7. Female fertility is normal in the <i>Sbtdr</i> mutant	143
Figure 4.8. <i>Sbtdr</i> anther development is abnormal after microsporocyte meiosis and anthers yield no pollen	145
Figure 4.9. The <i>SbTDR</i> gene Sb04g001650 (Sobic.004G017500 locus) and <i>Sbtdr</i> mutation sites.....	145

Figure 4.10. The *SbTDR* gene is expressed in anthers only from tetrads to pollen

stages 146

LIST OF TABLES

Table 3.1. Classification of floral developmental stages in <i>Sorghum bicolor</i>	106
Table S3.1. Analysis of <i>SbTCP</i> gene expression in WT (stages 5, 6, 10) and <i>msd1</i> mutant (stages 6, 10)	107
Table S3.2. Differentially expressed cell cycle genes in <i>S. bicolor</i> WT (stages 5, 6, 10) and <i>msd1</i> mutant (stages 6, 10).....	108
Table S3.3. Differentially expressed MADS-box genes in <i>S. bicolor</i> (stages 5, 6, 10) and <i>msd1</i> mutant (stages 6, 10)	109
Table S3.4 Differentially expressed key jasmonic acid genes in <i>S. bicolor</i> WT (stages 5, 6, 10) and <i>msd1</i> mutant (stages 6, 10)	111
Table S3.5. Differentially expressed <i>SbIAA</i> genes in <i>S. bicolor</i> WT (stages 5, 6, 10) and <i>msd1</i> mutant (stages 6, 10)	112
Table S3.6. Differentially expressed gibberellic acid genes in <i>S. bicolor</i> WT (stages 5, 6, 10) and <i>msd1</i> mutant (stages 6, 10)	113
Table S3.7. Differentially expressed brassinosteroid genes in <i>S. bicolor</i> WT (stages 5, 6, 10) and <i>msd1</i> mutant (stages 6, 10)	114
Table 4.1. Primers used in this study	147

LIST OF ABBREVIATIONS

AC1	ACTIN1
bHLH	basic Helix-Loop-Helix
BR	Brassinosteroid
BSE	Backscattered electron
CMS	Cytoplasmic male sterility
DTD	DELAYED TAPETAL DEGENERATION
EAT1	ETERNAL TAPETUM1
FPKM	Fragments Per Kilobase of transcript per Million mapped reads
GA	Gibberellic acid
GID1	GA INSENSITIVE DWARF1
HSP	Heat shock protein
IAA	Indole-3-acetic acid
JA	Jasmonic acid
MS8	MALE STERILE8
MSAL	MALE STERILE ANTHERLESS
MSD1	MULTISEEDED1
NMS	Nuclear male sterility
PCD	Programmed cell death
PMC	Pollen mother cell
PS	Pedicellate spikelet
QTL	Quantitative trait loci

TGMS	Thermo-sensitive genic male-sterile
<i>S. bicolor</i>	<i>Sorghum bicolor</i>
SEM	Scanning electron microscope
SS	Sessile spikelet
TCP	TEOSINTE BRANCHED 1, CYCLOIDEA, PCF1
TDR	TAPETAL DEGENERATION RETARDATION
VRS	SIX-ROWED SPIKE
WT	Wild type

ACKNOWLEDGEMENTS

First, deepest thanks are extended to Dr. Dave Zhao for taking a chance on me. This work would not exist without your guidance, support, and friendship. I am eternally grateful to you for this opportunity. Further thanks to Dr. Jian Huang our lab postdoc who has been with me from the start of my PhD work and a constant source of advice, a mentor, and a friend. Additionally, thank you Paul Engevoold for helping to grow the nearly endless crops of sorghum and for advice on plants and beyond. Deep thanks and appreciation to Dr. Heather Owen for years of help in microtomy, microscopy, countless lab supplies, and many laughs. Thank you to Dr. Xin of the USDA for the seeds and guidance needed to begin and continue to quite literally grow this work. I would further like to thank all my committee members at University of Wisconsin-Milwaukee including Dr. Dave Heathcote, Dr. Chuck Wimpee, Dr. Erica Young, and Dr. Filipe Alberto for their advice helping to shape this work.

Additional gratitude must be extended to my wonderful husband who has provided me with unconditional love. Thank you for supporting me more than just emotionally but by pot washing, planting, and cutting when my sorghum allergies were in full swing. From these experiences you have earned the title of honorary plant biologist. Finally, thank you to my friends and family. Your support and love have made all the difference during this journey.

Chapter 1

Introduction

This chapter contains modified portions of a review paper published in *Frontiers in Plant Science* (Smith and Zhao, 2016).

1.1 Origins and uses of Sorghum bicolor

Sorghum bicolor (L.) Moench is a widely grown cereal grain native to Africa currently cultivated throughout many arid environments including regions across all habitable continents. Sorghum grain is surpassed only by wheat, maize, rice and barley production (Doggett, 1988). The ten highest sorghum producing countries according to current data include: United States, Nigeria, Sudan, Mexico, Ethiopia, India, Argentina, China, and Niger (FAOSTAT, 2019). Members of the *Sorghum* genus are used in food, feed, fiber and fuel production (Palmer, 1992; Rooney et al., 2007). Sorghum varieties also contain diverse sources of phenolic compounds which may confer health benefits (Dykes and Rooney, 2006). Grain sorghum varieties are used for harvesting large seed heads with easily digestible grains. In the food industry sorghum grain can be processed into starch, flour, grits, and flakes used in a variety of foods and beverages. Popular uses include breads, baked goods and malted beverages (Taylor et al., 2006). The sorghum grain is high in starch and protein content (Palmer, 1992). Sweet sorghum varieties are grown to have higher concentration of stalk sugars. These stalk sugars are milled and can be used for syrup, molasses, and crystal sugar. The plant products used

for human consumption provide a gluten free alternative for those with food sensitivities or celiac disease (Ciacci et al., 2007). Sorghum is also used in animal feeds and many forage varieties are available. These forage varieties generally have reduced lignin making them more prone to damage but more easily digestible by livestock. Sorghum use in feeds has increased partially due to its low cost, high protein levels, and the reduced prevalence of mycotoxins and parasites (Colombo et al., 2007). As a cattle feed, varieties like brown midrib (bmr)-6 forage sorghum are known to have digestibility similar to corn, producing similar yields of milk with high milk fat in lactating cows (Oliver et al., 2004). The fibers from both the leaves and stems have also been used to construct a jute-like product. The fibers possess the necessary length and fineness for use in composites, textiles and other applications. Currently sorghum leaf and stem byproducts are not commercially processed for fiber, however if manufacturing technologies were advanced the value of the plant could increase (Reddy and Yang, 2007).

Finally, sorghum is being developed for use as a major bioenergy crop. Many different varieties can be used for ethanol production including grain, sweet, and forage. Recently biomass varieties have shown promise as they can be grown to 30 ft in height. Sorghum has high levels of sugars that can be obtained from the stalk and seeds that can be used for ethanol production (Carpita and McCann, 2008). Some of the greatest strengths of sorghum as a bioenergy source include its adaptations to hot and dry climates, limited effect on food supply, and the high net energy ratio. Sweet sorghum ethanol yield per hectare is surpassed only by sugarcane, and produces more biomass than switchgrass and corn (Regassa and Wortmann, 2014; Rooney et al., 2007). While

sorghum can be grown on marginal lands, has higher ethanol yields per hectare than maize, and requires less energy input, maize study continues to dominate over sorghum in current bioenergy efforts (Regassa and Wortmann, 2014). In the future, bioenergy crops are expected to be grown predominantly on non-irrigated land, further highlighting the need for a drought tolerant bioenergy crop (Ferreira et al., 2013). There are a few limitations to using sorghum as a bioenergy crop. While the production of sugars is very high, it is more difficult to process the material resulting in reduced yield (Vermerris, 2011). If technologies to process sorghum sugars can be advanced there are huge possibilities for its use in the production of bioenergy.

Many hypotheses exist as to why sorghum displays more drought stress resistance compared to other cereals. The ability to maximize water use is partially due to its use of the C4 photosynthetic pathway and epicuticular wax deposits (Ebercon et al., 1977). An additional hypothesis is that root anatomy allows for high water extraction leading to growth in water limited environments. This may be due to silicification of the root epidermis improving the mechanical properties of the root, or other factors such as thick sclerenchyma cell walls and fewer metaxylem vessels (Lux et al., 2002; Salih et al., 1999). Others who study sorghum drought resistance emphasize the roles of the shoot system including higher solute concentration to maintain turgor and osmotic pressure, higher epicuticular wax load, and lower cuticular conductance (Premachandra et al., 1992). The higher levels of wax result in reflection of radiation and decreased transpiration resulting in less water loss in the plants (Ebercon et al., 1977). Increased wax production up to 0.067 g m^{-2} results in decreased transpiration rates, where beyond this thickness minimal changes in transpiration are observed (Jordan et al.,

1984). The bloomless (*bm*) mutants have decreased production of this protective epicuticular wax. Bloomless varieties in turn have lower water use efficiencies compared to their normal counterparts (Premachandra et al., 1994). Recently the *bm39* and *bm40* mutants were studied and the decreased wax production was attributed to mutations in *Sobic.001G269200* and *Sobic.001G228100* respectively which encode GDSL-like lipase/acylhydrolases (Jiao et al., 2018a; Uttam et al., 2017).

To improve yield under drought stress researchers have identified plants with a post-flowering drought adaptation mechanism known as stay-green. Stay-green allows the sorghum to avoid premature leaf senescence under osmotic stress and maintain photosynthetic activity. This adaptation has been mapped to four quantitative trait loci (QTL): *Stg1-Stg4* (Harris et al., 2007). These QTLs were then separated into two distinct groups, where Linkage group A (*Stg1*, and *Stg2*) contain key photosynthetic enzymes, heat shock proteins, and an abscisic acid responsive gene. The remaining QTLs *Stg3* and *Stg4* are on linkage groups D and J, respectively (Xu et al., 2000). Additionally, the QTLs for chlorophyll content (*Chl1-3*) all coincide with QTL regions (*Stg1-3*).

1.2 Heat stress resistance

Many stages of flower development, particularly the late stages of stamen development, are sensitive to heat stress. In *Arabidopsis* and cereal grains, sensitive stages include meiosis of pollen mother cells (PMCs), tapetum development, anther dehiscence/pollen

release, anthesis, and fertilization (De Storme and Geelen, 2014; Dupuis and Dumas, 1990; Kim et al., 2001; Oshino et al., 2007; Thakur et al., 2010; Zinn et al., 2010). The overall effects of heat stress on male sterility depend on duration, timing, and temperature (Schoper et al., 1987a; Schoper et al., 1986; Schoper et al., 1987b). The female organ is not as susceptible as the male organ to heat stress.

The tapetum in the anther is particularly vulnerable to heat stress (Parish et al., 2012). In *Arabidopsis*, the tapetum consists of a monolayer of cells, which surrounds successive stages of microsporocytes, tetrads, microspores, and developing pollen as anther development progresses. Tapetal cells undergo three stages: differentiation, maturation, and programmed cell death (PCD). First, the early differentiated tapetal cells secrete the callase enzyme that is required for the release of haploid microspores from meiotic tetrads. Second, mature tapetal cells produce a large amount of specialized non-photosynthetic plastids (elaioplasts) and tapetosomes, which provide lipids, proteins, and sporopollenin essential for pollen wall formation. Finally, tapetal cells are degenerated via PCD, and the remnants are important for the completion of pollen wall formation (McCormick, 1993; Parish and Li, 2010; Wu and Cheung, 2000).

Abnormal tapetum or altered timing of its degeneration causes pollen defects and consequently male sterility. Barley and wheat grown at elevated temperatures (barley: 30–35°C day/20–25°C night, wheat: 30°C for 1–3 days, or varied 30/20°C day/night at meiosis) display precocious tapetum degradation (Omidi et al., 2014; Oshino et al., 2007; Saini and Aspinall, 1982; Saini et al., 1984). In rice, tapetal genes including *YY1* and *YY2* are down regulated following heat stress [39/30°C (day/night) for 5 days],

affecting tapetum function and consequently pollen viability (Endo et al., 2009). Additionally in rice, male sterility in the thermo-sensitive genic male-sterile (TGMS) line *95850ms* is caused by premature tapetum PCD and consequent pollen grain collapse (Ku et al., 2001; Ku et al., 2003). A recent study shows that the TGMS trait in the *thermosensitive genic male sterile 5 (tms5)* mutant is caused by the loss of function of RNase Z^{s1}, which processes mRNAs of three ubiquitin fusion ribosomal protein genes (Ubl_{L40}) (Zhou et al., 2014). At restrictive temperatures, high levels of Ubl_{L40} results in abortive pollen and therefore male sterility. *Arabidopsis* plants under heat stress (31 and 33°C) show reduced expression of *YUCCA* genes especially in tapetum and PMCs. Inactivation of *YUC2* and *YUC6* leads to decreased male fertility, which can be reversed by exogenous application of auxin (Sakata et al., 2014; Sakata et al., 2010). More work needs to be done to understand the genetic pathways leading to decreased fertility during heat stress, especially the role of auxin in male fertility and tapetum development.

Another sensitive stage is in the meiosis of PMCs meiosis. Wheat and rice exposed to high or varied temperatures [wheat: high 30°C (1–3 days), varied 30°/20°C (day/night), rice: 39/30°C (day/night; 5 days)] at and prior to the onset of PMCs meiosis exhibit greatly reduced grain set (Endo et al., 2009; Omid et al., 2014; Saini and Aspinall, 1982; Saini et al., 1984). Impairments in rice division of PMCs occurs even 5°C over the ambient temperature [28.3/21.3°C (day/night)], resulting in decreased pollen production especially in susceptible cultivars (Prasad et al., 2006b). Anther dehiscence, anthesis, and fertilization are all known to be sensitive to elevated temperatures. Heat stress applied to wheat [two-day intervals of 36/31°C (day/night)] from floral emergence

to 3 days post anthesis results in male sterility due to abnormal pollen grains (Ferris et al., 1998; Tashiro and Wardlaw, 1990). Similarly, rice that receives a short-term (33.7°C, 1 h) or a long-term heat stress (35°C, 38°C, and 41°C, 5 days) at anthesis displays reduced fertility, but with less sterility when stress was applied before or after anthesis (Jagadish et al., 2007; Satake and Yoshida, 1978). Heat stressed rice [35/25°C (day/night)] has decreased anther dehiscence and pollen count (Das et al., 2014). Pollen germination is also very vulnerable to high temperature stress. When maize tassels and rice spikelets are subjected to high heat stress [maize: 6 h of 40°C, rice: 35/25°C (day/night) or greater for 3 days], the ability of pollen to fertilize the ear is lost, which is attributed to the failure of pollen tube growth (Das et al., 2014; Dupuis and Dumas, 1990). In *Arabidopsis*, disruption of *THERMOSENSITIVE MALE STERILE 1* (*TMS1*), which encodes the heat shock protein HSP40, causes pollen tubes to burst and/or decreased pollen tube length (Yang et al., 2009). Although the cause of the heat-induced sterility is not clear, it might be related to heat shock proteins such as HSP40 mentioned above (Yang et al., 2009). Mutations in the small heat shock protein gene *BOBBER1* (*BOB1*) result in a range of phenotypes, such as irregular flowers and sterile siliques (Perez et al., 2009). In maize, pollen infertility may be due to the lack of production of major protective HSPs (Dupuis and Dumas, 1990; Hopf et al., 1992), supported by the fact that pollen grains do not express *HSP* RNAs at dehiscence (Dietrich et al., 1991; Young et al., 2001). In wheat, heat-stress induces many HSPs, including HSP17, HSP26, and HSP70, as well as microRNA-targeted to *HSP* genes (Kumar et al., 2015). Heat stress in sorghum is discussed in detail in Chapter 2.

1.3 Floral anatomy and development in *S. bicolor*

Flower development is a long and complex process, which is mainly classified into four stages: flowering transition, floral meristem identity, floral organ identity, and floral organ morphogenesis. Mainly using model species *Arabidopsis thaliana* and snapdragon (*Antirrhinum majus*), extensive molecular genetic studies have identified numerous genes required for flower development, particularly during early stages. *Arabidopsis* plants produce raceme-type indeterminate inflorescences where flowers are indefinitely generated. A typical *Arabidopsis* flower contains four protective sepals in the first whorl, four petals in the second whorl, six stamens (male reproductive organs) in the third whorl, and two fused carpels (female reproductive structure) that form the gynoecium in the fourth whorl (Fig. 1.1A, B). Different from *Arabidopsis*, Poaceae plants, commonly known as grasses, produce determinate panicles where flowers (or florets) are organized into spikelets. The anatomical and genetic developmental progression is much better documented in maize in comparison to sorghum, and is outlined here. In maize, the spikelets are grouped into separate male and female inflorescences (Fig. 1.2A). The highly branched male inflorescence, the tassel, is composed of spikelet pairs, each of which comprises an upper and a lower floret surrounded by the leaf-like structures known as glumes (Fig. 1.2A). Similarly, spikelet pairs are formed in the female inflorescence, but the lower floret in each spikelet pair is aborted (Fig. 1.2A) (Cheng et al., 1983; Zhang and Yuan, 2014). Poaceae florets have stamens and carpels similar to eudicot flowers, such as *Arabidopsis*. In maize, the male floret contains three stamens (Fig. 1.1C, D), while the female floret produces three central carpels which are fused to form the pistil (Fig. 1.1E, F) (Zhang and Yuan, 2014). Maize

florets do not contain sepals and petals. Instead, the sepal-analogous organs lemma and palea are produced (Fig.1.1C–F) (Lombardo and Yoshida, 2015; Schmidt and Ambrose, 1998). Additionally, the petal analogous structures known as lodicules are essential for pollination via opening the bract organs (Yoshida, 2012).

A complete floral developmental series has not yet been documented in sorghum, and no studies discuss the cause for sterility of over half of the spikelets produced in the sorghum panicle. The basic development can be outlined as follows. In sorghum, the shoot apex elongates and produces primary branch primordia which give rise to secondary branch primordia, where some branches, often lower on the developing panicle, lead to the formation of tertiary and quaternary branch primordia. The higher ordered branches give rise to spikelets which in turn bring about florets (Kellogg, 2007; Lee et al., 1974). In sorghum the florets develop in pairs (along the flowering stem) or triplets (terminal floret) where a single sessile floret is bisexual and fertile, and the pedicellate florets (1-2) are sterile at maturity (Fig 1.2B). While the process leading to the development of florets has been studied, little is known about the development of the floral meristems or why sterile florets form. Sorghum florets are surrounded by an outer and inner glume. The most external layer of the floret is the lemma, followed by the palea, the lodicules (analogous to petals), 3 stamens, and a central carpel (Doggett, 1988; Lee et al., 1974; Schmidt and Ambrose, 1998).

Inflorescence development arises from the vegetative meristem where the plant essentially makes a switch from making vegetative structures to making spikelets. During floral organ morphogenesis, when plants undergo extensive genetic and

morphological remodeling, floral meristem identity genes, floral organ identity genes (ABC genes), and floral organ maturation genes are required for constructing flowers (Jack, 2004). In the grasses, less is known on the exact roles and interactions of these genes (Smith and Zhao, 2016). The ABC genes are classes of genes that specify the floral whorls and are critical for proper floral organ identification, but may also play a role in floral organ degeneration. The interactions of ABC genes in the grasses are less clear, although they have been clearly laid out in the model species *Arabidopsis* (Fig. 1.1G). In *Arabidopsis*, class A genes [*APETALA1* (*AP1*) and *AP2*] specify sepals in the first whorl. Class A and B genes [*AP3* and *PISTILLATA* (*PI*)] in combination control petal identity in the second whorl. Class B and C gene expression [*AGAMOUS* (*AG*)] results in stamen identity in the third whorl, while the class C gene alone specifies carpels in the fourth whorl (Bowman et al. 1991). The modified ABC model has been expanded to include class D gene [*SEEDSTICK* (*STK*), previously *AGL11*] which plays a role in ovule specification (Rounsley et al., 1995). Additionally, the redundant E function genes (*SEPALATTA1-4*) are necessary for the development of all of the whorls (Ditta et al., 2004; Pelaz et al., 2000).

The ABCDE model can be also applied to floral development in other plants including the Poaceae, although many modifications exist (Fig. 1.1H). Many of these classes of genes have been identified in maize, for example in *bd1-2* mutants, loss of expression of genes such as *ZAG1* (C Class), *ZAG2* (D Class), and *ZMM2* (D Class) is observed along with the loss of female fertility (Colombo et al., 1998). Although floral organ degeneration occurs after the establishment of floral meristem identity, floral organ identity genes are critical for final floral organ formation and for activation of the

floral organ building genes (Jack, 2004). Among these broad classes of genes there are many places where altered expression patterns can result in sterility.

1.4 Sterility in other cereal grains

During development in cereal grain crops such as wheat (*Triticum aestivum*), rice (*Oryza sativa*), oats (*Avena sativa*), barley (*Hordeum vulgare*), and sorghum (*Sorghum bicolor*), the arrest of stamen or carpel primordia, or both, potentially results in reduced fertility or completely sterile spikelets (Aryal and Ming, 2014; Bommert et al., 2005; Schmidt and Ambrose, 1998; Yoshida and Nagato, 2011). Additionally, abiotic stresses can cause floral sterility, which consequently results in yield loss.

Wild barley produce a central fertile floret surrounded by a pair of sterile florets known as the 2-rowed variety. More commonly cultivated is the 6-rowed fully fertile barley where the two infertile lateral spikelets become fertile, resulting in a large increase in yield. The six rowed barley phenotype is controlled by many loci and the pathways are being actively studied (Koppolu et al., 2013). In the floret pair of sorghum, one floret is bisexually fertile, whereas the other one is bisexually sterile. Mutants with fertile pedicellate florets exist; however, the seeds, while more plentiful, are reduced in size (Burow et al., 2014). In maize, abortion of the female reproductive organs in the tassel and the male reproductive organs in the ear is key to the formation of single-sex florets (Fig. 1.2B,C). Additionally, in maize the lower female floret lags in development prior to abortion, very similar to the lag and degeneration that is observed in sorghum

(Cheng et al., 1983). Even oats are known to form sterile florets at the apex of the rachilla (Schmidt and Ambrose, 1998). Genes underlying sterilization of floral male and/or female organ(s) are much better studied in barley (ex. *Vrs1*), maize (ex. *Tasselseed* genes), and rice (ex. *Long Sterile Lemma1 (G1)*) (Irish et al., 1994; Komatsuda et al., 2007; Malcomber and Kellogg, 2006; Yoshida et al., 2009).

1.5 Anther development

The Arabidopsis flower consists of four whorls: the outermost whorl (the calyx) with four sepals, the second whorl (the corolla) with four petals, the third whorl with six stamens (4 long and 2 short) and the fourth whorl with a central gynoecium (Smyth et al., 1990). Angiosperms such as Arabidopsis exhibit heterospory, forming specialized spores, the microspores and megaspores. In microsporogenesis, L2-derived archesporial cells in anthers divide and form the primary sporogenous cell and primary parietal cell. The primary parietal cell then divides giving rise to the secondary parietal layers which will eventually form the four types of anther wall cells. The primary sporogenous cell divides, forming pollen mother cells (PMCs) or microsporocytes. These diploid PMCs undergo meiosis, each forming four microspores which then develop into pollen grains (Sanders et al., 1999; Zhao et al., 2002). During sporogenesis, some key genes are identified to specify the sporangia. *NOZZLE*, also called *SPOROCYTLESS (NZZ/SPL)* is required for both male and female sporogenesis, where *nzz/spl* mutants do not form megaspore mother cells or PMCs (Schiefthaler et al., 1999; Yang et al., 1999). Loss of

genes such as *EXCESS MICROSPOROCTES1 (EMS1)* results in the production of additional microsporocytes (Zhao et al., 2002).

1.6 Male sterility and breeding systems

Understanding male fertility is important as many important breeding systems are based on male sterility. The major aim of this work centers on increasing seed yield. To increase seed yield by breeding, we must be able to outcross sorghum and maximize hybrid vigor/heterosis. Many cereals such as sorghum, reproduce predominantly by selfing. As the mass removal of sorghum anthers before pollination is not feasible, more complex breeding systems must be used if the avoidance of selfing is desired. For small scale experiments it is possible to remove most of the pollen viability, entire anthers, or delay anther dehiscence by hot-water emasculation, careful hand emasculation, and altering the humidity respectively (Schertz and Dalton, 1980). Traditionally, cytoplasmic male sterility (CMS) breeding has been used as a heritable means of maximizing yield. CMS has been documented in over 150 plant species (Laser and Lersten, 1972). The system utilizes three lines, the male sterile line as the female parent (A line), the maintainer (B line) as the male to pollinate A and continue the male sterile line, and the restorer male (R) line as the male parent that can complement the sterility of the A line to restore fertility (Rooney et al., 2007). CMS lines generally contain unusual open reading frames (ORFs) in mitochondrial genomes, which are maternally inherited. These plants are used as the female parent as they can pass these abnormal ORFs to their offspring. This sterility can be reversed if they are crossed with plants that have a

nuclear *Restorer-of-fertility* (*Rf*) gene (Chase and Gabay-Laughnan, 2004). The mechanism by which the *Rf* gene restores fertility is often similar in different systems and species. Common strategies include altered or enhanced CMS transcript processing (Tang et al., 1996).

In rice, the CMS-WA (wild abortive) system was the first to be widely used. Around 90% of CMS hybrid varieties in rice utilize this system. CMS-WA is a sporophytic system where two mapped loci (chromosomes 1, 10) are associated with fertility restoration (Yao et al., 1997). In addition there are several other gametophytic systems including: BT-, HL-, LD- and CW-CMS (Huang et al., 2014). CMS is not currently as widely used in maize. The use of CMS-T (CMS-Texas) to avoid manual detasseling was widely popular. Unbeknownst to researchers and farmers this line also conveyed susceptibility to southern corn leaf blight and a subsequent epidemic resulted in the popularity of this line (Ullstrup, 1972). Other CMS lines are available for maize including CMS-S and CMS-C (Tie et al., 2006). In wheat the CMS-K system is popular, where rearrangements have resulted in novel fusions between ORFs. K-type CMS has a large number of restorer lines in wheat also adding to its widespread use (Liu et al., 2011). Sorghum hybrid breeding is currently done exclusively using CMS. Sorghum CMS primarily uses the A₁ cytoplasm. These types of monocultures are worrisome, with potential to lead to a disaster similar to that which followed wide-spread use of CMS-T in maize. In sorghum, A₁, A₂, and A₃ cytoplasm can be used for the production of F₁ hybrids; however, A₃ has been associated with reduced yield (Moran and Rooney, 2003). Due to the strong similarity of A₂ to A₁ and the presence of multiple compatible

Rf genes, the intensified use of A_2 would be advantageous (Jordan et al., 2011; Praveen et al., 2015).

In addition to CMS systems, in some crops a two-line hybrid system that uses environmental triggers to cause male sterility is used. These two-line breeding systems use photoperiod-sensitive genic male-sterile (PGMS) or thermo-sensitive genic male-sterile (TGMS) lines. These PTGMS plant lines are used as the maternal parents which can be crossed to produce hybrid seeds. The PTGMS lines are generally sterile under restrictive conditions (high temperatures and long days), and fertile under permissive conditions (low temperatures and short days) where they act as a maintainer line. Current efforts in rice have maximized the usable restorer lines while removing any negative effects caused by the sterile cytoplasm (Yuan, 1990). When grown in stable conditions these varieties are highly productive.

Another two-line breeding system currently under study is nuclear male sterility (NMS), which is not as commonly used as the widespread CMS and PTGMS lines. In NMS lines the genetic defect in the nuclear genome causes sterility. In these sterile lines there is some mutation that produces inviable, absent, or inaccessible pollen. In order for these lines to be used for hybrid breeding they must have complete loss of male fertility. There are many known male sterility genes across the cereal grains that have led to lab engineered NMS lines. The largest hurdle in NMS systems is not identifying male sterility genes, but how to use these to generate sufficient quantities of male-sterile only seeds. Much work has been done to target sterility and detect sterile seeds. In various plants including wheat, *Brassica napus* (oilseed rape), and *Nicotiana*

tabacum (tobacco) the expression of the ribonuclease barnase under a tapetum-specific promoter drives loss of RNA in the developing microspores, resulting in sterile anthers. This targeted destruction does not affect female fertility or the vegetative development of the plant (Deblock and Debrouwer, 1993; DeBlock et al., 1997; Mariani et al., 1990). More recent work in rice has been done using *Oryza sativa No Pollen 1* (*OsNP1*) that may greatly increase the efficiency of NMS systems. *OsNP1* is only in the tapetum and microspores where it regulates tapetal degeneration and pollen wall formation. The *osnp1* mutant was transformed following the combination of *OsNP1* with α -amylase to disrupt the transgenic pollen and red fluorescent protein (*DsRed*) to identify the transgenic seeds (Chang et al., 2016). The *male sterility 7* (*ms7*) mutant in maize has a mutation in the anther specific *MS7* gene resulting in thin walls of microspores and abnormal tapetum development, and shows promise in 2-line breeding efforts (Zhang et al., 2018a). The classic NMS formula includes: a male fertility gene, a pollen-disrupting gene, and an indicator of transgene presence such as seed coat color. Additional pollen-disrupting genes and herbicide-resistance genes including *Bar* may further improve these systems by limiting transgene transmittance to the pollen and facilitating the spraying to remove non-transgenic seedlings (Zhang et al., 2018a).

1.7 Significance of research

As there is increased pressure for affordable food sources for growing populations, researching a crop that provides both excellent food and feed is desirable, especially for crops that can grow in semiarid regions (Morris et al., 2013). Models predict that it will

become increasingly dry and hot in arid regions including the American southwest (Seager et al., 2007). The near-surface temperature of the earth is anticipated to increase by 1.8 – 5.8°C by the end of the century (IPCC, 2013). This level of change is enough to affect the crop yield of many cereals, as described above. Sorghum could be grown in many of these areas when these expectations become a reality. We are in the unique position where research to maximize sorghum yield can have immediate and long-term global benefits. With global climate change driving increased temperatures and water shortages, growing sufficient grain will become increasingly difficult. This challenge, combined with the anticipated need of 1,500 more million metric tonnes of food over the next decades, spells a recipe for catastrophe. This problem intensifies particularly in developing countries with limited access to irrigation (Rosenzweig and Parry, 1994). In addition to ever-increasing needs for feed and food there is a need for new energy sources and to lower carbon emissions. Between 2015 and 2040 the United States will need to produce 8% more energy. It is expected that renewable liquid fuels will grow from 5% to 15% of fuels by 2035 (USDOE, 2016). The study of sorghum could help meet this goal of producing more biofuel while reducing carbon emissions. The potential biomass supply for all crops in the United States is estimated to exceed one billion tons without affecting food, feed, and fiber supply and could replace 30% of the petroleum used (USDOE, 2016). While the potential biomass supply for biofuels is vast, there is hesitation to use large quantities of the US corn crop to produce ethanol. This hesitation is often due to an inherent fear that the overuse of corn could somehow affect feed and food supplies and that a sharp increase in price may follow the intensification of corn derived biofuels. It is estimated that corn stover, containing the stalks, leaves,

and cobs left after harvest could supply over 100 million metric tons (Graham et al., 2007; USDOE, 2016). Additionally, sorghum is poised to become a model research organism within C4 grasses with a fully sequenced diploid genome of approximately 730 Mb, providing an alternative to traditional maize with a genome size of 2500 Mb (Paterson et al., 2009). Despite its great agricultural and research potential, little is known about the process of floral development, and few male sterile mutants are available for hybrid breeding.

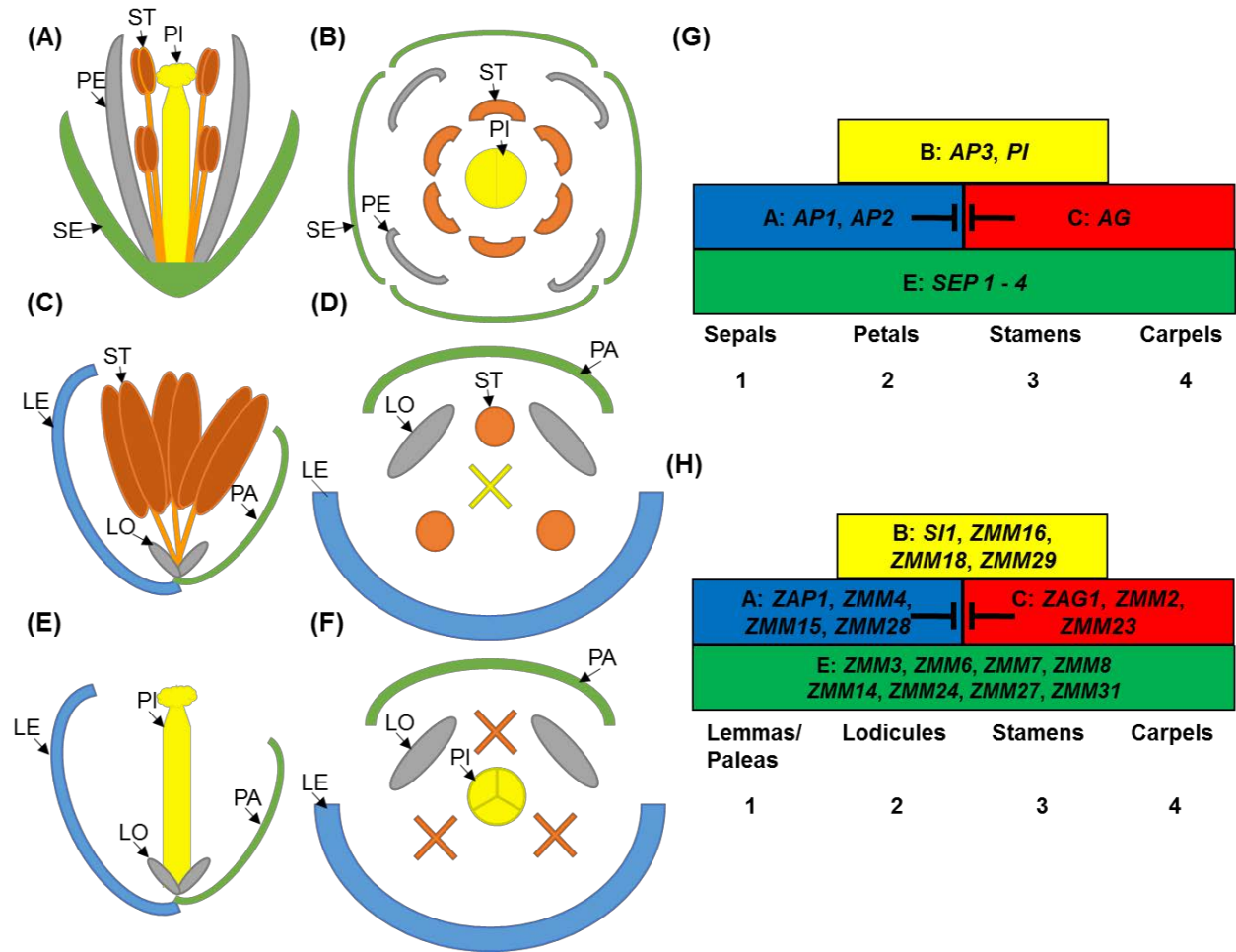


Figure 1.1. Flower and floret structures in *Arabidopsis* and maize with corresponding ABCE models. (A) A longitudinal view through a mature *Arabidopsis* flower (only 2 of 4 long stamens shown). (B) A cross view through an *Arabidopsis* flower. (C) A longitudinal view through a mature male upper floret in maize. (D) A cross view through a male maize floret. (E) A longitudinal view through a mature female upper floret in maize. (F) A cross section view a female maize floret. LE, lemma; LO, lodicule; PA, palea; PE, petal; PI, pistil; SE, sepal; and ST, stamen. X indicates the aborted carpels. (G) The ABCE model in *Arabidopsis*. (H) The ABCE model in maize with most likely orthologous genes.

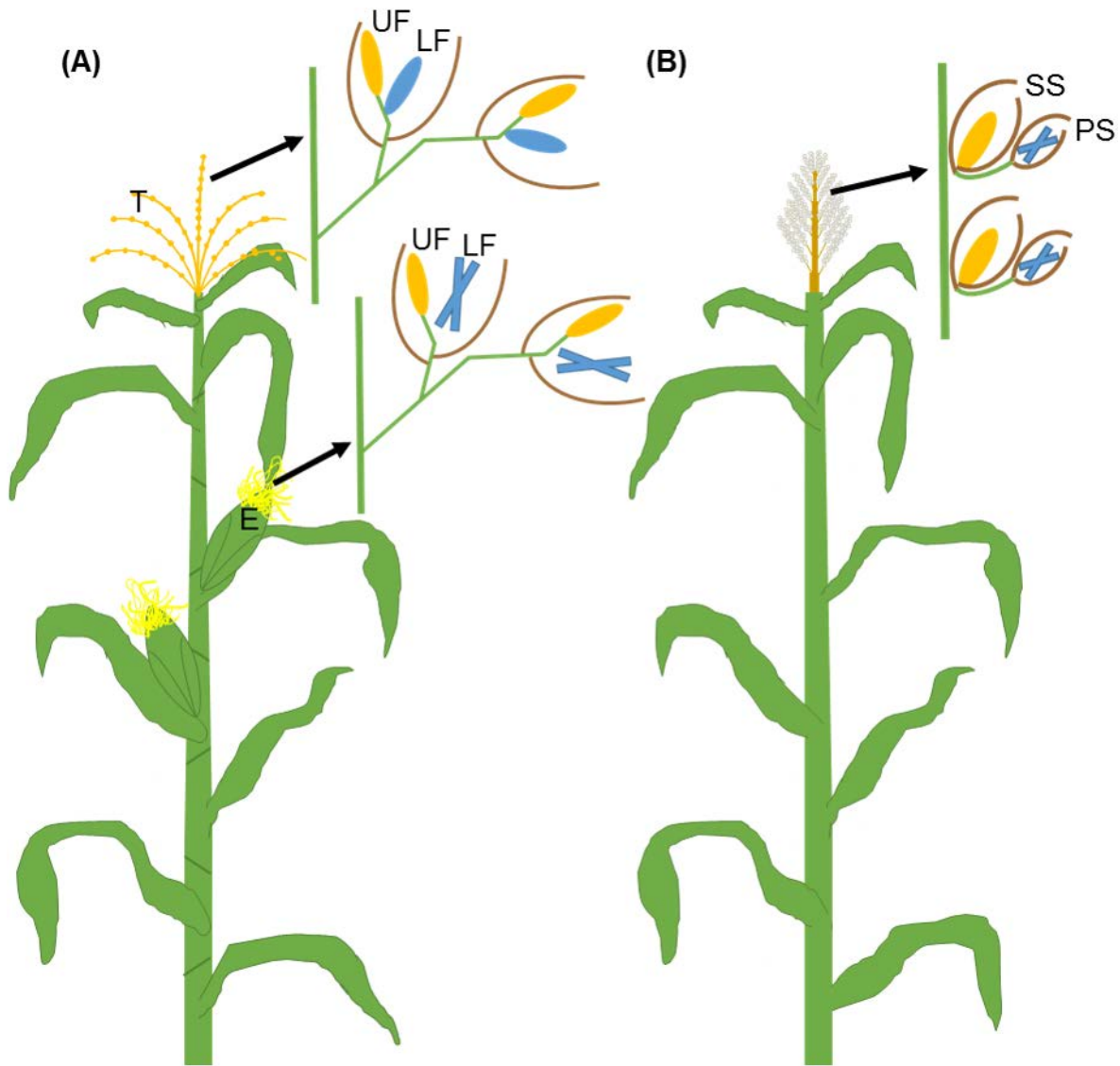


Figure 1.2. Positioning of fertile and sterile maize and sorghum spikelets at maturity. (A) Mature maize plant with positions of the Tassel (T) and the Ears (E) indicated. Arrangement of the fertile upper and lower florets (UF/LF) of the tassel and the fertile upper and sterile lower floret of the ear shown. (B) Mature sorghum plant with the formation of fertile sessile spikelets (SS) and sterile pedicellate spikelets (PS) shown. All sterile florets are indicated with an X. (A) Modified from Bortiri and Hake, 2007.

1.8 Thesis Statement

My research fills a large gap in the study of sorghum and key questions that are addressed include: How does heat stress at PMCs stage affect grain yield in sorghum? How does pedicellate spikelet development differ from sessile spikelet development? At these key stages, what genes are differentially expressed? Does anther development in sorghum mirror the development seen in other cereal grains? When during anther development does sterility of the *ms8* and *Sbtdr* mutants occur? Which genes underlie sterility in the *ms8* and *SbTDR* mutations, and are they similar to known orthologs? With ever increasing pressure for affordable food that can be grown in diversifying conditions, there is a heightened necessity to study heat and drought resistant crops including sorghum. To increase grain yield, we need to determine the heat-sensitive developmental stages, the specifics of spikelet development, manipulate spikelets to increase seed yield, and improve hybrid breeding systems. In other model organisms and crops, including *Arabidopsis* and maize, the stages of floral development have been studied extensively using scanning electron microscopy (SEM) starting decades ago (Cheng et al., 1983; Smyth et al., 1990). In sorghum, no complete series such as these currently exists. It is necessary to create this resource and to use that information to better understand sorghum flowering, sterility, and yield.

It is essential that we add to the collection of available male sterile mutants. Current hybrid lines available in sorghum focus only on the traditional three line cytoplasmic male sterility (CMS) systems in contrast to two line nuclear male sterility

(NMS) systems. While a few male sterility cytoplasm exist, the vast majority of hybrid seed production in sorghum exploits the A₁ cytoplasm (*milo*). In order to better breed sorghum for higher yielding plants and to avoid potential agricultural disasters associated with monocultures, these resources must be improved (Jordan et al., 2011; Praveen et al., 2015; Ullstrup, 1972). Similarly, little study has been done on the development of sorghum anthers and pollen. The study of pollen is critical as failure to form pollen or development of inviable pollen is a key cause of plant sterility, as demonstrated in my review (Smith and Zhao, 2016). The study of anther development is also crucial to understanding and studying male sterile mutants such as *ms8* and *Sbtdr* for hybrid breeding use and for increasing sorghum yield.

These contributions are significant, as the work provides an excellent resource for studying spikelet and anther development in sorghum and other cereal grains. The identification of key floral genes responsible for sterility can be directly used by manipulating these genes, performing complementation experiments and producing fully fertile sorghum varieties. Additionally, the predicted differential expression in the pedicellate and sessile spikelets may provide insight into floral evolution in grasses when comparing to similar phenomena such as sterile lemmas in rice and sterile florets in barley and maize. With the characterization of the *ms8* and *Sbtdr* mutants and cloning of the genes responsible for sterility, the mutants are closer to use in 2-line breeding systems. The use of NMS technology not only simplifies hybrid seed production but also can add to the diversity of plants used in hybrid seed production (Xin et al., 2017).

Chapter 2

The wide-ranging effects of heat stress on floral fertility and vegetative growth in

Sorghum bicolor

2.1 Abstract

With the world facing an ever intensifying climate, heat stress has increasingly detrimental effects on plant growth and development, reducing overall biomass and grain yield in many crops. Although heat stress in *Sorghum bicolor* (L.) Moench during late developmental stages including anthesis, pollen germination, and grain filling decreases the grain yield, it is unclear whether heat stress affects male fertility and seed production in early male development. Here we showed that heat stress beginning at pollen mother cells (PMCs) and through early pollen stages impairs pollen development and reduces grain yield in sorghum. Plants heat stressed for less than 9 days at the PMCs stage showed normal pollen development and seed set, but those heat stressed for 12 days had almost complete loss of grain yield and production of inviable pollen grains. Panicles heat-stressed for 3 days at the early pollen stage had few or no seeds. Further analysis revealed reduced pollen viability, failed anther dehiscence, and aborted pollen tube growth or germination in those 3-day heat stressed plants. Interestingly, besides inhibiting plant height, heat stress for 12 days at the PMCs stage promotes basal tiller formation, while 3-day heat stress at the early pollen stage (booting) stimulates the formation of apical tillers, which salvaged seed yield following the heat stress condition, with no statistical significant difference in total yield. Collectively, our findings demonstrated that heat stress during early male reproductive development

severely decreases grain yield via impaired pollen and anther development, which could help elucidate the molecular mechanisms underlying heat stress-caused male sterility in many cereal crops.

2.2 Introduction

Sorghum bicolor (L.) Moench is a widely grown cereal grain, which is native to Africa and currently cultivated throughout many arid environments including regions across all habitable continents. Sorghum is the fifth most harvested cereal grain globally (Doggett, 1988). The United States produced 9,241,760 tonnes in 2017 over 2,041,660 hectares, which is more than any other country by approximately 2.3 million tonnes (FAOSTAT, 2019). Members of the *Sorghum* genus are used in food, feed, fiber and fuel production (Palmer, 1992; Rooney et al., 2007). In cereal grains, heat stress is a major problem limiting yield (Smith and Zhao, 2016). Since the baseline growing temperature of sorghum is higher than many other cereal grains, it is often claimed that sorghum is more heat resistant; however, heat stress in sorghum is also associated with delays in flowering, decreases in plant height, and reductions in seed yield (Craufurd and Peacock, 1993; Prasad et al., 2008). Maintaining both biomass and seed yields are essential in agricultural and bioenergy production. Sweet sorghum sugars, mainly produced from stalks are used in syrup production, forage, silage, and ethanol production (Reddy et al., 2005). Due to the importance of the stalk and leaves in food, feed, and fuel production, it is essential to maintain biomass under heat stress conditions. Similarly, keeping high seed yield is crucial for grain sorghum; therefore, it is

important to identify key developmental stages during reproduction which are susceptible to heat stress in order to maximize seed yield under heat stress.

So far, few studies have highlighted the effects of heat stress on sorghum fertility and grain yield compared to other crops. When sorghum was subjected to heat stress of 10 days at 40/30°C (day/night) before and during flowering, seed yield loss was observed (Prasad et al., 2008). Heat and drought stresses during booting (spikelets surrounded by the sheath of the flag leaf) and flowering had strong negative effects on grain yield in sorghum, while plants receiving similar stress at the vegetative stage showed normal yield (Craufurd and Peacock, 1993). Pollen development in sorghum is susceptible to heat stress (36/26°C), since microspores from stressed plants were starch-deficient and resulting pollen grains had reduced germination rates (Jain et al., 2007). The starch deficiency was attributed to decreased sucrose biosynthesis and subsequent carbohydrate metabolism (Jain et al., 2007). Under similar conditions, a shorter exposure of 5-10 days, as well as season-long exposure, led to aberrant panicles that were shorter, narrower, contained necrotic regions, and ultimately produced fewer seeds (Jain et al., 2007; Prasad et al., 2006a). These effects were exacerbated at increased CO₂ levels (Prasad et al., 2006a). Heat stress caused by extreme high temperatures (40/30 and 44/34°C) caused more severe phenotypes, such as delayed floral transition, late or failed panicle emergence, nonviable pollen, and complete loss of seed yield (Jain et al., 2007; Prasad et al., 2006a). So far, studies have mainly focused on heat stress occurring late in development at the time of anthesis, pollen germination, and grain filling (Nguyen et al., 2013; Prasad et al., 2015). Proper anther development is critical for the production of viable pollen and consequently

seeds in sorghum. Sorghum is similar to maize in terms of their anther structure. In maize and sorghum anthers have four lobes (microsporangia); within each lobe, the central pollen mother cells are surrounded by four layers of somatic cells: the epidermis, endothecium, middle layer, and tapetum (Cheng et al., 1979; Christensen et al., 1972). Once these layers are established PMCs in maize over the next 14-17 days will undergo meiosis, resulting in microspores and then pollen grains prior to anthesis (Tsou et al., 2015). In sorghum prior to anthesis, young buds are enclosed in a bulged leaf sheath known as the boot. So far, studies have mainly focused on heat stress occurring late in development surrounding anthesis, pollen germination, and grain filling (Nguyen et al., 2013; Prasad et al., 2015).

In this study, our aim was to examine the effects of heat stress applied at the PMCs stage. We hypothesized that heat stress applied during early anther development would result in pollen sterility and decreased seed yield. We applied heat stress of 42/32°C (day/night) to sorghum plants at the PMCs stage for 3 to 12 days. Our results showed that the long-term heat stress (9 to 12 days) at the PMCs stage significantly decreased grain yield and impaired pollen development. After observing the strong effects of heat stress from 9 to 12 days, we further targeted early pollen stage (post PMCs) at booting with a heat stress for 3 days. This short-term heat stress at the post PMCs stage had similar effects. Furthermore, we found that 12-day heat stress at the PMCs stage promoted basal tiller formation, but reduced the plant height. Interestingly, plants under 3-day heat stress at the post PMCs stage produced apical tillers, which could rescue seed loss from the aborted main panicle. Taken together, our findings demonstrated the effects of heat stress during early male reproductive development on

seed production and pollen development, which fills an important gap in the study of sorghum heat stress.

2.3 Materials and Methods

2.3.1 Growing conditions and heat stress treatment

Sorghum bicolor BTx623 WT seeds were grown as single potted plants (triple potted for IAA experiment only) containing SUN GRO Metro-Mix 360. The plants were grown under greenhouse conditions of 28/23°C (day/night), with 10 hours of light (8am-6pm), 14 hours of dark (6pm-8am), and a relative humidity of 50%. Plants were watered daily and fertilized weekly using a Young Mixer-Proportioner Injector at a rate of 60:1, with Sprint 330 and Peterson's Water Soluble General Purpose 20-20-20 fertilizer (250 ppm N and 20 ppm Fe). All plants for long-term heat stress were grown until the anthers reached pollen mother cells (PMCs) stage. The PMCs stage was confirmed by sacrificing a plant and collecting anthers from the mid-panicle. These anthers were stained with 0.5% Toluidine Blue. Stained anthers were squashed and observed by light microscope. After confirming the correct stage, plants were moved into heat stress conditions. Plants grown for short-term heat stress were grown until the booting stage was visible.

For long-term heat stress, 10 plants each were heat-stressed at 42/32°C (day/night) for 3, 6, 9, and 12 days. For short-term heat stress, 10 plants were heat-stressed at 42/32°C (day/night) for 3 days only. Plants were monitored and watered as needed twice a day and humidity was maintained to ensure adequate soil moisture and

limit potential drought stress effects. Plants were returned to normal growing conditions after the desired length of heat stress and grown until the production of mature seeds.

2.3.2 Sample collection and Alexander pollen staining

After the top of the panicle began anthesis and anthers were visible, the spikelets just below were collected and processed. Anthers were dissected and collected for Alexander pollen staining. The anthers were placed in the Alexander stain and left overnight at 42°C. Anthers were then placed in water and imaged on an Olympus BX51 microscope equipped with an Olympus DP70 digital camera. The anthers were evaluated as fertile if they contained large red pollen grains indicating staining of viable cytoplasm and mitochondria. The anthers were labeled as sterile if they contained no pollen or if the pollen appeared small, shrunken, and blue/green indicating only the presence of the pollen wall (Alexander, 1969; Xin et al., 2017).

2.3.3 Pollen germination

Pollen tubes were germinated *in vivo* on stigmas as described previously (Lu, 2011). Briefly, spikelets were fixed in acetic acid overnight, softened in 1 M NaOH overnight, and washed thrice in KPO₄ buffer. Tissue was stained in aniline blue for 2 hours and imaged under UV (Lu, 2011).

2.3.4 Data collection and statistical analysis

The height of plant, number of tillers, seed count, and seed weight were analyzed. The height of the plant was obtained by measuring from the soil surface to the top of the

panicle. The number of tillers was counted as the number of shoots not including the main culm. After drying mature seed heads in a dry oven, seeds were removed from heads. The seeds produced per plant were counted and weighed for analysis. The statistical analyses were completed using JMP. Statistical analyses performed on PMC stage heat stress were One-way ANOVAs and considered significant at $p < 0.05$. Statistical analysis of the three-day heat stress looking at yield were Wilcoxon Rank-Sum Tests.

2.4 Results

2.4.1 Heat stress has limited effects on the vegetative development of *S. bicolor*

All plants in the initial study were heat-stressed starting at the early anther development stage (PMCs stage) for 3-12 days to maximize the likelihood of observing decreased grain yield relative to the control. Heat stress that ranged from 3 to 9 days had minimal effects on plant height ($p > 0.05$), but plant height and tiller formation were significantly affected under a 12-day heat stress (long-term) ($p < 0.0001$). The long-term heat stress caused significant reductions in plant height ($p < 0.0001$) (Fig. 1, 2A). Few tillers were formed on plants heat stressed from 3-9 days, while plants heat-stressed for 12 days formed on average nearly 4 tillers during the same growth period (Fig. 1, 2B). In sorghum, tiller growth is a normal developmental step occurring late in development surrounding anthesis or upon removal of the main stem. Our results suggest that the long-term heat stress promotes tiller formation but inhibits the height in sorghum.

2.4.2 Long-term heat stress beginning at PMCs stage causes male sterility in *S. bicolor*

To examine the effects of heat stress on male fertility, we treated plants starting at the PMCs stage for 3 to 12 days. The developing panicles were deeply embedded in the culm when the heat treatments started. Heat stress for 3-6 days had minimal effects on grain yield in terms of seed count and weight ($p > 0.05$) (Fig. 3). Plants heat-stressed for 9 days produced significantly fewer numbers of seeds and seed weight per panicle was lower, compared to control plants ($p < 0.0001$) (Fig. 3B, C). The seed yield was almost completely lost in plants that were heat stressed for 12 days (Fig. 3). To test the cause of yield loss by heat stress, we performed Alexander staining to examine pollen viability. On average, over 90% of pollen grains were viable in anthers from plants that were heat stressed for 0, 3, 6, and 9 days, as indicated by large red pollen grains with viable cytoplasm (Fig. 4A, B, E; Fig. S2.1). In contrast, anthers examined from plants heat-stressed for 12 days showed nearly 100% inviable pollen grains with blue color, with a significant decrease in viability ($p < 0.0001$) (Fig. 4C, D, E). Our results suggest that the long-term heat stress beginning at the PMCs stage had a severe effect on pollen development, which consequently caused substantial grain yield loss in sorghum.

2.4.3 Heat stress at pollen stage abolished male fertility and promotes tiller formation at the plant apex in *S. bicolor*

To determine the effects of heat stress on male fertility in late male reproductive development stages, we treated sorghum plants just prior to anthesis (early pollen stage). Specifically, we selected plants whose inflorescence were entirely in the boot

and then heat-stressed these plants for 3 days. The control plant developed a single mature panicle with a full seed set (Fig. 5A); however, the panicle in the 3-day heat-stressed plant was small and had few or no seeds (Fig. 5B). Compared with pollen from control plants (Fig. 6A), pollen viability was severely affected by the 3-day heat stress ($p < 0.001$) (Fig. 6B, C). First, very few pollen grains were released from the heat-stressed anther after strong squash (Fig. 6B), suggesting abnormal anther dehiscence. Second, approximately 50% of pollen grains observed were inviable in the heat-stressed anther (Fig. 6C, 4E). In control plants, pollen grains were attached to the hairy sorghum stigmas and pollen tubes were clearly visible (Fig. 6D). In contrast, on the surface of the 3-day heat-stressed stigma, pollen grains failed to germinate (Fig. 6E).

In the control plants, nine nodes on average were observed prior to flowering. In addition to the effects observed on male fertility and seed yield of the main panicle, heat stress at pollen stage caused a rapid growth of additional tillers near the top of plant, generally at the eighth node on the main culm (Fig. 5B). Conversely, these apical tillers were not observed in the control plants (Fig. 5A). Interestingly, the combined seed weight and seed count that arose from these multiple apical tillers were not statistically different when compared to the single seed head of the control plants (Fig. 5C, D). Taken together, our results suggest that a short-term heat stress applied at the early pollen stage abolished male fertility via affecting pollen viability, anther dehiscence, and pollen tube germination. Furthermore, heat stress at this stage promotes the formation of apical tillers, which salvaged seed yield.

2.5 Discussion

2.5.1 Significant agricultural impacts of heat stress on sorghum

The results from our study may have significant impacts on production of sorghum and other grains. The reduction in height caused by heat stress is detrimental, since many sorghum varieties are harvested for biomass and stalk sugars (Rocateli et al., 2012). Similar plant height reductions have been documented in sorghum at 40/30°C (day/night) for 10 days prior to and at flowering (Prasad et al., 2008). In our study, plants heat-stressed at 42/32°C (day/night) for less than 9 days appeared shorter but vigorous; while plants stressed for 12 days often became very small and bush-like with many basal tillers.

Plant architecture is an important feature in maximizing yield. One way to alter plant architecture in sorghum is by modifying tillering. This study demonstrated that heat stress induced tillers that formed at the top plant node. Typically, plants with large carbohydrate sinks such as sorghum and maize produce a single culm under normal conditions. A previous study demonstrated that tillers generally emerged from low numbered nodes whereas higher numbered nodes displayed decreased fertility in sorghum (Lafarge et al., 2002). In our study, the long-term (12 days) heat stress at the vegetative stage caused the formation of numerous tillers, with each tiller displaying greatly reduced seed production. In contrast, tillers at the apex of plants induced by the short-term (3 days) heat stress in the booting stage had the opposite effect. In these plants, tillers each quickly produced seed heads with minimal additional vegetative growth. In *B. distachyon*, plants consistently formed less tillers as temperature was

increased (Harsant et al., 2013). This ability to form large tiller numbers under heat stress conditions might be special to more heat resistant grains such as sorghum.

Increasing the number of tillers may increase the biomass and/or seed production, however not all plants or varieties demonstrated the same benefits. Typically heat stress has been associated with decreased yield; however the ability to form tillers at the apex could maintain yield by compensating for the loss of the main panicle under heat stress while simultaneously having few impacts on harvest date. Increasing tiller number in wheat may only have minimal increases in biomass, since high tiller varieties are often also dwarf (Peng et al., 1999). In rice, transplanting seedlings at different ages increased tiller production, and therefore increased seed yield (Pasuquin et al., 2008). Conversely, high tiller rice varieties have been shown to only increase the vegetative biomass as tillers generally do not have complete grain filling (Sakamoto and Matsuoka, 2004). Moreover, the maize ancestor teosinte produces a large number of tillers with very small cobs and few kernels, with overall low seed yield. In sorghum, a high grain yield might be achievable if both the main seed bearing panicle and additional apical tillers are produced under the normal condition; however, the mechanism of formation of tillers at the apex is not known.

2.5.2 Potential mechanism for altered tillering in heat-stressed sorghum

We found that heat stress induced the formation of apical tillers. In lines possessing strong apical dominance, tillering is not normally induced until anthesis of the primary inflorescence (Isbell and Morgan, 1982). The plants may perceive the functional loss of the apical dominance via sugar and/or hormonal changes which could trigger tiller

development. Several phytohormones, such as auxin, cytokinin, strigolactone, and gibberellic acid, may play some roles in apical tiller formation. The polar transport of auxin in particular is known to block lateral growth. Auxin is produced at the shoot apical meristem and passes basipetally down the stem to inhibit axillary bud development (Booker et al., 2003; Thimann et al., 1934). In *Arabidopsis* the MORE AXILLARY BRANCHING (MAX) pathway inhibits shoot branching via regulating the activity of PIN auxin efflux transporters (Bennett et al., 2006). Mutations of MAX orthologous genes RAMOSUS (RMS) in peas and DECREASED APICAL DOMINANCE (DAD) in petunia led to increased branching (Beveridge et al., 1994; Napoli, 1996). In addition, auxin works with cytokinin to maintain bud dormancy and with strigolactone (SL) to regulate shoot branching (Bennett et al., 2006; Gomez-Roldan et al., 2008). Signaling of SL and cytokinin might be partially integrated with auxin signaling via BRANCHED1/TEOSINTE BRANCHED1 (BRC1/TB1) which regulate auxin transport (Dun et al., 2012; Moreno-Pachon et al., 2018; Seale et al., 2017). Moreover, repression of genes including BRC1 has been associated with sugar redistribution prior to the loss of apical auxin (Mason et al., 2014).

Our preliminary findings showed that auxin might play an important role in apical tiller formation in sorghum. Under normal conditions, plants developed basal tillers after anthesis, but no apical tillers were observed (Fig. S2A). Plants that were decapitated and received lanolin but did not receive IAA grew apical tiller(s), although the seed maturation was slightly delayed compared to the control plants (Fig. S2B). Plants that were decapitated and had IAA applied, failed to grow apical tillers (Fig. S2C). The fact that heat stress also promotes the formation of apical tillers suggests that heat stress

may inhibit auxin biosynthesis or signaling in the apex of sorghum. It will be interesting to investigate the role of auxin in tiller formation under normal and heat stress conditions in the future.

2.5.3 Heat stress severely impacts male fertility and seed yield in sorghum

Our study showed that the cause for reduced fertility following heat stress is attributable to problems in anther and pollen development. In addition, duration and the timing of heat stress are critical for affecting male fertility and seed yield. We found that male fertility is susceptible to heat stress at pollen stage in sorghum. A short-term heat stress (3 – 6 days) beginning at the early male reproductive PMCs stage did not impact fertility; however, we observed complete sterility in anthers heat-stressed for 12 days beginning at the same stage. Over the duration of the 12 day heat stress, the PMCs divided forming microspores and then pollen. Similarly, the 3 day heat-stressed anthers also were at pollen stage. When heat-stressed during pollen development, dead pollen grains were observed in both experiments. This finding highlighted pollen susceptibility to heat stress. Interestingly, only partial pollen grain death was observed in anthers heat-stressed for 3 days after the formation of the boot. Because of this finding it can be inferred that stress applied early in anther development compounded the negative effects observed on later pollen viability and seed yield. In further support, the pollen grains with the long-term heat stress beginning at the PMCs stage also appeared to be reduced in size and lacked the rounded appearance typical of the non-stressed pollen. It is possible that decreased starch accumulation resulted in smaller inviable grains. In other cereals including wheat and barley, stress applied at an earlier stage, such as

meiosis in the anthers, is known to cause abnormal tapetal degeneration and sterility (Saini et al., 1984; Sakata et al., 2000). Tapetal cells are known to be important for nourishing microspores and pollen development, and sensitive to stress (Smith and Zhao, 2016). Heat stress during early anther development may impair the normal function of tapetal cells, which consequently leads to the formation of inviable pollen. In addition to affecting pollen viability, the short-term heat stress at the early pollen booting stage also caused the failure of anther dehiscence. Similarly in rice, heat stress during late development resulted in anther indehiscence (Matsui and Omasa, 2002; Satake and Yoshida, 1978). Our results are consistent with previous studies as pollen did not release from squashed anthers and less pollen grains reached the surface of the stigma (Jain et al., 2007; Matsui et al., 2000; Sato et al., 1973). Next, it will be necessary to study how heat stress affects tapetal cell differentiation and pollen development at the molecular level. Overall, in ever diversifying environments sorghum may experience heat stress $>42^{\circ}\text{C}$ with variable durations. Further work to elucidate the molecular mechanisms underlying male sterility, decreased seed yield, reduced plant height, and increased apical tillering under heat stress would be highly beneficial in sorghum cultivation.



Figure 2.1. Comparison of control and heat-stressed (HS) plants beginning at the PMCs stage. Scale bars: 10 cm.

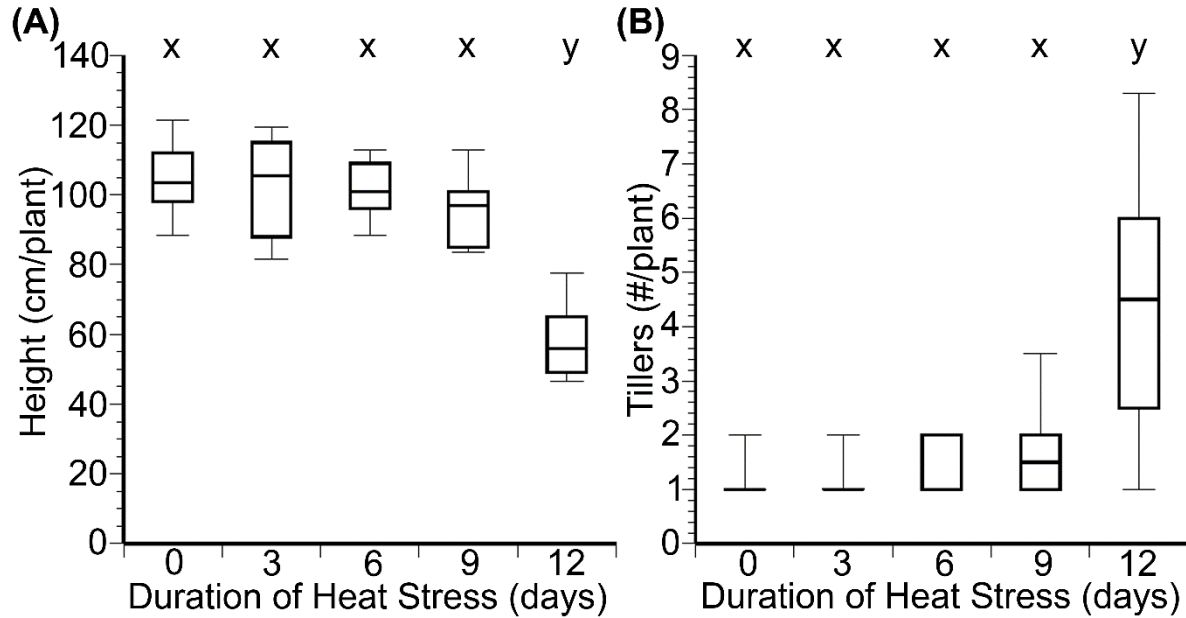


Figure 2.2 Effects of heat stress applied beginning at the PMCs stage on plant height tiller formation. (A,B) Box plots include median values with standard error.

One-way ANOVAs with levels that differ significantly ($p < 0.05$) are indicated. (A) The plant height is significantly affected by heat stress ($F_{4,45} = 24.0897$, $p < 0.0001$), and 12-day heat-stressed plants are significantly shorter, p value < 0.0001 . (B) The tiller number is significantly affected by heat stress ($F_{4,45} = 24.0897$, $p < 0.0001$), and 12-day heat-stressed plants have significantly more tillers, p value < 0.0001 .

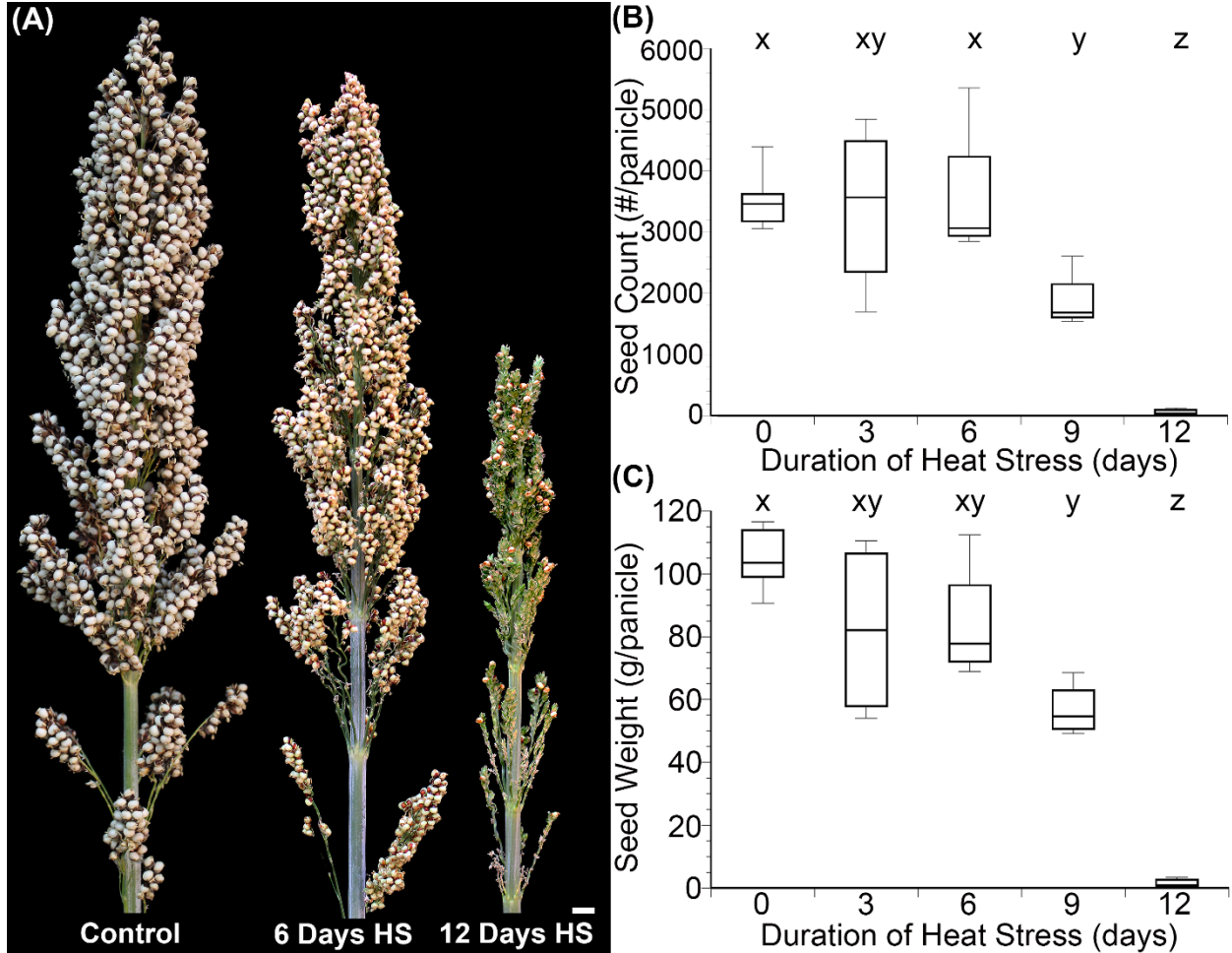


Figure 2.3. Effects of heat stress on seed count and weight. (A) Mature seed heads from non-heat stressed plants, and plants heat stressed for 6 and 12 days. (B, C) Box plots contain median values with standard error. Levels that differ ($p < 0.05$) via one-way ANOVA are indicated. (B) Seed count is negatively affected by prolonged heat stress ($F_{4,21} = 19.6204$, $p < 0.0001$) and 12-day heat stressed plants have reduced seed count, $p < 0.0001$. (C) Seed weight is negatively affected by prolonged heat stress ($F_{4,21} = 41.4148$, $p < 0.0001$), and 9- and 12-day heat stressed plants have significantly reduced seed weight, $p = < 0.0001$. Scale bar: 1 cm.

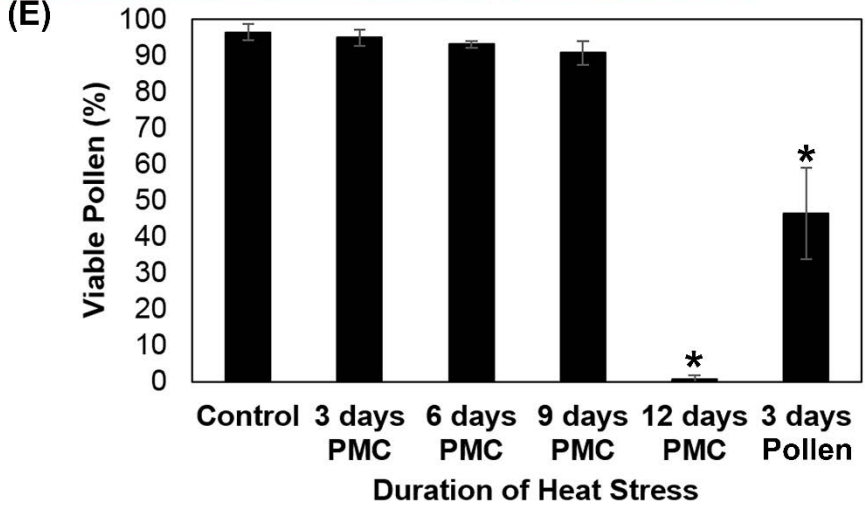
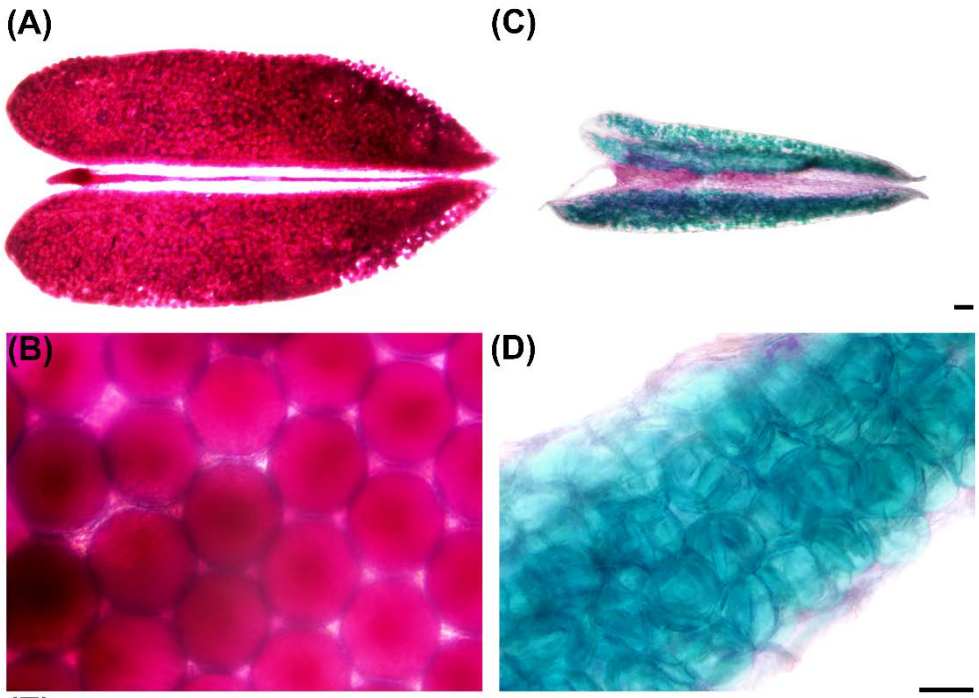


Figure 2.4. Pollen viability examined via Alexander staining in control and 12-day heat-stressed plants starting at PMCs stage. (A) A full-size control anther. (B) High magnification of image (A) showing red viable pollen grains. (C) A full-size anther from the 12-day heat-stressed plant. (D) A high magnification of image (C) displaying dead blue pollen grains. (E) Mean percent of viable pollen from the control and heat-treated plants starting at PMC and pollen stage with standard error shown. Pollen viability is significantly impacted by heat stress ($F_{5,24} = 201.68$, $p < 0.0001$) with significantly less viable pollen in 12 days at PMC and 3 days at pollen (booting) $p < 0.0001$ as indicated by asterisk. (other durations $p > 0.05$). Scale bars: 100 μm (A and C) and 25 μm (B and D).

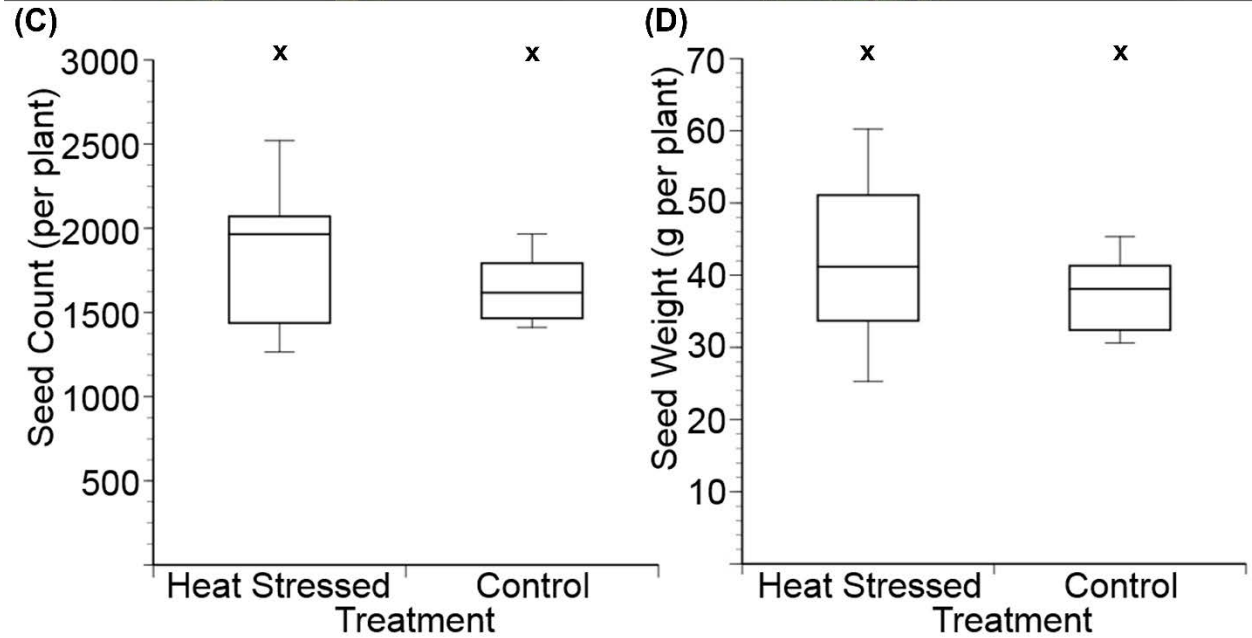


Figure 2.5. Similar total grain yield per plant in control and 3-day heat-stressed plants at the booting stage. (A) The control plant showing a single seed head and no tillers at the apex. (B) The 3-day pollen stage heat-stressed plant exhibiting a dead main panicle and 2 tillers at the apex. (C, D) Seed counts (C) and seed weight (D) per plant with median and standard error shown in boxplots. Seed yield was similar between the control and heat-stressed plants with no statistical differences (Wilcoxon Rank-Sum Test) in either total seed count per plant ($\chi^2_1 = 0.5634$ $p = 0.4799$) (C) or total seed weight per plant ($\chi^2_1 = 0.7037$ $p = 0.4015$) (D). Arrow indicates sterile main panicle used for pollen staining and germination studies. Scale bars 10 cm (A, B).

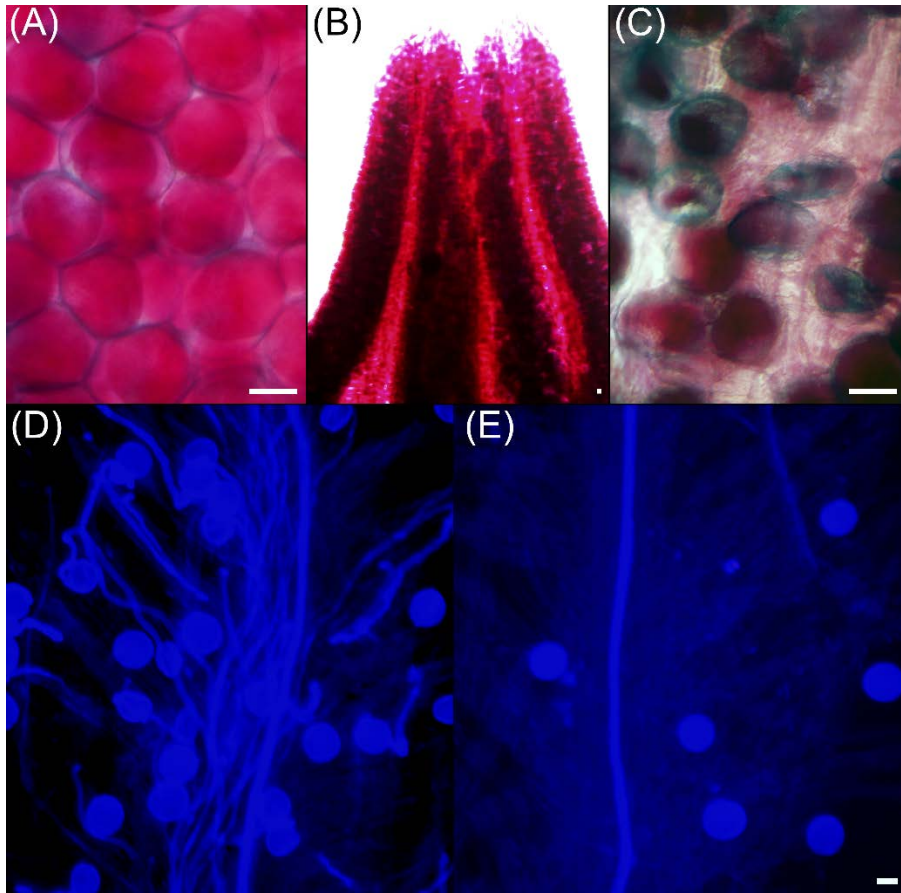


Figure 2.6. Pollen fertility in control and 3-day heat-stressed plants. (A) Red viable pollen grains in the control anther. (B) A portion of the squished 3-day heat-stressed anther. (C) Mix of fertile (red) and sterile (blue-green) pollen grains from the 3-day heat-stressed anther. (D) Normal pollen tube germination in the stigma of control plant. (E) No pollen tube germination in the stigma of 3-day heat-stressed plant. Scale bars 20 μm .

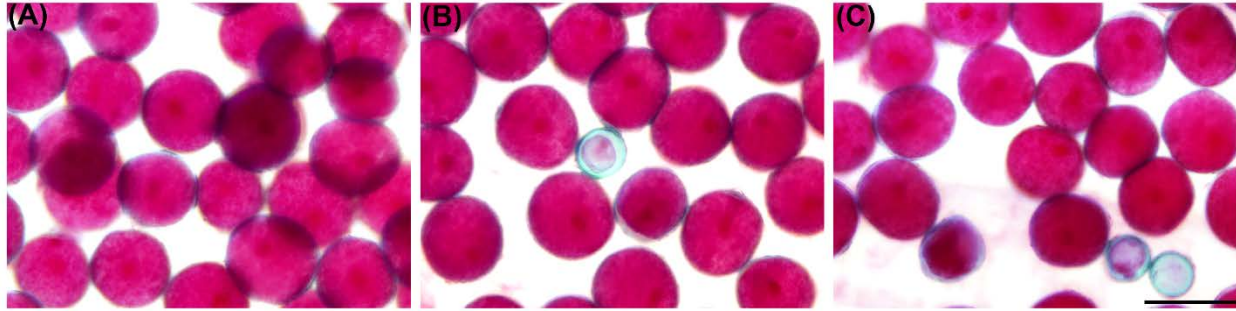


Figure S2.1. Alexander staining of mature pollen grains showing viable pollen grains are produced under 3-9 day heat stress. Pollen shown at 3 (A), 6 (B), and 9 (C) days heat stress applied beginning at pollen mother cell anther stage. Scale bar 50 μm .

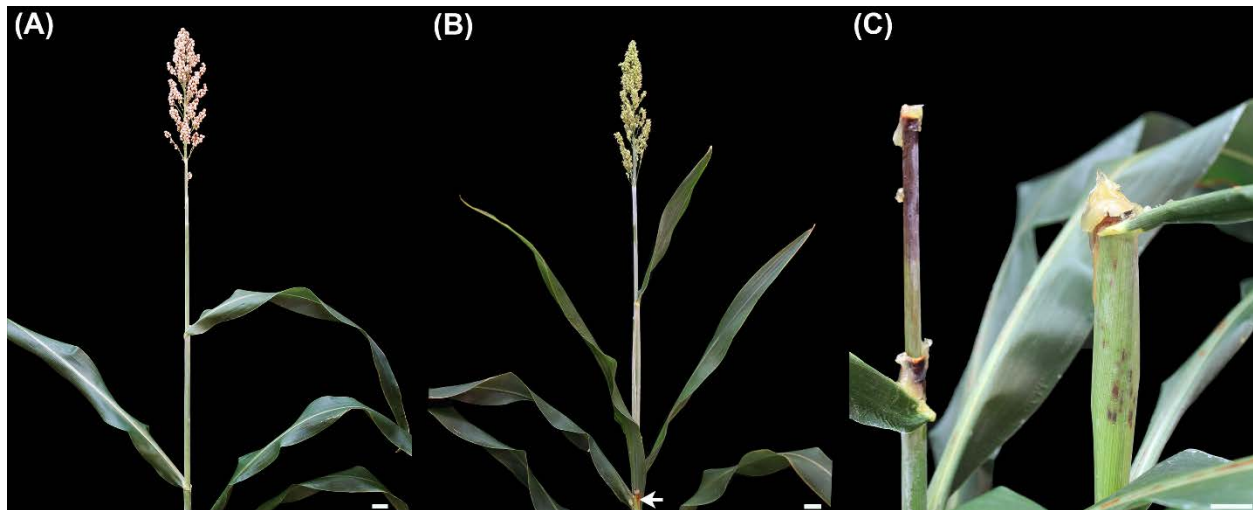


Figure S2.2. Effects of decapitation and IAA treatment on apical tiller formation. (A) The control plant showing a single mature panicle. (B) The plant whose primary inflorescence was removed (arrow) and mock-treated with lanolin exhibiting a panicle from the apical tiller. (C) The plant whose primary inflorescence was removed and treated with lanolin IAA and lanolin failed to develop the apical tiller. Scale bars 2.5 cm.

Chapter 3

Spikelet development in *Sorghum bicolor* and the genetic basis for pedicellate floret sterility

3.1 Abstract

In cereal crops including *Sorghum bicolor* (L.) Moench, it is important to maximize the grain number to increase the yield. Sorghum forms a spikelet pair containing a fertile sessile spikelet and 1-2 sterile pedicellate spikelets, resulting in over half of the florets failing to produce seed. Despite the significance of the grain reduction, the complete morphological differences between the sessile and pedicellate spikelets have not been documented, and little is known about the genes that control pedicellate sterility. Based on scanning electron microscopy analysis, here we provide a comprehensive floral developmental series in sorghum wild type BTx623 WT as well as two mutants, *multiseeded1* (*msd1*) and *malesterile antherless* (*msa1*). We identified key developmental stages corresponding to major morphological alterations between sessile and pedicellate spikelets. We showed that sessile and pedicellate spikelets have uniform early development of the outer floral whorls; however, during the transition to form the androecium and gynoecium a developmental lag is initiated in all pedicellate florets. This developmental lag continues, leading to degeneration of the stamens and carpel, and ultimately, sterility in wild-type pedicellate spikelets. In contrast, the *msd1* mutant overcame the developmental lags in pedicellate spikelets, continued to develop, and formed seeds in all spikelets, greatly increasing grain yield. In *msa1* we further show that sessile spikelets fail to form stamens and instead form abnormal numbers of

carpels. Transcriptomic analysis revealed altered expression of genes encoding TEOSINTE BRANCHED 1, CYCLOIDEA, PROLIFERATING CELL FACTOR 1 (TCP), and MADS-box transcription factors as well as genes involved in cell cycle and phytohormone biosynthesis and signaling in developing sessile and pedicellate spikelets. We proposed that upregulated expression of the *SbTCP2* gene which is orthologous with the maize *TEOSINTE BRANCHED 1 (TB1)* and barley *SIX-ROWED SPIKE 5 (VRS5, INT-C)* might inhibit lateral growth of the pedicellate spikelets. Collectively, we for the first time morphologically characterized the development of sessile and pedicellate spikelets in sorghum. Furthermore, we proposed key pathways and genes that control pedicellate sterility, providing a valuable molecular basis for increasing grain yield in sorghum.

3.2 Introduction

Sorghum bicolor (L.) Moench is a drought resistant monocot native to Africa currently cultivated throughout India, Asia, Southern United States, Mexico, and South America. Sorghum is the fifth most harvested cereal grain globally (Doggett, 1988). Members of the *Sorghum* genus are used in food, feed, fiber and fuel production. As there is increased pressure for affordable food sources for growing populations, researching a crop that provides both excellent food and feed is desirable, especially in plants grown in semiarid regions (Morris et al., 2013). After extensive climate modeling, it has been shown that the American southwest is anticipated to become increasingly arid in upcoming decades (Seager et al., 2007). Simultaneously, the need for world cereal production is expected to increase, with an estimated need of 3,286 million metric tons (m.m.t.) by 2060, an increase of nearly 1,500 m.m.t. from 1990 (Rosenzweig and Parry, 1994). Even though technologies improve and irrigation is used, in many countries, particularly non-developed countries, decreased grain yield is anticipated due to climate changes (Rosenzweig and Parry, 1994). As the production of this protein and carbohydrate rich grain is facilitated by the development of spikelets, all aspects of spikelet development must be understood if yield is to be increased.

In sorghum, the basic developmental process has been previously documented. Following vegetative growth, the primary-branch primordia are initiated, followed by the formation of secondary and higher-order branch primordia, initiation of spikelet primordia, morphogenesis of spikelets, as well as elongation and emergence of the panicle (Lee et al., 1974). So far, detailed developmental of spikelets is not clear and the specific stages of spikelet development are not classified. In model organisms and

other crops, such as *Arabidopsis* and maize, the stages of floral development have been studied extensively using scanning electron microscopy (SEM) (Cheng et al., 1983; Smyth et al., 1990). Grasses including sorghum possess florets that are organized into spikelets, each of which contains at least one floret. In sorghum, these spikelets are arranged into groups of one sessile spikelet with one or two pedicellate spikelets (two in terminal spikelet pairs). Individual florets are surrounded by a pair of bracts known as the outer and inner glume (Doggett, 1988; Schmidt and Ambrose, 1998). In the first whorl, in lieu of sepals, the sorghum BTx623 wild-type (WT) forms the lemma and palea. The lemma and palea are in the relative position of the sepals but their similarity to sepals and homology to each other have been long debated (Ambrose et al., 2000; Keijzer et al., 1996; Lombardo and Yoshida, 2015; Schmidt and Ambrose, 1998). In the second whorl two lodicules are present in the typical position of petals (Yoshida, 2012). The third whorl, the androecium, contains three stamens, and in the fourth whorl, a central gynoecium with bipid stigma is formed. In sorghum, the sterile pedicellate spikelets of the BTx623 WT grown in our greenhouse conditions contain only the glumes (outside of the floret) and a single lemma/palea like organ at maturity. Past studies show pedicellate spikelets were observed to occasionally form anthers (Jiao et al., 2018b).

Besides the lack of knowledge about spikelet morphogenesis, the molecular mechanisms underlying floral organ specification are not known in *S. bicolor*. In flowering plants, the MADS-box genes, particularly the ABCE genes control floral organ identity. Several studies have identified sorghum MADS-box genes that likely play important roles in development and fertility (Chen et al., 2017; Greco et al., 1997; Zhao

et al., 2011). The functions of these sorghum MADS-box genes are not as well studied as in the *Arabidopsis* pathways or in their increasingly well documented rice and maize orthologs. Due to the fact that many genes display consistent roles in these diverse species, it is likely that similar functions are found in sorghum. Class E genes specify ABCD gene activity to promote meristem and floral organ identity. *SEPALLATA* genes including *Arabidopsis* *SEP1-4*, rice *SEP*-like *LEAFY HULL STERILE1* (*LHS1/OsMADS1*), and Maize gene *SEP4*-like *BDE* are essential to fertility (Ditta et al., 2004; Jeon et al., 2000a; Malcomber and Kellogg, 2005; Pelaz et al., 2000; Prasad et al., 2001; Thompson et al., 2009). A-class genes are required for sepal and petal identity. A class MADS-box genes includes the *Arabidopsis* *APETALA1* (*AP1*), maize *ZAP1*, and the potentially redundant rice *OsMADS14/15/18/20* orthologs (Fornara et al., 2004; Huijser et al., 1992; Jeon et al., 2000b; Lim et al., 2000; Mandel et al., 1992; Mena et al., 1995). C-class genes are essential in petal (*Arabidopsis*) and lodicule (grasses) formation. This includes *Arabidopsis* C-class gene *AGAMOUS* (*AG*), and in rice, *OSMADS3/58* (Bowman et al., 1991; Bradley et al., 1993; Yamaguchi et al., 2006). B-class genes specify the petals/lodicules and stamen identity. In *Arabidopsis* this function is attributed to *APETALA3* (*AP3*) and *PISTILLATA* (*PI*) (Goto and Meyerowitz, 1994; Jack et al., 1992; Sommer et al., 1990; Trobner et al., 1992). Similarly, in grains the *AP3* orthologous genes *Silky1* (*Si1*) in maize and *SUPERWOMAN1* (*SPW1*) in rice and *PI* orthologues *ZMM16/18/29* in maize and *MADS2/4* in rice specify the identity of the lodicules and stamens (Ambrose et al., 2000; Chung et al., 1995; Munster et al., 2001; Nagasawa et al., 2003; Yoshida, 2012). D-class MADS-box genes function in ovule development. In *Arabidopsis*, *STK* is involved in seed development (Mizzotti et al.,

2014). The potential rice homolog *OsMADS32* functions in stamen and lodicule identity regulation by negatively regulating *DROOPING LEAF (DL)* expression (Sang et al., 2012; Wang et al., 2015).

In addition to genes specifying floral organs, key genes in cereals have also been identified in controlling the development of lateral spikelets. WT barley is a 2-rowed variety, while common cultivars are a 6-rowed fully fertile barley whose two lateral sterile spikelets are fertile (Koppolu et al., 2013). Five genes contribute to the conversion of two-row to six-row barley and, in total, 11 independent loci (*HEXASTICHON (HEX)*, *SIX-ROWED SPIKE (VRS)* and *INTERMEDIUM (INT)*) are known to affect lateral spikelet fertility (Bull et al., 2017). Loss of function of *VRS* genes causes various phenotypes ranging from small increases to complete lateral-spikelet fertility. The *vrs1* mutants display a complete conversion of sterile lateral spikelets to fertile spikelets (Komatsuda et al., 2007). Loss of the wheat *VRS1* ortholog *Grain Number Increase 1 (GNI1)* leads to increased fertile floret number and seed yield (Sakuma et al., 2019). *VRS1* which is expressed in immature lateral-spikelet primordia, encodes a basic helix-loop-helix (bHLH) transcription factor (Komatsuda et al., 2007; Koppolu et al., 2013). *VRS2* encodes a SHORT INTERNODES (SHI) transcriptional regulator, and when mutated, fertile lateral spikelets are only observed at the basal nodes, although further functions in organ patterning and phase duration are proposed (Youssef et al., 2017). The *VRS3* (syn. INT-A) gene encodes a putative Jumonji C-type H3K9me2/me3 demethylase, functioning as a regulator of the chromatin state. The *vrs3* mutants form six-rowed barley with the exception of the basal spikelets, and *VRS3* is likely involved in spikelet identity and meristem determinacy (Bull et al., 2017; Zwirek et

al., 2018). *vrs4* mutants form 6-rowed barley similar to *vrs1*. Acting upstream of *VRS1*, *VRS4* (syn. INT-E) encodes a LATERAL ORGAN BOUNDARY domain transcription factor (Koppolu et al., 2013). Double mutants *vrs1vrs3*, *vrs1vrs4*, and *vrs1vrs5* all have increased seed number (Zwirek et al., 2018). *VRS5* (syn. INT-C) in barley plays a role in lateral spikelet fertility by modifying or complementing the effect of *VRS1* alleles (Ramsay et al., 2011). *VRS5* homologs such as *TEOSINTE BRANCHED1 (TB1)* are known to repress elongation of the tiller buds and promote apical dominance (Doebley et al., 1997; Ramsay et al., 2011). In maize, *TB1* represses axillary organs and supports the formation of the female inflorescence. Modern maize has high *TB1* expression compared to its highly branched ancestor teosinte (Doebley et al., 1997). Altered expression of homologous *VRS* genes has not been documented in sorghum. This work explores the potential effects of the *SbTB1* ortholog.

The aim of this work is to provide a complete developmental series in sorghum, classify the key stages associated with pedicellate sterility, and use these key stages to identify the differences in gene expression underlying pedicellate sterility. Due to past work in cereals, the hypothesis was made that developmental may mirror the sterility of the lower ear floret of maize. Here we report a detailed morphological characterization of sessile and pedicellate spikelet development in WT sorghum and compare it to that in *msd1* and *msal* mutants. We show key anatomical differences during development between the spikelet types and the mutants. Specifically, we demonstrate a clear developmental lag in pedicellate spikelets in the WT and mutants. We further show that this developmental lag is resolved in the fully fertile *msd1* mutant, while it intensifies and leads to complete sterility in the WT. Using these anatomical differences and the

developmental lag identified in this work, we targeted key stages 5, 6, and 10 for RNA-seq to identify the genetic basis for sterility in sorghum pedicellate florets. Specifically, we propose the molecular mechanism in which TCP transcription factors, MADS-box genes, and jasmonic acid (JA) control pedicellate spikelet sterility.

3.3 Materials and Methods

3.3.1 Sorghum lines and growing conditions

The BTx623 WT, *msd1* and *msal* mutants were utilized in this study. The *msd1* and WT sessile spikelets are identical, however *msd1* pedicellate spikelets form fully fertile florets due to a mutation in the Sb07g021140 gene which encodes a class II TCP transcription factor *SbTCP16* gene (Burow et al., 2014; Jiao et al., 2018b). The *msal* mutant characterized in this study is male sterile and fails to produce stamens at any point in development. All lines were all grown in SUN GRO Metro-Mix 360 at a temperature of 28/23°C (day/night), with 10 hours of light (8am to 6pm), and 14 hours of dark (6pm to 8am), at a relative humidity of 50%. Plants were watered daily and fertilized weekly using a Young Mixer-Proportioner Injector at a rate of 60:1, using a concentrate of Sprint 330 and Peterson's Water-Soluble General Purpose 20-20-20 fertilizer that contains 250 ppm nitrogen and 20 ppm iron. Spikelets were imaged using an Olympus SZX7 dissecting microscope equipped with an Olympus DP70 digital camera.

3.3.2 Sample preparation and scanning electron microscopy

Sorghum floral tissue was harvested 6 to 10 weeks after planting and placed in modified Trump's 4:1 primary fixative (4% paraformaldehyde, 1% glutaraldehyde, in 0.1 M HEPES buffer (pH 7.2), and 0.02% Triton X-100) (McDowell and Trump, 1976). Plants were harvested between approximately 6 and 10 weeks after emergence by cutting the plant at the base. The outer layers of the stem were then removed by hand. Once these layers were removed, the floral primordia through mature spikelets were collected.

Samples were vacuum infiltrated with fixative for 30 minutes and left in primary fixative for a minimum of two days and subsequently stored at 4°C. To prepare samples for scanning electron microscopy (SEM) they were first washed twice in ddH₂O. Samples were post fixed in 1% osmium tetroxide overnight at room temperature. The osmium tetroxide was then removed and the samples were rinsed twice in ddH₂O. Dehydration was performed in 10% ethanol increments for a minimum of 1.5 hours per step. The samples were then critical point dried using a BALZERS UNION CPD 020. After mounting and dissections, samples were sputter coated with iridium using an Emitech 575X sputter coater. The florets and floral primordia were viewed on a Hitachi S-4800 SEM.

Sections that were imaged were prepared following OsO₄ post-fixation (as above) using a 10% acetone gradient for 3 hours each up until 100% which was performed three times. Floral tissues were then infiltrated with a 10% modified Spurr's resin gradient for a minimum of three hours each (Holdorf et al., 2012). 100% resin was exchanged for 5-7 days prior to embedding in flat molds. Floral tissue in resin was cured for 3 days at 60°C. Tissue was sectioned at 500 nm on a RMC-MT7 ultramicrotome. To

generate SEM backscattered electron (BSE) images, the approach outlined by Micheva and Smith (2007) was modified. Tissue was sectioned at 400 nm by ultramicrotome. Sections were placed on a 22 mm round glass coverslip and the coverslip mounted with carbon tape to a one inch stub. The coverslip with sections was carbon coated using an Edwards Coating System 306A using carbon string. This coated coverslip was then surrounded by carbon paint and the tissue sections were imaged by SEM to generate backscattered images (Micheva and Smith, 2007).

3.3.3 RNA-seq library preparation

Floral tissue from key stages, as detected in our developmental study, including sorghum WT stages 5, 6, and 10 and *msd1* stages 6 and 10, were dissected fresh and placed immediately into RNAlater™ solution (Sigma-Aldrich, St Louis, MO, USA) to preserve RNA. Floral tissues for RNA-seq were collected from three biological replicates from a minimum of three plants per replicate. Samples were then placed at -20°C prior to RNA extraction. RNA was extracted using the RNeasy plant mini kit (Qiagen, Manchester, UK) according to the manufacturer's instructions. After RNA extraction, libraries were prepared using TruSeq Stranded Total RNA with Ribo-Zero Plant kit (Illumina, San Diego, CA) following the manufacturer's protocol. On-column DNase digestion was carried out using the RNase-free DNase (Qiagen). RNA amounts were determined with a Qubit 3.0 Fluorimeter (Fisher Scientific) and 500 ng of total RNA was used for preparing each RNA-seq library (Zhao et al., 2018). The amplified cDNA was transported to the UW-Madison Biotechnology Center where the libraries were validated, standardized, and sequenced on an Illumina HiSeq 2500 using a TruSeq

SBS sequencing kit version 3 (Illumina) and processed with Casava 1.8.2 to obtain stranded, 100 bp, single end reads. The average number of reads obtained from each library was 33.4 M.

3.3.4 RNA-seq data analysis

After sequencing, the data was first analyzed for quality scores using *FASTQC* (<http://www.bioinformatics.bbsrc.ac.uk/projects/fastqc>) (Andrews, 2014). Data was processed using the CyVerse computation infrastructure (<http://www.cyverse.org/>). To pre-process the data, it was trimmed to remove adapters and low quality sequences using the programs *Scythe* and *Sickle*. Reads with a base quality of 20 on the Phred scale (confidence or accurate base calling of >99%) and longer than 20 nt were further analyzed (Huang et al., 2016). Reads were analyzed using the hierarchical indexing for spliced alignment of transcripts program (HISAT2), StringTie, and Ballgown to detect differentially expressed genes (Kim et al., 2015; Pertea et al., 2016). Briefly, reads were aligned with the HISAT2 program to the *Sorghum bicolor* v3.1.1 genome downloaded from phytozome (<https://phytozome.jgi.doe.gov/pz/portal.html>). These transcripts were assembled using StringTie. The assembled transcripts were then merged, and differentially expressed genes between stages, lines, and spikelet types were detected using Ballgown (Kim et al., 2015; Pertea et al., 2016). Data was once again checked on *FASTQC*. All genes with significant differential expression ($p < 0.05$) were analyzed and genes with log₂fc greater than 2 were further analyzed. Genes were clustered into pathways using STRING (<https://string-db.org/cgi/input.pl>) and functional categories via

AgriGO2 (<http://systemsbiology.cau.edu.cn/agriGOv2/>) to identify the gene families or gene networks that were highly represented.

3.4 Results

3.4.1 *S. bicolor* spikelets display uniform development prior to the formation of reproductive floral organs

We performed scanning electron microscopy (SEM) and classified sessile and pedicellate spikelet development into 13 stages. We then used our standards to study the spikelet phenotypes of two floral mutants. The *msd1* mutant was chosen, as it has known pedicellate fertility, providing an interesting comparison to the WT. The second mutant, *msal*, has an interesting uncharacterized male sterility phenotype, allowing a comparison between male and female reproductive development.

Stages were classified using terminology consistent with past work in maize (Cheng et al., 1983). Sorghum stage 1 is characterized by the formation of spikelet primordia. The spikelet primordia cannot be anatomically distinguished from each other at stage 1, however two clear primordia are present (Fig. 3.1A). At stage 1, these primordia contain the floral meristem as the floral organ primordia have not yet formed. At stage 2, the pedicels begin to form allowing what will become the pedicellate spikelets to extend higher and distinguishing the spikelet primordia (Fig. 3.1B). At stage 3, both the outer (1st) and then inner (2nd) glume primordia are initiated (Fig. 3.1C). At stage 4, these develop and extend, residing below the floral meristem (Fig. 3.1D). At stage 5, the lemma and then palea primordia are formed giving the developing spikelets a distinctive four layers that can easily be counted (Fig. 3.1E). Stage 5 prior to formation

of the reproductive whorls, is the last stage when all spikelet types and lines are identical.

3.4.2 WT pedicellate spikelet development lags behind the sessile spikelet

After the establishment of the outermost layers, the developing spikelet enters into a very active period. At stage 6, many key events occur in the developing sessile spikelet. The lodicule primordia form a distinct ridge in the sessile spikelet (Fig. 3.2A). The three stamen primordia become visible around the central dome that will form the carpel (Fig. 3.2A). The pedicellate spikelet at this stage first demonstrates the developmental lag that will characterize all future growth. In the developing pedicellate spikelet, the lodicules, stamens, and gynoecium primordia have not yet formed (Fig. 3.2A). The lag initiated at stage 6 continues throughout development up until the point of degeneration in the WT pedicellate spikelet (Fig. 3.2). At stage 7 in the sessile spikelet, the palea forms a distinctive peak (Fig. 3.2B). The reproductive primordia expand in the sessile spikelet, and the developing anther below the peak of the palea begins to lobe in the WT (Fig. 3.2B). In maize, the lateral stamens develop ahead of what is termed the third stamen or abaxial stamen (Cheng et al., 1983). In contrast, this non-lateral or adaxial stamen develops ahead of the lateral stamens in sorghum. The central developing gynoecium becomes increasingly domed in all lines (Fig. 3.2B). At stage 7, in the developing pedicellate spikelet, the reproductive primordia begin to develop (Fig. 3.2B). During stage 8, the gynoecium flattens in the sessile spikelet (Fig. 3.2C). The 'first' anther in the WT spikelet also begins to lobe (Fig. 3.2C). In the pedicellate spikelet the reproductive primordia begin to expand (Fig. 3.2C). At stage 9, WT anthers of the

pedicellate spikelet surge in growth, containing four distinct lobes, and the peak anther reaches a taller height than the lateral anthers (the two not below the palea peak) (Fig. 3.2D). The gynoecium begins to develop the styles and it takes on a distinctive u-shaped appearance with a slight depression at the base (Fig. 3.2D). In the WT pedicellate spikelet, the 'first' anther lobes ahead of the lateral anthers which flatten and begin to lobe (Fig. 3.2D). At stage 10, the size difference between the sessile and pedicellate spikelets becomes great (Fig. 3.2E). The sessile spikelet anthers continue to elongate, and the lateral anthers reach the height of the 'first' anther (Fig. 3.2E). The styles elongate greatly in all lines but do not reach the height of the anthers (Fig. 3.2E). In the WT pedicellate spikelet, the anthers do slightly lobe but do not elongate (Fig. 3.2E). Over the mid developmental stages the WT pedicellate spikelet begins to develop but at stage 10 fail to progress, marking the beginning of degeneration.

As floral development nears completion, the WT sessile spikelet continues to advance, intensifying the developmental lag. Degeneration continues in the WT pedicellate spikelet. In WT, the sessile spikelet has great extension of the styles by stage 11, formation of obvious feathery stigmas by stage 12, and growth of the stigmas over the top of the anthers by stage 13, which is prior to anthesis (Fig 3.3A, B, C). By the end of development, the sterile spikelet undergoes little to no development or growth (Fig. 3.3D, E, F). Prior to complete degeneration of the WT pedicellate spikelet, it contains abnormal anthers that have minimal extension (Fig. 3.3D, E, F). Ultimately, the pedicellate spikelet undergoes complete degeneration of the innermost whorls.

At pollen mother cells (PMCs) anther stage, clearly formed epidermis, endothecium, middle layer, and tapetum layers are visible in the sessile spikelet anther

(Fig. 3.4A) The developmental lag is visible at this early stage where the pedicellate anther has not divided to form the proper anther wall layers (Fig. 3.4B). In these sections, cells that were alive with nuclei and organelles can be similarly observed (Fig. 3.4B). As development continues the progression of the sessile spikelet results in formation of microspores with clear enlargement of the tapetum and completed degeneration of the middle layer (Fig. 3.4C). The pedicellate spikelet anther at this time point contains only the epidermal layer with the remaining contents having degenerated and clear cells are no longer visible. Consistent with the SEM findings the late-stage pedicellate anther collapses (Fig. 3.4D). At the end of the developmental series the WT sessile spikelet is bisexually fertile and the pedicellate spikelet is bisexually sterile with only remnants of degenerated inner whorls (Fig. 3.3C, F). When the end stages of development in sorghum were compared to other cereal grains, many similarities were observed. Similar to the degeneration of the sorghum pedicellate spikelets, maize undergoes degeneration of the lower ear florets, rice forms the sterile structures known as the sterile lemmas, the apical florets of wheat are typically sterile, and the lateral spikelets of wild 2-rowed barley fail to form seeds (Fig. 3.5).

From all the SEM work and comparisons to other cereal grains displaying sterile organs and florets, the key stages of spikelet development for the RNA-seq study were identified as stages 5, 6, and 10. Firstly, stage 5, was where the last synchronous development of the pedicellate and sessile was observed. Secondly, stage 6, was the beginning of reproductive development in sessile spikelets and the onset of the pedicellate lag. Thirdly, stage 10, was where no further pedicellate reproductive development was observed and degeneration commenced in pedicellate spikelets.

3.4.3 *msd1* pedicellate development overcomes the developmental lag

We compared *msd1* and WT to identify what stages varied in development, leading to pedicellate fertility. Consistent with the WT, early anatomical development of the sessile and pedicellate spikelets is identical (Fig. 3.1F, G, H, I, J). Further, at stage 6 a clear developmental lag forms between the sessile and pedicellate spikelet (Fig. 3.2F). The development of the *msd1* pedicellate spikelet mirrors that of the WT through stage 9 of development (Fig. 3.2F, G, H, I). Beginning at stage 10, a clear difference is observable in the *msd1* pedicellate spikelet. At this stage the pedicellate spikelet begins a surge in growth where it approaches the developmental stage of the sessile spikelet (Fig. 3.2J). Unlike in WT, the lag does not intensify in *msd1* (Fig. 3.3J, K, L). As the *msd1* pedicellate spikelet develops it maintains a one stage delay behind the sessile spikelet (Fig. 3.3J, K, L). When sessile *msd1* anthers begin to dehisce, nearly mature anthers are observed in the pedicellate spikelet (Fig. 3.3I, L). Eventually all florets open, pollen is released, and complete seed-set is observable in both spikelet types.

3.4.4 Male sterile mutant *msal* fails to develop stamens while producing numerous carpels

In our study, we compared WT sessile development to a male sterile mutant to better characterize normal reproductive development. We observed that *msal* mutants vary compared to WT sessile but not WT pedicellate spikelet development. The *msal* mutant displayed normal WT-like development prior to the formation of the reproductive whorls (Fig. 3.1K, L, M, N, O). Similar to the WT, *msal* mutant spikelets demonstrate the

pedicellate lag beginning at stage 6 and eventually pedicellate sterility (Fig. 3.2K). At stage 6, the *msal* mutant demonstrates abnormal male and female reproductive development (3.2K). At stage 6, we expected to identify a central gynoecium primordia surrounded by three stamen primordia (Fig. 3.2A). At this time point we instead identified two major findings. The first is that no male reproductive structures were formed at stage 6 or any subsequent stage (Fig. 3.2K, L, M, N, O, 3.3M, N, O). The second is that in their place a variable number of increased ovaries and stigmas form (Fig. 3.2K, L, M, N, O, 3.3M, N, O). Every *msal* mutant contained at least 2 carpels and the most common finding was the presence of four carpels (mean 3.84 ± 0.92) (Fig. 3.6C). In the WT every sessile spikelet examined contained a pair of lodicules. In *msal*, only a single lodicule was present in some spikelets (Fig. 3.6C). Not only did the numbers of floral organs vary greatly from the WT but many of the individual carpels contained a single style/stigma unit in place of the WT, which has one central bifid stigma (Fig. 3.3A, B, C, M, N, O, 3.6B). Logically, the mutant yielded no seed naturally. After the *msal* was pollinated with BTx623 WT pollen the spikelets formed a single seed, likely due to fertilization of only the central, normally positioned carpel (personal observations). This central carpel typically was largest, developed at the same time as the carpel of the WT sessile spikelet, and contained a central bifid stigma.

3.4.5 RNA-seq reveals differential expression of many key cell cycle, development, phytohormone, and TCP transcription factor genes between sessile and pedicellate spikelets

To identify the cause of pedicellate sterility, RNA-seq data from key developmental stages was analyzed as previously selected based on extensive SEM studies. These stages included stage 5 with no morphological differences, stage 6 with the onset of the pedicellate lag, and stage 10 the earliest WT pedicellate degeneration. Over the course of the WT analysis, expression of over 34,000 genes were detected in the samples. Most of these (over 33,000) were detectable in all the stages, with some transcripts that appeared unique to each stage (Fig. 3.7A, B, D, E). After compiling these gene lists, the differentially expressed genes were compared between the WT pedicellate and sessile spikelets and the *msd1* pedicellate and sessile spikelets. Additionally, comparisons were made between *msd1* and WT. Several key groups were identified with numerous differentially expressed genes including genes known to be involved in TCP, cell cycle, development, and phytohormone production and signaling. The sessile and pedicellate spikelets displayed different transcriptomes, with the largest differences observed between the stage 10 pedicellate and sessile spikelets. This was not surprising, as the stage 10 fertile spikelets are completing their reproductive maturation whereas the stage 10 sterile spikelets were halting reproductive development, potentially degenerating the inner layers, and only the outermost layers including the leaf-like glumes appeared to be elongating (Fig. 3.2E).

In the WT, nearly 2500 genes had significantly lower expression in sessile spikelets than in pedicellate while around 2100 had higher expression in sessile

spikelets (Fig. 3.7A, B). When more stringent cut-offs were placed on the data to examine only the genes with the greatest and significant log₂ fold changes of 2 or greater, less than 300 genes were identified in the WT (Fig. 3.7C). Similarly, in *msd1* sessile and pedicellate comparisons, over 2900 genes had significantly lower sessile expression and just under 2800 genes had significantly greater sessile expression than (Fig. 3.7D, E). When examining log₂ fold changes of 2 or greater, this was reduced to just over 500 differentially expressed genes (Fig. 3.F). During the WT study only three genes displayed these consistent high log₂ fold changes including *Sobic.003G269700*, *Sobic.004G216600*, and *Sobic.005G018500* (Fig. 3.7C). *Sobic.003G269700* had higher WT pedicellate expression (compared to sessile) and its product is predicted to function in terpene biosynthesis as a methyltransferase (MT) (Hay, 2018). *Sobic.004G216600* had higher WT sessile expression (compared to pedicellate) functioning encoding a glutaredoxin. *Sobic.005G018500* likely encodes a *NAC-LIKE, ACTIVATED BY AP3/PI (NAP)* where in our study it displayed lower WT sessile (compared to pedicellate) expression. Functional annotation showed that compared to pedicellate spikelets, sessile spikelets had higher expression of genes for transcription, translation, and protein production. These spikelets are rapidly developing and forming new floral whorls in contrast to the pedicellate spikelets that have lagged behind. In contrast, the pedicellate spikelets were dominated by increased expression of photosynthesis, metabolic, fatty acid, and genes related to metabolism. The pedicellate spikelets contain a higher ratio of glume tissue to internal floral whorls. Compared to sessile spikelets, the increased pedicellate expression of photosynthetic genes may reflect their more leaf-like appearance and eventual function.

3.4.6 A group of master regulators, the TCP factor genes, are differentially expressed in sterile spikelets with limited effects on cell cycle gene expression

All known sorghum TCP factors were examined in the current study except for *SbTCP4*, which was not detected at any stage in this study. Many different expression patterns were observed across the study. In general, compared to pedicellate spikelets, several TCP factors had significantly lower expression in sessile spikelets over various stages including *SbTCP3*, 5, 7, 9, 15, 16, and 19 (Fig. 3.8, Table S3.1). Higher expression of TCPs in WT tissue (compared to *msd1*) was observed in many samples and stages including *SbTCP1*, 3, 6, 7, 9, 11, 13, 15-19. Only four TCP factors had significantly lower expression in WT spikelets compared to *msd1* spikelets, including *SbTCP1*, 5, 16, 19. One piece of data that appears particularly significant is the high expression of *SbTCP2* and *SBTCP14* in WT sessile tissue. *SbTCP2* is the ortholog of the maize gene *TB1*. It is the only TCP factor to have consistently high and significant expression in all sessile WT spikelets, and to some extent, *msd1* sessile spikelets (compared to pedicellate spikelets) (Fig. 3.8, Table S3.1). *SbTCP14* has a similar expression pattern to *SbTCP2* but the results were not statistically significant ($p > 0.05$) (Fig. 3.8, Table S3.1). *SbTCP14* is the ortholog of rice *PCF1*. The tri-seed *msd1* mutant has a mutation in *SbTCP16* (Jiao et al., 2018b). *SbTCP16* in this study has lower expression in stage 6 and stage 10 sessile spikelets (compared to pedicellate) as well as higher expression in WT stage 10 pedicellate spikelets compared to the *msd1* mutant. Consistent with the large developmental differences between *msd1* 10P and WT 10P, there was significant

differential expression of 12/19 quantifiable TCP factors. Within this group, 11 of these TCP factors have higher expression in the WT spikelets than in pedicellate spikelets.

A first glance, the expression of cell cycle genes appeared to reveal dramatic changes. Upon closer examination, few significant differentially expressed genes in the WT pedicellate and sessile comparisons were found, and those identified were scattered over stages 5, 6, and 10 (Fig. 3.9, Table S3.2). Similarly, *msd1* gene expression showed some pedicellate vs. sessile differences over early development with fewer differences in cell cycle gene expression at stage 6. Overall, *msd1* and WT displayed similar gene expression at stage 6 in both pedicellate and sessile spikelets. Gene expression varied greatly when comparing WT and *msd1* spikelets at stage 10p and also when comparing *msd* 10S and *msd* 10P (Fig. 3.9, Table S3.2). Broadly speaking, sessile and WT tissue demonstrated higher expression of many categories of cell cycle related genes; however, few genes were significantly differentially expressed in the WTP/WTS comparisons (Table S3.2).

3.4.7 MADS-box genes play a role in establishing and maintaining the development of sessile spikelets

Differential expression of MIKCC-type MADS-box genes revealed a pattern of predominately higher expression in WT and *msd1* sessile spikelets over time including *SbMADS3*, 8, 10, 11, 16, 17, 22, 26, 27, 31, and 32 (Fig. 3.10, Table S3.3). Altered gene expression was detected for several ABCDE gene homologs. In the WT, E-class orthologs (*SEP*) *SbMADS3/8/22* had higher expression in sessile spikelets over stages 6 and 10. Dramatic changes were observed in *SbMADS22*, with higher expression in all

stage 6 and 10 sessile spikelets. The A class AP1 orthologs *SbMADS9/33* did not display differential expression (Chen et al., 2017) (Fig. 3.10, Table S3.3). B class AG-homologous MADS-box genes *SbMADS10/S26* had significantly higher WT sessile expression in stages 5 and 10 (*SbMADS10*) and 6 (*SbMADS26*) (Fig. 3.10, Table S3.3). The C class genes orthologous to *AP3* and *PI* showed the most consistent altered expression. *SbMADS27* is orthologous to *PI* and had higher expression in all sessile spikelets (Fig. 3.10, Table S3.3). Another *PI* clade gene, *SbMADS11*, has higher expression in multiple sessile spikelets but was only significant at WT stage 6 and *msd1* stage 10 (Fig. 3.10, Table S3.3). Similar to *SbMADS10*, *SbMADS11* has higher expression in *msd1* at stage 10. *Arabidopsis* *AP3* homolog and rice *SUPERWOMAN* ortholog *SbMADS31* had higher expression in all sessile spikelets and higher expression at *msd1* stage 10P (Fig. 3.10, Table S3.3). The D class gene *SbMADS32* is homologous to *SEEDSTICK* (*STK*) (formerly *AGL11*) and *OsMADS32* (Also named *Chimeric Floral Organs1*), and had higher expression in stage 6/10S spikelets. MIKC^C MADS-box genes displayed an interesting trend with increased expression of select genes in the WT and *msd1* sessile spikelets (compared to pedicellate spikelets).

3.4.8 Expression of genes involved in JA biosynthesis, response, signaling, and transport is altered in sterile pedicellate spikelets

In the dataset, one apparent trend was the increase in JA gene expression in WT pedicellate (compared to WT 10S), as well as stage 10P spikelets compared to *msd1* 10P. Genes orthologous to *Arabidopsis* JA biosynthesis genes showed significant increased expression in the WT late stage pedicellate spikelets compared to the *msd1*

mutant, consistent with past findings (Jiao et al., 2018b) (Fig. 3.11, Table S3.4). WT sessile spikelets overall had lower levels of JA biosynthesis gene expression compared to their pedicellate counterparts. Clear trends in expression were observed when following through JA biosynthesis. In sequential biosynthesis order, *DEFECTIVE ANTHWER DEHISCENCE (DAD1)* ortholog *Sobic.005G032700*, displays higher expression in late sterile WT compared to the mutant. Next in order is *LIPOXYGENASE3 (LOX3)* *Sobic.006G09560* which is also the likely *TASSELSEED1 (TS1)* ortholog in sorghum. The sorghum *LOX3* has higher expression in WT 10P compared to *msd1* 10P. In sorghum, *TS2* may also function in JA biosynthesis. The likely *TS2* homolog *Sobic.006G153100* has significantly decreased expression in all WT sessile spikelets, and higher expression in stage 10P sterile spikelets, compared to the fertile *msd1* pedicellate spikelets. Continuing the trend of increased JA biosynthesis gene expression in pedicellate spikelets, *ALLENE OXIDE SYNTHASE (AOS)* homologs *Sobic.001G077400* and *Sobic.001G449700* had generally lower expression in WT sessile spikelets and both had higher expression in WT stage 10P compared to *msd1* stage 10P (Fig. 3.11, Table S3.4). *ALLENE OXIDE CYCLASE (AOC) 1/4* homolog *Sobic.001G329800* and *12-OXO-PHYTODIENOIC ACID 10,11 REDUCTASE (OPR3)* homolog *Sobic.007G151100* displayed lower WT 10S expression and higher expression in WT10P when compared to *msd1* 10P (Fig. 3.11, Table S3.4). An additional JA gene of interest, *Sobic.003G269700*, was differentially expressed with log₂fc greater than 2 in all WT comparisons. Its homologs have functions as Jasmonic acid carboxyl Methyltransferases catalyzing methyljasmonate formation and as jasmonic or a salicylate carboxymethyltransferase (Kakei et al., 2015; Yang et al., 2006). Overall,

while the changes in JA gene expression often were not large, they were dependably significant demonstrating a consistent higher expression profile in the WT (compared to *msd1*) and pedicellate (compared to WT) comparisons.

3.4.9 Auxin, gibberellic acid, and brassinosteroid genes do not strongly affect pedicellate fertility

Differentially expressed IAA, GA, and BR genes were present between sessile and pedicellate WT spikelets and the patterns were not consistent. Several genes had unique and significant differential expression between *msd1* and WT stage 6P and 10P suggesting there could be some differences in auxin production (Fig. 3.12, Table S3.5). Few genes had differential expression in the WT comparisons, with no reliable patterns. For example, Sobic.009G203700 (*SbIAA22*) and Sobic.009G069700 (*SbIAA20*) have the greatest increased and decreased expression in sessile spikelets respectively and are both *PAP1* orthologs in *Arabidopsis*. Genes expressed early in the GA biosynthesis pathway including *CPS1*, *KS1*, *KO1*, and *KAO1* largely showed no significant changes in expression, with the exception of *KAO1* which overall had higher expression in sessile and WT tissues. The enzymes that catalyze the 2 β -hydroxylation steps to form bioactive forms of GA overall had limited differential expression and likely did not impact the final levels of bioactive GA (Hedden and Phillips, 2000). Within the enzymes that catalyze the conversion of GA₁₂ to inactive GA₁₁₀ and GA₅₃ to inactive GA₉₇, most comparisons did not yield significant results, while those that did often had opposing results (Lo et al., 2008; Schomburg et al., 2003)

Decreased signaling or perception of GA may have minimal impacts on pedicellate sterility. Signal perception by GA binding to GA INSENSITIVE DWARF1 (GID1) may be affected as *GID1* had lower expression in sessile and WT tissues except at the *msd1* stage 10P where its expression was increased. DELLA proteins are transcriptional regulators which repress GA signaling. As the GID1/GA complex interacts with DELLA resulting in DELLA degradation by the SCF^{GID2/SLY1} complex in a proteasome pathway GA activity may be further affected (Dill et al., 2004; McGinnis et al., 2003; Murase et al., 2008). Overall *GID2* and the potential *SLY1* homolog *Sobic.004G358900* were not differentially expressed with the exception of higher *Sobic.004G358900* expression in WT 10P compared to *msd1* (Fig. 3.13, Table S3.6). Overall, few meaningful changes in biosynthesis, inactivation, and *DELLA* gene expression were present (Fig. 3.13, Table S3.6). The last analyzed phytohormone group was the brassinosteroids. There was no indication that in the WT, brassinosteroid biosynthesis, response, or perception affected pedicellate fertility (Fig. 3.14, Table S3.7). Several genes had altered expression when comparing the WTP and WTS and *msd1* and WT. These differences were not consistent and groups of genes were split between increased and decreased expression.

3.5 Discussion

3.5.1 Development between sessile and pedicellate spikelets is distinctive

Despite the great agricultural potential, little prior to this study was known about the process of floral development and the reason that over half of the spikelets fail to form seeds. With ever-increasing pressure for affordable food that can be grown in

diversifying conditions, there is a heightened necessity to study heat and drought resistant crops including sorghum. To increase grain yield, we need to determine the specifics of floral development, manipulate florets to increase seed yield, and improve hybrid breeding systems. The establishment of this clear and complete developmental series allows a better understanding of sorghum flowering, sterility, and yield. It also allows for interesting comparisons of sorghum to other cereal grains. During early spikelet development in all lines in this study, floral development was identical. All spikelets were able to progress and eventually formed all the floral primordia starting with the non-reproductive structures of the spikelet over identical developmental stages. Over time, the different lines and spikelet types became distinct. Notably at stage 6 the sessile spikelet surged in reproductive development, separating them from their pedicellate counterpart. This developmental lag continued throughout development in the three lines we studied. While the lag was initially present in *msd1*, the pedicellate spikelets were able to form fertile reproductive organs (Jiao et al., 2018b). In contrast, the previously uncharacterized *msal* mutant formed only carpels starting at stage 6. The central *msal* carpel typically was the largest, but all carpels developed at a similar pace, identical to the WT sessile carpel with the exception of their high number. The *msal* mutant demonstrated complete sterility as no anthers or pollen were produced beginning at this earliest stage.

The spikelet developmental series observed in sorghum is consistent with other cereal grains. In maize and rice, floral development follows nearly an identical progression of establishing the glumes, lemma, palea, lodicules, stamens and anthers (Cheng et al., 1983; Ikeda et al., 2004). During maize development both the tassel and

ear form pairs of florets within a spikelet. In both the tassel and the ear the lower florets lag developmentally behind the upper floret (Cheng et al., 1983). Analysis of WT pedicellate spikelet sections revealed that the reproductive structures were gradually degenerated and collapsed primarily over floral stages 10-13. In maize studies, vacuolated anther cells and collapsed lobes in the female ear resemble sorghum stage 9 sections which showed large vacuoles (Cheng et al., 1983). The exact stage of degeneration did vary somewhat between spikelets but in the SEM studies no WT pedicellate spikelets had full extension of any of the reproductive structures, lodicules, or formed a completed pair of lemma/palea. Terminal sorghum spikelets form two sterile spikelets. As the glumes are not considered true floral organs the pedicellate sorghum spikelet grouping shares remarkable similarity with the fertile spikelet and paired sterile lemmas found in rice. While the origin of these rice structures is still actively debated, more recent findings suggest that they are remnants of a pair of lateral florets. This idea is supported by an elongation and homeotic conversion of sterile lemmas to lemmas in several mutants, such as *long sterile lemma (g1)/elongated empty glume (ele)* and *osmads34/panicle phytomer2 (pap2)* (Gao et al., 2010; Hong et al., 2010; Kobayashi et al., 2010; Yoshida et al., 2009). Further support of the developmental delay and subsequent degeneration is observed in 2-rowed barley. In 2-rowed barley the lateral florets begin to develop normally, like the central florets. As development proceeds, the stamen primordia arrest and appear to lag behind the central floret, consistent with sorghum pedicellate spikelets (Youssef et al., 2014). Some similarity is also observed compared to the wheat spike. Wheat spikelets contain a large number of florets with increased sterility in the basal spikelets and the more apical florets within spikelets

(Rawson and Evans, 1970). The florets show an increased developmental lag and likelihood of sterility as you ascend in the spikelet, similar to the effects of the observed pedicellate lag in sorghum (Feng et al., 2017; Rawson and Evans, 1970).

3.5.2 The pedicellate spikelet developmental lag and sterility are likely connected to TCP factor gene expression.

TCP family members play many roles in plant development, including control of flowering and flower development via the cell cycle and hormonal signaling. TCP factors are involved in many hormone pathways including gibberellic acid (GA), jasmonic acid (JA), salicylic acid (SA), cytokinin (CK), abscisic acid (ABA), and brassinosteroids (BR) (Nicolas and Cubas, 2016). In sorghum, 20 TCP factors including 7 potential paralogs make up 2 distinct clades that could influence plant morphology and abiotic stress tolerance (Francis et al., 2016). TCP proteins, with the exception of SbTCP4, all contain a complete TCP domain, basic helix I, loop, and Helix II regions. In class I proteins there is a four-amino acid deletion in the basic region (Francis et al., 2016). Our study found several differentially expressed TCP genes. One of interest was identified as *SbTCP2* (Fig. 3.6). Past studies demonstrate that *SbTB1* (*SbTCP2*) and *MSD1* (*SbTCP16*) are both detected at high levels in the young inflorescence (Francis et al., 2016; Jiao et al., 2018b; Makita et al., 2014). A comparative study of transcriptomic data indicates that both *SbTCP16* and *SbTCP2* frequently have low expression (based on FPKM values compared to other TCPs); however, their highest expression values are both found in the inflorescence where they are the most highly expressed sub-clade G TCP factors (Francis et al., 2016). Sub-clade G including CYC/TB1-like genes that are specifically

expressed in the inflorescence (Francis et al., 2016). In maize, the increased expression of *TB1* compared to its teosinte ancestor resulted in suppression of axillary branching (Hubbard et al., 2002). *TB1* is expressed in tissues with limited growth including axillary meristems, the stamen primordia of the ear, and weaker expression in the stamen primordia of the tassel (Hubbard et al., 2002). The question posed here is why is the expression of *TB1* significantly greater in all WT sessile spikelets? We hypothesize that in sorghum it may act as a lateral blockade. *TB1* expression is associated with the suppression of axillary growth, reduced lateral branching, and arresting growth as in maize, potato, tomato, *Arabidopsis*, barley, rice and others (Aguilar-Martinez et al., 2007; Hubbard et al., 2002; Martin-Trillo et al., 2011; Nicolas et al., 2015; Ramsay et al., 2011; Takeda et al., 2003). While the end product of *TB1* is consistent, the expression of *TB1* would typically be highest in the sterile tissues themselves.

Much study has been done on *TB1*, particularly in the cereal grains. As demonstrated in maize, the function of *TB1* may be more complicated than generally described as demonstrated by the expression (although weaker) in the tassel stamens and the overexpression of *TB1* not affecting axillary bud propagation in rice (Takeda et al., 2003). Similar to in maize, in overexpression and ectopic overproduction of *OsTB1* in wheat decreases lateral branching and generates fewer tillers (Takeda et al., 2003). The rice *TB1* homolog *FINE CULM1* integrates multiple hormonal signals, suppressing axillary bud development likely downstream of the strigolactone pathway (Minakuchi et al., 2010). The homologous potato gene *BRANCHED1a* is affected by the ratio of far red to red light and auxin levels causing alternate splicing. Higher expression of the transcriptional activator *BRC1a*^{Long} (unspliced) was associated with decreased

branching and apical auxin application, far-red light, and darkness. Expression of the unspliced *BRC1a* results in suppressed lateral growth. The dominant negative factor *BRC1a^{Short}* (spliced) antagonizes *StBRC1a^{Long}*, increasing shoot and stolon branching (Nicolas et al., 2015). In barley, the *VRS* genes control fertility of the lateral spikelets. The *VRS5/INT-C* gene is the barley homolog of maize *TB1*, and can affect lateral spikelet fertility in different mutant backgrounds (Ramsay et al., 2011). A recent study has demonstrated that the role of *TB1* may be associated with the formation of paired spikelets where increased dosage of *TB-D1* (D-genome) promotes the paired spikelet trait in wheat (Dixon et al., 2018). It is proposed here that the increased *TB1* expression somehow blocks the formation of their adjacent axillary pedicellate spikelets. The mechanism or potential transport of *TB1* would require future study to better support this hypothesis. Similar ideas have been put forward in the past where branch meristem fate is controlled by inflorescence genes that define the boundary domain (Kellogg, 2007).

Glutaredoxins are known to regulate transcription factors. Interactions occurring between some TCP factors and plant-specific CC-type glutaredoxins (GRX) such as *ROXY1* have been documented (Ziemann, 2010). While the exact interactions of the *Sobic.004G216600* GRX are unknown, future studies could determine whether there are interactions between *TB1* and this GRX. *Sobic.004G216600* had large and significant log₂ fold change in all WT samples with lower expression in sessile spikelets in this study and higher *msd1* expression. *Sobic.004G216600* was expressed in the early inflorescence with typically lower expression in vegetative tissues. The maize ortholog is *GRMZM2G148387*. In maize, glutaredoxins are essential for anther development and maintaining plant fertility (Hong et al., 2012). The rice ortholog

OsGRX9 was induced under several conditions, particularly by the addition of different hormones, where higher expression of *OsGRX9* was present when SA, JA, ABA, and IAA were applied (Garg et al., 2010).

3.5.3 Altered MADS-box gene expression is crucial for establishing and maintaining the developmental lag and sterility of the pedicellate spikelet

MADS-box genes encode a transcription factor family which plays essential roles in plant development including flower development (Becker et al., 2000). In *Arabidopsis* there are five distinct groups of MADS-box genes: M α , M β , M γ , M δ , and MIKC (Parenicova et al., 2003). Few M α and M β genes detected had significant changes between lines or stages. However, many MIKC genes had altered expression. The finding of differential expression of several key MADS-box genes is an important finding impacting sorghum fertility. There are strong connections between the roles of many of these MADS-box genes in *Arabidopsis* and the cereal grains. Notably there was little differential expression of likely A class *AP1*-like genes so these genes likely do not play a role in pedicellate sterility. Outer pedicellate spikelet layers such as the lemma/palea like organ that remain were relatively unaffected, highlighting that A class function may still partially function in these spikelets. In contrast, several B, C, D, and E class homologous genes were examined in sorghum with known expression profiles in the developing inflorescence and reproductive whorls. These genes overall had differential expression consistent with the lag and loss of the lodicules, stamens, carpels, and overall fertility. These *AP3*, *PI*, *AG*, *STK*, and *SEP*, MADS-box gene homologs typically had decreased expression in the WT pedicellate spikelets, particularly at stages 6 and

10 (Fig. 3.7). These B and C class genes as well as *SEP2*-like E class genes had lower expression in WT spikelets compared to *msd1* mutant spikelets, particularly at stage 10 in both pedicellate and sessile WT spikelets. It is known that the AP3 and PI heterodimer regulates many aspects of floral development and the expression of several developmental genes including *GATA22/GNL* and *GATA21/GNC*, and *NAP* (Mara and Irish, 2008; Sablowski and Meyerowitz, 1998). *Sobic.005G018500* was one of the genes of interest in this study due to its high log₂fc. Its potential *Arabidopsis* homolog is AT1G69490 or *NAC-LIKE, ACTIVATED BY AP3/PI (NAP)*. Expression of *NAP* is specifically detected below the inflorescence meristem, in flower pedicels, and in the developing sepals. As flowers matured the expression shifted in the flower extending to aspects of the petals, ovules, and sepals (Sablowski and Meyerowitz, 1998). *NAP* expression is directly activated by AP3 and PI (Sablowski and Meyerowitz, 1998). The reason for decreased expression in sessile spikelets observed is unclear. Other orthologs including the maize ortholog GRMZM2G127379 (*ZmNAC111*), the brachypodium ortholog BRADI4G44000, and the wheat ortholog TaNAC29 function heavily in stress response, suggesting that the role of *Sobic.005G018500* cannot be predicted based on its homologs alone (Mao et al., 2015; Matzrafi et al., 2017; Xu et al., 2015).

The development (stage 6) and the maturation (stage 10) of floral organs are both heavily dependent on the expression of MADS-box genes. MADS-box genes are believed to regulate many important developmental pathways (Chen et al., 2017; Greco et al., 1997; Zhao et al., 2011). Similarly, TCP factors regulate many aspects of plant development and fertility (Aggarwal et al., 2011; Li et al., 2005; Li et al., 2012b; Zhang

et al., 2018b). Some evidence has suggested that there are molecular connections between these important developmental genes. The MADS-Box gene *SEP3* (*SbMADS22*), for example, integrates many pathways and shows enrichment in TCP binding sites with higher expression in key tissues including the panicle, early inflorescence, pistil, anther and endosperm (Kaufmann et al., 2009). Higher expression of *SbMADS22* in stage 6 and 10 sessile spikelets suggest one potentially important connection. Overall the decreased expression across so many MADS-box genes could play a crucial role in the developmental lag and may also contribute to pedicellate sterility particularly in the lodicules, stamens, and carpel.

Failures in cell cycle progression are not the cause of pedicellate spikelet sterility or the developmental lag

Despite the known roles of TCP factors, it is unlikely that they regulate sorghum pedicellate development or initiate the developmental lag by influencing cell cycle progression (Aggarwal et al., 2011; Li et al., 2005; Li et al., 2012b; Zhang et al., 2018b). One common conclusion is that class I TCP factors promote cell cycle progression while class II TCP factors repress cell proliferation. Specifically, Class I TCP factors can bind cell-cycle gene promoters (Daviere et al., 2014). The Class I TCP factors were not differentially expressed in this study and did not drive the sessile spikelets to have greater cell cycle progression. The class II TCP factors did show limited higher expression in pedicellate spikelets and greater WT expression compared to *msd1* at stage 10 which originally suggested to us that these spikelets may have less and more repression of cell cycle, respectively. This finding includes the mentioned *msd1* gene

SbTCP16. In our study, however, there were few cell cycle genes with differential expression in the WT despite these changes in TCP gene expression. In WT spikelets at stage 5 and 6 the pedicellate and sessile spikelets were both actively dividing and maturing. While the development slightly lagged in the pedicellate spikelets starting at stage 6, this lag did not appear to be driven by known cell cycle gene expression in sorghum. In support of this finding *msd1* at stage 6 also lacked differential expression in cell cycle genes but did show the developmental lag. Better future annotation of the sorghum genome may be necessary to fully understand a potential role for cell cycle genes in pedicellate sterility. While few genes were differentially expressed between WT stage 10 pedicellate and sessile spikelets, the differences between *msd1* and WT were quite extreme. We consider two possibilities for this finding. The first is that there are major genetic differences between *msd1* and WT. This is unlikely as demonstrated in recent work on *msd1* (Jiao et al., 2018b). The second may be due to the experimental method, which may have caused some variation between the WT and *msd1* plants. Spikelets in pedicellate and sessile comparisons were made using adjacent spikelet tissue, greatly minimizing the likelihood that non-relevant results would be found. In the *msd1* and WT comparison the plants themselves were completely different, which could have added some of the additional variability observed here. This idea was supported by the overlap of the differentially expressed genes in both pedicellate and sessile datasets.

3.5.4 JA signaling is strongly correlated with pedicellate spikelet sterility

Altered levels of JA biosynthesis and other JA genes identified in WT pedicellate and sessile spikelets and in the *msd1* and WT comparisons likely play an important role in pedicellate sterility. The expression changes which were typically quite large and significant were observed in key biosynthesis genes including *DAD1*, *LOX3*, *LOX4*, *AOS*, *AOC*, and *OPR3*. Later in development, most of these key genes had higher expression in the WT sessile spikelets and in the WT compared to *msd1* pedicellate spikelets. *DAD1* encodes a Phospholipase A1, which catalyzes the first step in JA biosynthesis. In *Arabidopsis* *DAD1* is active in stamen filaments and is required for filament development, pollen grain development, anther dehiscence and flower openings where *dad1* mutant anthers do not dehisce and release no pollen grains (Ishiguro et al., 2001). Next, hydroperoxy derivatives are formed via the activity of 13-lipoxygenases (13-LOXs). In *Arabidopsis* (*Columbia-0*), 4 of these 13S-LOXs are found including *LOX2*, *LOX3*, *LOX4*, and *LOX6* (Bannenberg et al., 2009). *LOX2* is more active in wound response in comparison to *LOX3* and *LOX4*, which are essential to global proliferative arrest and male fertility (Caldelari et al., 2011; Glauser et al., 2009). The double mutant *lox3 lox4* is male sterile producing an abnormal feminized floret (Caldelari et al., 2011). *LOX3* (*TS1*) increase in WT stage 10P combined with increased pedicellate *TS2* expression and no corresponding increases in the pistil protective *SK1*, may be a root cause of pedicellate female sterility (Calderon-Urrea and Dellaporta, 1999). In maize *ts1* and *ts2*, mutants fail to abort the pistils of the lower ear floret and tassel florets (Acosta et al., 2009).

Continuing in JA biosynthesis, 13S-hydroperoxy-octadecatrienoic acid (13-HPOT) is dehydrated following catalysis by AOS to form an unstable and highly reactive allene oxide (Kubigsteltig et al., 1999). The *aos* mutant in *Arabidopsis* is sterile with stamens that fail to elongate and anthers that do not dehisce (Park et al., 2002). AOS generally had lower WT sessile spikelet expression and higher expression in WT 10P versus *msd1* 10P. This allene oxide is immediately converted to the first cyclic intermediate *cis*-12-oxophytodienoic acid (OPDA) by AOC (Hamberg and Fahlstadius, 1990). The OPDA reductase OPR3 catalyses the reduction of OPDA to 3-oxo-2-(2'(Z)-pentenyl)-cyclopentane-1 octanoic acid (OPC-8:0) (Schaller et al., 2000). In the reductase mutant *opr3*, the plants are deficient in JA and are male sterile due to failure to elongate the stamen filaments, problems in anther dehiscence, and limited anthesis (Stintzi and Browse, 2000). The expression pattern of both *AOC* and *OPR3* was observed to be lower in WT 10S versus 10P expression and higher expression was present in WT10P compared to *msd* 10P. The overall pattern of increased JA biosynthesis gene expression in sterile spikelets and decreased JA biosynthesis gene expression in fertile spikelets was consistent in across the samples in our study.

Because of the large differences between JA expression in WT and *msd1* sessile spikelets early in development where spikelets are identical, it seemed unlikely that JA alone affects fertility. Additionally, the varied expression of genes involved in JA biosynthesis did not explain the uniform developmental lag between the *msd1* and WT as the *msd1* undergoes the lag even with decreased pedicellate JA production (Jiao et al., 2018b). At a similar developmental stage, arbitrarily designated stage 3 by Jiao et al., few differences were seen in JA biosynthesis gene expression (Jiao et al., 2018b).

Later in development when comparing *msd1* and WT, pedicellate spikelets the WT had higher expression of JA biosynthesis genes compared to the *msd1* mutant, consistent with the arbitrarily named stage 4 in the same Jiao et al. study (2018b). While the role of JA in fertility and in *msd1* is documented, the mechanisms by which it controls fertility and the target genes are still unclear. Past studies have demonstrated strong connections between male fertility and JA. JA biosynthesis mutants including *dad1*, *lox3*, *lox 4*, *aos*, and *opr3* all possess similar phenotypes with clear male sterility (Caldelari et al., 2011; Ishiguro et al., 2001; Park et al., 2002; Stintzi and Browse, 2000) Past biosynthesis overexpression of the JA catabolism gene *CYP94B3* and mutated JA signaling in *coi1* also display similar male sterility due to failures late in development including decreased stamen elongation and indehiscent anthers (Koo et al., 2011; Xie et al., 1998). For a review of the function of JA in fertility, see Smith and Zhao 2016. The loss of JA signaling in the *msd1* mutant was proposed to cause complete pedicellate fertility possibly due to programmed cell death (Jiao et al., 2018b). Exogenous application of JA reversed the mutant phenotype and sterile pedicellate spikelets were once again observed (Jiao et al., 2018b). Limited information supports this JA-mediated PCD process. The expression of *TS1* and JA production is associated with pistil cell death in maize tassels during the normal formation of the tassel spikelets (Acosta et al., 2009). What the testing of this hypothesis failed to explain and what is not supported by the literature was the male sterility observed with higher JA biosynthesis in WT pedicellate spikelets. Further, previous studies have failed to explain the cause for the clear developmental lag in WT and *msd1*. More work on JA needs to be done to

determine why pedicellate spikelets have increased JA production later in development and how broadly this impacts fertility.

3.5.5 No clear connection is detected between the TCP factors and other phytohormones

TB1 expression is associated with repressed axillary growth, similar to the classical role of auxin in apical dominance. Auxin plays a pivotal role in driving cell elongation, cell division, growth and development of many plant organs. During the cessation of growth in WT pedicellate spikelets, decreases in auxin biosynthesis and downstream genes were hypothesized to occur, either as a driving force or an effect of the reduced observed growth. Further study would be needed to better elucidate the role of auxin in fertility. Both Aux/IAA (indole-3-acetic acid) and Auxin Response Factors (ARFs) regulate auxin responsive genes. These gene families in sorghum have been recently compiled (Wang et al., 2010). Auxin interacts with the phytohormone strigolactone (SL) and reduces the axillary growth promoting cytokinin to regulate bud dormancy (Bennett et al., 2006; Shimizu-Sato et al., 2009). *TB1* is activated and likely functions downstream of SL and is repressed by CK and GA (Dun et al., 2012; Moreno-Pachon et al., 2018). Study of strigolactones and identification of key genes in sorghum may provide future insight into these interactions. Overall, the minimal differential IAA expression observed indicated that any altered IAA expression was likely a product rather than a cause of sterility.

TB1 and lateral growth share important connections to the gibberellic acid (GA) pathway. Gibberellic acid is an essential phytohormone regulating aspects of plant

development including seed germination, stem elongation, leaf expansion, flower development (particularly anther and pollen development), and embryo development. Several sorghum genes have been identified that function in GA biosynthesis, signaling, and regulation (Gao et al., 2012; Ordonio et al., 2014). In our study decreased GA receptor *GID1* (*GA INSENSITIVE DWARF1*) expression may have led to less GA sensitivity; however, there were not any direct effects easily observed in the sessile tissues as they maintained fertility. It is possible that sufficient GA is still being bound by *GID1* despite decreased expression. Production of bioactive GAs negatively regulates *TB1*, playing a direct role in tillering and the overexpression of GA2oxs results in increased tillers and adventitious growth (Lo et al., 2008). Additionally, TCPs cannot bind to cell cycle gene promoters when blocked by DELLA proteins (Daviere et al., 2014). As demonstrated, GA gene expression had few significant differences in levels between study lines and between spikelet types, and these changes in expression were not consistent in terms of the known GA biosynthesis pathway, signaling mechanisms, and repression. While these genes may play a role in fertility, it is unlikely that they are the driving force of pedicellate sterility. *TB1* expression is higher in sorghum sessile spikelets but no corresponding decreases in GA biosynthesis genes (or increase in GA2ox inactivation genes) are consistently present in the current study (Fig. 3.8 and Table S3.5).

Brassinosteroids (BR) do not control the developmental lag or fertility in pedicellate spikelets. Brassinosteroids are often associated with the transition to flowering where proper BR biosynthesis and sensitivity are required for proper and timely transitions. In double mutants with mutations in *BRASSINOSTEROID-*

INSENSITIVE 1 (BRI1) and known flower-timing genes, elevated expression of the flowering repressor *FLOWERING LOCUS C (FLC)* was observed (Domagalska et al., 2007). It is known that TCP1 in *Arabidopsis* positively regulates BR biosynthesis by binding to the promoter and enhancing the transcription of the biosynthesis rate limiting gene *DWARF4 (DWF4)*. Further, plants similarly display a dwarfed BR-deficient mutant phenotype with overexpression of the dominant-negative mutant *TCP1-SRDX* in the WT background (Gao et al., 2015; Guo et al., 2010). Few interactions between BR and TCP factors have been described and no connection between BR and sterility or BR and the differentially expressed TCPs was found.

3.5.6 The proposed pathway for controlling pedicellate spikelet sterility

Sorghum contains both perfect sessile spikelets and sterile pedicellate spikelets. The developmental lag of the pedicellate spikelet begins at stage 6 and continues and intensifies, leading to degeneration of stamens and gynoecium in the inner whorls. Over floral development key *TCP* genes are differentially expressed including higher *SbTCP2 (SbTB1)* expression in sessile spikelets. We propose that *SbTB1* regulates a cascade of developmental events similar to its role in maize and *Arabidopsis* as a master signal integrator. One possibility is that *SbTB1* works as described in maize by interacting with *TEOSINTE GLUME ARCHITECTURE1* which represses key meristem and flower identity genes (Studer et al., 2017). Altered MADS-box genes might restrain the morphogenesis of stamens and gynoecium by affecting hormone production and signaling like the role of *AGAMOUS* in JA biosynthesis (Ito et al., 2007). The main future direction is to determine the function of *SbTB1* in sorghum spikelet development.

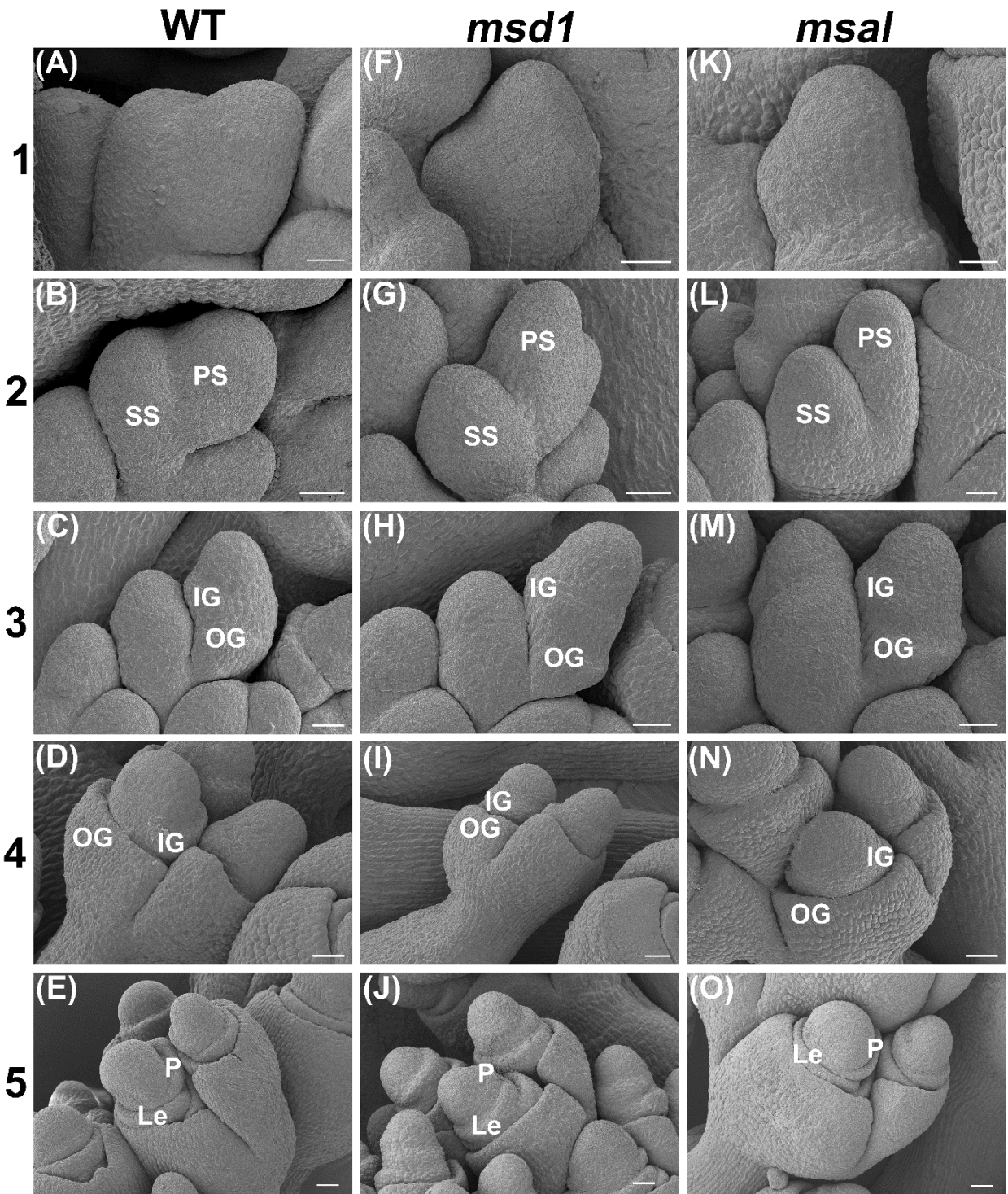


Figure 3.1. Early sorghum floral developmental stages 1-5 prior to the developmental lag of the pedicellate spikelet. (A-E) WT development, (F-J) *msd1* development, and (K-O) *msa1* development. Development for both sessile spikelets (SS) and pedicellate spikelets (PS) shown. Abbreviations: IG- Inner Glume, Le- Lemma, OG- Outer Glume, and P- Palea. Scale bars: 25 μ m.

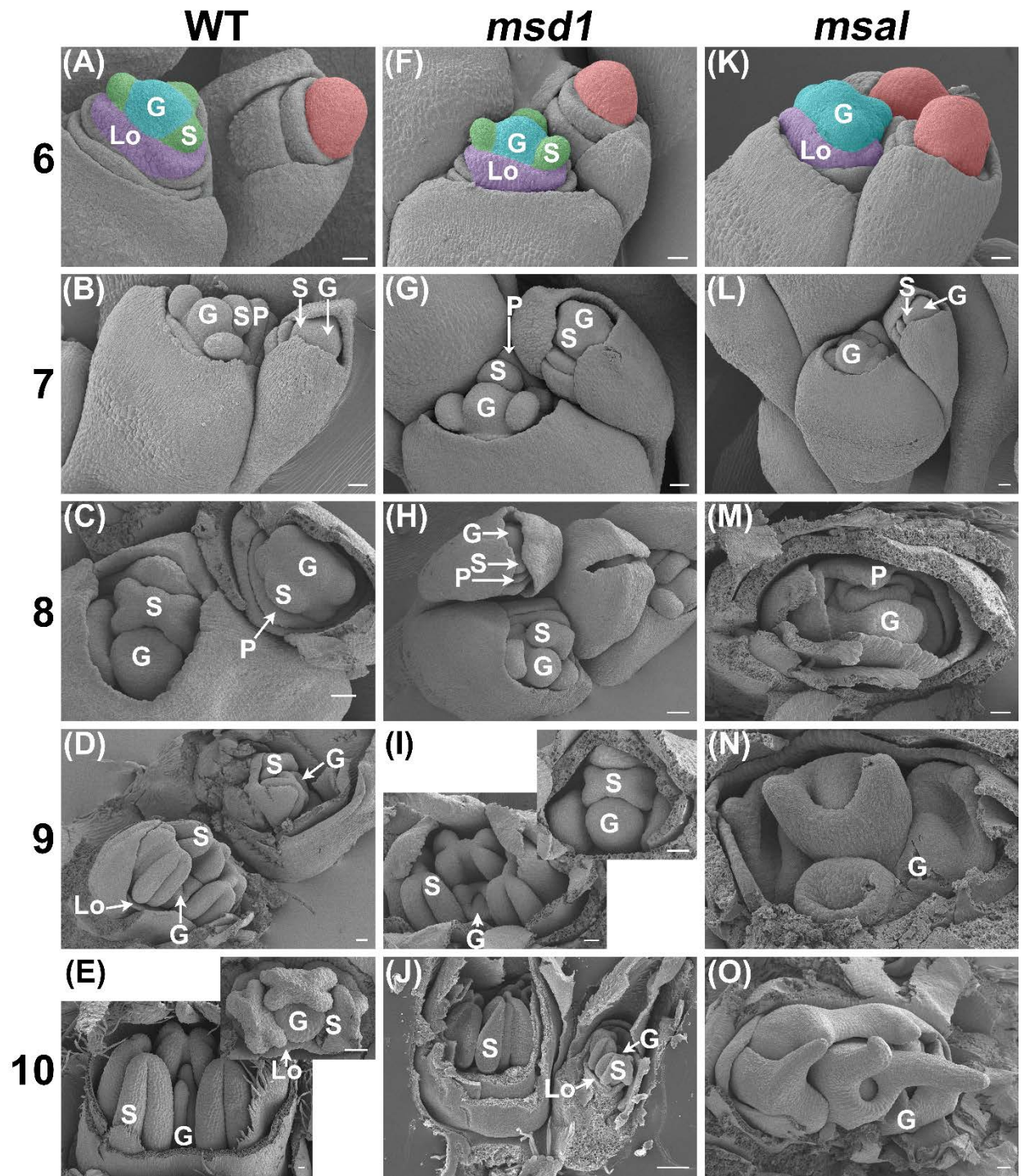


Figure 3.2. Middle sorghum floral developmental stages 6-10 and the onset of the developmental lag of the pedicellate spikelet. (A-E) WT development, (F-J) *msd1* development, and (K-O) *msal* development. Development for all sessile spikelets and all pedicellate except *msal* from stages 8-10. (A-C) Stage 6 spikelets are pseudocolored to highlight the onset of the developmental lag in all pedicellate spikelets (blue- gynoecium, green- stamens, pink- floral dome, and purple- lodicules). Abbreviations: G- Gynoecium, Lo- Lodicule, P- Palea, S- Stamen. Scale bars: 25 μ m.

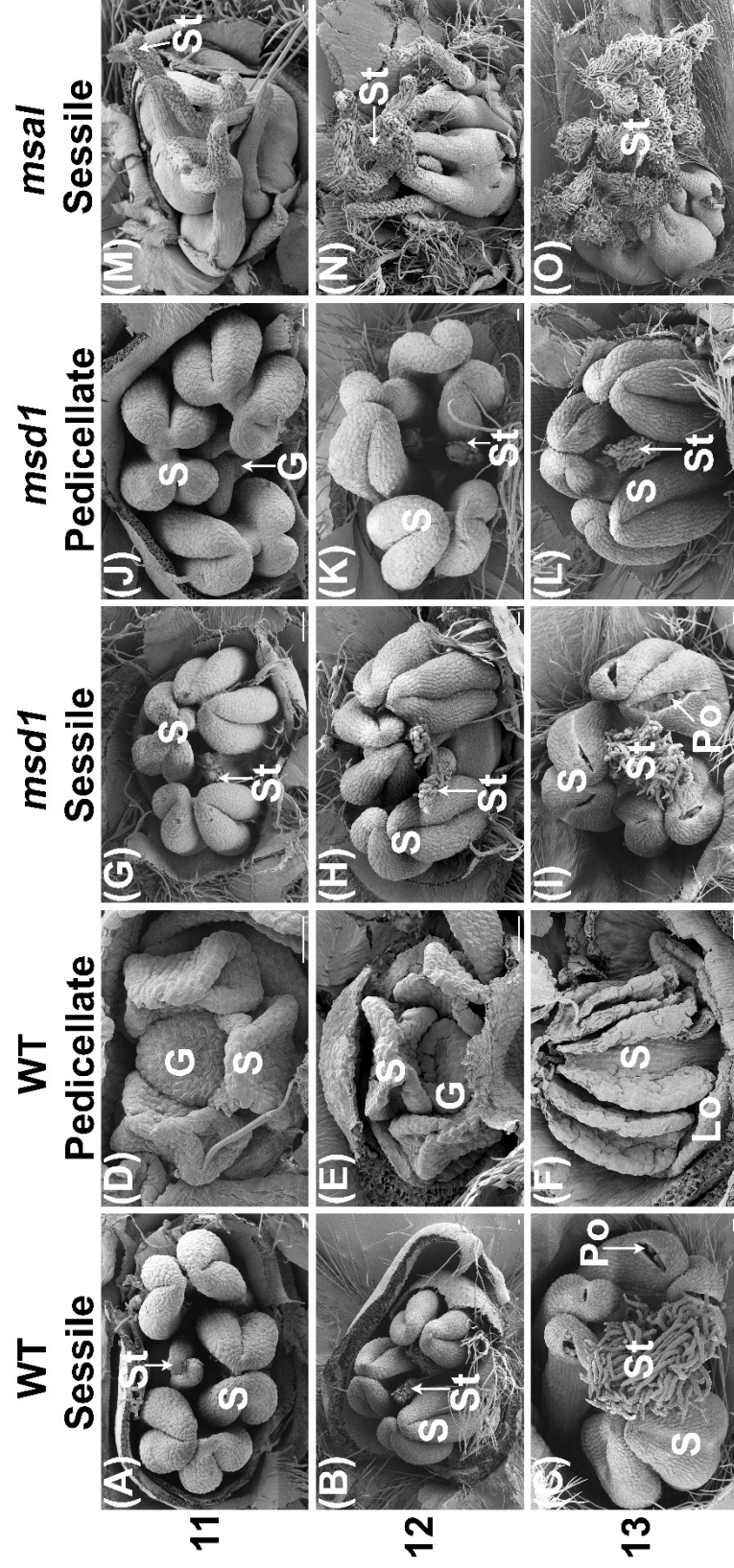


Figure 3.3. Late sorghum floral developmental stages 11-13 and degeneration of the pedicellate spikelet.

(A-C) WT sessile spikelet development, (D-F) WT pedicellate spikelet development, (G-I) *msd1* sessile spikelet development, (J-L) *msd1* pedicellate spikelet development, and (M-O) *msal* sessile spikelet development.

Abbreviations: G- Gynoecium, Lo- Lodicule, Po- Pollen, S- stamen, and St- Stigmas. Scale bars: 25 μm.

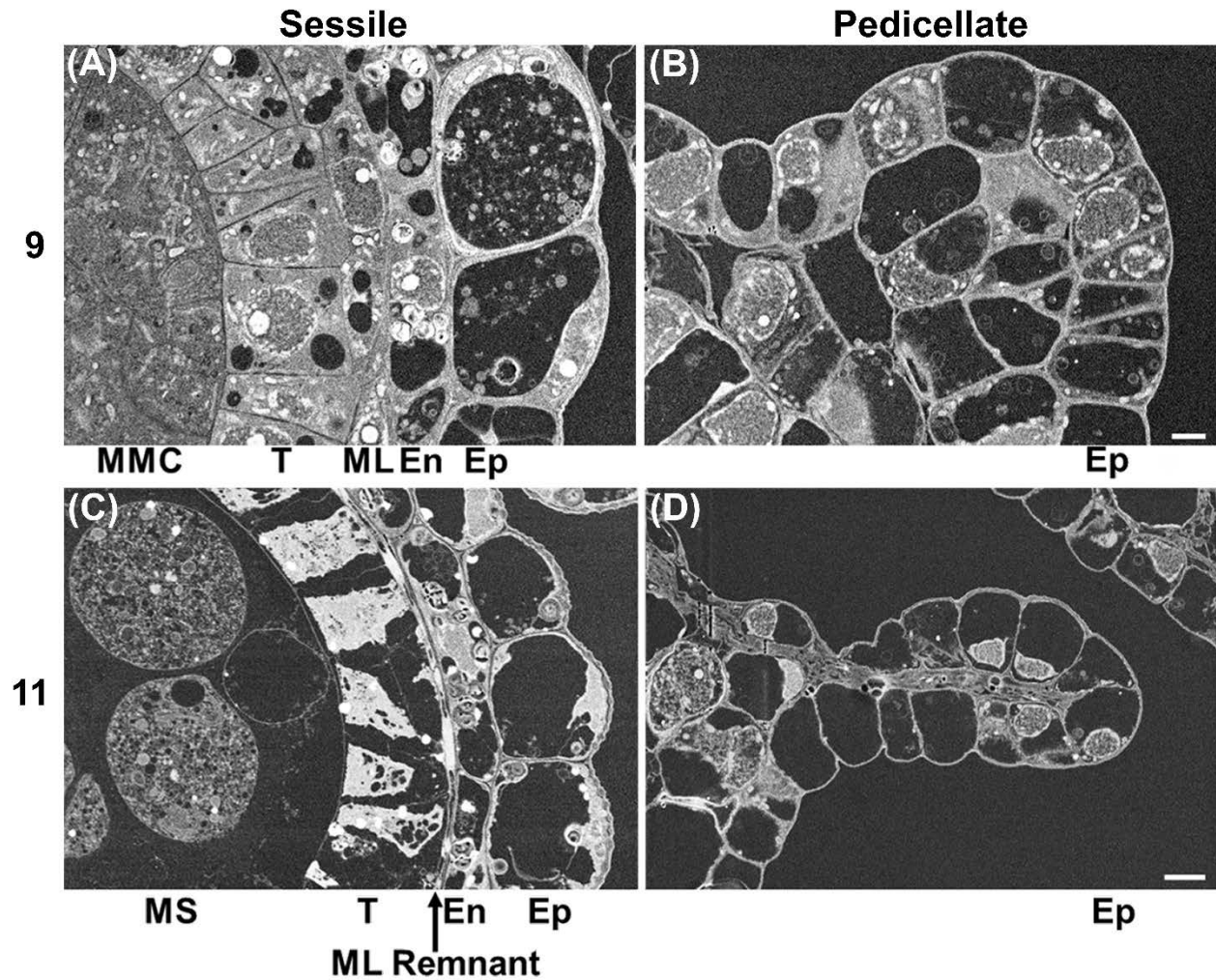


Figure 3.4. SEM micrographs of anther sections from spikelet pairs at stage 9 and 11. (A, B) WT anther lobes from stage 9 spikelet pair. (A) Sessile anther lobe displaying normal anther wall and pollen mother cells. (B) Pedicellate anther with only the outer epidermal cells formed. (C, D) WT anther lobes from stage 11 spikelet pair. (C) Anther development in WT sessile with normal degeneration of middle layer and development of microspores. (D) Pedicellate spikelet anther with only epidermal cells and degenerated lobe contents. Abbreviations: En- Endothecium, Ep- Epidermis, ML- Middle Layer, MS- Microspores, PMC- Pollen Mother Cells and T- Tapetum. Scale bars: 5 μm (A/B) and 10 μm (C/D).

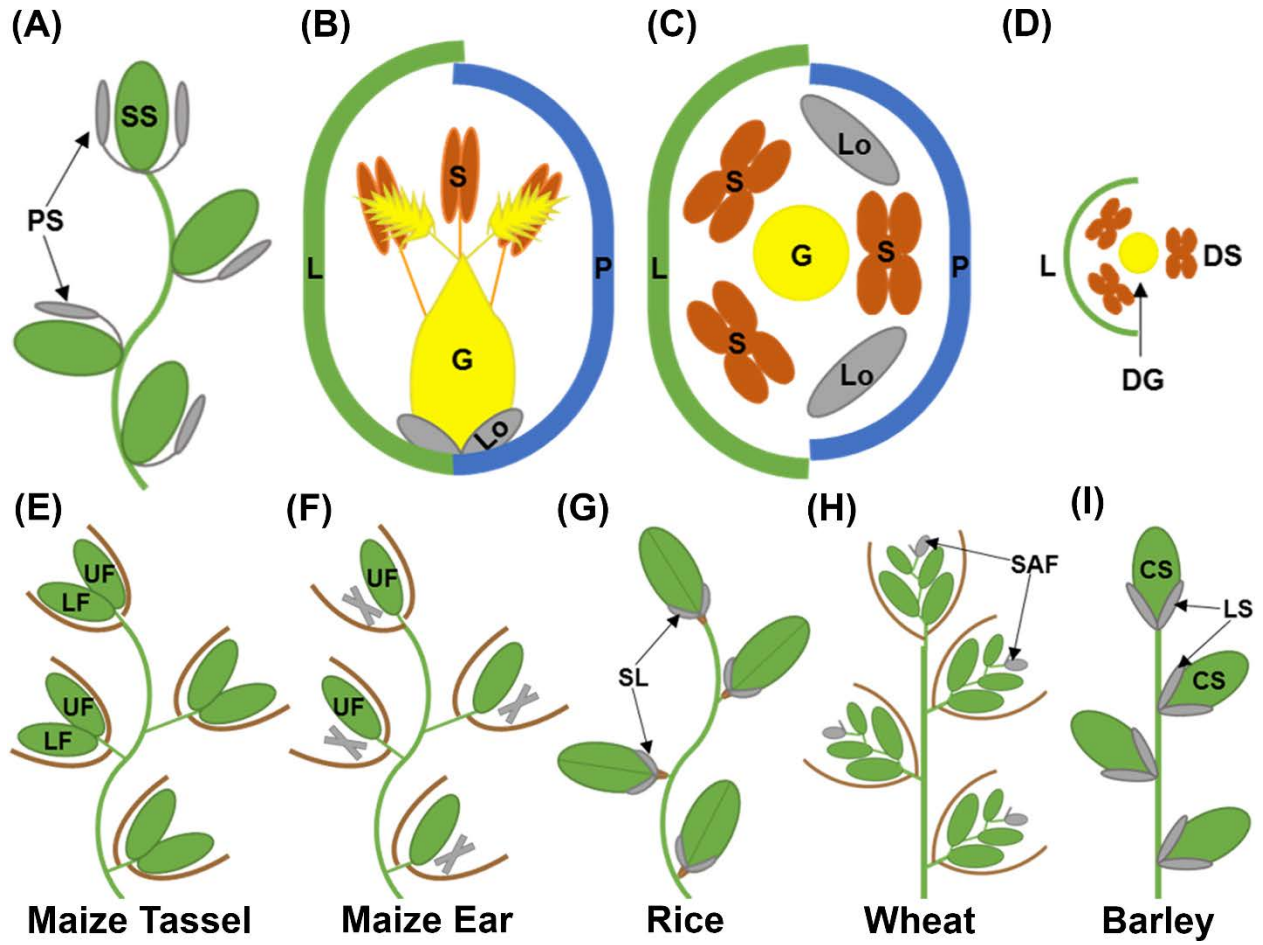


Figure 3.5. *Sorghum bicolor* spikelet structure and floral comparisons to other cereal grains. (A-D) *Sorghum* spikelets and spikelets with glumes removed (B-D). (A) Positioning of sessile spikelets (SS) and pedicellate spikelets (PS) on the flowering branch. (B) Longitudinal section diagram depicting the sessile spikelet containing the lemma (L), lodicules (Lo), palea (P), stamens (S) and central gynoecium (G). (C) Cross section floral diagram of sessile spikelets with the same floral organs identified. (D) Cross section diagram of degenerating pedicellate spikelets with a lemma-like organ remaining (L), degenerating gynoecium (DG), and degenerating stamen (DS). (E) Maize tassel spikelets branch with upper florets (UF) and lower florets (LF). (F) Maize ear spikelets branch with upper florets (UF) and degenerated lower florets absent. (G) Rice spikelets branch with sterile lemmas (SL). (H) Wheat spikelets on rachis with sterile apical florets indicated (SAF). (I) Front view of barley spikelets on rachis from wild 2-rowed barley with central fertile spikelets (CS) surrounded by sterile lateral spikelets (LS). Glumes surrounding multiple spikelets or at floral base indicated with brown. All sterile florets, spikelets, and other structures indicated with gray.

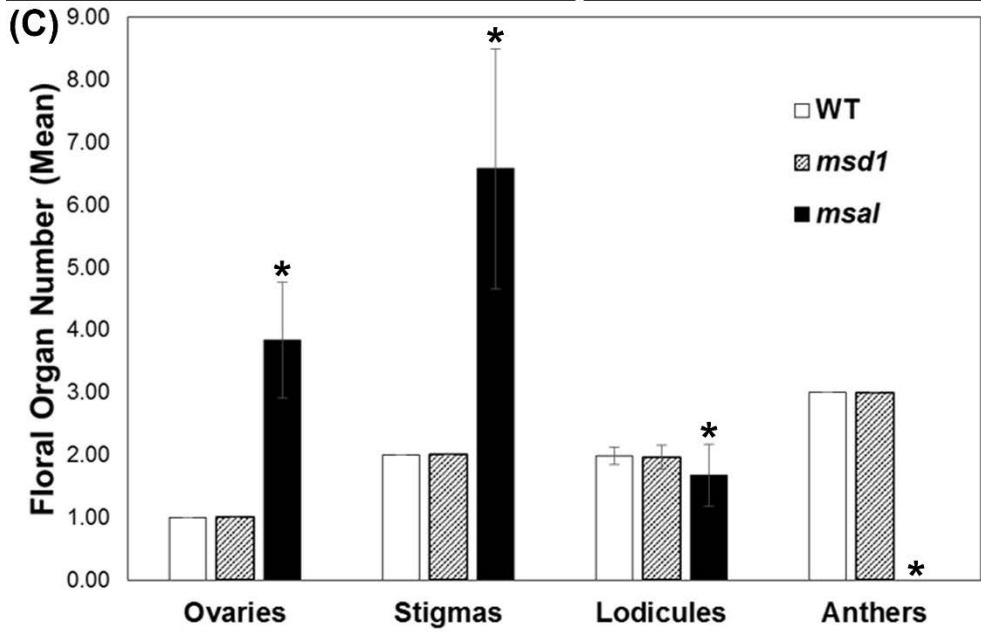
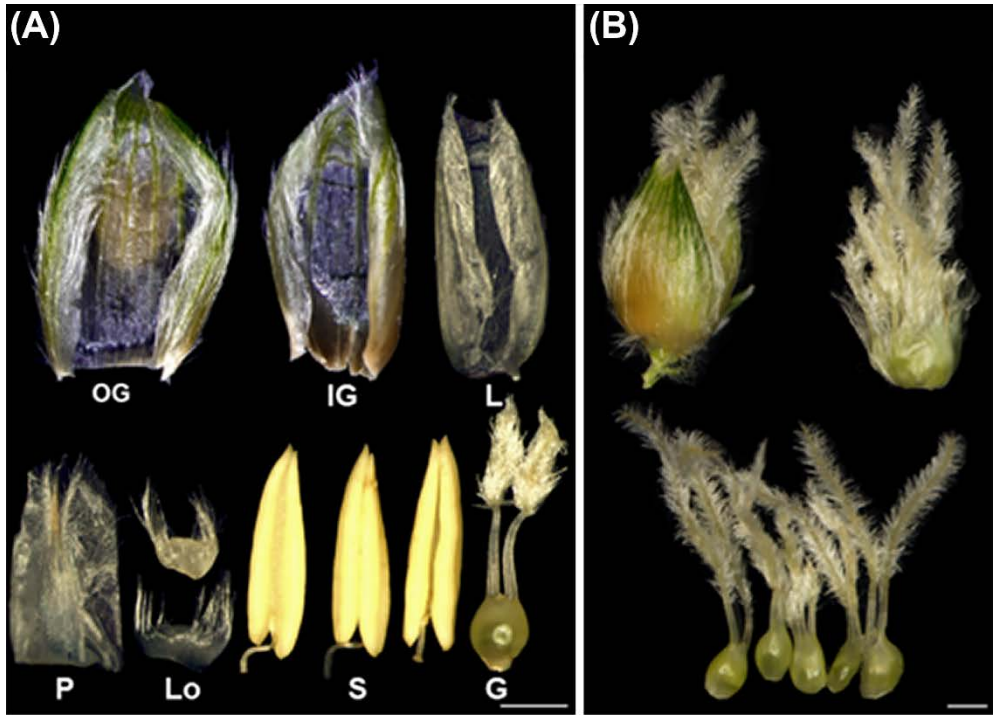


Figure 3.6. Comparisons between WT and *msal* floral organs. (A) Sorghum sessile spikelet floral organs and glumes. (B) *msal* floral structure with increased carpel number. (C) *msal* has altered number of ovaries ($F_{2,197} = 476.07$, $p < 0.0001$), stigmas ($F_{2,197} = 531.5331$, $p < 0.0001$), lodicules ($F_{2,197} = 16.4471$, $p < 0.0001$), and anthers (no variance, $p < 0.0001$) as demonstrated in one-way ANOVA and indicated by asterisk. All WT and *msd1* spikelets contained a single ovary, pair of stigmas and lodicules, and three anthers. Abbreviations: G- Gynoecium, IG- Inner Glume, L- Lemma, Lo- Lodicule, OG- Outer Glume, P-Palea, and S- Stamen. Significant values indicated with an asterisk. Scale bars 1.0 mm.

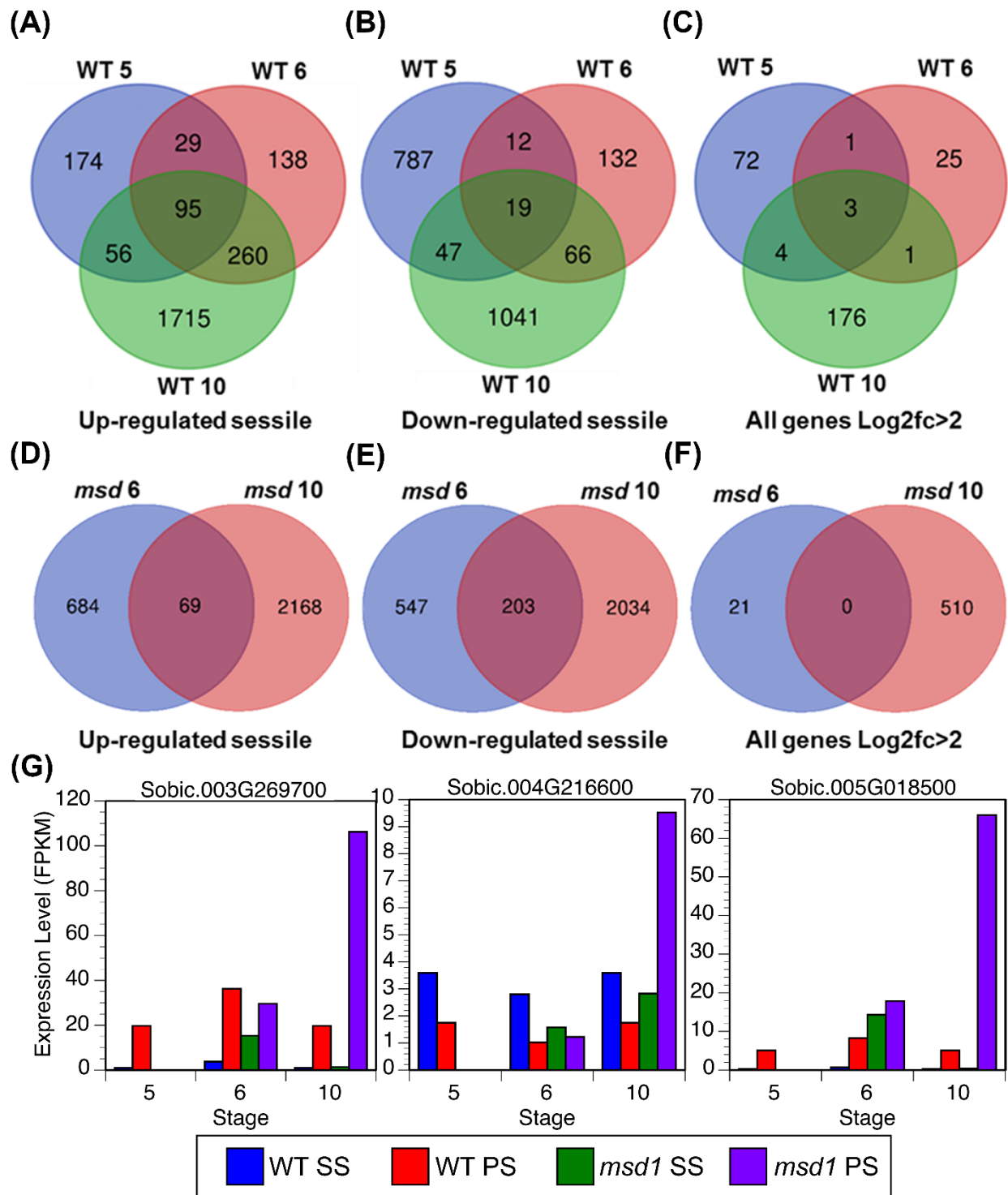


Figure 3.7. Differentially expressed transcripts across WT and *msd1* sessile and pedicellate spikelets. (A-C) Altered WT gene expression with significantly lower sessile expression (A), higher sessile expression (B) and log₂fold changes greater than 2 (C). (D-F) Altered *msd1* gene expression with significantly lower sessile expression (D), higher sessile expression (E) and log₂fold changes greater than 2 (F). (G) Expression levels of the three overlapping WT genes with highest log₂fc values over the course of the study.

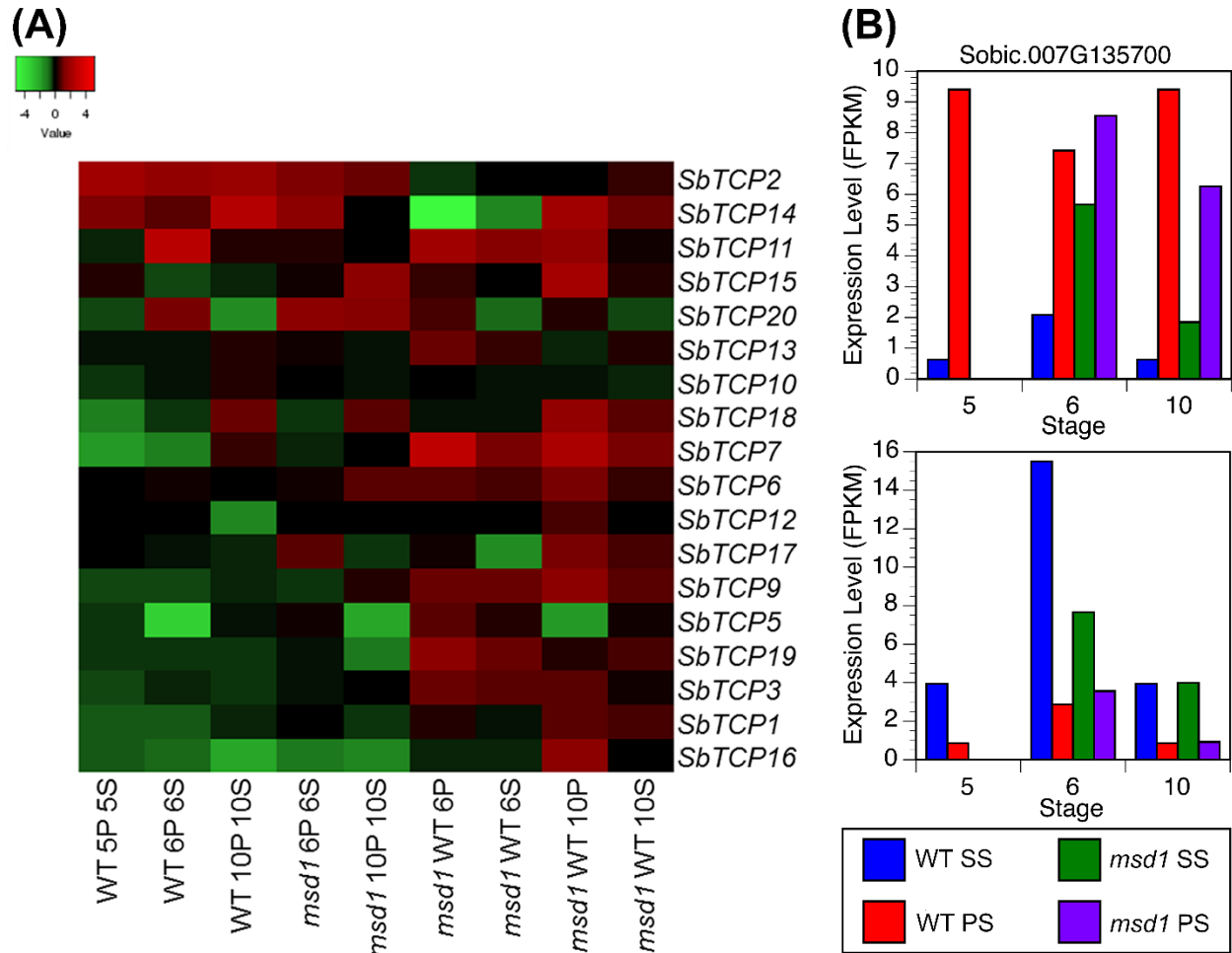


Figure 3.8. Key *SbTCP* transcription factor genes are differentially expressed. (A)

Heat map of *SbTCP* gene expression with log₂ fold change values of sessile spikelet gene expression (compared to pedicellate) and WT spikelet gene expression

(compared to *msd1*) shown (*SbTCP4* omitted as it was not detected). (B)

Sobic.007G135700 (*MSD1/SbTCP16*) and Sobic.001G121600 (*SbTB1/SbTCP2*)

Fragments Per Kilobase of transcript per Million mapped reads (FPKM) values over the course of the study in WT and *msd1*.

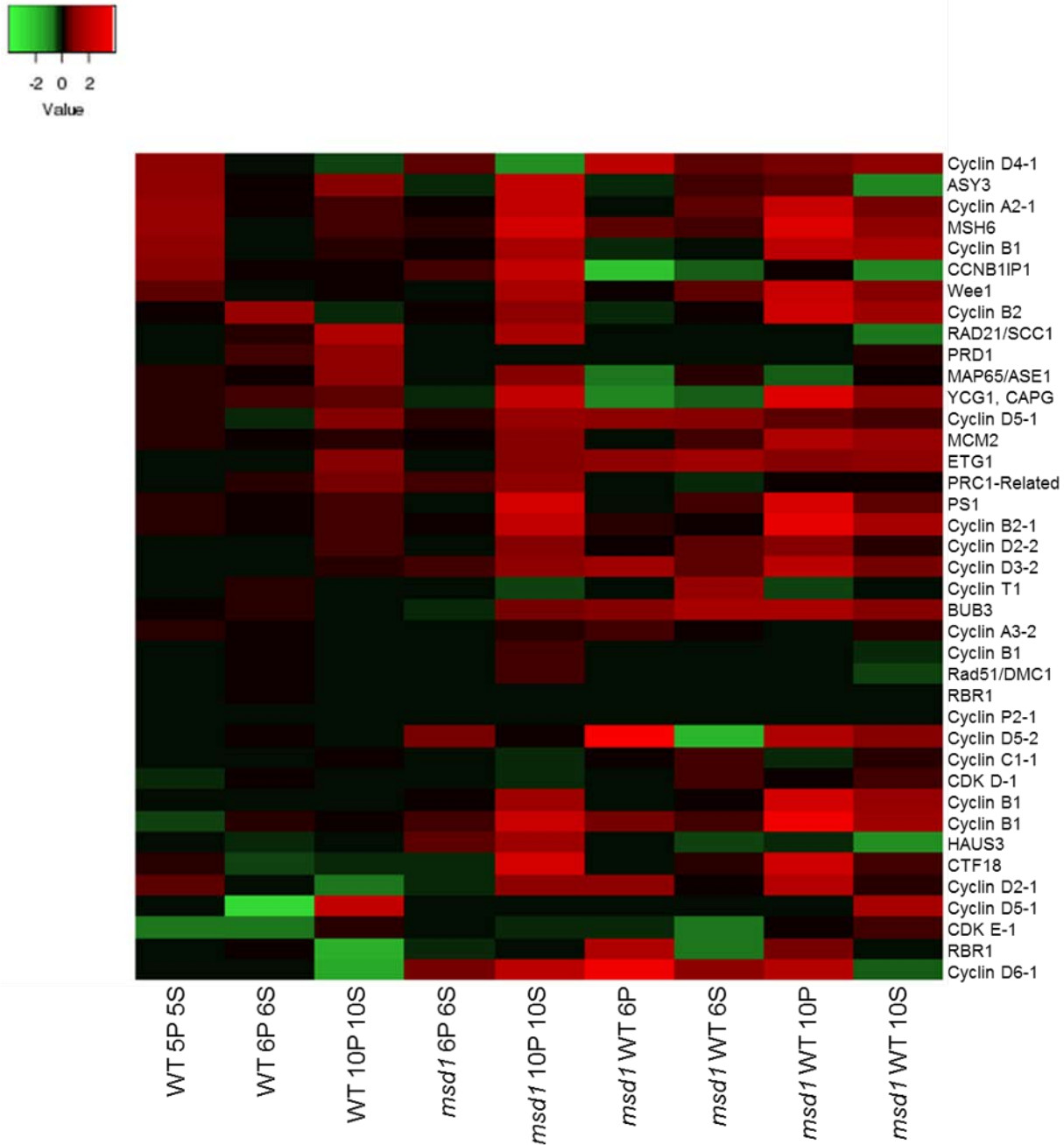


Figure 3.9. Differentially expressed cell cycle genes. Few differentially expressed cell cycle genes were detected and likely differential expression of cell cycle genes does not establish or maintain the developmental lag. Heat map shows log₂ fold changes of sessile spikelet gene expression (compared to pedicellate) and WT spikelet gene expression (compared to *msd1*).

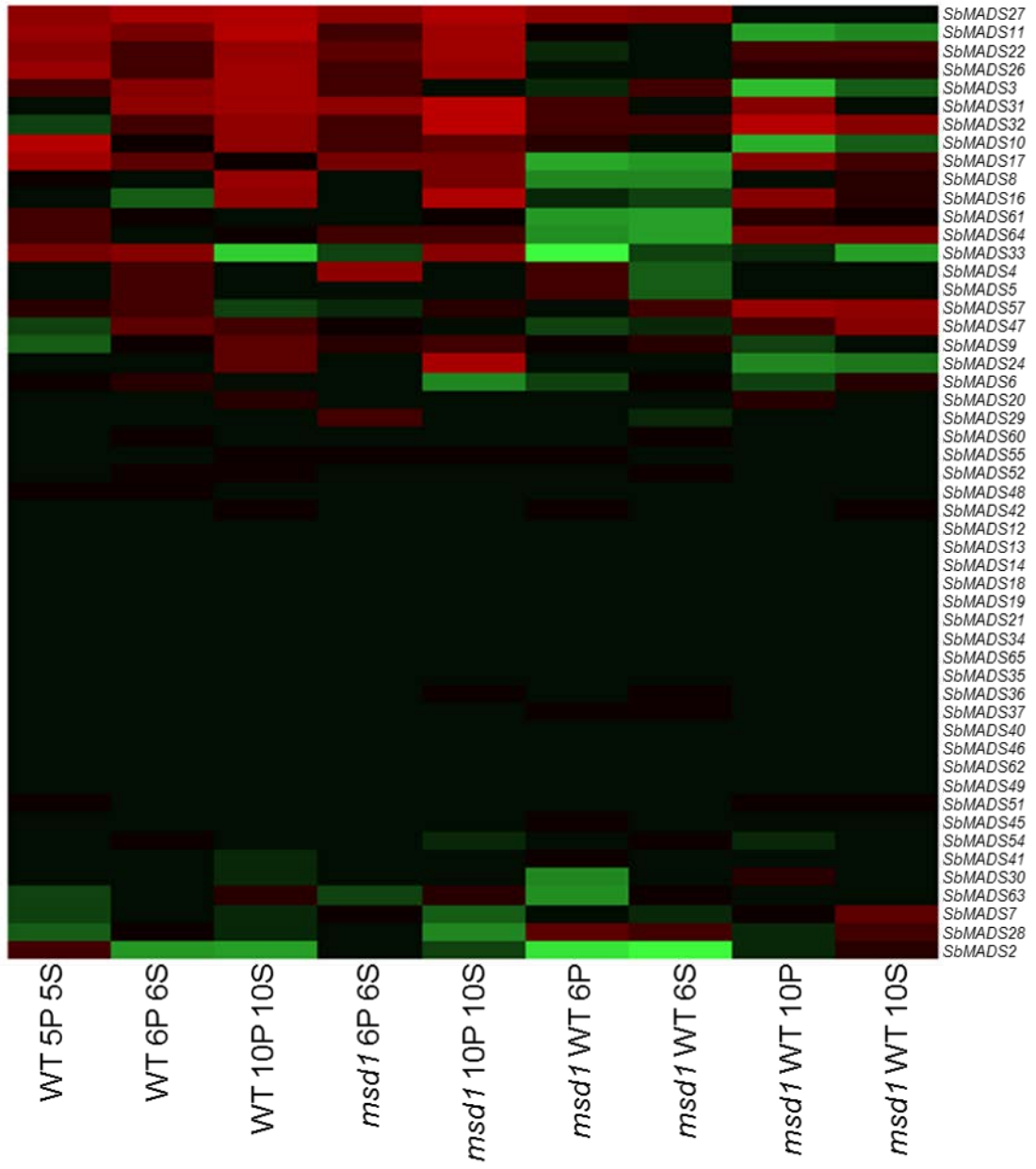
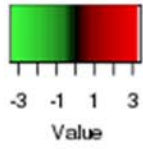


Figure 3.10. Differentially expressed MADS-box genes. ABCDE-class MADS-box genes are differentially expressed while other MADS-box genes are not. Heat map indicates log₂ fold changes in sessile spikelet gene expression (compared to pedicellate) and WT spikelet gene expression (compared to *msd1*).

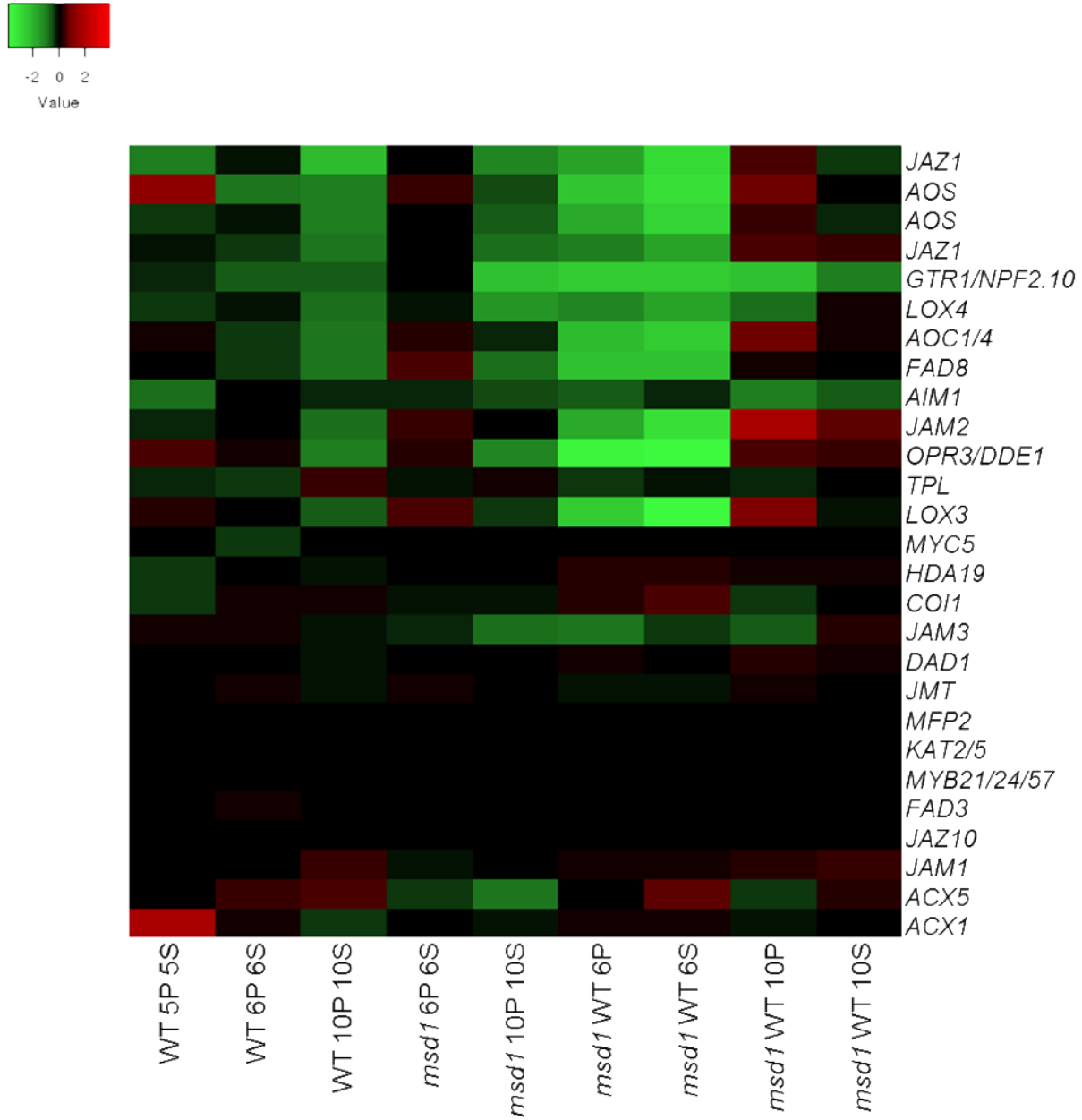


Figure 3.11. Differentially expressed genes involved in jasmonic acid, biosynthesis, response, signaling, and transport genes. Down-regulation of genes expression particularly those involved in jasmonic acid biosynthesis is found in fertile spikelets. Heat map demonstrates log₂ fold changes of sessile spikelet gene expression (compared to pedicellate) and WT spikelet gene expression (compared to *msd1*).

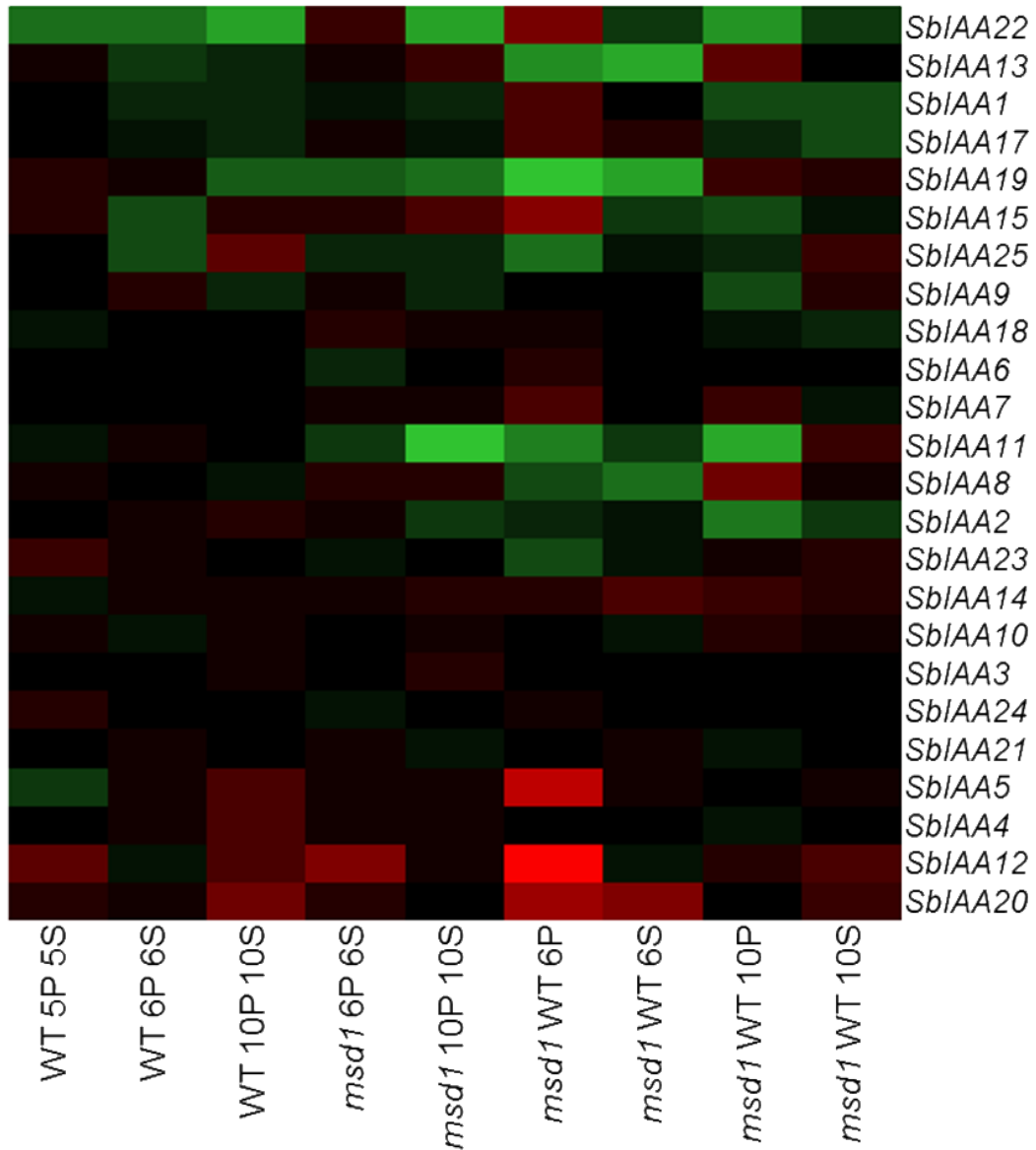
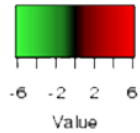


Figure 3.12. Differentially expressed *SbIAA* genes. Few genes have differential expression of IAA genes. Heat map indicates log₂ fold changes of sessile spikelet gene expression (compared to pedicellate) and WT spikelet gene expression (compared to *msd1*).

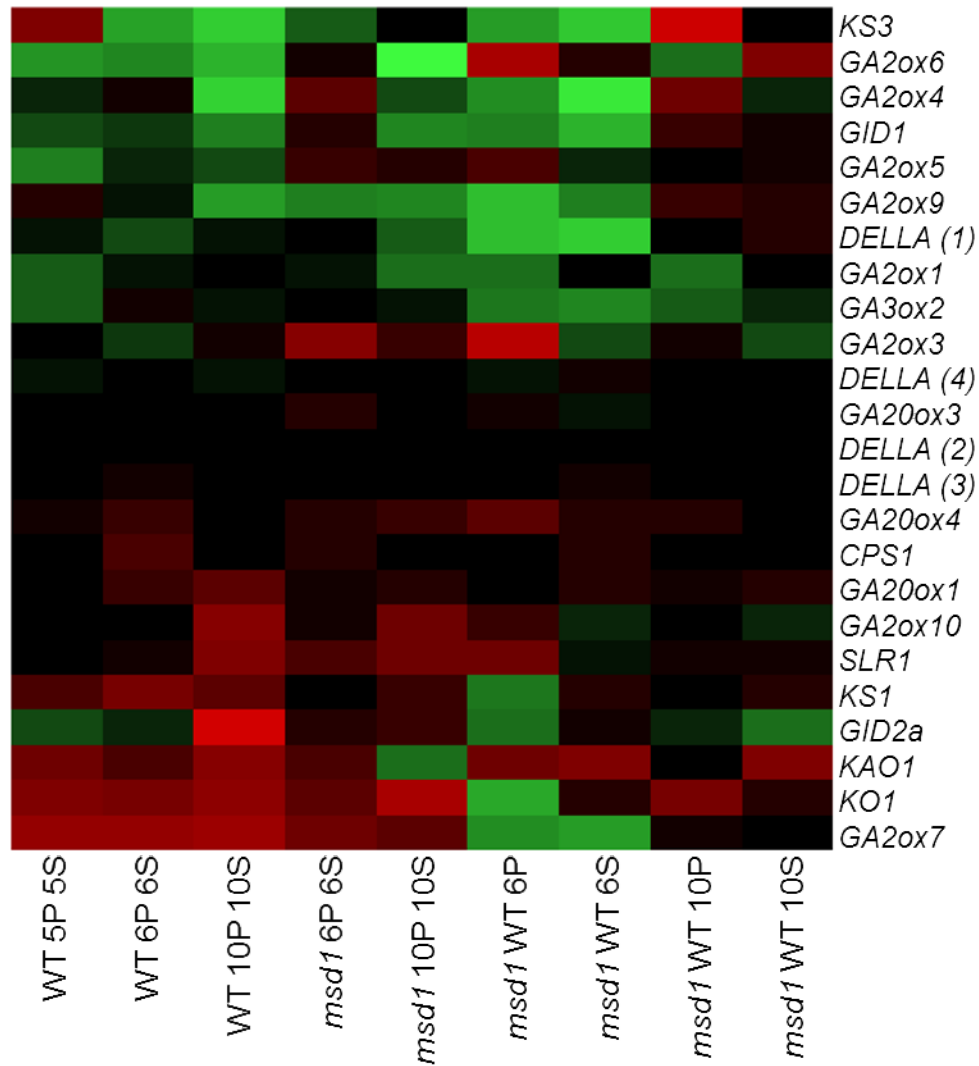


Figure 3.13. Differentially expressed genes involved in gibberellic acid

biosynthesis, inactivation, regulation and signal transduction. No consistent

patterns in genes associated with GA are detected. Heat map values are log₂ fold

changes of sessile spikelet gene expression (compared to pedicellate) and WT spikelet

gene expression (compared to *msd1*).

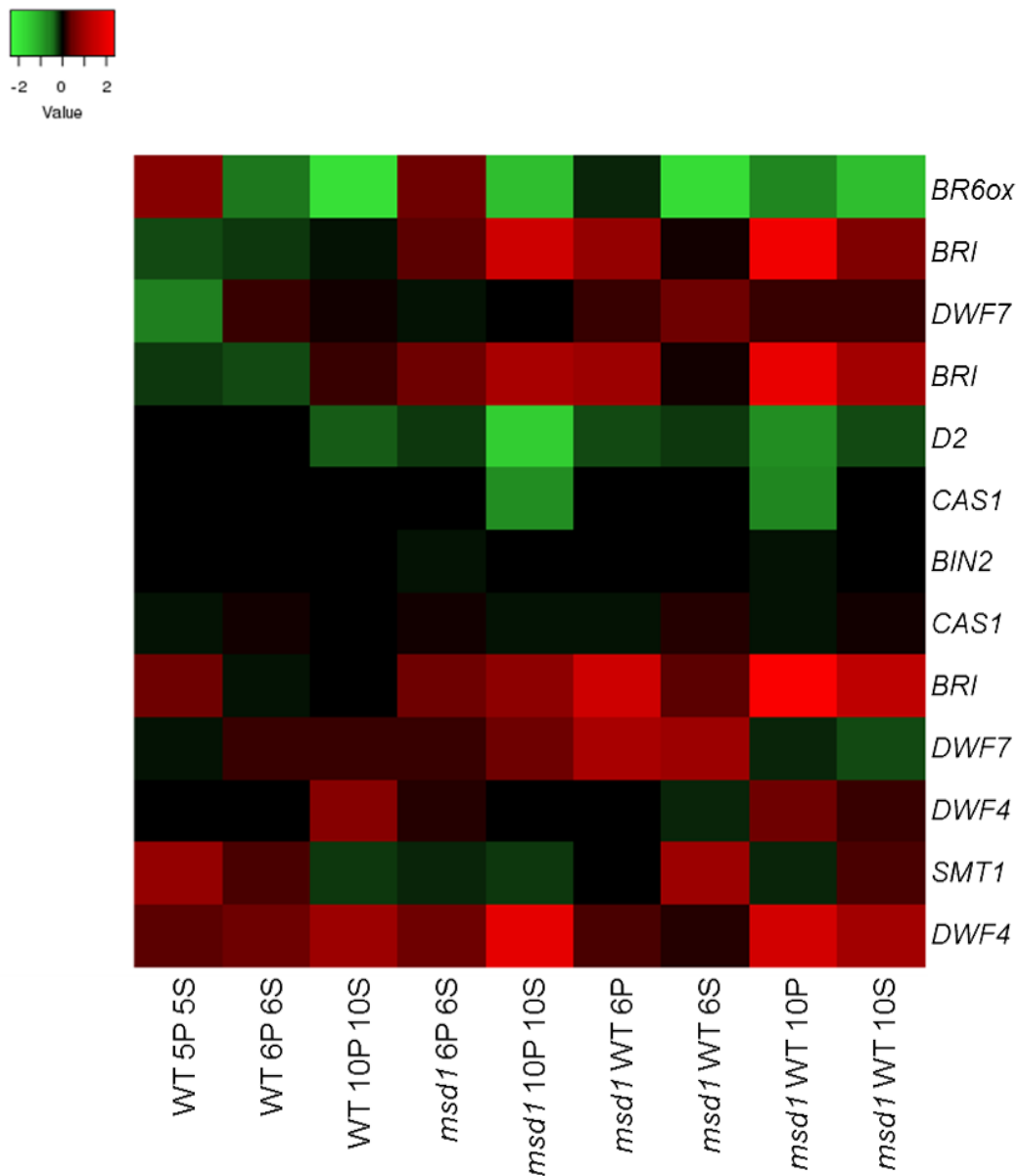


Figure 3.14. Differentially expressed genes involved in brassinosteroid biosynthesis, perception, and negative signal response. No consistent patterns in genes associated with brassinosteroid are detected. Values on heat map are log2 fold changes of sessile spikelet gene expression (compared to pedicellate) and WT spikelet gene expression (compared to *msd1*).

Table 3.1. Classification of floral developmental stages in *Sorghum bicolor*

Stage	Major Developmental Milestones
1	Spikelet primordia are visible, but the sessile and pedicellate spikelet primordia are not distinguishable from each other.
2	Sessile and pedicellate spikelets primordia become distinct due to the formation of the pedicel. No additional floral whorls initiate.
3	Outer and inner glume primordia arise, pedicels elongate in the spikelet.
4	Developing glumes grow close to the base of the floral primordia.
5	The lemma and palea originate on the sessile and pedicellate spikelets.
6	In the sessile spikelet the lodicule primordia form, three stamen primordia are visible, and the developing gynoecium domes. In the pedicellate spikelet the outer glume begins to enclose the inner floral whorls. In <i>msa1</i> no stamen primordia form and a varied number of carpel primordia develop.
7	Reproductive primordia enlarge on the sessile spikelet and first form on the pedicellate spikelet. In the sessile spikelet the palea forms a distinctive peak behind the adaxial anther. The glumes nearly enclose the pedicellate spikelet.
8	On the sessile spikelet the developing carpels flatten and the adaxial anther begins to lobe. The pedicellate spikelet reproductive primordia enlarge and the curling of the glumes over the reproductive primordia is nearly complete.
9	On the sessile spikelet the central developing carpel invaginates, the styles form, and the anthers fully lobe and elongate. On the pedicellate spikelet the adaxial anthers begin to lobe and the carpel flattens.
10	The sessile spikelet styles and anthers elongate. The pedicellate spikelet has little invagination of the developing carpel with no visible growth.
11	The sessile spikelet stigmas form hairs and the anthers elongate. The pedicellate spikelet fails to develop and begins degeneration.
12	The sessile spikelet stigmas reach the top of the anthers and the ovary enlarges. The pedicellate spikelet fails to develop and degenerates.
13	In sessile and <i>msd1</i> spikelets the stigmas and anthers emerge and the anthers dehisce as the lodicules enlarge. In pedicellate WT and <i>msa1</i> spikelets only the bract organs and a single lemma/palea like organ remain at maturity

Table S3.1. Analysis of *SbTCP* gene expression in WT (stages 5, 6, 10) and *msd1* mutant (stages 6, 10). Genes with significantly higher expression are indicated with red and genes with significant lower expression are indicated with green. All values are log2 fold changes where - indicates no data was obtained.

Name	Gene Name	Class	WT			<i>msd1</i>			<i>msd1</i>		
			5P 5S	6P 6S	10P 10S	6P 6S	10P 10S	6P 6S	10P 10S	6P 6S	10P 10S
<i>SbTCP1</i>	Sobic.001G066100 II		-0.748	-0.692	-0.368	0.335	-0.502	0.307	-0.102	0.738	0.601
<i>SbTCP2</i>	Sobic.001G121600 II		1.968	1.698	1.718	1.170	0.956	-0.436	0.038	-0.002	0.374
<i>SbTCP3</i>	Sobic.002G035500 II		-0.580	-0.346	-0.370	0.129	-0.018	0.951	0.747	0.719	0.216
<i>SbTCP4</i>	Sobic.002G141450 II		-	-	-	-	-	-	-	-	-
<i>SbTCP5</i>	Sobic.002G198400 II		-0.425	-3.392	-0.217	0.215	-2.062	0.666	0.330	-1.715	0.151
<i>SbTCP6</i>	Sobic.002G268600 I		-0.073	0.143	0.000	0.119	0.666	0.807	0.537	1.036	0.390
<i>SbTCP7</i>	Sobic.003G018700 II		-1.752	-1.112	0.487	0.000	0.019	2.778	1.056	2.146	1.079
<i>SbTCP8</i>	Sobic.003G299700 II		0.000	0.000	0.000	0.564	0.000	0.000	0.000	0.000	0.000
<i>SbTCP9</i>	Sobic.003G305000 II		-0.631	-0.644	-0.359	0.282	0.355	0.958	0.899	1.420	0.715
<i>SbTCP10</i>	Sobic.003G408400 I		-0.463	-0.147	0.305	-0.006	-0.100	0.010	-0.196	-0.109	-0.272
<i>SbTCP11</i>	Sobic.004G225400 I		-0.248	2.679	0.367	1.004	0.000	1.880	1.322	1.562	0.084
<i>SbTCP12</i>	Sobic.004G237300 I		0.000	0.000	-1.384	-0.263	0.000	0.000	0.000	0.635	0.000
<i>SbTCP13</i>	Sobic.004G354700 I		-0.121	-0.183	0.299	-0.387	-0.111	0.894	0.485	-0.247	0.316
<i>SbTCP14</i>	Sobic.006G025000 I		1.247	0.728	2.571	0.000	0.000	-5.096	-1.346	1.967	0.881
<i>SbTCP15</i>	Sobic.006G154000 I		0.316	-0.605	-0.364	-0.122	1.473	0.504	-0.058	2.002	0.334
<i>SbTCP16</i>	Sobic.007G135700 II		-0.696	-0.928	-2.063	-0.008	-1.277	-0.293	-0.306	1.407	-0.004
<i>SbTCP17</i>	Sobic.007G182101 I		0.000	-0.206	-0.224	-0.199	-0.430	0.163	-1.489	1.058	0.524
<i>SbTCP18</i>	Sobic.008G172200 II		-1.247	-0.372	0.830	-0.561	0.810	-0.162	-0.108	1.565	0.686
<i>SbTCP19</i>	Sobic.009G195000 II		-0.475	-0.410	-0.417	0.049	-1.007	1.472	0.883	0.273	0.559
<i>SbTCP20</i>	Sobic.010G092100 II		-0.608	1.048	-1.498	0.109	1.327	0.539	-0.881	0.352	-0.531

Table S3.2. Differentially expressed cell cycle genes in *S. bicolor* WT (stages 5, 6, 10) and *msd1* mutant (stages 6, 10). Genes with significantly higher expression are indicated with red and genes with significant lower expression are indicated with green. All values are log2fold changes. Cell Differentiation Repression (CDR), Cyclin Dependent kinase (CDK), Tyrosine Kinase (TK).

Name*	Gene Name	Group	WT	WT	WT	<i>msd1</i>	<i>msd1</i>	<i>msd1</i>	<i>msd1</i>	<i>msd1</i>	<i>msd1</i>
			5P	6P	10P	6P	10P	WT	WT	WT	WT
			5S	6S	10S	6S	10S	6P	6S	10P	10S
CDK E-1	Sobic.001G281600.1	CDK	-0.773	-0.797	0.204	-0.037	-0.206	-0.289	-0.675	0.009	0.378
RBR1	Sobic.005G138300.1	CDK	0.000	0.049	0.000	0.000	0.000	0.000	0.000	0.000	0.000
RBR1	Sobic.009G010600.3	CDK	0.000	0.144	-1.653	-0.190	0.000	1.621	-0.739	0.715	0.000
CDK D-1	Sobic.009G126600.1	CDK	-0.206	0.152	-0.001	-0.079	-0.267	-0.064	0.344	0.095	0.345
Cyclin D5-1	Sobic.001G166800.1	Cyclin	0.000	-2.853	2.158	0.000	0.000	0.000	0.000	0.000	1.467
Cyclin D5-1	Sobic.001G464800.1	Cyclin	0.288	-0.274	0.833	0.258	1.195	0.961	0.914	0.585	0.463
Cyclin D3-2	Sobic.002G144800.1	Cyclin	-0.125	-0.097	0.279	0.383	1.043	1.368	0.550	1.992	0.776
Cyclin D2-1	Sobic.002G190700.2	Cyclin	0.488	-0.095	-0.671	-0.233	1.019	1.022	0.001	1.883	0.275
Cyclin D4-1	Sobic.002G230900.1	Cyclin	1.015	-0.027	-0.325	0.513	-0.986	1.947	0.597	0.680	0.960
Cyclin C1-1	Sobic.002G256200.1	Cyclin	-0.105	0.000	0.052	-0.120	-0.163	0.089	0.369	-0.160	0.259
Cyclin D6-1	Sobic.002G335900.1	Cyclin	-0.144	0.000	-1.488	0.673	2.072	3.513	1.076	1.856	-0.534
Cyclin D2-2	Sobic.002G378600.1	Cyclin	-0.071	0.000	0.455	-0.050	0.862	0.061	0.562	0.886	0.308
Cyclin B1	Sobic.003G134500.1	Cyclin	1.022	0.000	0.283	0.113	1.481	-0.298	-0.085	1.967	1.541
Cyclin B1	Sobic.003G328500.1	Cyclin	-0.005	0.000	-0.136	0.132	1.411	-0.082	0.006	2.680	1.256
Cyclin P2-1	Sobic.006G171400	Cyclin	0.000	0.000	0.000	0.000	0.000	0.000	0.000	0.000	0.000
Cyclin B2-1	Sobic.006G179200.1	Cyclin	0.225	0.060	0.321	0.154	2.164	0.177	0.022	3.338	1.473
Cyclin A2-1	Sobic.008G104000.1	Cyclin	1.180	0.081	0.373	0.011	2.187	-0.061	0.547	2.339	0.748
Cyclin A3-2	Sobic.008G143800.2	Cyclin	0.190	0.085	-0.028	-0.009	0.173	0.374	0.084	-0.022	0.234
Cyclin D5-2	Sobic.008G147500.1	Cyclin	-0.050	0.111	-0.087	0.771	0.080	3.989	-1.904	1.742	0.892
Cyclin B1	Sobic.009G087100.1	Cyclin	0.000	0.152	0.000	0.000	0.380	0.000	0.000	0.000	-0.298
Cyclin B1	Sobic.009G181500.1	Cyclin	-0.425	0.166	0.048	0.388	2.333	0.642	0.476	3.640	1.396
Cyclin T1	Sobic.010G086600.4	Cyclin	0.000	0.298	0.000	0.000	-0.370	0.000	1.137	-0.383	0.000
Cyclin B2	Sobic.010G274000.3	Cyclin	0.127	1.137	-0.225	0.089	0.987	-0.293	0.087	2.419	1.298
ASY3	Sobic.004G063300.1	Meiosis	1.024	0.008	0.912	-0.169	2.087	-0.295	0.354	0.631	-0.823
CCNB1IP1	Sobic.004G101500.1	Meiosis	0.832	0.021	0.110	0.449	2.222	-2.091	-0.545	0.057	-0.916
Rad51/DMC1	Sobic.008G010900.1	Meiosis	0.000	0.080	0.000	0.000	0.330	0.000	0.000	-0.072	-0.473
RAD21/SCC1	Sobic.009G245400.1	Meiosis	0.000	0.190	1.735	0.000	1.490	0.000	0.000	0.000	-0.645
PRD1	Sobic.010G222900.1	Meiosis	0.000	0.428	1.036	0.000	0.000	0.000	0.000	0.000	0.230
CTF18	Sobic.001G427400.2	Mitosis	0.270	-0.355	-0.191	-0.162	2.564	-0.081	0.191	2.426	0.435
HAUS3	Sobic.002G057400.1	Mitosis	0.000	-0.261	0.000	0.492	1.344	0.000	-0.386	-0.215	-1.065
MSH6	Sobic.003G041700.1	Mitosis	1.194	0.000	0.334	0.173	2.565	0.487	0.361	2.984	1.027
ETG1	Sobic.003G055600.1	Mitosis	-0.126	0.000	0.911	-0.019	0.949	1.033	1.417	0.936	0.966
PS1	Sobic.005G056800.1	Mitosis	0.187	0.023	0.471	-0.014	2.638	-0.068	0.354	2.859	0.626
MCM2	Sobic.005G110535.1	Mitosis	0.275	0.038	0.225	0.025	0.921	-0.030	0.324	1.669	1.246
MAP65/ASE1	Sobic.006G215800.1	Mitosis	0.229	0.070	1.039	-0.145	0.905	-0.778	0.213	-0.527	0.004
PRC1-Rel.	Sobic.009G132400.3	Mitosis	-0.143	0.163	0.721	0.400	1.103	-0.069	-0.274	0.137	0.044
BUB3	Sobic.010G032400.1	Mitosis	0.158	0.201	-0.102	-0.199	0.727	0.847	1.469	1.482	0.857
YCG1, CAPG	Sobic.010G105400.1	Mitosis	0.279	0.400	0.517	-0.188	2.189	-0.855	-0.538	2.880	0.928
Wee1	Sobic.004G032900.1	TK	0.485	0.000	0.021	-0.100	1.589	0.013	0.534	2.294	0.859

Table S3.3. Differentially expressed MADS-box genes in *S. bicolor* (stages 5, 6, 10) and *msd1* mutant (stages 6, 10). Genes with significantly higher expression are indicated with red and genes with significant lower expression are indicated with green. All values are log2 fold changes.

Name	Gene Name	Type	WT	WT	WT	<i>msd1</i>	<i>msd1</i>	<i>msd1</i>	<i>msd1</i>	<i>msd1</i>	<i>msd1</i>
			5P	6P	10P	6P	10P	WT	WT	WT	WT
			5S	6S	10S	6S	10S	6P	6S	10P	10S
<i>SbMADS1</i>	Sobic.001G086400.1	MIKC	0.21	0.12	-1.87	0.18	-0.63	-1.24	-1.22	-0.86	-1.06
<i>SbMADS2</i>	Sobic.001G314400.1	MIKC ^C	0.27	-0.96	-1.15	0.01	-0.25	-2.67	-3.33	-0.22	0.25
<i>SbMADS3</i>	Sobic.001G455900.1	MIKC ^C	0.25	0.82	1.18	0.36	0.02	-0.20	0.40	-1.66	-0.48
<i>SbMADS4</i>	Sobic.001G478400.1	MIKC ^C	0.00	0.43	0.00	0.87	0.00	0.31	-0.53	0.00	0.00
<i>SbMADS5</i>	Sobic.001G478400.1	MIKC ^C	0.00	0.43	0.00	0.00	0.00	0.31	-0.53	0.00	0.00
<i>SbMADS6</i>	Sobic.001G526800.1	MIKC ^C	0.06	0.21	-0.01	0.04	-0.68	-0.34	0.15	-0.44	0.20
<i>SbMADS7</i>	Sobic.002G010100.1	MIKC ^C	-0.26	0.03	-0.21	0.08	-0.51	-0.14	-0.17	0.07	0.47
<i>SbMADS8</i>	Sobic.002G258000.1	MIKC ^C	0.05	-0.09	0.97	0.04	0.59	-0.74	-0.77	-0.13	0.24
<i>SbMADS9</i>	Sobic.002G368700.1	MIKC ^C	-0.49	0.08	0.52	0.16	0.27	0.11	0.21	-0.30	-0.02
<i>SbMADS10</i>	Sobic.003G027000.1	MIKC ^C	1.64	0.13	0.93	0.39	0.46	0.16	-0.03	-1.40	-0.53
<i>SbMADS11</i>	Sobic.003G379000.1	MIKC ^C	0.96	0.61	1.45	0.34	1.18	0.08	0.01	-1.20	-0.73
<i>SbMADS12</i>	Sobic.003G381100.1	MIKC ^C	0.00	0.00	0.00	0.00	0.00	0.00	0.00	0.00	0.00
<i>SbMADS13</i>	Sobic.004G003400.1	MIKC ^C	0.00	0.00	0.00	0.00	0.00	0.00	0.00	0.00	0.00
<i>SbMADS14</i>	Sobic.004G056000.2	MIKC ^C	0.00	0.00	0.00	0.00	0.00	0.00	0.00	0.00	0.00
<i>SbMADS16</i>	Sobic.004G281000.1	MIKC ^C	-0.05	-0.52	0.88	-0.06	1.41	-0.21	-0.33	0.77	0.22
<i>SbMADS17</i>	Sobic.004G306500.1	MIKC ^C	1.15	0.52	0.14	0.58	0.63	-1.31	-0.98	0.68	0.42
<i>SbMADS18</i>	Sobic.006G091500.1	MIKC ^C	0.00	0.00	0.00	0.00	0.00	0.00	0.00	0.00	0.00
<i>SbMADS19</i>	Sobic.006G189500.1	MIKC ^C	0.00	0.00	0.00	0.00	0.00	0.00	0.00	0.00	0.00
<i>SbMADS20</i>	Sobic.006G213900.1	MIKC ^C	0.00	0.00	0.24	0.00	0.00	0.00	0.00	0.21	0.00
<i>SbMADS21</i>	Sobic.007G013800.1	MIKC ^C	0.00	0.00	0.00	0.00	0.00	0.00	0.00	0.00	0.00
<i>SbMADS22</i>	Sobic.007G193300.1	MIKC ^C	0.68	0.37	1.03	0.49	1.09	-0.21	-0.11	0.43	0.42
<i>SbMADS24</i>	Sobic.008G072900.1	MIKC ^C	0.00	0.00	0.50	0.00	1.31	0.00	0.00	-0.66	-0.64
<i>SbMADS26</i>	Sobic.009G075500.4	MIKC ^C	0.96	0.37	1.09	0.30	0.98	-0.15	-0.01	0.17	0.25
<i>SbMADS27</i>	Sobic.009G142500.1	MIKC ^C	0.87	1.25	1.44	0.88	1.38	0.88	0.72	-0.06	-0.13
<i>SbMADS28</i>	Sobic.010G050500.1	MIKC ^C	-0.47	0.06	-0.18	0.01	-0.77	0.54	0.43	-0.19	0.28
<i>SbMADS29</i>	Sobic.010G085400.1	MIKC ^C	0.00	0.00	0.00	0.28	0.00	0.00	-0.18	0.00	0.00
<i>SbMADS30</i>	Sobic.010G221500.1	MIKC ^C	0.00	0.00	-0.19	-0.03	0.00	-0.67	-0.12	0.25	0.00
<i>SbMADS31</i>	Sobic.010G261800.1	MIKC ^C	0.03	0.89	1.12	0.91	1.70	0.42	-0.02	0.70	0.04
<i>SbMADS32</i>	Sobic.003G282400.1	MIKC ^C	-0.35	0.37	0.92	0.32	1.69	0.35	0.35	1.59	0.66
<i>SbMADS33</i>	Sobic.001G086500.1	MIKC ^C	0.61	0.74	-2.06	-0.39	0.70	-3.38	-0.42	-0.23	-1.12
<i>SbMADS34</i>	Sobic.005G204600.1	MIKC [*]	0.00	0.00	0.00	0.00	0.00	0.00	0.00	0.00	0.00
<i>SbMADS35</i>	Sobic.010G090200.2	MIKC [*]	0.00	0.00	0.00	0.00	0.00	0.00	0.00	0.00	0.00
<i>SbMADS36</i>	Sobic.002G026500.1	Ma	0.00	0.04	0.05	0.00	0.06	0.03	0.09	-0.01	-0.07
<i>SbMADS37</i>	Sobic.002G026600.1	Ma	0.03	-0.01	-0.02	0.03	-0.01	0.14	0.06	0.02	0.05
<i>SbMADS40</i>	Sobic.002G080500.1	Ma	-0.02	-0.04	-0.04	0.00	0.00	0.02	0.00	0.02	0.05
<i>SbMADS41</i>	Sobic.002G080600.1	Ma	0.00	-0.03	-0.17	0.02	0.01	0.14	0.05	-0.02	0.04
<i>SbMADS42</i>	Sobic.002G080700.1	Ma	0.00	-0.03	0.06	0.00	0.01	0.05	0.00	-0.01	0.13
<i>SbMADS45</i>	Sobic.003G216800.1	Ma	0.00	-0.10	-0.06	-0.02	0.00	0.14	0.02	0.01	0.01
<i>SbMADS46</i>	Sobic.003G216900.1	Ma	0.00	0.00	0.00	0.00	0.00	0.00	0.00	0.00	0.00
<i>SbMADS47</i>	Sobic.003G406800.1	Ma	-0.25	0.51	0.41	0.12	-0.12	-0.35	-0.17	0.31	0.76
<i>SbMADS48</i>	Sobic.004G051500.1	Ma	0.08	0.05	-0.04	0.00	0.04	-0.07	0.03	0.00	-0.01
<i>SbMADS49</i>	Sobic.004G191900.1	Ma	0.00	0.00	0.00	0.00	0.00	0.00	0.00	0.00	0.00
<i>SbMADS51</i>	Sobic.K042700.1	Ma	0.08	-0.07	0.00	-0.05	-0.01	-0.04	-0.05	0.08	0.07
<i>SbMADS52</i>	Sobic.007G090412.1	Ma	0.00	0.08	0.10	0.00	-0.01	0.02	0.12	0.00	0.00
<i>SbMADS54</i>	Sobic.007G086100.1	Ma	-0.08	0.14	0.00	0.03	-0.18	0.00	0.12	-0.23	-0.03
<i>SbMADS55</i>	Sobic.007G086200.1	Ma	0.00	0.00	0.10	0.12	0.12	0.07	-0.02	-0.01	-0.06
<i>SbMADS57</i>	Sobic.007G192900.1	Ma	0.17	0.35	-0.38	-0.18	0.19	0.00	0.31	1.00	0.90

<i>SbMADS60</i>	Sobic.009G239000.1	M α	-0.03	0.07	0.00	0.00	0.00	0.00	0.08	0.03	0.01
<i>SbMADS61</i>	Sobic.010G029200.1	M α	0.38	0.09	-0.11	0.01	0.09	-1.02	-1.17	0.18	0.06
<i>SbMADS62</i>	Sobic.010G162300.1	M α	0.00	0.00	0.00	0.00	0.00	0.00	0.00	0.00	0.00
<i>SbMADS63</i>	Sobic.010G148100.1	M α	-0.30	-0.02	0.18	-0.32	0.16	-0.92	0.09	0.01	0.02
<i>SbMADS64</i>	Sobic.003G156600.1	M β	0.43	-0.01	0.10	0.33	0.30	-0.94	-1.17	0.63	0.62
<i>SbMADS65</i>	Sobic.002G352300.1	M β	0.00	0.00	0.00	0.00	0.00	0.00	0.00	0.00	0.00

Table S3.4 Differentially expressed key jasmonic acid genes in *S. bicolor* WT (stages 5, 6, 10) and *msd1* mutant (stages 6, 10). BS- Biosynthesis, RES- Responsive, SIG-Signaling, TRAN- Transporter.

Name	Gene Name	Role	WT	WT	WT	<i>msd1</i>	<i>msd1</i>	<i>msd1</i>	<i>msd1</i>	<i>msd1</i>	<i>msd1</i>
			5P	6P	10P	6P	10P	WT	WT	WT	WT
			5S	6S	10S	6S	10S	6P	6S	10P	10S
AOS	Sobic.001G077400	BS	1.305	-0.94	-1	0.412	-0.5	-2.37	-3.11	0.75	0
AOC1/4	Sobic.001G329800	BS	0.11	-0.37	-0.86	0.191	-0.24	-2.16	-2.58	0.748	0.074
FAD8	Sobic.001G407600	BS	-0.06	-0.34	-0.83	0.571	-0.77	-2.34	-2.32	0.187	0.062
AOS	Sobic.001G449700	BS	-0.41	-0.13	-1.03	0.013	-0.61	-1.75	-2.74	0.353	-0.27
LOX4	Sobic.001G483400	BS	-0.37	-0.12	-0.77	-0.13	-1.45	-1.16	-1.62	-0.75	0.109
MFP2	Sobic.003G158300	BS	0	-0.02	0	0	0	0	0	0	0
AIM1	Sobic.004G124200	BS	-0.72	0	-0.2	-0.26	-0.54	-0.63	-0.28	-0.98	-0.58
DAD1	Sobic.005G032700	BS	-0.03	0	-0.11	0.032	0.056	0.066	0.034	0.258	0.116
LOX3	Sobic.006G095600	BS	0.276	0.016	-0.6	0.523	-0.4	-2.6	-3.87	1.055	-0.15
OPR3/DDE1	Sobic.007G151100	BS	0.513	0.076	-0.98	0.285	-1.16	-3.67	-3.82	0.564	0.379
FAD3	Sobic.008G003200	BS	0	0.086	0	0	0	0	0	0	0
JMT	Sobic.009G000900	BS	-0.06	0.094	-0.1	0.129	0.034	-0.07	-0.16	0.176	0.043
ACX1	Sobic.010G001900	BS	1.734	0.162	-0.33	0.009	-0.13	0.154	0.157	-0.12	0.023
ACX5	Sobic.010G049100	BS	0	0.426	0.529	-0.35	-0.86	-0.01	0.659	-0.37	0.266
MYC5	Sobic.001G287600	RES	0	-0.44	0	0	0	0	0	0	0
JAM1	Sobic.003G004500	RES	-0.06	-0.05	0.364	-0.15	0.004	0.152	0.098	0.223	0.331
MYB21/24/57	Sobic.003G232800	RES	0	0	0	0	-0.05	0	0	-0.05	0
JAM2	Sobic.003G272200	RES	-0.26	0	-0.74	0.377	0.001	-1.8	-2.99	1.746	0.68
JAM3	Sobic.009G088100	RES	0.107	0.108	-0.06	-0.25	-0.7	-0.86	-0.37	-0.6	0.23
JAZ1	Sobic.001G343900	SIG	-0.08	-0.37	-0.89	0.05	-0.81	-1.04	-1.66	0.446	0.441
TPL	Sobic.001G433800	SIG	-0.29	-0.34	0.318	-0.07	0.08	-0.38	-0.07	-0.22	-0.01
JAZ1	Sobic.002G214800	SIG	-1.02	-0.07	-2.13	-0.06	-1.13	-1.66	-2.98	0.564	-0.33
HDA19	Sobic.004G091200	SIG	-0.35	0	-0.09	-0.03	0.063	0.274	0.281	0.092	0.155
JAZ10	Sobic.006G056400	SIG	0	0.011	0	0	0	0	0	0	0
COI1	Sobic.009G157200	SIG	-0.41	0.115	0.151	-0.08	-0.11	0.192	0.551	-0.36	-0.05
GTR1/NPF2.10	Sobic.001G133900	TRAN	-0.23	-0.62	-0.66	0.052	-2.3	-2.49	-2.55	-2.25	-1.01

Table S3.5. Differentially expressed *SbIAA* genes in *S. bicolor* WT (stages 5, 6, 10) and *msd1* mutant (stages 6, 10).

Name	Gene Name	WT			<i>msd1</i>		<i>msd1</i>		<i>msd1</i>	
		5P	6P	10P	6P	10P	WT	WT	WT	WT
		5S	6S	10S	6S	10S	6P	6S	10P	10S
SbIAA1	Sobic.001G056100.1	0	-0.36	-0.33	-0.2	-0.33	0.881	-0.08	-0.7	-0.76
SbIAA2	Sobic.001G094800.1	-0.06	0.263	0.341	0.136	-0.53	-0.48	-0.14	-1.31	-0.5
SbIAA3	Sobic.001G161500.1	0	0	0.264	0	0.37	0	0	0	-0.04
SbIAA4	Sobic.001G161601.1	0	0.165	0.799	0.253	0.256	0	0.009	-0.23	-0.02
SbIAA5	Sobic.002G055900.1	-0.50	0.165	0.785	0.257	0.101	3.558	0.2	0.038	0.166
SbIAA6	Sobic.002G273400.1	0	0	0	-0.31	0	0.405	0	0	0
SbIAA7	Sobic.003G035700.2	-0.04	0.087	0.021	0.146	0.215	0.743	-0.06	0.667	-0.25
SbIAA8	Sobic.003G044900.1	0.215	0.032	-0.11	0.433	0.386	-0.84	-1.14	1.097	0.249
SbIAA9	Sobic.003G137200.1	0	0.333	-0.3	0.296	-0.48	0	-0.02	-0.74	0.39
SbIAA10	Sobic.003G254800.1	0.101	-0.22	0.268	0.076	0.185	0.075	-0.16	0.309	0.225
SbIAA11	Sobic.003G291200.1	-0.12	0.138	0.065	-0.54	-3.83	-1.65	-0.67	-2.7	0.637
SbIAA12	Sobic.004G099600.2	1.04	-0.22	0.837	1.533	0.205	6.215	-0.28	0.43	0.777
SbIAA13	Sobic.004G336500.1	0.247	-0.62	-0.44	0.137	0.554	-1.98	-2.78	0.927	0.055
SbIAA14	Sobic.004G345600.1	-0.22	0.211	0.125	0.148	0.306	0.463	0.763	0.69	0.403
SbIAA15	Sobic.005G098400.1	0.357	-0.81	0.393	0.349	0.755	1.773	-0.51	-0.76	-0.12
SbIAA17	Sobic.008G156900.1	0.089	-0.14	-0.37	0.181	-0.18	0.763	0.456	-0.47	-0.76
SbIAA18	Sobic.008G157000.1	-0.17	0.063	0.046	0.369	0.272	0.227	-0.04	-0.26	-0.45
SbIAA19	Sobic.009G065000.1	0.466	0.222	-0.99	-0.95	-1.18	-3.68	-2.58	0.615	0.406
SbIAA20	Sobic.009G069700.1	0.376	0.247	1.204	0.433	0	2.338	1.491	0	0.608
SbIAA21	Sobic.009G085100.2	0.039	0.291	0.052	0.125	-0.16	-0.09	0.249	-0.22	0.034
SbIAA22	Sobic.009G203700.1	-1.19	-1.09	-2.6	0.595	-2.6	1.315	-0.57	-2.12	-0.59
SbIAA23	Sobic.009G229200.1	0.538	0.124	-0.04	-0.18	0.035	-0.78	-0.16	0.17	0.448
SbIAA24	Sobic.010G052700.1	0.372	0	0	-0.23	0	0.263	0	0	0
SbIAA25	Sobic.010G146400.1	0	-0.72	0.905	-0.43	-0.44	-1.27	-0.28	-0.44	0.574

Table S3.6. Differentially expressed gibberellic acid genes in *S. bicolor* WT (stages 5, 6, 10) and *msd1* mutant (stages 6, 10). BS- Biosynthesis, IN- Inactivation, ST- Signal Transduction, UN-Unknown, NR- Negative Signal Regulator

Name	Gene Name	Role	WT	WT	WT	<i>msd1</i>	<i>msd1</i>	<i>msd1</i>	<i>msd1</i>	<i>msd1</i>	<i>msd1</i>
			5P	6P	10P	6P	10P	WT	WT	WT	WT
			5S	6S	10S	6S	10S	6P	6S	10P	10S
<i>GA20ox1</i>	Sobic.001G005300	BS	0.00	0.35	0.67	0.07	0.28	0.02	0.28	0.17	0.33
<i>CPS1</i>	Sobic.001G248600	BS	0.00	0.57	0.00	0.33	0.00	0.00	0.31	0.00	0.00
<i>GA20ox3</i>	Sobic.002G046500	BS	0.00	0.00	0.00	0.21	0.00	0.08	-0.17	0.00	0.00
<i>GA3ox2</i>	Sobic.003G045900	BS	-0.68	0.14	-0.10	-0.06	-0.16	-0.99	-1.28	-0.68	-0.24
<i>KS1</i>	Sobic.006G211500	BS	0.60	0.94	0.66	0.03	0.45	-1.01	0.21	-0.01	0.30
<i>GA20ox4</i>	Sobic.009G142400	BS	0.17	0.44	-0.07	0.31	0.36	0.70	0.24	0.34	-0.02
<i>KAO1</i>	Sobic.010G007700	BS	0.81	0.56	1.30	0.48	-0.76	0.82	1.14	0.02	1.15
<i>KO1</i>	Sobic.010G172700	BS	1.16	0.94	1.31	0.66	1.89	-1.85	0.31	0.92	0.33
<i>GA2ox6</i>	Sobic.003G300800	IN	-1.45	-1.19	-2.19	0.18	-4.31	1.90	0.26	-0.79	1.04
<i>GA2ox9</i>	Sobic.004G222500	IN	0.26	-0.15	-1.59	-1.08	-1.24	-2.42	-1.15	0.40	0.33
<i>GA2ox10</i>	Sobic.006G150800	IN	0.00	0.00	1.17	0.10	0.79	0.35	-0.28	0.00	-0.30
<i>GA2ox1</i>	Sobic.009G053700	IN	-0.70	-0.10	0.00	-0.17	-0.76	-0.82	0.00	-0.76	0.00
<i>GA2ox7</i>	Sobic.009G196300	IN	1.48	1.49	1.63	0.76	0.73	-1.35	-1.63	0.11	0.02
<i>SLR1</i>	Sobic.001G120900	ST	0.00	0.12	1.14	0.61	0.77	0.85	-0.08	0.08	0.15
<i>GID2a</i>	Sobic.004G192400	ST	-0.50	-0.26	3.06	0.24	0.44	-0.81	0.09	-0.25	-0.83
<i>GID1</i>	Sobic.009G134600	ST	-0.61	-0.38	-1.10	0.26	-1.28	-1.10	-2.14	0.35	0.15
<i>GA2ox3</i>	Sobic.003G022700	UN	0.00	-0.46	0.11	1.16	0.45	2.32	-0.49	0.17	-0.55
<i>KS3</i>	Sobic.006G211400	UN	1.14	-1.78	-2.84	-0.71	0.00	-1.58	-2.69	2.81	0.00
<i>GA2ox4</i>	Sobic.009G077500	UN	-0.27	0.11	-3.01	0.71	-0.59	-1.34	-3.71	0.77	-0.21
<i>GA2ox5</i>	Sobic.009G230800	UN	-1.12	-0.28	-0.60	0.43	0.25	0.50	-0.31	0.00	0.08
<i>DELLA</i>	Sobic.002G354900	NSR	-0.13	-0.54	-0.20	-0.03	-0.62	-2.51	-2.86	0.00	0.25
<i>DELLA</i>	Sobic.005G123000	NSR	0.00	0.00	0.00	-0.01	0.00	0.00	0.00	0.00	0.00
<i>DELLA</i>	Sobic.008G168400	NSR	0.00	0.08	-0.02	0.00	-0.04	0.03	0.10	-0.01	0.02
<i>DELLA</i>	Sobic.003G392800	NSR	-0.09	0.01	-0.07	0.05	-0.02	-0.07	0.07	0.00	-0.02

Table S3.7. Differentially expressed brassinosteroid genes in *S. bicolor* WT (stages 5, 6, 10) and *msd1* mutant (stages 6, 10). BS- Biosynthesis, NSR- Negative Signal Response, and PE- Perception.

Name*	Gene Name	Role	WT		WT		<i>msd1</i>		<i>msd1</i>		<i>msd1</i>	
			5P	6P	10P	6P	10P	WT	WT	WT	WT	
			5S	6S	10S	6S	10S	6P	6S	10P	10S	
<i>BR6ox</i>	Sobic.001G172400	BS	0.67	-0.55	-1.85	0.48	-1.37	-0.13	-1.80	-0.68	-1.37	
<i>DWF4</i>	Sobic.001g445900	BS	0.00	0.00	0.66	0.18	0.00	0.00	-0.14	0.48	0.21	
<i>D2</i>	Sobic.003G030600	BS	0.00	0.00	-0.35	-0.20	-1.56	-0.31	-0.19	-0.74	-0.33	
<i>DWF7</i>	Sobic.003g083300	BS	-0.11	0.26	0.25	0.19	0.47	1.04	0.94	-0.18	-0.31	
<i>CAS1</i>	Sobic.004g037200	BS	-0.09	0.11	0.02	0.05	-0.04	-0.09	0.15	-0.10	0.10	
<i>DWF4</i>	Sobic.006g114600	BS	0.37	0.44	0.93	0.43	1.92	0.29	0.17	1.68	1.00	
<i>CAS1</i>	Sobic.007g085800	BS	0.00	0.00	0.00	0.00	-0.73	0.00	0.00	-0.71	0.00	
<i>SMT1</i>	Sobic.009g244900	BS	0.86	0.30	-0.25	-0.17	-0.26	0.02	0.91	-0.14	0.27	
<i>DWF7</i>	Sobic.010g277300	BS	-0.60	0.19	0.04	-0.11	-0.01	0.21	0.42	0.23	0.21	
<i>BIN2</i>	Sobic.003G024800	NSR	0.00	0.00	0.00	-0.04	0.00	0.00	0.00	-0.05	0.00	
<i>BRI</i>	Sobic.001g403200	PE	0.45	-0.05	0.03	0.43	0.76	1.60	0.35	2.37	1.32	
<i>BRI</i>	Sobic.005g005700	PE	-0.31	-0.20	-0.06	0.36	1.57	0.86	0.06	2.20	0.62	
<i>BRI</i>	Sobic.008g006800	PE	-0.19	-0.28	0.26	0.46	1.03	0.94	0.10	2.04	0.96	

Chapter 4

Functional identification of *MS8* and *SbTDR* genes in tapetal cell differentiation and degeneration in *Sorghum bicolor*

This chapter contains *ms8* characterization work previously published in PLoS ONE (Xin et al., 2017).

4.1 Abstract

Anthers and male fertility are essential in normal seed plant reproduction. In agriculture, the production of hybrid seed typically involves manipulating male fertility. Sorghum (*Sorghum bicolor* L. Moench) is an important cereal grain with increasing use in both agriculture and research. However, little is known about anther development or what genes control anther cell differentiation and male fertility in sorghum. Here, we report the morphological characterization of the BTx623 WT and two *Sorghum bicolor* male sterile mutants, *male sterile 8* (*ms8*) and *tapetal degeneration retardation* (*Sbtdr*), as well as the cloning of causal genes. Our results showed that wild-type sorghum plants produced large yellow anthers visible after anthesis, while both *ms8* and *Sbtdr* mutants formed small white anthers. Further examination revealed that *ms8* and *Sbtdr* are completely male sterile due to the failure of pollen production. Analysis performed on semi-thin sections of anthers demonstrated that both mutants are defective in tapetum development and degeneration. Whole genome and Sanger sequences showed that *MS8* and *SbTDR* encode bHLH transcription factors. Moreover, RT-PCR analysis showed that both *MS8* and *SbTDR* were highly expressed in anthers at stages which are critical for tapetum development. Our results shed light on the molecular mechanisms by which *MS8* and *SbTDR* bHLH transcription factors control tapetal cell

differentiation in sorghum anther development. Moreover, our findings may help develop new hybrid breeding systems in sorghum.

4.2 Introduction

Sorghum bicolor (L.) Moench is a cereal grain and food staple in many semi-arid regions where it is difficult to cultivate less drought-resistant grains. Sorghum is the fifth most harvested grain globally behind wheat, maize, rice and barley. Proper stamen development is crucial for male fertility and seed yield in flowering plants. Stamens include the anther with developing pollen (male gametophyte) and the filament that attaches the anther to the flower. Anther development is well studied in many cereal grains and model organisms including rice, maize and *Arabidopsis* (Cheng et al., 1979; Raghavan, 1988; Sanders et al., 1999; Zhang et al., 2011); however, little is known about anther cell differentiation at both morphological and molecular levels in sorghum. During early development in well studied cereal grains and in *Arabidopsis*, anthers form four lobes (microsporangia) (Cheng et al., 1979; Raghavan, 1988; Sanders et al., 1999; Zhang et al., 2011). At the center, these four lobes contain microsporocytes (pollen mother cells, PMCs) that will later divide meiotically to give rise to microspores and then mitotically to form pollen. Outside of the PMCs the anther wall is organized into four concentric layers of somatic cells. From the external to internal these layers include the epidermis, endothecium, middle layer, and tapetum.

Tapetal cells have three major functions. First, In *Arabidopsis*, tapetal cells secrete the callase enzyme (β -1,3-glucanase) that releases the haploid microspores in the locule by breaking down the callose surrounding the meiotic tetrads (Stieglitz and

Stern, 1973). The timing of the callose dissolution must be precise, where early (prophase one, and early meiotic stages) or late enzyme activity (after the establishment of tetrads) results in sterility (Izhar and Frankel, 1971; Worrall et al., 1992). Second, with endoreduplication mature tapetal cells contain multiple nuclei and specialized non-photosynthetic plastids (elaioplasts) and tapetosomes, which provide lipids, proteins, polysaccharides and sporopollenin necessary for pollen wall formation (Hernandez-Pinzon et al., 1999; Hsieh and Huang, 2007). Finally, tapetal cells degenerate via programmed cell death (PCD), and depending on the plant species, materials such as tryphine and pollenkit are deposited forming the pollen coat (Hsieh and Huang, 2007; Li et al., 2011). As mentioned, tapetal cell function is often specific to plant groups. For example, late in development, maize tapetal cells do not contain elaioplasts and tapetosomes, instead tapetal cells synthesize glucanase, xylanase, and *Zea mays* pollen coat protease proteins which are found on the pollen surface after tapetal PCD (Li et al., 2012a). Tapetal degeneration is a stress-sensitive stage, where applying stress surrounding tapetal degeneration (e.g. drought and heat) frequently results in altered timing of the degeneration and loss of pollen fertility (Smith and Zhao, 2016). Additionally, male sterile mutants commonly demonstrate abnormal tapetal differentiation, development and degeneration resulting in abnormal pollen development and male sterility (Fu et al., 2014; Niu et al., 2013a; Parish and Li, 2010; Zhang et al., 2011).

In sorghum, there are 6 known lines with nuclear gene mutations, termed nuclear male sterility (NMS) mutants, including *ms1*, *ms2*, *ms3*, *ms7*, *msa1*, and *ms8*. These male sterile mutants were discovered following mutagenesis of the BTx623 WT line by

ethyl methane sulfonate (EMS) (Xin et al., 2017). *ms8* (now *ms8-1*) is important as it is the first of these mutants in sorghum that were fully characterized (Xin et al., 2017). Recently, increased efforts have led to the development of new NMS mutants named *tapetum degeneration retardation* (*Sbtdr1*, *Sbtdr2*, and *Sbtdr3*). To study these mutants a complete anther developmental series is necessary, allowing for comparison of the normal differentiation, development, and degeneration of the anther wall cell layers and reproductive cells.

Many basic helix-loop-helix (bHLH) transcription factors have been identified as playing key roles in tapetal cell differentiation and degeneration. In rice *bHLH142*, UNDEVELOPED TAPETUM1 (UDT1), TDR INTERACTING PROTEIN2 (TIP2), ETERNAL TAPETUM1 (EAT1)/DELAYED TAPETUM DEGENERATION (DTD), and TAPETUM DEGENERATION RETARDATION (TDR), work in a complex pathway to regulate the proper timing of tapetal PCD (Fu et al., 2014; Ji et al., 2013; Jung et al., 2005; Ko et al., 2014; Li et al., 2006; Niu et al., 2013b). Altered expression of these genes including loss of function and over-expression has demonstrated delayed or precocious (respectively) tapetal PCD and male sterility (Fu et al., 2014; Ji et al., 2013; Ko et al., 2014; Li et al., 2006; Niu et al., 2013b). These bHLH transcription factors comprise a complex web of interactions in rice. It has been proposed that the TIP2 and UDT1 heterodimer may activate *EAT1* which is further promoted by EAT1/UDT1 (Ono et al., 2018). Additionally, it has been reported that the TIP2/TDR heterodimer directly activates *EAT1* transcription (Ko et al., 2014). As TDR also dimerizes with EAT1, EAT1 competes for TDR (Niu et al., 2013b). EAT1 directly activates aspartic protease genes

by binding to the promoters of *AP25* and *AP37* which induce PCD in yeast and plants (Li et al., 2006).

The aim was to characterize the male sterile mutants. To do so, the complete characterization of anther development was necessary. Based on past work in known orthologs we hypothesized that male sterility due to delayed or abnormal tapetal cell degeneration was present. In our work, we established a complete anther developmental series for properly staging sorghum anthers which was used to characterize every stage in the *ms8* mutant and key stages in *Sbtdr* line ARS-67. In both mutant lines, we observed complete male sterility with no viable pollen production. During *ms8* development the tapetal cells did not develop properly or degenerate at the necessary time. Building on this work, we collaborated to clone the first male sterile gene in sorghum. Our sequencing results confirmed that the *ms8* mutation is in the Sb04g030850 gene and expression of this gene was restricted to anther and spikelet development from PMCs to microspores stage. Similarly, in *Sbtdr* line ARS-67 we observed hypervacuolated tapetal cells that remained late into development. Our *Sbtdr* mutant sequencing and RT-PCR work confirmed the mutation in the rice *TDR* orthologous gene Sb04g001650. *SbTDR* expression was restricted to tetrads, microspores, and pollen anthers with no expression detected in the other floral whorls. Our findings provide insight into the molecular mechanisms by which *MS8* and *SbTDR* genes control male sterility by regulating tapetal cell differentiation in sorghum. Moreover, our results have potential applications for generating new hybrid breeding systems in sorghum.

4.3 Materials and Methods

4.3.1 Sorghum lines and growing conditions

Sorghum bicolor BTx623 WT, *ms8-1*, *ms8-2*, *Sbtdr-1* (ARS-67), *Sbtdr-2* (ARS-84) and *Sbtdr-3* (ARS-250) seeds were grown in SUN GRO Metro-Mix 360 soil. The plants were grown under greenhouse conditions of 28/23°C (day/night), with 10 hours of light (8am-6pm), 14 hours of dark (6pm-8am), and a relative humidity of 50%. Plants were watered daily and fertilized weekly using a Young Mixer-Proportioner Injector at a rate of 60:1, with Sprint 330 and Peterson's Water Soluble General Purpose 20-20-20 fertilizer (250 ppm N and 20 ppm Fe).

4.3.2 Alexander staining

After the top of the panicle began anthesis, the spikelets just below were collected and processed. Anthers were dissected and collected for Alexander staining to detect viable pollen (Alexander, 1969). The anthers were placed in Alexander stain and left overnight at 42°C. Anthers were then placed in a drop of water and imaged. The anthers were evaluated as fertile if they contained large red pollen grains indicating staining of cytoplasm and mitochondria. The anthers were labeled as sterile if they contained no pollen or if the pollen appeared small, shrunken, and blue/green indicating only the presence of the pollen wall (Alexander, 1969).

4.3.3 Female fertility testing

After panicle emergence at the top of each plant, mutant and WT phenotypes were identified. The exposed portion of the panicle was cut and bagged. The following

morning the freshly opened spikelets were fertilized with BTx623 WT pollen and then bagged again. 2 and 3 days after pollination tissue was collected and the enlargement of the ovaries was observed in the mutant and WT lines and imaged with the Olympus SZX7 dissection microscope equipped with an Olympus DP 70 digital camera.

4.3.4 Sample preparation, semi-thin sectioning, and imaging

Panicles from the WT (BTx623), *ms8* (*ms8-1*), and *Sbtdr* (*Sbtdr-1*) were harvested after 6 to 10 weeks and floral tissues were fixed in modified Trump's 4:1 primary fixative (containing 1% glutaraldehyde, 4% Paraformaldehyde, in 0.1 M HEPES buffer (pH 7.2), and 0.02% Triton X-100) (McDowell and Trump, 1976). Samples were vacuum infiltrated in primary fixative for 10-30 minutes. Fixed tissue was left at room temperature overnight and stored at 4°C until use. Samples were washed twice in ddH₂O. Samples were post-fixed in 1% osmium tetroxide overnight at room temperature. After washing 2 times, samples were dehydrated in 10% increments (10:90; 20:80, 30:70, 40:60, 50:50, 60:40, 70:30, 80:20, 90:10) and then 100% acetone with 2-3 hours for each step. The 100% acetone was exchanged 3 times to ensure complete dehydration. After dehydration the floral tissues were infiltrated with a modified Spurr's resin gradient at 10% increments with 3 hours per change (Holdorf et al., 2012). 100% resin was exchanged twice daily for 5 days on average. Tissue was then embedded in molds filled with 100% resin and placed at 60°C to cure for 3 days. After curing the blocks were removed and rough-faced into trapezoids using razor blades. Semi-thin sections of 500 nm were then cut on a RMC-MT7 ultramicrotome. These sections were placed onto cleaned glass slides with a droplet of 10% acetone and set

onto a heat block to allow the acetone to evaporate and the sections to adhere. The slides were then stained with toluidine blue and rinsed with water (Dykstra, 1993). Sections were imaged on an Olympus Bx51 microscope equipped with an Olympus DP70 digital camera. From these images a developmental series for WT and *ms8* were constructed. To generate scanning electron microscopy (SEM) backscattered images the approach outlined by Micheva and Smith (2007) was modified. Tissue was sectioned at 400 nm by and placed on a 22 mm diameter glass coverslip, mounted with carbon tape to a one inch stub. The coverslip with sections was carbon coated using an Edwards Coating System 306A. The coated coverslips were then surrounded by carbon paint and the tissue sections were imaged by Hitachi S-4800 SEM to generate backscattered images (Micheva and Smith, 2007).

4.3.5 Sequencing verification of *ms8* and *Sbtdr* mutations

DNA was extracted using a CTAB DNA extraction method. The major steps include grinding tissue, extracting DNA, precipitating the DNA from solution, and purifying DNA. The protocol was followed from Xin and Chen (2012) with few modifications including grinding the tissue with liquid nitrogen and centrifugation rather than magnetic beads (Xin and Chen, 2012). The *MS8* and *SbTDR* genes were amplified by PCR from BTx623WT, *ms8-1*, *ms8-2*, *Sbtdr-1*, *Sbtdr-2*, and *Sbtdr-3*, primers available in Table 4.1. Sanger sequencing was performed by GENEWIZ of the WT and mutants. These mutant sequences were aligned to the WT sequence downloaded from phytozome (<https://phytozome.jgi.doe.gov/pz/portal.html>) to determine the presence and location of the mutations.

4.3.6 Semi-quantitative RT-PCR

Samples were collected from seedlings and from spikelets including pre-PMCs through mature spikelet stage. Floral samples were dissected fresh and from PMCs through pollen stage anthers were removed and separately processed. All tissue was stored in RNAlater™ solution (Sigma-Aldrich) at -20°C until sufficient material was collected for RNA extraction (RNeasy Plant Mini Kit, Qiagen). The RNA was then transcribed to cDNA (Qiagen's Quantitect Reverse Transcription Kit). Kits were used according to manufacturer's instructions. Actin trials were performed to calibrate the cDNA used for the final *MS8* and *SbTDR* RT-PCR. All primers are listed in Table 4.1. The PCR products were run on a 0.8% agarose gel to detect expression. ImageJ was then used to quantify the relative intensity of the bands.

4.4 Results

4.4.1 Vegetative development, non-male floral organs, and female fertility are normal in the *ms8* mutant.

During the development of the *ms8* line there were no quantifiable or qualitative vegetative differences between the WT and mutant plants. Both the WT and *ms8* lines formed full size plants (Xin et al., 2017). After observing male sterility in the *ms8* line it was important to ensure that the rest of the flower was unaffected by the mutation. The flowers appeared identical, with the exception of the small, pale to white anthers produced in the *ms8* line (Fig. 4.1A, B). When the WT and *ms8* carpels were observed after anthesis, they appeared nearly identical, with the exception that WT stigmas were

covered in pollen and the male sterile *ms8* had barren stigmas (Fig. 4.1A-C). After hand pollination of the sterile plants, the enlargement of the ovary was monitored. The ovary of the WT and *ms8* mutant continued to enlarge after pollination and no differences were observed in female fertility (Fig. 4.1D). The anthers were stained to identify viable pollen, where the WT line displayed numerous large, round, and red-stained pollen grains (Fig. 1E). In contrast, no pollen was observed in the smaller *ms8* anthers (Fig. 4.1F). These data along with normal seed yield following manual pollination in the lab and the field showed that the gynoecium is unaffected in *ms8* mutants (Xin et al., 2017).

4.4.2 The *ms8* mutant displays abnormal anther development after PMCs stage leading to the ultimate collapse of the anther lobes.

Early anther development in sorghum proceeds similarly to other grasses, and it is particularly similar to rice (Zhang et al., 2011). Pre-meiotic *ms8* anther development is similar to that of WT up to stage 5. In both WT and the *ms8* mutant at stage 1, Layer 1, 2, 3 (L1, L2, L3) cells are visible (Fig. 4.1A, B). All anther cells originate from the L1, 2, 3. In the WT and *ms8*, the L1 layer divides and forms the epidermis and divisions of the L2 layer form the archesporial cells at stage 2 (Fig. 4.2C, D) (Sanders et al., 1999). The L3 cells contribute to vascular and connective tissue formation. At anther stage 2 the anther begins to take shape and smaller connective cells and inner-most vascular cells form in the center (Fig. 4.2C, D). In WT and *ms8* stage 3, the epidermal cells continue to enlarge, and the large central archesporial cells divide, forming the primary parietal cells (Fig. 4.2E, F) (Zhang et al., 2011). Next, at WT and *ms8* stage 4, these primary parietal cells divide and form two (outer and inner) secondary parietal layers that are

surrounded by large epidermal cells. These secondary parietal cells surround the sporogenous cells (Fig. 4.2 G, H) (Li et al., 2006; Zhang et al., 2011).

At stage 5 in the WT and *ms8* mutant, the secondary parietal cells differentiate into endothecium, and the inner secondary parietal cells further divide into the middle layer and tapetum, completing the anther wall cell differentiation (Li et al., 2006; Zhang et al., 2011) (Fig. 4.2I, J). The *ms8* mutant does not have defects in establishing anther wall cells (Fig. 4.2J). At stage 6, microsporocytes should begin their first meiotic division. In the WT, microsporocytes associate with tapetal cells which have visible vacuoles (Fig. 4.2K) (Li et al., 2011; Zhang et al., 2011). Some *ms8* stage 6 anthers form an enlarged tapetum, but do not enter meiosis (Fig. 4.2L). Following two rounds of meiosis in the WT, dyads are formed at stage 7 (Fig. 4.2M), and tetrads are produced at stage 8 (Fig. 4.2O) (Li et al., 2006; Zhang et al., 2011). In the *ms8* mutant, the tapetum appears partially condensed at stage 7 and the presence of the middle layer wanes in stages 7 and 8 (Fig. 4.2N, P). The majority of *ms8* PMCs fail to divide to form any viable dyads, tetrads, or microspores during stage 7-8 and beyond.

In the WT at stage 9, the callose that holds tetrads degrades and microspores are released. Additionally, tapetal cells lose their vacuolated appearance as they condense and the middle layer degenerates (Fig. 4.2Q) (Li et al., 2011; Zhang et al., 2011). In the *ms8* mutant at stage 9, the anther wall has some similarities to WT including normal degeneration of the middle layer. In *ms8* stage 9, anthers that progress into meiosis demonstrate abnormal degeneration of the tapetum that most closely resembles WT stage 9. The inner cells at *ms8* stage 9 resemble the dyad-like cells observed in WT stage 7 (Fig. 4.2M, Q, R). In *ms8* stage 9, no viable microspores have been observed

(Fig. 4.2R, T). At stage 10 in WT, the microspores enlarge, vacuolate, and organize in a ring near the condensed tapetal surface, as the tapetum increasingly degenerates (Fig. 4.2S). In the *ms8* anther at stage 10, irregularly shaped microspores are randomly located in the central lobe (Fig. 4.2T). Moreover, a large and heavily vacuolated tapetal layer is also present (Fig. 4.2T). In the WT anther at stage 11, pollen mitosis occurs and two nuclei with separated cells are visible in the developing grains, demonstrating bicellular pollen stage (Fig. 4.2U). The developing pollen remain associated with the anther wall and the tapetum is no longer present (Fig. 4.2U). In *ms8* anther stage 11, no pollen grains were observed (Fig. 4.2V, X, Z). In some *ms8* anthers, the lobe appears to be filled with microspores at first glance; however, it is more likely that these cells represent a hypervacuolated tapetal layer. In the WT anther at stage 12, the endothecium is greatly reduced but remnants are present, and the septum breaks down (Fig. 4.2W). The development of the pollen is close to completion and the grains are mostly round and densely stained. Conversely, in the *ms8* stage 12 anther, the lobe is empty and the anther wall is similar to the WT, containing the epidermis, endothecium and only remnants of inner layers. Finally, pollen releases during anther dehiscence in the WT at stage 13, with clear breakdown of the anther lobes (Fig. 4.2Y). In the *ms8* anther at stage 13, the lobe collapses and the lobe contents further degenerate (Fig. 4.2Z). SEM backscattered (BSE) images allowed for a more detailed look at the anther cell wall development. In these images, early pre-meiotic stage 5 anther development is unaffected in *ms8* anthers, with no obvious defects observed in the semi-thin work (Fig 4.3A, B).

4.4.3 The *ms8* phenotype is attributed to mutations in *Sb04g030850*, and normally expressed in the sorghum spikelet and anthers from PMCs to microspores stage.

Ethyl methanesulfonate (EMS) mutagenesis and identification of the *ms8* mutants was performed by Dr. Zhanguo Xin (USDA). Whole genome sequencing by Dr. Xin of the *ms8* mutant revealed 8 potential mutations that mapped to a single locus. To remove unlinked mutations that occurred during mutagenesis, the *ms8* mutants were backcrossed six times to the BTx623 WT line (Xin et al., 2017). The *ms8* X BTx623 cross yielded fertile F1 plants and the F2 segregated at a 1:3 ratio, suggesting that *ms8* is a recessive mutation. One mutation in the *Sb04g030850* (locus: Sobic.004G270900) gene (Fig. 4.4A), resulted in a premature stop codon. Specifically, the glutamine (CAA:Q) at position 150 was converted to a stop codon (TAA, Fig. 4.4). An additional independent allele was discovered named *ms8-2*. Similarly, a C-T mutation was observed where glutamine (CAG:Q) at position 148 was converted to a stop codon (TAG, Fig. 4.4). In our lab, independent DNA extraction and sequencing results supported the findings that the male sterility in the *ms8* mutants is caused by the mutation of *Sb04g030850*, which encodes a basic helix-loop-helix (bHLH) DNA-binding superfamily protein (Xin et al., 2017). In rice, the orthologous gene is *Delayed Tapetum Degeneration (DTD)*. Due to the nature of the mutation, this gene was selected as the likely candidate for the *ms8* mutation. The expression of *MS8* and the actin control *SbAC1* were examined in seedling, prePMCs whole spikelets, and for both spikelets and anthers for PMCs, meiotic cells, released microspores, and pollen. RT-PCR revealed that expression of *MS8* is highest in PMCs through microspores stage with higher expression in the anthers at all stages (Fig. 4.4A). This finding was evaluated

using ImageJ to evaluate band intensity which confirmed the observed pattern, and further demonstrating that *MS8* is expressed at the highest level at middle anther development stages 5-10 (Fig. 4.4B).

4.4.4 *Sbtdr* mutant plants display normal vegetative development with a similar anther sterility phenotype to *ms8*.

The *Sbtdr* mutant is similar to WT, except that its pale and thin anthers failed to form pollen. Specifically, the vegetative structures appeared WT-like in appearance and the panicle fully extended from the boot (Fig. 4.6A, B). In the WT large yellow anthers are produced (Fig. 4.6A, C, E, G). During late stage 12, flower development and after anthesis at stage 13 small and pale anthers emerged (Fig 4.5D, F, H). The other floral whorls had typical WT appearances (Fig. 4.4F). After bagging these panicles to exclude outcrossing, no seeds were produced, consistent with the *ms8* phenotype. Normally in WT development after self-fertilization, ovaries enlarge as the embryo increases in size (Fig. 4.7). Similarly, when *Sbtdr* flowers were hand pollinated using BTx623 WT pollen, normal enlargement of the ovary was observed (Fig. 4.7). Upon closer examination of the anthers small hair-like extensions were visible from the anther tips on all mutant anthers, which are not observed in the WT (Fig. 4.6G, H; Fig. 4.8A, B). Alexander staining demonstrated large viable pollen grains in the WT (Fig. 4.8A). Like the the *ms8* mutant line, no pollen were present in the *Sbtdr* anthers and complete sterility was confirmed (Fig. 4.8B). Preliminary semi-thin sectioning results demonstrated that the *Sbtdr*, like the WT anther, had normal development at anther stage 5 (PMCs) (Fig. 4.8C, D). Both WT and *Sbtdr* produced all anther cell layers with epidermis,

endothecium, middle layer, tapetum, and the inner pollen mother cells (Fig. 4.68C, D). In normal development, meiosis should form completed dyads at anther stage 7 and tetrads at anther stage 8 (Fig. 4.8E, G). Similar to *ms8*, few anthers progressed through meiosis. Some *Sbtdr* lobes filled with what has been documented previously as tapetal cells with no microspores or precursors present (Fig. 4.8F) (Li et al., 2006). Other *Sbtdr* anthers demonstrate condensed tapetal cells and degeneration of the middle layer, but fail to form viable microspores (Fig. 4.8H). Late in development, sorghum anthers form large round pollen grains with only the outermost epidermal cells and endothecium remnants remaining (Fig. 4.8J). In *Sbtdr*, tapetum hypervacuolated tapetal cells were common and filled the inner anther lobe prior to degeneration and exhibited collapse of the lobe and complete sterility (Fig. 4.8F, J). In *ms8*, hypervacuolated tapetal cells typically presented at anther stage 11; however, the middle layer was still present in *Sbtdr*. It is possible the middle layer failed to degenerate or the tapetum became hypervacuolated at an earlier stage

4.4.5 The Sbtdr mutant phenotype is attributed to a mutation in Sb04g001650 which is expressed in anthers from PMCs through early pollen stage.

Mutation of the Sb04g001650 (*SbTDR*) gene results in anther sterility. Previous to this work, whole genome sequencing was performed and results shared by Dr. Xin (USDA). In this study, the BTx623-WT and ARS-67 lines were used. The *SbTDR* gene was sequenced in our lab in the WT and ARS-67 mutant and the mutation was confirmed. The mutation detected in the Sb04g001650 (locus: Sobic.004G017500) gene resulted in a premature stop codon in exon 5 (Fig. 4.9). Further sequencing of the ARS-84 and

ARS-250 mutants in the Sb04g001650 gene detected a single nucleotide change in each. These point mutations in exon 6 resulted in altered amino acid sequences in both lines (Fig. 4.9). In rice, the orthologous gene is *TDR*. The expression of the sorghum actin control, *SbAC1*, and *SbTDR* genes were examined at seedling, prePMCs whole spikelets, and for both spikelets and anthers for PMCs, tetrads, microspores, and mature spikelets containing pollen stages. RT-PCR revealed that expression of *SbTDR* is highest in meiotic anthers but some expression was detected in PMCs anthers and low expression in early pollen anthers (Fig. 4.10A). Using ImageJ to evaluate band intensity further highlighted the relative high expression of *SbTDR* in meiotic anthers. *Sbtdr* was not detected in the floral whorls outside of the stamens. Spikelets with anthers removed showed only background signal via imageJ analysis (Fig. 4.10B).

4.5 Discussion

4.5.1 Anther development in Sorghum is similar to other cereal grains.

Early anther developmental events in sorghum were similar to rice and maize (Cheng et al., 1979; Zhang et al., 2011). Different from Arabidopsis, meiosis led to the production of dyads and tetrads, then the release of microspores. After the formation of microspores, a few differences were observed between sorghum and rice development. In rice, microspores become filled with starch and other reserves, resulting in a more rounded shape as they developed to form mature pollen. Because of this process, a bicellular pollen appeared to form hook shaped cells. In processing sorghum anther samples, it seemed more likely that hook shaped cells were due to tissue processing errors and are not an accurate depiction of bicellular pollen in either plant (Zhang et al.,

2011). In sorghum, the hook shaped cells were not found in most anther samples. Another difference occurred in late sorghum anther development, where the septum appeared to break down earlier in rice (Zhang et al., 2011). Additionally, some series included shrunken epidermal cells in late pollen stages suggesting that sample processing errors may have been more prevalent in late anther stages (Li et al., 2011; Zhang et al., 2011). The elongated processing time used in this study, particularly for dehydration and infiltration, may have resulted in improved preservation. These improved sections demonstrated rounded cells of the microspores and bicellular pollen as well as better preserved anther walls late in development.

4.5.2 Anther development in *ms8* and *Sbtdr* show obvious defects in tapetal cell development and differentiation.

The sections and staining work provide a clear look at sorghum WT, *ms8*, and *Sbtdr* anther development of both the anther wall and the developing pollen grains. In the mutants, the developmental patterns were not always consistent. The anthers observed showed the earliest defects during meiosis of the microsporocytes with no observed effects on the earlier formation of the anther wall. As demonstrated above, anther development proceeded normally in the *ms8* and *Sbtdr* mutants up until the PMCs stage, after which difficulties progressing through meiosis and formation of microspores occurred. This finding is consistent with studies in known orthologs, where early anther development is unaffected (Ji et al., 2013; Ko et al., 2014; Li et al., 2006; Niu et al., 2013b). In contrast with these past studies, few meiotic cells or microspore-like cells were identified throughout this study in either *ms8* or *Sbtdr* (Ji et al., 2013; Ko

et al., 2014; Li et al., 2006; Niu et al., 2013b). While the inner lobe contents at this stage were not consistent, the effects observed on tapetal degeneration were similar. In sorghum and rice the tapetal walls of the *ms8/eat1* and *Sbtdr/tdr* (respectively) became hypervacuolated and also vacuolated/degenerated at the incorrect time point. This finding was significant, as the proper degeneration via a proposed programmed cell death of the tapetum is essential to developing microspores and to form viable pollen (Vizcay-Barrena and Wilson, 2006). In rice, *tdr* and the homologous *Arabidopsis malesterile1 (Atms1)* mutants fail to undergo proper tapetal cell degeneration or delayed degeneration resulting in sterility (Li et al., 2006; Vizcay-Barrena and Wilson, 2006). Additionally, in *ms8* and *Sbtdr* mutants during late development, the inner most cells including abnormal microspore like cells or hypervacuolated tapetal cells degenerated. The end of development is characterized by empty lobes and complete lobe collapse. At the end of development, only an epidermal layer and possible remnants of the endothecium remained. Unfortunately, this late stage is not shown in the studies of *eat1* or *tdr* (Li et al., 2006; Niu et al., 2013b). It is unclear if later collapse occurred in these lines or if this stage is unique to sorghum mutants. Ultimately, no pollen was produced or released in either the *ms8* or *Sbtdr* mutants consistent with its known orthologs.

4.5.3 Sorghum MS8 and SbTDR have similar functions to orthologs in rice

Loss of functional *MS8* or *SbTDR* resulted in complete male sterility in sorghum, similar to the mutants identified in rice. The *ms8* rice ortholog *dtd* and its allelic mutant *eat1* mutant are characterized by a delay in programmed cell death of the tapetal cells, and production of abnormal anthers that do not form viable pollen (Ji et al., 2013; Niu et al.,

2013b). In the *eat1/dtd* mutant the anther cells can undergo meiosis to form microspores but the microspores degrade and no mature pollen is produced (Ji et al., 2013; Niu et al., 2013b). Consistent with our study, abnormal and degrading microspores were detected; however, clear evidence of meiotic divisions was not. Partially consistent with past work, *MS8* expression was detected from PMCs to microspores stages. Past study has shown two major expression patterns. The original work demonstrates anther expression from meiotic cells through pollen with highest levels in tetrads and microspores (Niu et al., 2013b). Later study demonstrated a bimodal expression pattern with earliest expression at pre-PMCs and reduced expression at the tetrads stage (Ono et al., 2018). Interestingly, our preliminary result shows a combination of these findings with decreased expression at the tetrads stage. Consistent with function in tapetal degeneration, these genes have highest expression in the tapetal cell layer.

In rice, *EAT1* acts with *TDR* to control tapetal degeneration. Additionally, *TDR1* and *bHLH142* likely form a heterodimer and bind to the *EAT1* promoter to regulate programmed cell death. When *bHLH142* (*ms142*), *EAT1* or *TDR1* were mutated, the anthers were small, pale and sterile. Mutants from this pathway overall are associated with sterility, possessing small and pale anthers that do not yield viable pollen (Ji et al., 2013; Ko et al., 2014; Li et al., 2006; Niu et al., 2013b). Similar to *EAT1*, different expression patterns have been documented for *TDR*. In past study, expression is highest in the tapetal layer of the anthers, consistent with its function in tapetal degeneration. Studies vary on when *TDR* is expressed; however, there is consensus that *TDR* is expressed at tetrads and microspores stages, similar to our study (Li et al.,

2006; Ono et al., 2018). Overall, consistent with previous rice studies, our study of *MS8* and *SbTDR* genes and their mutants highlight the necessity of these genes in male fertility. Loss of these genes results in complete sterility due to improper tapetal cell differentiation and degeneration.

4.5.4 Use of *ms8* and *Sbtdr* in hybrid breeding

Both the *ms8* and *Sbtdr* mutants displayed complete male sterility as demonstrated by the absence of viable pollen. In addition, both mutants had normal female fertility and could be manually pollinated to make seed. There is a growing demand for NMS mutants in sorghum. The traditional cytoplasmic male sterility (CMS) system requires more time and expense. Furthermore, the limited genetic diversity and number of lines has caused past agricultural disasters (Ullstrup, 1972). Specifically in CMS there are three required lines, the male sterile female (A line), the maintainer male (B line) to pollinate A, and the restorer male (R) line that can complement the defect of the A line to restore fertility (Rooney et al., 2007). In contrast, NMS mutants do not have cytoplasmic mutations but possess alterations to the nuclear DNA. NMS lines are used in 2-line breeding systems, and allow for complementation with any line not containing the mutation of the male sterile line. Due to the specificity of both of the *MS8* and *SbTDR* genes in the flower and anther and the complete loss of male fertility, both lines demonstrate great potential for use in NMS breeding systems.

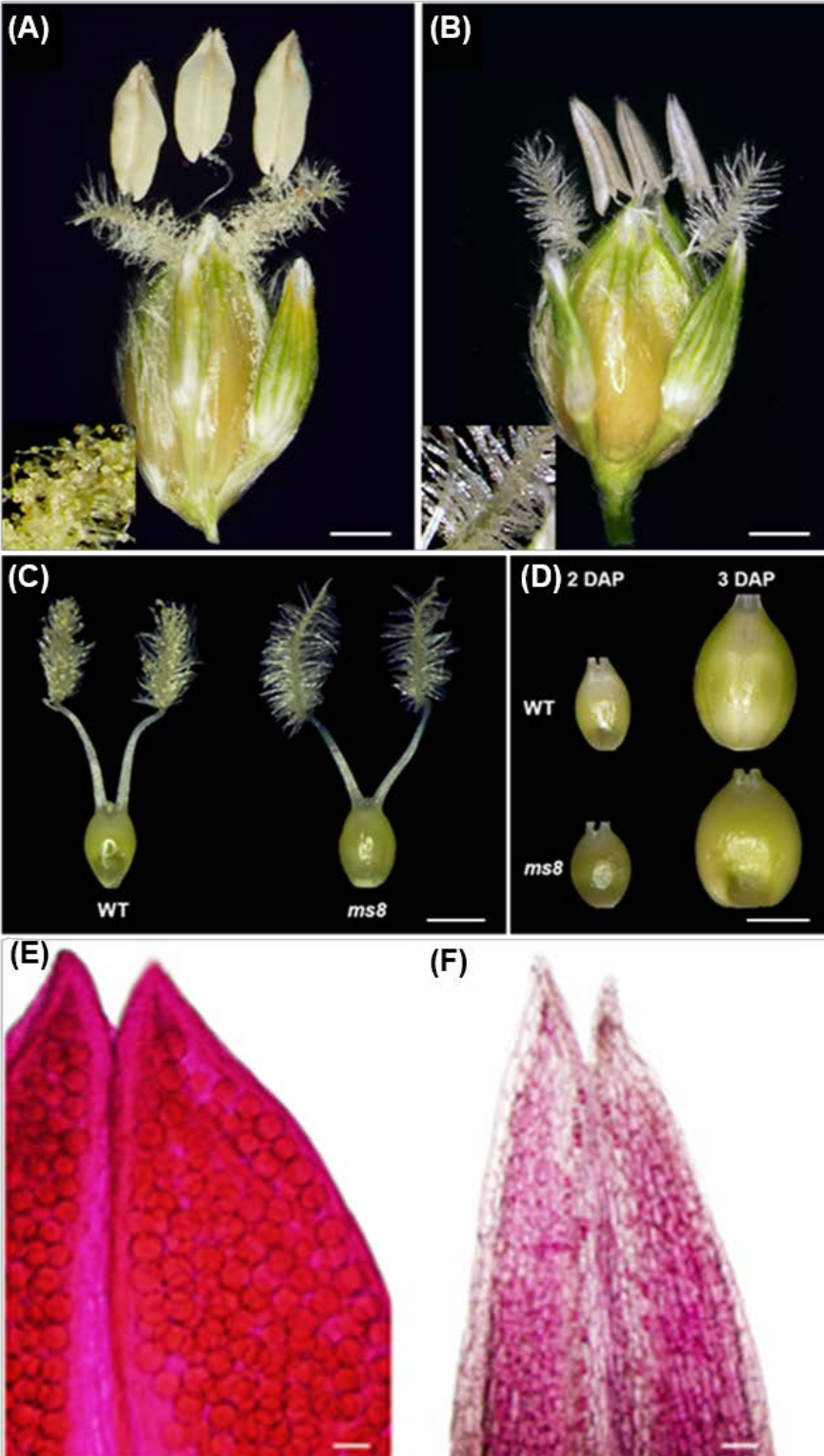


Figure 4.1. WT and *ms8* spikelet comparisons and evaluation of female and male fertility. (A) Mature WT external spikelet with enlarged view of stigma. (B) *ms8* external spikelet at maturity with zoom in on barren stigma. (C) WT and *ms8* gynoecium the day of anthesis with pollen visible on the stigmas of the WT only. (D) Ovary enlargement in both WT and *ms8* (after stigmas are manually pollinated). (E) Alexander staining of WT anther filled with viable pollen. (F) Alexander staining of thin *ms8* anther devoid of pollen. DAP- Days After Pollination. Scale bar 0.5 mm (A/B), 1.0 mm (C/D) and 20 μ m (E/F).

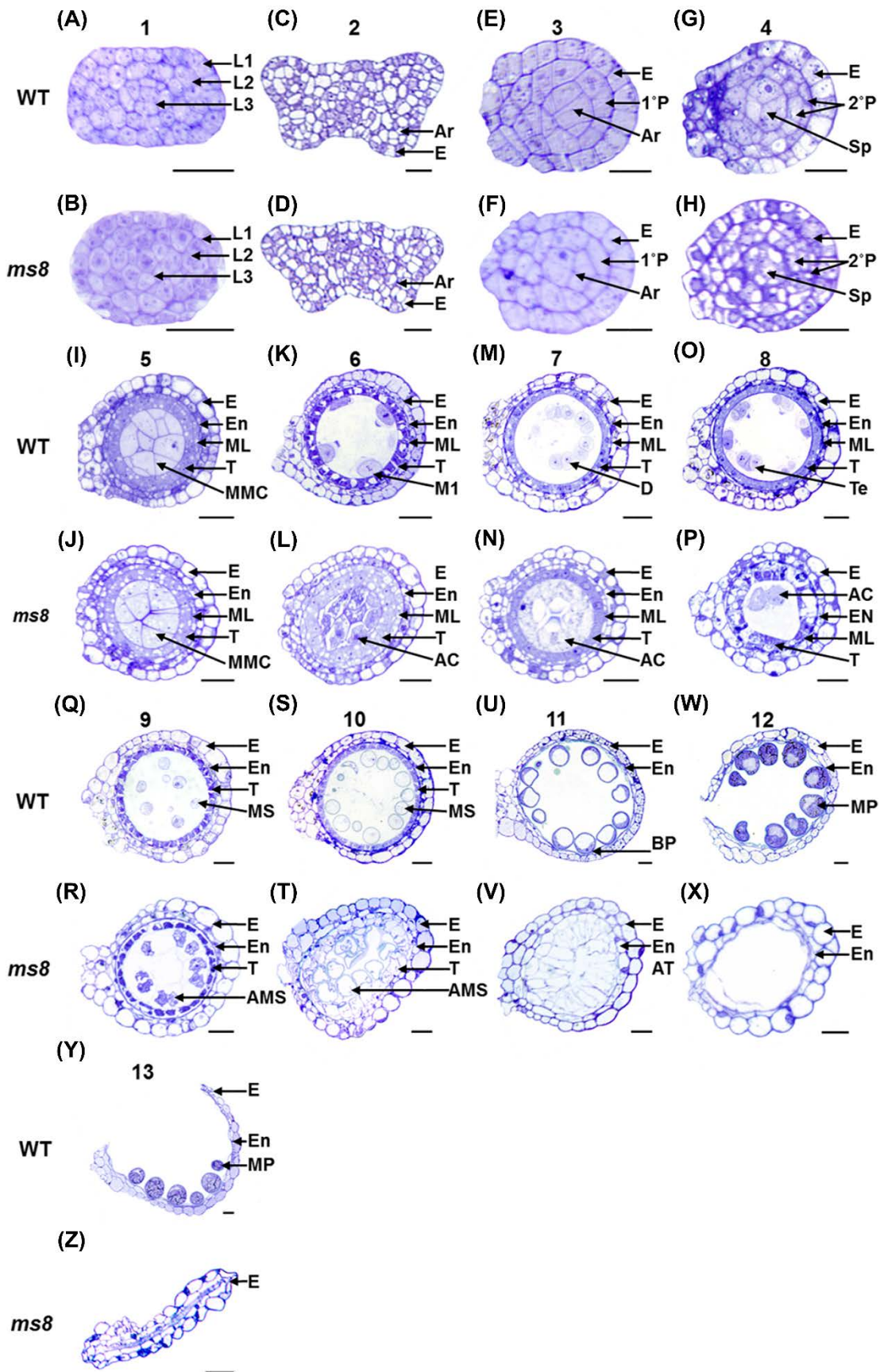


Figure 4.2. Successive anther development in WT and *ms8*. Irregular anther development of the *ms8* mutant is visible after the formation of the anther wall resulting in abnormal tapetal degeneration, abnormal microspores, and no pollen production. (A,C,E,G,I,K,M,O,Q,R,S,U,W,Y) Semi-thin sections with the development of the WT anthers. (B,D,F,H,J,L,N,P,R,T,V,X,Z) *ms8* anther stage comparisons. (A-D) Stages 1-2 entire anther view. (E-Z) Stages 3-13 with individual anther lobes shown. Abbreviations- 1°P- Primary Parietal, 2°P-Secondary Parietal, AMS- Abnormal Microsporocyte, Ar- Archesporial Cells, AT- Abnormal Tapetum, BP- Bicellular Pollen, E- Epidermis, En- Endothecium, L1- Layer 1, L2- Layer 2, L3- Layer 3, MP-Mature Pollen Sp-Sporogenous. Scale bars: 25 μ m.

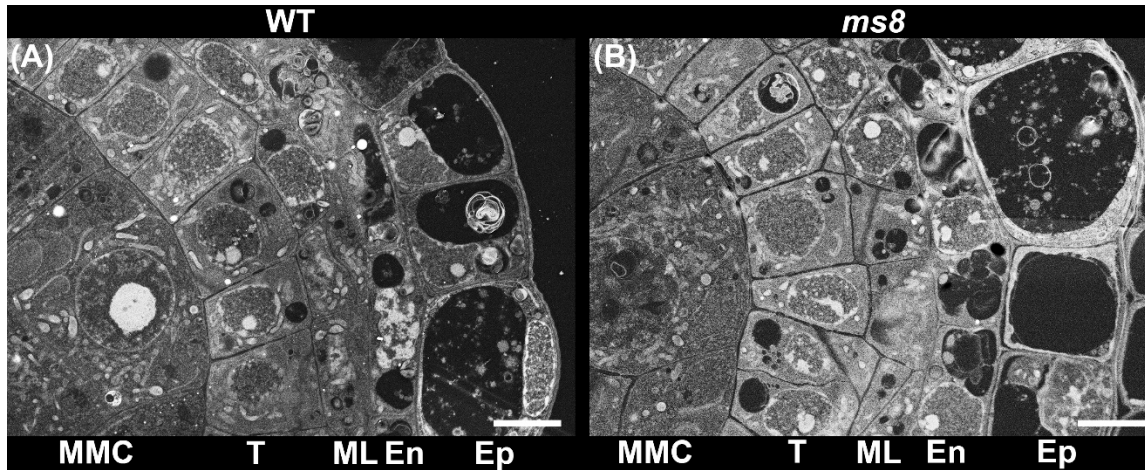


Figure 4.3. SEM micrographs of WT and *ms8* anther sections demonstrating normal PMCs development in *ms8*. Closer view of the PMCs stage highlights that development is normal at the formation of the anther wall. (A, B) Stage 9 WT anther (A) and *ms8* anther (B). Abbreviations: En- Endothecium, Ep- Epidermis, ML- Middle Layer, PMC- Pollen Mother Cells, and T- Tapetum. Scale bars 5 μ m

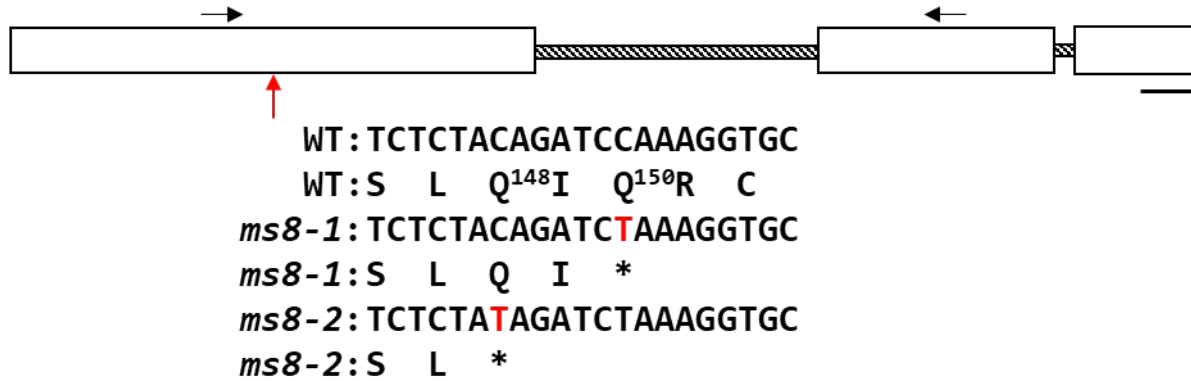


Figure 4.4. Sb04g030850 (Sobic.004G270900 locus) gene and mutation sites in *ms8* mutants. Diagram of Sb04g030850 containing 3 exons (open boxes) and 2 introns (dashed boxes) with the RT primer pair indicated with arrows. The *ms8* mutation sites are in exon 1 as indicated, both resulting in a premature stop codon. Scale bar 100bp.

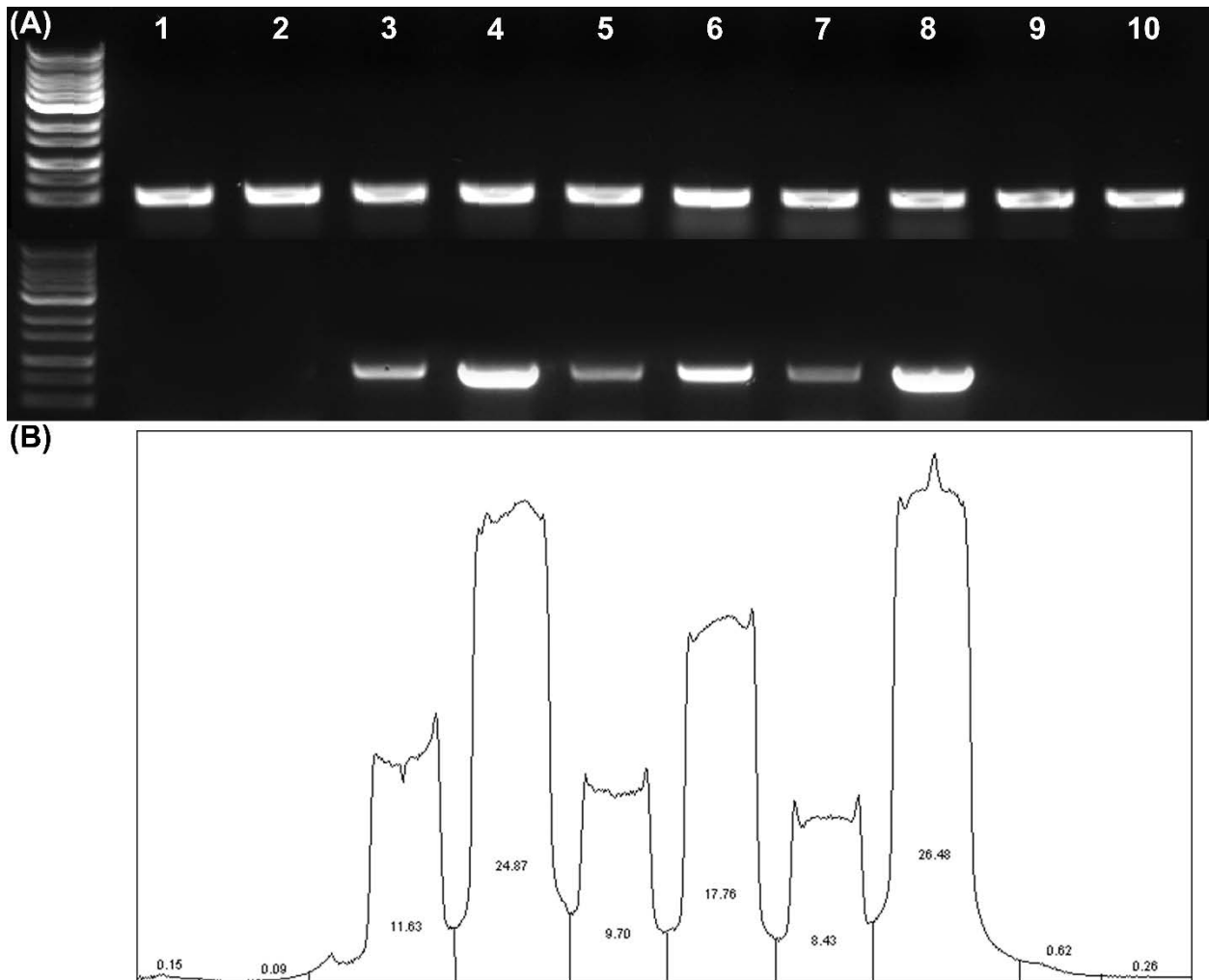


Figure 4.5. The *MS8* gene is expressed in flowers and anthers from PMCs to microspores stage. (A) Expression of actin and *SbTDR* in seedlings, spikelets, and anthers over development as detected by RT-PCR. (B) Semi-quantitative output of *SbTDR* expression using band intensity over all stages. Stages: 1- seedling, 2- pre-PMC spikelets with anther primordia 3- PMCs spikelets 4- PMCs anthers 5- tetrads spikelets 6- tetrads anthers 7- microspores spikelets 8- microspores anthers, 9- mature spikelets, and 10- mature anthers.

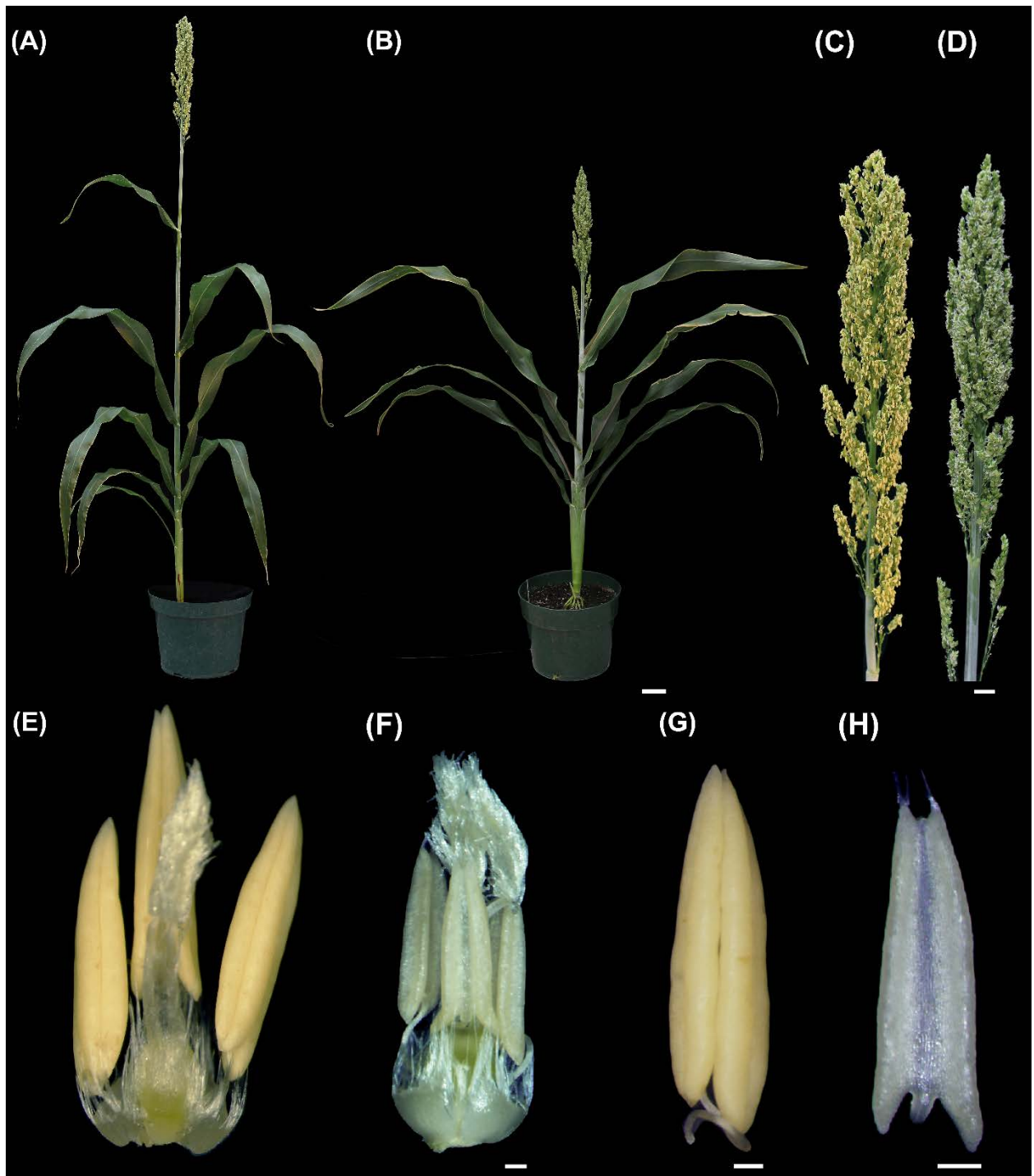


Figure 4.6. *Sbtdr* mutant plants display normal vegetative development but abnormal anthers. (A) Complete WT plant. (B) Complete *Sbtdr* plant. (C) WT panicle at dehiscence. (D) *Sbtdr* panicle with small white anthers visible. (E) WT internal spikelet structures. (F) *Sbtdr* internal spikelet structures. (G) WT single anther. (H) Single pale *Sbtdr* anther with hair like extensions. Scale bars 2 cm (A,B) and 250 μ m (C-E).



Figure 4.7. Female fertility is normal in the *Sbtdr* mutant. WT plants display clear ovary enlargement after self-pollination with BTx623. *Sbtdr* displays normal ovary enlargement after manual pollination using the BTx623 WT pollen. Scale bar 1 mm.

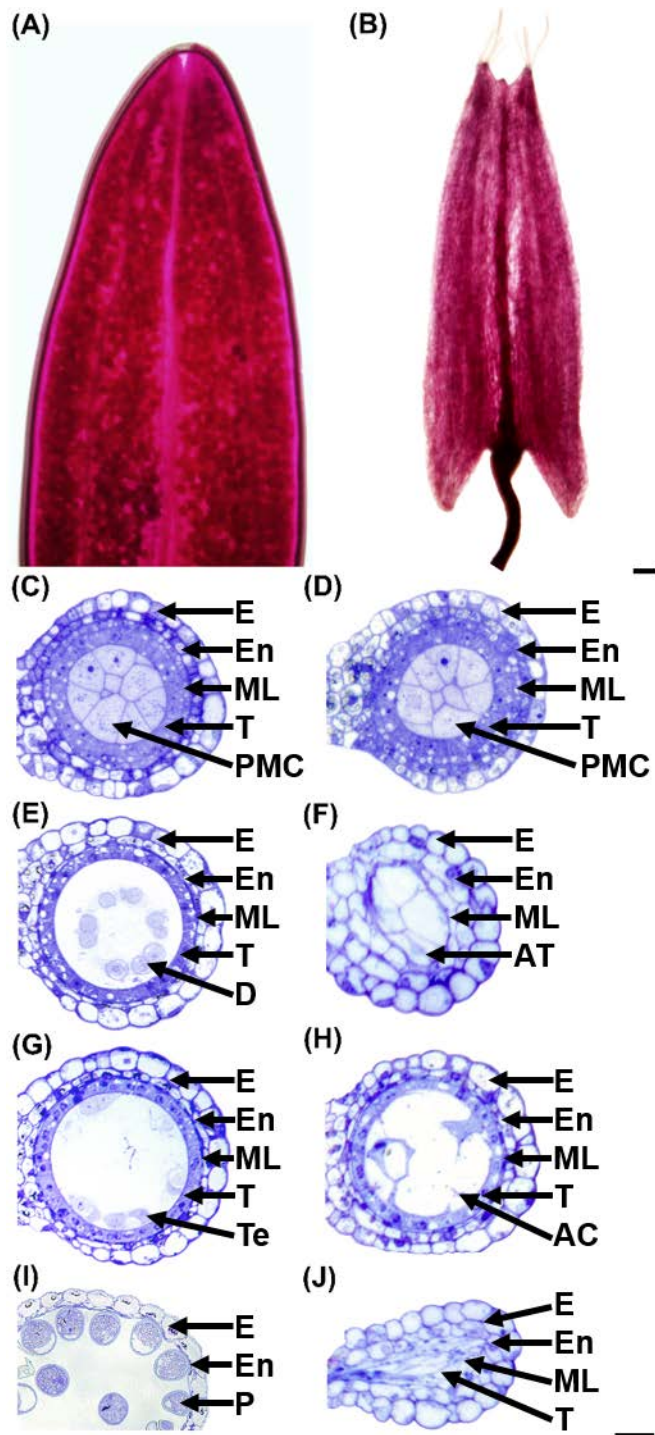


Figure 4.8. *Sbtdr* anther development is abnormal after microsporocyte meiosis and anthers yield no pollen. A/B) Alexander staining reveals viable pollen in WT but lack of pollen and hairy anthers in the *Sbtdr* mutant (B). C/D) Normal development up to pollen mother cell (PMCs) at stage 5 is observed in WT (C) and *Sbtdr* (D). E/F) WT progresses into meiotic divisions at stage 7 with dyads observed (E) where some *Sbtdr* fail to enter meiosis and display hypervacuolated tapetal cells (F). G/H) Wild type continues to divide and forms tetrads at stage 8 (G) while some *Sbtdr* produce abnormal meiotic cells (H). I/J) WT completes pollen formation at stage 12 (I) while *Sbtdr* mutant anthers collapse (J). Abbreviations: AC- Abnormal Cells, D- Dyad, E- Epidermis, En- Endothecium, ML- Middle Layer, PMC- Pollen Mother Cells, T- Tapetum, Te- Tetrads. Scale bars 100 μm (A,B) and 50 μm (C-J).

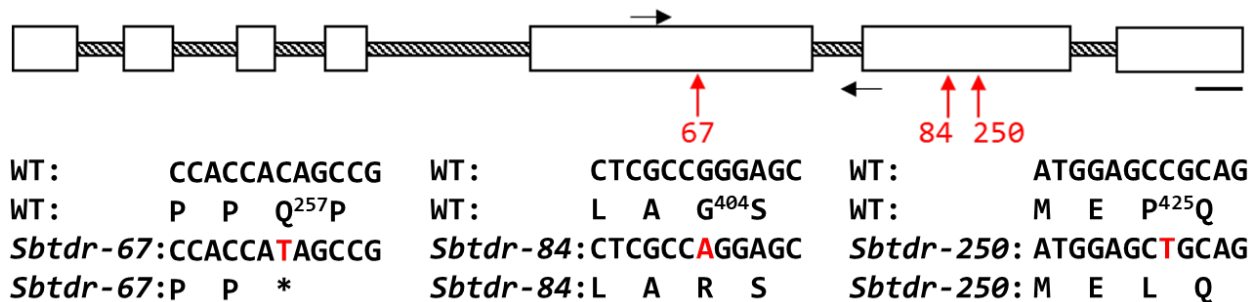


Figure 4.9. The *SbTDR* gene Sb04g001650 (Sobic.004G017500 locus) and *Sbtdr* mutation sites. Diagram of *SbTDR* containing 7 exons (open boxes) and 6 introns (dashed boxes), with the RT primer pair indicated with black arrows. The *Sbtdr* mutation sites are indicated in exons 5 and 6. Scale bar 100bp.

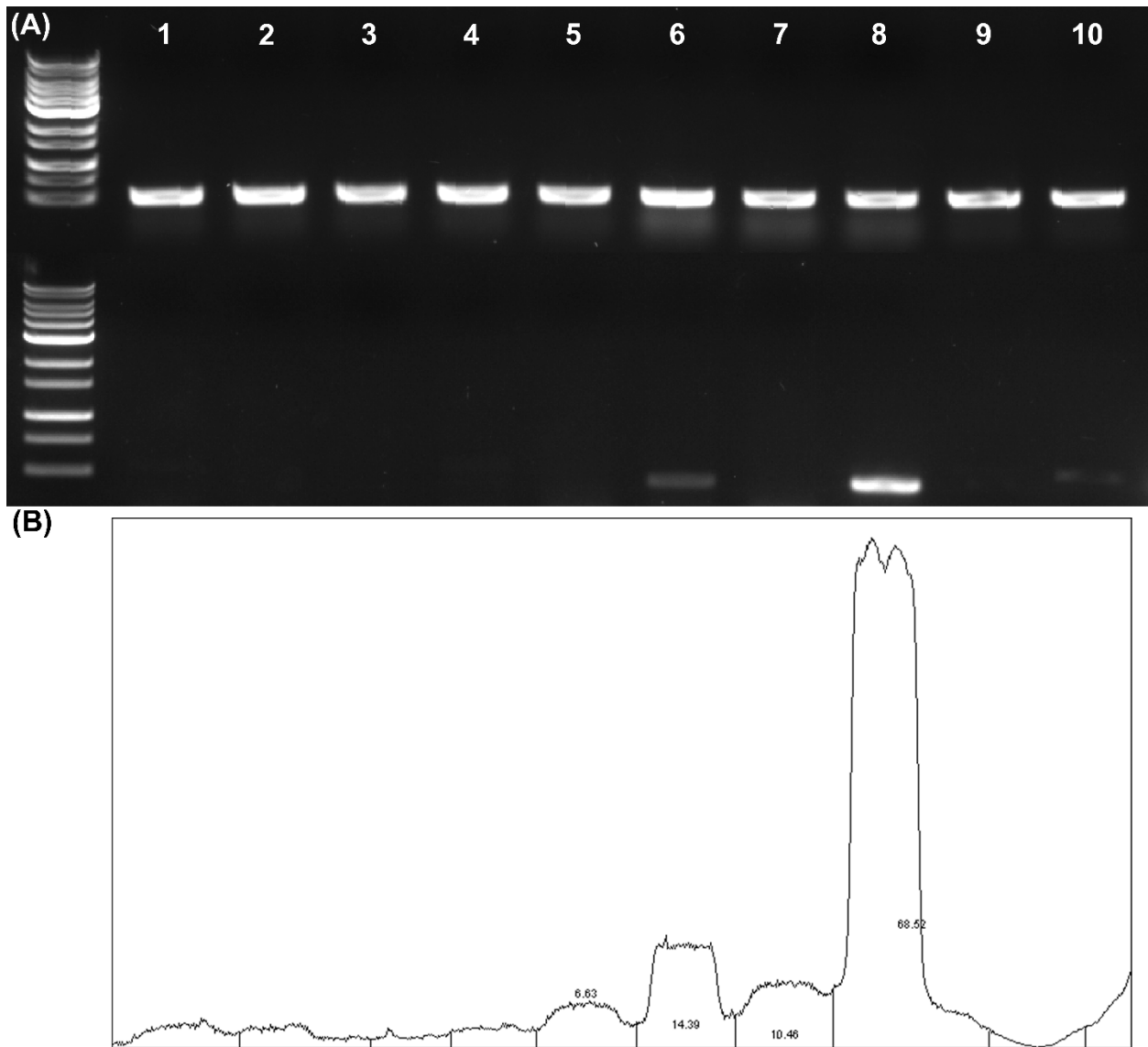


Figure 4.10. The *SbTDR* gene is expressed in anthers only from tetrads to pollen stages. (A) Expression of actin and *SbTDR* in seedlings, spikelets, and anthers over development as detected by RT-PCR. (B) Semi-quantitative output of *SbTDR* expression using band intensity over all stages. Stages: 1- seedling, 2- pre-PMCs spikelets with anther primordia 3- PMCs spikelets 4- PMCs anthers 5- tetrads spikelets 6- tetrads anthers 7- microspores spikelets 8- microspores anthers, 9- mature spikelets, and 10- mature anthers.

Table 4.1. Primers used in this study

Primer Name	Sequence	Purpose
Sb04g030850 Seq 1F	GTTTTGTCTCCTGCCTTTGC	<i>ms8</i> sequencing
Sb04g030850 Seq 1R	CATGTTCCAATACATCCTGTACG	<i>ms8</i> sequencing
Sb04g030850 Seq 2F	CTCATTTTCCACAGTTGCATGG	<i>ms8</i> sequencing
Sb04g030850 Seq 2R	CTAAAGAGCAGACCAGCATG	<i>ms8</i> sequencing
Sb04g001650 Seq F	GACCCGTTCCAGGCGGTG	<i>Sbtdr</i> sequencing
Sb04g001650 Seq R	ACGGCAGCGCGGAAGACG	<i>Sbtdr</i> sequencing
Sb05g003880 RT F	TTCACGAGACTACCTACAAC	<i>ACTIN1</i> RT-PCR control
Sb05g003880 RT R	ATCAAGTGAGAAGCATAGGT	<i>ACTIN1</i> RT-PCR control
Sb04g030850 RT F	GTCCAAGATCGTATCCTCAG	<i>MS8</i> RT-PCR
Sb04g030850 RT R	TATGCGGACATCAACATCGC	<i>MS8</i> RT-PCR
Sb04g001650 RT F	GACCCGTTCCAGGCGGTG	<i>Sbtdr</i> RT-PCR
Sb04g001650 RT R	GTTCTGCAGACCCACGATGT	<i>Sbtdr</i> RT-PCR

Chapter 5

Summary

5.1 Summary of key findings

Using *S. bicolor* as my study organism, this study evaluated several key areas of fertility to further the efforts to maximize sorghum seed yield. First, I studied the effects of heat stress. The presented work filled a key void in understanding sorghum heat stress by using different durations of heat stress, observing the effects of heat stress beginning at pollen mother cell (PMCs) anther stage 5, and focusing on early pollen production at booting. It was identified that mild heat stress has minimal effects on plant size and tiller number. I further demonstrated that male fertility is particularly sensitive to heat stress in sorghum. Heat stress applied beginning at PMCs for 12 days and at booting stage for 3 days had devastating effects on seed yield. Interestingly, when heat stress was applied from PMCs through booting, maximum yield loss occurred, suggesting that heat stress during early anther development increased the effects of heat stress treatment. In the three day booting experiment problems were observed in anther dehiscence, pollen germination, and tillers that formed at the apex of the plant. I proposed that altered auxin signaling may be responsible for the apical tiller formation in heat-stressed plants.

Second, I studied flower development in *S. bicolor*. Maximizing grain yield is a driving force in cereal grain research. To maximize yield, it is important to have a complete understanding of the steps leading to the formation of seed, starting with the production of spikelets. The sorghum BTx623 WT produces two spikelet types, the

bisexually fertile sessile spikelets and the bisexually sterile pedicellate spikelets.

Previously, little was known why over half of the spikelets yielded no seeds. I completely characterized spikelet development. In doing so, I identified key developmental stages surrounding a pedicellate developmental lag and pedicellate floret degeneration in the WT. In *msd1*, I observed this developmental lag followed by rapid pedicellate growth and bisexual pedicellate fertility. In *msal*, I characterized the mutant as producing an increased but variable number of carpels and no stamen development. After the SEM studies I targeted the developmental lag and the onset of degeneration using RNA-seq to study genes important for sessile floret fertility. I identified key potential pathways involved in TCP transcription factors, MADS-box genes and phytohormones (particularly jasmonic acid), which likely contribute to pedicellate sterility.

Third, and finally, I examined anther development in *S. bicolor*. I established a complete anther developmental series for both the WT and the *ms8* mutant and compared key stages in the *Sbtdr* mutant. I demonstrated that the differentiation of anther wall cells in *ms8* and *Sbtdr* anthers is normal, but defects are first detected after meiosis. The primary findings were: hypervacuolated tapetal cells that filled the anther lobes, delayed tapetal degeneration, no pollen production, and complete anther collapse. We cloned the *MS8* and *SbTDR* genes. I showed that *MS8* was specifically expressed in spikelets and anthers from PMCs through the pollen stage. In *SbTDR*, the expression pattern was even more specific, with only expression in the anthers from tetrads through early pollen.

5.2 Future work on sorghum heat stress

Complete sterility resulted from 12 days of heat stress at PMCs and near sterility from 3 days of heat stress at early pollen (booting stage). I hypothesized that the additional heat stress applied at PMCs had devastating effects on fertility. To test this idea, sectioning tissue from the 6 and 9 day heat stress samples to look for variations from my recently completed normal anther developmental series. Transmission electron microscopy during stages like early pollen would test whether heat stress damaged the ultrastructure of organelles or perhaps altered tapetal cell degeneration. Additionally, there is a *heat sensitive (hs)* sorghum mutant available that has not been fully characterized. Work on the *hs* mutant would provide a valuable addition to heat stress studies in sorghum.

In the three day heat stressed plants, the formation of tillers at the apex was unexpected. Tillers typically emerge from basal nodes and form complete plants, while the tillers from the apical nodes quickly formed seed heads and salvaged yield. The preliminary work suggested that auxin signaling may play a key role in the formation of these tillers. Auxin applied in the pilot study blocked the formation of all tillers, consistent with the known role of auxin in blocking lateral growth and promoting apical dominance (Booker et al., 2003). Quantifying auxin and its precursors in the apical plant tissues could better explore the role of auxin in sorghum tillering. Several approaches exist and the basic protocol includes extraction, purification, and analysis using a technique like Gas chromatography–mass spectrometry. In addition, genes involved in auxin biosynthesis and signaling have been described in sorghum. In particular, three auxin genes *SbIAA1*, *SbGH3-13*, and *SbLBD32* have been associated with abiotic

stress response (Wang et al., 2010). To better support the auxin-based hypothesis, I would collect plant samples from control and heat-stressed plant apices and measure or quantify the expression of these genes with qRT. In addition to testing auxin gene expression and production, there are key tillering mutants including *monoculm* (*moc*), *multiple tillers* (*mtl*) and *nodal tillers* (*ntl*) that could provide an alternate way to look at the role of auxin signaling in sorghum tillering. Of particular interest is the currently uncharacterized *ntl* mutant which produces upper nodal tillers (Jiao et al., 2016). Future work to elucidate and manipulate this proposed auxin signaling mechanism in sorghum could stimulate formation of multiple seed heads and greatly improve yield.

5.3 Future work to manipulate pedicellate spikelet sterility

Of particular significance in the study of pedicellate fertility was the altered expression of *SbTCP2*. *SbTCP2* is the sorghum ortholog of *TB1* in maize and *VRS5 (INT-C)* in barley, which affects the fertility of lateral branching. While generally *TB1* limits growth, recent work in wheat suggested that the paired spikelet trait may be promoted by *TB1* expression (Dixon et al., 2018). I have two opposing hypotheses. The first is that *SbTB1* in sorghum promotes spikelet formation. In this case, increased pedicellate expression would convert this sterile floret to a fertile floret. An over-expression study could test this hypothesis. The second is that *SbTB1* acts as the proposed block to pedicellate fertility. Future work to knock out *SbTB1* using RNAi or CRISPR/Cas9 to remove this blockade would show if the *SbTB1* does negatively regulate pedicellate fertility. Further functional studies should be completed in key jasmonic acid genes. This work would better explain the sterility pathway and support past study in *msd1* (Jiao et al., 2018b). In particular,

studying the connection between jasmonic acid genes, *TASSELSEED* genes, and reproductive floral whorl development in sorghum would be very interesting. Currently, the sorghum MADS-box genes have received little study, and few have been cloned. Interesting expression patterns were detected, particularly in the B- and C-class MADS-box genes. Manipulating these genes as described may have the greatest promise in overcoming the pedicellate developmental lag.

5.4 Future work to use the *ms8* and *Sbtdr* mutants in 2-line breeding systems

I characterized two new male sterile mutants in sorghum with clear defects in tapetal cell development and degeneration. There are several projects that are in progress. First, I will perform *in situ* hybridization to show the expression pattern of *MS8* and *SbTDR* in sorghum spikelets and anthers. Second, in the lab we are working to finalize constructs using *ms8-1* to utilize in 2-line breeding systems, and have already transformed one construct that is currently being analyzed. Third and finally, to study the upstream and downstream genes in this network. As described, there are numerous bHLH transcription factors controlling tapetal PCD. In the future, it would be interesting to compare expression of other possible genes in the pathway (based on known orthologs) in the mutant and WT background to detect differences. Alternatively, over-expressing *MS8* and *SbTDR* and looking at its effects on possible downstream genes would also be useful. Further work using ChIP-seq could also be used for genome-wide mapping of transcription factor binding sites. More information about these genes in sorghum is key to understanding male fertility and in future development of lines for hybrid breeding.

5.5 Concluding remarks

Throughout these studies of *S. bicolor*, my results have important implications ranging from agricultural work including planting dates/times and hybrid breeding possibilities to vast future genetic work to maximize yield. One important gap that I addressed was establishing important foundational resources in sorghum. Both the anther series and the sessile and pedicellate floral developmental series comparison had not been previously completed. In addition to these valuable resources for future researchers, this work added greatly to the study of fertility in sorghum. In this fertility work, I highlighted the impressive heat stress resistance of sorghum and determined the most sensitive floral stages to improve future growing of this important crop. Additionally, I proposed here a new area of study with the potential to increase the number of seed heads produced. In my floral development work, altered gene expression pathways were identified that may control pedicellate sterility. The continued study of these genes could lead to the production of high yielding sorghum varieties. Finally, I characterized the development of two valuable male sterile mutants. These male sterile mutants are actively being studied for use in NMS breeding systems and have strong potential to improve yield through hybrid breeding efforts. Overall, these studies greatly improve what is known about sorghum flower development and fertility and provide important resources to launch future work.

References

- Acosta, I.F., Laparra, H., Romero, S.P., Schmelz, E., Hamberg, M., Mottinger, J.P., Moreno, M.A., Dellaporta, S.L., 2009. *tasse/seed1* is a lipoxygenase affecting jasmonic acid signaling in sex determination of maize. *Science* 323, 262-265. <https://doi.org/10.1126/science.1164645>.
- Aggarwal, P., Padmanabhan, B., Bhat, A., Sarvepalli, K., Sadhale, P.P., Nath, U., 2011. The TCP4 transcription factor of *Arabidopsis* blocks cell division in yeast at G1 -> S transition. *Biochem. Bioph. Res. Co.* 410, 276-281. <https://doi.org/10.1016/j.bbrc.2011.05.132>.
- Aguiar-Martinez, J.A., Poza-Carrion, C., Cubas, P., 2007. *Arabidopsis* *BRANCHED1* acts as an integrator of branching signals within axillary buds. *Plant Cell* 19, 458-472. <https://doi.org/10.1105/tpc.106.048934>.
- Alexander, M.P., 1969. Differential staining of aborted and nonaborted pollen. *Stain Technol.* 44, 117-122. <https://doi.org/10.3109/10520296909063335>.
- Ambrose, B.A., Lerner, D.R., Ciceri, P., Padilla, C.M., Yanofsky, M.F., Schmidt, R.J., 2000. Molecular and genetic analyses of the *silky1* gene reveal conservation in floral organ specification between eudicots and monocots. *Mol. Cell* 5, 569-579. [https://doi.org/10.1016/s1097-2765\(00\)80450-5](https://doi.org/10.1016/s1097-2765(00)80450-5).
- Andrews, S., 2014. FastQC a quality control tool for high throughput sequence data. <http://www.bioinformatics.babraham.ac.uk/projects/fastqc/>
- Aryal, R., Ming, R., 2014. Sex determination in flowering plants: Papaya as a model system. *Plant Sci.* 217, 56-62. <https://doi.org/10.1016/j.plantsci.2013.10.018>.
- Bannenberg, G., Martínez, M., Hamberg, M., Castresana, C., 2009. Diversity of the enzymatic activity in the lipoxygenase gene family of *Arabidopsis thaliana*. *Lipids* 44, 85. <https://doi.org/10.1007/s11745-008-3245-7>.
- Becker, A., Winter, K.U., Meyer, B., Saedler, H., Theissen, G., 2000. MADS-box gene diversity in seed plants 300 million years ago. *Mol. Biol. Evol.* 17, 1425-1434. <https://doi.org/10.1093/oxfordjournals.molbev.a026243>.
- Bennett, T., Sieberer, T., Willett, B., Booker, J., Luschnig, C., Leyser, O., 2006. The *Arabidopsis* MAX pathway controls shoot branching by regulating auxin transport. *Curr. Biol.* 16, 553-563. <https://doi.org/10.1016/j.cub.2006.01.058>.
- Beveridge, C.A., Ross, J.J., Murfet, I.C., 1994. Branching mutant *rms-2* in *Pisum sativum* (grafting studies and endogenous indole-3-acetic acid levels). *Plant Physiol.* 104, 953-959. <https://doi.org/10.1104/pp.104.3.953>.
- Bommert, P., Satoh-Nagasawa, N., Jackson, D., Hirano, H.Y., 2005. Genetics and evolution of inflorescence and flower development in grasses. *Plant Cell Physiol.* 46, 69-78. <https://doi.org/10.1093/pcp/pci504>.
- Booker, J., Chatfield, S., Leyser, O., 2003. Auxin acts in xylem-associated or medullary cells to mediate apical dominance. *Plant Cell* 15, 495-507. <https://doi.org/10.1105/tpc.007542>.
- Bowman, J.L., Drews, G.N., Meyerowitz, E.M., 1991. Expression of the *Arabidopsis* floral homeotic gene *AGAMOUS* is restricted to specific cell types late in flower development. *Plant Cell* 3, 749-758. <https://doi.org/10.1105/tpc.3.8.749>.
- Bradley, D., Carpenter, R., Sommer, H., Hartley, N., Coen, E., 1993. Complementary floral homeotic phenotypes result from opposite orientations of a transposon at the *plena* locus of *Antirrhinum*. *Cell* 72, 85-95. [https://doi.org/10.1016/0092-8674\(93\)90052-R](https://doi.org/10.1016/0092-8674(93)90052-R).
- Bull, H., Casao, M.C., Zwirek, M., Flavell, A.J., Thomas, W.T.B., Guo, W.B., Zhang, R.X., Rapazote-Flores, P., Kyriakidis, S., Russell, J., Druka, A., McKim, S.M., Waugh, R., 2017. Barley *SIX-ROWED SPIKE3* encodes a putative Jumonji C-type H3K9me2/me3 demethylase that represses lateral spikelet fertility. *Nat. Commun.* 8. <https://doi.org/10.1038/s41467-017-00940-7>.
- Burow, G., Xin, Z.G., Hayes, C., Burke, J., 2014. Characterization of a multiseeded (*msd1*) mutant of Sorghum for increasing grain yield. *Crop Sci.* 54, 2030-2037. <https://doi.org/10.2135/cropsci2013.08.0566>.

- Caldelari, D., Wang, G.G., Farmer, E.E., Dong, X.N., 2011. *Arabidopsis lox3 lox4* double mutants are male sterile and defective in global proliferative arrest. *Plant Mol. Biol.* 75, 25-33. <https://doi.org/10.1007/s11103-010-9701-9>.
- Calderon-Urrea, A., Dellaporta, S.L., 1999. Cell death and cell protection genes determine the fate of pistils in maize. *Development* 126, 435-441.
- Carpita, N.C., McCann, M.C., 2008. Maize and Sorghum: genetic resources for bioenergy grasses. *Trends Plant Sci.* 13, 415-420. <https://doi.org/10.1016/j.tplants.2008.06.002>.
- Chang, Z.Y., Chen, Z.F., Wang, N., Xie, G., Lu, J.W., Yan, W., Zhou, J.L., Tang, X.Y., Deng, X.W., 2016. Construction of a male sterility system for hybrid rice breeding and seed production using a nuclear male sterility gene. *Proc. Natl. Acad. Sci. U. S. A.* 113, 14145-14150. <https://doi.org/10.1073/pnas.1613792113>.
- Chase, C.D., Gabay-Laughnan, S., 2004. Cytoplasmic male sterility and fertility restoration by nuclear genes, in: Daniell, H., Chase, C. (Eds.), *Molecular biology and biotechnology of plant organelles: Chloroplasts and mitochondria*. Springer Netherlands, Dordrecht, pp 593-621.
- Chen, F., Zhang, X.T., Liu, X., Zhang, L.S., 2017. Evolutionary analysis of MIKCC-type MADS-box genes in gymnosperms and angiosperms. *Front. Plant Sci.* 8. <https://doi.org/10.3389/fpls.2017.00895>.
- Cheng, P.C., Greyson, R.I., Walden, D.B., 1979. Comparison of anther development in genic male-sterile (*ms10*) and in male-fertile corn (*Zea mays*) from light microscopy and scanning electron microscopy. *Can. J. Bot.* 57, 578-596. <https://doi.org/10.1139/b79-076>.
- Cheng, P.C., Greyson, R.I., Walden, D.B., 1983. Organ initiation and the development of unisexual flowers in the tassel and ear of *Zea mays*. *Am. J. Bot.* 70, 450-462. <https://doi.org/10.2307/2443252>.
- Christensen, J.E., Horner, J., H. T., Lersten, N.R., 1972. Pollen wall and tapetal orbicular wall development in *Sorghum bicolor* (Gramineae). *Am. J. Bot.* 59, 43-58. <https://doi.org/10.1002/j.1537-2197.1972.tb10061.x>.
- Chung, Y.Y., Kim, S.R., Kang, H.G., Noh, Y.S., Park, M.C., Finkel, D., An, G.H., 1995. Characterization of 2 rice MADS box genes homologous to *GLOBOSA*. *Plant Sci.* 109, 45-56. [https://doi.org/10.1016/0168-9452\(95\)04153-L](https://doi.org/10.1016/0168-9452(95)04153-L).
- Ciacci, C., Maiuri, L., Caporaso, N., Bucci, C., Del Giudice, L., Massardo, D.R., Pontieri, P., Di Fonzo, N., Bean, S.R., Loerger, B., Londei, M., 2007. Celiac disease: In vitro and in vivo safety and palatability of wheat-free sorghum food products. *Clin. Nutr.* 26, 799-805. <https://doi.org/10.1016/j.clnu.2007.05.006>.
- Colombo, D., Crovetto, G.M., Colombini, S., Galassi, G., Rapetti, L., 2007. Nutritive value of different hybrids of sorghum forage determined in vitro. *Ital. J. Anim. Sci.* 6, 289-291. <https://doi.org/10.4081/ijas.2007.1s.289>.
- Colombo, L., Marziani, G., Masiero, S., Wittich, P.E., Schmidt, R.J., Gorla, M.S., Pe, M.E., 1998. *BRANCHED SILKLESS* mediates the transition from spikelet to floral meristem during *Zea mays* ear development. *Plant J.* 16, 355-363. <https://doi.org/10.1046/j.1365-3113x.1998.00300.x>.
- Craufurd, P.Q., Peacock, J.M., 1993. Effect of heat and drought stress on sorghum (*Sorghum bicolor*). II. Grain yield. *Exp. Agr.* 29, 77-86. <https://doi.org/10.1017/S0014479700020421>.
- Das, S., Krishnan, P., Nayak, M., Ramakrishnan, B., 2014. High temperature stress effects on pollens of rice (*Oryza sativa* L.) genotypes. *Environ. Exp. Bot.* 101, 36-46. <https://doi.org/10.1016/j.envexpbot.2014.01.004>.
- Daviere, J.M., Wild, M., Regnault, T., Baumberger, N., Eisler, H., Genschik, P., Achard, P., 2014. Class I TCP-DELLA interactions in inflorescence shoot apex determine plant height. *Curr. Biol.* 24, 1923-1928. <https://doi.org/10.1016/j.cub.2014.07.012>.
- De Storme, N., Geelen, D., 2014. The impact of environmental stress on male reproductive development in plants: biological processes and molecular mechanisms. *Plant. Cell Environ.* 37, 1-18. <https://doi.org/10.1111/pce.12142>.
- Deblock, M., Debrouwer, D., 1993. Engineered fertility control in transgenic *Brassica napus* L.: Histochemical analysis of anther development. *Planta* 189, 218-225. <https://doi.org/10.1007/Bf00195080>.
- DeBlock, M., Debrouwer, D., Moens, T., 1997. The development of a nuclear male sterility system in wheat. Expression of the *barnase* gene under the control of tapetum specific promoters. *Theor. Appl. Genet.* 95, 125-131. <https://doi.org/10.1007/s001220050540>.

- Dietrich, P.S., Bouchard, R.A., Casey, E.S., Sinibaldi, R.M., 1991. Isolation and characterization of a small heat shock protein gene from maize. *Plant Physiol.* 96, 1268-1276.
<https://doi.org/10.1104/pp.96.4.1268>.
- Dill, A., Thomas, S.G., Hu, J.H., Steber, C.M., Sun, T.P., 2004. The *Arabidopsis* F-box protein SLEEPY1 targets gibberellin signaling repressors for gibberellin-induced degradation. *Plant Cell* 16, 1392-1405. <https://doi.org/10.1105/tpc.020958>.
- Ditta, G., Pinyopich, A., Robles, P., Pelaz, S., Yanofsky, M.F., 2004. The *SEP4* gene of *Arabidopsis thaliana* functions in floral organ and meristem identity. *Curr. Biol.* 14, 1935-1940.
<https://doi.org/10.1016/j.cub.2004.10.028>.
- Dixon, L.E., Greenwood, J.R., Bencivenga, S., Zhang, P., Cockram, J., Mellers, G., Ramm, K., Cavanagh, C., Swain, S.M., Boden, S.A., 2018. *TEOSINTE BRANCHED1* Regulates Inflorescence Architecture and Development in Bread Wheat (*Triticum aestivum*). *Plant Cell* 30, 563-581.
<https://doi.org/10.1105/tpc.17.00961>.
- Doebley, J., Stec, A., Hubbard, L., 1997. The evolution of apical dominance in maize. *Nature* 386, 485-488. <https://doi.org/10.1038/386485a0>.
- Doggett, H., 1988. Sorghum, Second ed. Longman, New York.
- Domagalska, M.A., Schomburg, F.M., Amasino, R.M., Vierstra, R.D., Nagy, F., Davis, S.J., 2007. Attenuation of brassinosteroid signaling enhances *FLC* expression and delays flowering. *Development* 134, 2841-2850. <https://doi.org/10.1242/dev.02866>.
- Dun, E.A., de Saint Germain, A., Rameau, C., Beveridge, C.A., 2012. Antagonistic action of strigolactone and cytokinin in bud outgrowth control. *Plant Physiol.* 158, 487-498.
<https://doi.org/10.1104/pp.111.186783>.
- Dupuis, I., Dumas, C., 1990. Influence of temperature stress on in vitro fertilization and heat shock protein synthesis in maize (*Zea mays* L.) reproductive tissues. *Plant Physiol.* 94, 665-670.
<https://doi.org/10.1104/pp.94.2.665>.
- Dykes, L., Rooney, L.W., 2006. Sorghum and millet phenols and antioxidants. *J. Cereal. Sci.* 44, 236-251.
<https://doi.org/10.1016/j.jcs.2006.06.007>.
- Dykstra, M.J., 1993. A manual of applied techniques for biological electron microscopy. Plenum Press, New York.
- Ebercon, A., Blum, A., Jordan, W., 1977. A rapid colorimetric method for epicuticular wax content of sorghum leaves *Crop Sci.* 17, 179-180.
<https://doi.org/10.2135/cropsci1977.0011183X001700010047x>.
- Endo, M., Tsuchiya, T., Hamada, K., Kawamura, S., Yano, K., Ohshima, M., Higashitani, A., Watanabe, M., Kawagishi-Kobayashi, M., 2009. High temperatures cause male sterility in rice plants with transcriptional alterations during pollen development. *Plant Cell Physiol.* 50, 1911-1922.
<https://doi.org/10.1093/pcp/pcp135>.
- FAOSTAT, 2019. FAOSTAT statistics database. <http://www.fao.org/faostat/en/#home>.
- Feng, N., Song, G.Y., Guan, J.T., Chen, K., Jia, M.L., Huang, D.H., Wu, J.J., Zhang, L.C., Kong, X.Y., Geng, S.F., Liu, J., Li, A.L., Mao, L., 2017. Transcriptome profiling of wheat inflorescence development from spikelet initiation to floral patterning identified stage-specific regulatory genes. *Plant Physiol.* 174, 1779-1794. <https://doi.org/10.1104/pp.17.00310>.
- Ferreira, S.D., Nishiyama, M.Y., Paterson, A.H., Souza, G.M., 2013. Biofuel and energy crops: high-yield Saccharinae take center stage in the post-genomics era. *Genome Biol.* 14.
<https://doi.org/10.1186/gb-2013-14-6-210>.
- Ferris, R., Ellis, R.H., Wheeler, T.R., Hadley, P., 1998. Effect of high temperature stress at anthesis on grain yield and biomass of field-grown crops of wheat. *Ann. Bot.* 82, 631-639.
<https://doi.org/10.1006/anbo.1998.0740>.
- Fornara, F., Parenicova, L., Falasca, G., Pelucchi, N., Masiero, S., Ciannamea, S., Lopez-Dee, Z., Altamura, M.M., Colombo, L., Kater, M.M., 2004. Functional characterization of *OsMADS18*, a member of the *AP1/SQUA* subfamily of MADS box genes. *Plant Physiol.* 135, 2207-2219.
<https://doi.org/10.1104/pp.104.045039>.
- Francis, A., Dhaka, N., Bakshi, M., Jung, K.H., Sharma, M.K., Sharma, R., 2016. Comparative phylogenomic analysis provides insights into TCP gene functions in *Sorghum*. *Sci. Rep.* 6.
<https://doi.org/10.1038/srep38488>.

- Fu, Z., Yu, J., Cheng, X., Zong, X., Xu, J., Chen, M., Li, Z., Zhang, D., Liang, W., 2014. The rice basic helix-loop-helix transcription factor TDR INTERACTING PROTEIN2 is a central switch in early anther development. *Plant Cell* 26, 1512-1524. <https://doi.org/10.1105/tpc.114.123745>.
- Gao, S., Xie, X., Yang, S., Chen, Z., Wang, X., 2012. The changes of GA level and signaling are involved in the regulation of mesocotyl elongation during blue light mediated de-etiolation in *Sorghum bicolor*. *Mol. Biol. Rep.* 39, 4091-4100. <https://doi.org/10.1007/s11033-011-1191-6>.
- Gao, X., Liang, W., Yin, C., Ji, S., Wang, H., Su, X., Guo, C., Kong, H., Xue, H., Zhang, D., 2010. The *SEPALLATA*-like gene *OsMADS34* is required for rice inflorescence and spikelet development. *Plant Physiol.* 153, 728-740. <https://doi.org/10.1104/pp.110.156711>.
- Gao, Y.H., Zhang, D.Z., Li, J., 2015. TCP1 modulates *DWF4* expression via directly interacting with the GGCC motifs in the promoter region of *DWF4* in *Arabidopsis thaliana*. *J. Genet. Genomics* 42, 383-392. <https://doi.org/10.1016/j.jgg.2015.04.009>.
- Garg, R., Jhanwar, S., Tyagi, A.K., Jain, M., 2010. Genome-wide survey and expression analysis suggest diverse roles of glutaredoxin gene family members during development and response to various stimuli in rice. *DNA Res.* 17, 353-367. <https://doi.org/10.1093/dnares/dsq023>.
- Glaser, G., Dubugnon, L., Mousavi, S.A.R., Rudaz, S., Wolfender, J.L., Farmer, E.E., 2009. Velocity estimates for signal propagation leading to systemic jasmonic acid accumulation in wounded *Arabidopsis*. *J. Biol. Chem.* 284, 34506-34513. <https://doi.org/10.1074/jbc.M109.061432>.
- Gomez-Roldan, V., Fermas, S., Brewer, P.B., Puech-Pages, V., Dun, E.A., Pillot, J.P., Letisse, F., Matusova, R., Danoun, S., Portais, J.C., Bouwmeester, H., Becard, G., Beveridge, C.A., Rameau, C., Rochange, S.F., 2008. Strigolactone inhibition of shoot branching. *Nature* 455, 189-194. <https://doi.org/10.1104/pp.15.00014>.
- Goto, K., Meyerowitz, E.M., 1994. Function and regulation of the *Arabidopsis* floral homeotic gene *PISTILLATA*. *Genes Dev.* 8, 1548-1560. <https://doi.org/10.1101/gad.8.13.1548>
- Graham, R.L., Nelson, R., Sheehan, J., Perlack, R.D., Wright, L.L., 2007. Current and potential US corn stover supplies. *Agron. J.* 99, 1-11. <https://doi.org/10.2134/argonj2005.0222>.
- Greco, R., Stagi, L., Colombo, L., Angenent, G.C., SariGorla, M., Pe, M.E., 1997. MADS box genes expressed in developing inflorescences of rice and sorghum. *Mol. Gen. Genet.* 253, 615-623. <https://doi.org/10.1007/s004380050364>.
- Guo, Z.X., Fujioka, S., Blancaflor, E.B., Miao, S., Gou, X.P., Li, J., 2010. TCP1 modulates brassinosteroid biosynthesis by regulating the expression of the key biosynthetic gene *DWARF4* in *Arabidopsis thaliana*. *Plant Cell* 22, 1161-1173. <https://doi.org/10.1105/tpc.109.069203>.
- Hamberg, M., Fahlstadius, P., 1990. Allene oxide cyclase: a new enzyme in plant lipid metabolism. *Arch. Biochem. Biophys.* 276, 518-526. [https://doi.org/10.1016/0003-9861\(90\)90753-L](https://doi.org/10.1016/0003-9861(90)90753-L).
- Harris, K., Subudhi, P.K., Borrell, A., Jordan, D., Rosenow, D., Nguyen, H., Klein, P., Klein, R., Mullet, J., 2007. Sorghum stay-green QTL individually reduce post-flowering drought-induced leaf senescence. *J. Exp. Bot.* 58, 327-338. <https://doi.org/10.1093/jxb/erl225>.
- Harsant, J., Pavlovic, L., Chiu, G., Sultmanis, S., Sage, T.L., 2013. High temperature stress and its effect on pollen development and morphological components of harvest index in the C-3 model grass *Brachypodium distachyon*. *J. Exp. Bot.* 64, 2971-2983. <https://doi.org/10.1093/jxb/ert142>.
- Hay, R., 2018. Investigation of the role of gene clusters in terpene biosynthesis in *Sorghum bicolor*. Master of Science. <https://irl.umsl.edu/thesis/320>
- Hedden, P., Phillips, A.L., 2000. Gibberellin metabolism: new insights revealed by the genes. *Trends Plant Sci.* 5, 523-530. [https://doi.org/10.1016/S1360-1385\(00\)01790-8](https://doi.org/10.1016/S1360-1385(00)01790-8).
- Hernandez-Pinzon, I., Ross, J.H., Barnes, K.A., Damant, A.P., Murphy, D.J., 1999. Composition and role of tapetal lipid bodies in the biogenesis of the pollen coat of *Brassica napus*. *Planta* 208, 588-598. <https://doi.org/10.1007/s004250050597>.
- Holdorf, M.M., Owen, H.A., Lieber, S.R., Yuan, L., Adams, N., Dabney-Smith, C., Makaroff, C.A., 2012. *Arabidopsis* *ETHE1* encodes a sulfur dioxygenase that is essential for embryo and endosperm development. *Plant Physiol.* 160, 226-236. <https://doi.org/10.1104/pp.112.201855>.
- Hong, L., Qian, Q., Zhu, K., Tang, D., Huang, Z., Gao, L., Li, M., Gu, M., Cheng, Z., 2010. ELE restrains empty glumes from developing into lemmas. *J. Genet. Genome Res.* 37, 101-115. [https://doi.org/10.1016/S1673-8527\(09\)60029-1](https://doi.org/10.1016/S1673-8527(09)60029-1).

- Hong, L.L., Tang, D., Zhu, K.M., Wang, K.J., Li, M., Cheng, Z.K., 2012. Somatic and reproductive cell development in rice anther is regulated by a putative glutaredoxin. *Plant Cell* 24, 577-588. <https://doi.org/10.1105/tpc.111.093740>.
- Hopf, N., Plesofskyvig, N., Brambl, R., 1992. The heat shock response of pollen and other tissues of maize. *Plant Mol. Biol.* 19, 623-630. <https://doi.org/10.1007/bf00026788>.
- Hsieh, K., Huang, A.H., 2007. Tapetosomes in Brassica tapetum accumulate endoplasmic reticulum-derived flavonoids and alkanes for delivery to the pollen surface. *Plant Cell* 19, 582-596. <https://doi.org/10.1105/tpc.106.049049>.
- Huang, J., Wijeratne, A.J., Tang, C., Zhang, T., Fenelon, R.E., Owen, H.A., Zhao, D., 2016. Ectopic expression of *TAPETUM DETERMINANT1* affects ovule development in *Arabidopsis*. *J. Exp. Bot.* 67, 1311-1326. <https://doi.org/10.1093/jxb/erv523>.
- Huang, J.Z., E, Z.G., Zhang, H.L., Shu, Q.Y., 2014. Workable male sterility systems for hybrid rice: Genetics, biochemistry, molecular biology, and utilization. *Rice* 7. <https://doi.org/10.1186/s12284-014-0013-6>.
- Hubbard, L., McSteen, P., Doebley, J., Hake, S., 2002. Expression patterns and mutant phenotype of *teosinte branched1* correlate with growth suppression in maize and teosinte. *Genetics* 162, 1927-1935.
- Huijser, P., Klein, J., Lönning, W., Meijer, H., Saedler, H., Sommer, H., 1992. Bracteomania, an inflorescence anomaly, is caused by the loss of function of the MADS-box gene *squamosa* in *Antirrhinum majus*. *EMBO J.* 11, 1239-1249. <https://doi.org/10.1002/j.1460-2075.1992.tb05168.x>.
- Ikeda, K., Sunohara, H., Nagato, Y., 2004. Developmental course of inflorescence and spikelet in rice. *Breed. Sci.* 54, 147-156. <https://doi.org/10.1270/jsbbs.54.147>.
- IPCC, 2013. Climate change 2013: The physical science basis. Working group I contribution to the fifth assessment report of the intergovernmental panel on climate change.
- Irish, E.E., Langdale, J.A., Nelson, T.M., 1994. Interactions between *tassel seed* genes and other sex determining genes in maize. *Dev. Genet.* 15, 155-171. <https://doi.org/10.1002/dvg.1020150206>.
- Isbell, V.R., Morgan, P.W., 1982. Manipulation of apical dominance in sorghum with growth regulators. *Crop Sci.* 22, 30-35. <https://doi.org/10.2135/cropsci1982.0011183X002200010007x>.
- Ishiguro, S., Kawai-Oda, A., Ueda, J., Nishida, I., Okada, K., 2001. The *DEFECTIVE IN ANTHHER DEHISCENCE1* gene encodes a novel phospholipase A1 catalyzing the initial step of jasmonic acid biosynthesis, which synchronizes pollen maturation, anther dehiscence, and flower opening in *Arabidopsis*. *Plant Cell* 13, 2191-2209. <https://doi.org/10.1105/tpc.13.10.2191>.
- Ito, T., Ng, K.H., Lim, T.S., Yu, H., Meyerowitz, E.M., 2007. The homeotic protein AGAMOUS controls late stamen development by regulating a jasmonate biosynthetic gene in *Arabidopsis*. *Plant Cell* 19, 3516-3529. <https://doi.org/10.1105/tpc.107.055467>.
- Izhar, S., Frankel, R., 1971. Mechanism of male sterility in *Petunia*: The relationship between pH, callase activity in the anthers, and the breakdown of the microsporogenesis. *Theor. Appl. Genet.* 41, 104-108. <https://doi.org/10.1007/BF00277751>.
- Jack, T., 2004. Molecular and genetic mechanisms of floral control. *Plant Cell* 16 Suppl, S1-17. <https://doi.org/10.1105/tpc.017038>.
- Jack, T., Brockman, L.L., Meyerowitz, E.M., 1992. The homeotic gene *APETALA3* of *Arabidopsis thaliana* encodes a MADS box and is expressed in petals and stamens. *Cell* 68, 683-697. [https://doi.org/10.1016/0092-8674\(92\)90144-2](https://doi.org/10.1016/0092-8674(92)90144-2).
- Jagadish, S.V.K., Craufurd, P.Q., Wheeler, T.R., 2007. High temperature stress and spikelet fertility in rice (*Oryza sativa* L.). *J. Exp. Bot.* 58, 1627-1635. <https://doi.org/10.1093/jxb/erm003>.
- Jain, M., Prasad, P.V.V., Boote, K.J., Hartwell, A.L., Chourey, P.S., 2007. Effects of season-long high temperature growth conditions on sugar-to-starch metabolism in developing microspores of grain sorghum (*Sorghum bicolor* L. Moench). *Planta* 227, 67-79. <https://doi.org/10.1007/s00425-007-0595-y>.
- Jeon, J.S., Jang, S., Lee, S., Nam, J., Kim, C., Lee, S.H., Chung, Y.Y., Kim, S.R., Lee, Y.H., Cho, Y.G., An, G., 2000a. *leafy hull sterile1* is a homeotic mutation in a rice MADS box gene affecting rice flower development. *Plant Cell* 12, 871-884. <https://doi.org/10.1105/tpc.12.6.871>.
- Jeon, J.S., Lee, S., Jung, K.H., Yang, W.S., Yi, G.H., Oh, B.G., An, G.H., 2000b. Production of transgenic rice plants showing reduced heading date and plant height by ectopic expression of rice MADS-box genes. *Mol. Breeding* 6, 581-592. <https://doi.org/10.1023/A:1011388620872>.

- Ji, C.H., Li, H.Y., Chen, L.B., Xie, M., Wang, F.P., Chen, Y.L., Liu, Y.G., 2013. A novel rice bHLH transcription factor, DTD, acts coordinately with TDR in controlling tapetum function and pollen development. *Mol. Plant* 6, 1715-1718. <https://doi.org/10.1093/mp/sst046>.
- Jiao, Y.P., Burke, J., Chopra, R., Burow, G., Chen, J.P., Wang, B., Hayes, C., Emendack, Y., Ware, D., Xin, Z.G., 2016. A sorghum mutant resource as an efficient platform for gene discovery in grasses. *Plant Cell* 28, 1551-1562. <https://doi.org/10.1105/tpc.16.00373>.
- Jiao, Y.P., Burow, G., Gladman, N., Acosta-Martinez, V., Chen, J.P., Burke, J., Ware, D., Xin, Z.G., 2018a. Efficient identification of causal mutations through sequencing of bulked F2 from two allelic Bloomless mutants of *Sorghum bicolor*. *Front. Plant Sci.* 8. <https://doi.org/10.3389/fpls.2017.02267>.
- Jiao, Y.P., Lee, Y.K., Gladman, N., Chopra, R., Christensen, S.A., Regulski, M., Burow, G., Hayes, C., Burke, J., Ware, D., Xin, Z.G., 2018b. MSD1 regulates pedicellate spikelet fertility in sorghum through the jasmonic acid pathway. *Nat. Commun.* 9. <https://doi.org/10.1038/s41467-018-03238-4>.
- Jordan, D.R., Klein, R.R., Sakreowski, K.G., Henzell, R.G., Klein, P.E., Mace, E.S., 2011. Mapping and characterization of *Rf5*: a new gene conditioning pollen fertility restoration in A1 and A2 cytoplasm in sorghum (*Sorghum bicolor* (L.) Moench). *Theor. Appl. Genet.* 123, 383-396. <https://doi.org/10.1007/s00122-011-1591-y>.
- Jordan, W.R., Shouse, P.J., Blum, A., Miller, F.R., Monk, R.L., 1984. Environmental physiology of sorghum. II. Epicuticular wax load and cuticular transpiration. *Crop Sci.* 24, 1168-1173. <https://doi.org/10.2135/cropsci1984.0011183X002400060038x>.
- Jung, K.-H., Han, M.-J., Lee, Y.-S., Kim, Y.-W., Hwang, I., Kim, M.-J., Kim, Y.-K., Nahm, B.H., An, G., 2005. Rice *Undeveloped Tapetum1* is a major regulator of early tapetum development. *Plant Cell* 17, 2705-2722. <https://doi.org/10.1105/tpc.105.034090>.
- Kakei, Y., Mochida, K., Sakurai, T., Yoshida, T., Shinozaki, K., Shimada, Y., 2015. Transcriptome analysis of hormone-induced gene expression in *Brachypodium distachyon*. *Sci. Rep.* 5. <https://doi.org/10.1038/srep14476>.
- Kaufmann, K., Muino, J.M., Jauregui, R., Airoidi, C.A., Smaczniak, C., Krajewski, P., Angenent, G.C., 2009. Target genes of the MADS transcription factor SEPALLATA3: Integration of developmental and hormonal pathways in the *Arabidopsis* flower. *Plos Biol.* 7, 854-875. <https://doi.org/10.1371/journal.pbio.1000090>.
- Keijzer, C.J., Reinders, M.C., LeferinkTenKlooster, H.B., 1996. The mechanics of the grass flower: The extension of the staminal filaments and the lodicules of maize. *Ann. Bot.* 77, 675-683. <https://doi.org/10.1006/anbo.1996.0084>.
- Kellogg, E.A., 2007. Floral displays: genetic control of grass inflorescences. *Curr. Opin. Plant Biol.* 10, 26-31. <https://doi.org/10.1016/j.pbi.2006.11.009>.
- Kim, D., Landmead, B., Salzberg, S.L., 2015. HISAT: a fast spliced aligner with low memory requirements. *Nat. Methods* 12, 357-U121. <https://doi.org/10.1038/Nmeth.3317>.
- Kim, S.Y., Hong, C.B., Lee, I., 2001. Heat shock stress causes stage-specific male sterility in *Arabidopsis thaliana*. *J. Plant Res.* 114, 301-307. <https://doi.org/10.1007/pl00013991>.
- Ko, S.S., Li, M.J., Sun-Ben Ku, M., Ho, Y.C., Lin, Y.J., Chuang, M.H., Hsing, H.X., Lien, Y.C., Yang, H.T., Chang, H.C., Chan, M.T., 2014. The bHLH142 transcription factor coordinates with TDR1 to modulate the expression of *EAT1* and regulate pollen development in rice. *Plant Cell* 26, 2486-2504. <https://doi.org/10.1105/tpc.114.126292>.
- Kobayashi, K., Maekawa, M., Miyao, A., Hirochika, H., Kyojuka, J., 2010. *PANICLE PHYTOMER2* (*PAP2*), encoding a SEPALLATA subfamily MADS-box protein, positively controls spikelet meristem identity in rice. *Plant Cell Physiol.* 51, 47-57. <https://doi.org/10.1093/pcp/pcp166>.
- Komatsuda, T., Pourkheirandish, M., He, C.F., Azhaguvel, P., Kanamori, H., Perovic, D., Stein, N., Graner, A., Wicker, T., Tagiri, A., Lundqvist, U., Fujimura, T., Matsuoka, M., Matsumoto, T., Yano, M., 2007. Six-rowed barley originated from a mutation in a homeodomain-leucine zipper I-class homeobox gene. *Proc. Natl. Acad. Sci. U. S. A.* 104, 1424-1429. <https://doi.org/10.1073/pnas.0608580104>.
- Koo, A.J.K., Cooke, T.F., Howe, G.A., 2011. Cytochrome P450 CYP94B3 mediates catabolism and inactivation of the plant hormone jasmonoyl-L-isoleucine. *Proc. Natl. Acad. Sci. U. S. A.* 108, 9298-9303. <https://doi.org/10.1073/pnas.1103542108>.

- Koppolu, R., Anwar, N., Sakuma, S., Tagiri, A., Lundqvist, U., Pourkheirandish, M., Rutten, T., Seiler, C., Himmelbach, A., Ariyadasa, R., Youssef, H.M., Stein, N., Sreenivasulu, N., Komatsuda, T., Schnurbusch, T., 2013. *Six-rowed spike4 (Vrs4)* controls spikelet determinacy and row-type in barley. *Proc. Natl. Acad. Sci. U. S. A.* 110, 13198-13203. <https://doi.org/10.1073/pnas.1221950110>.
- Ku, S.J., Cho, K.H., Choi, Y.J., Baek, W.K., Kim, S., Suh, H.S., Chung, Y.Y., 2001. Cytological observation of two environmental genic male-sterile lines of rice. *Mol. Cells* 12, 403-406.
- Ku, S.J., Yoon, H., Suh, H.S., Chung, Y.Y., 2003. Male-sterility of thermosensitive genic male-sterile rice is associated with premature programmed cell death of the tapetum. *Planta* 217, 559-565. <https://doi.org/10.1007/s00425-003-1030-7>.
- Kubigsteltig, I., Laudert, D., Weiler, E., 1999. Structure and regulation of the *Arabidopsis thaliana* allene oxide synthase gene. *Planta* 208, 463-471. <https://doi.org/10.1007/s004250050583>.
- Kumar, R.R., Pathak, H., Sharma, S.K., Kala, Y.K., Nirjal, M.K., Singh, G.P., Goswami, S., Rai, R.D., 2015. Novel and conserved heat-responsive microRNAs in wheat (*Triticum aestivum* L.). *Funct. Integr. Genomics* 15, 323-348. <https://doi.org/10.1007/s10142-014-0421-0>.
- Lafarge, T.A., Broad, I.J., Hammer, G.L., 2002. Tillering in grain sorghum over a wide range of population densities: Identification of a common hierarchy for tiller emergence, leaf area development and fertility. *Ann. Bot.* 90, 87-98. <https://doi.org/10.1093/aob/mcf152>.
- Laser, K.D., Lersten, N.R., 1972. Anatomy and cytology of microsporogenesis in cytoplasmic male sterile angiosperms. *Bot. Rev.* 38, 425-454. <https://doi.org/10.1007/bf02860010>.
- Lee, K.-w., Lommasson, R.C., Eastin, J.D., 1974. Developmental studies on the panicle initiation in Sorghum. *Crop Sci.* 14, 80-84. <https://doi.org/10.2135/cropsci1974.0011183X001400010024x>.
- Li, C.X., Potuschak, T., Colon-Carmona, A., Gutierrez, R.A., Doerner, P., 2005. *Arabidopsis* TCP20 links regulation of growth and cell division control pathways. *Proc. Natl. Acad. Sci. U. S. A.* 102, 12978-12983. <https://doi.org/10.1073/pnas.0504039102>.
- Li, H., Yuan, Z., Vizcay-Barrena, G., Yang, C.Y., Liang, W.Q., Zong, J., Wilson, Z.A., Zhang, D.B., 2011. PERSISTENT TAPETAL CELL1 encodes a PHD-finger protein that is required for tapetal cell death and pollen development in rice. *Plant Physiol.* 156, 615-630. <https://doi.org/10.1104/pp.111.175760>.
- Li, N., Zhang, D.S., Liu, H.S., Yin, C.S., Li, X.X., Liang, W.Q., Yuan, Z., Xu, B., Chu, H.W., Wang, J., Wen, T.Q., Huang, H., Luo, D., Ma, H., Zhang, D.B., 2006. The *Rice Tapetum Degeneration Retardation* gene is required for tapetum degradation and anther development. *Plant Cell* 18, 2999-3014. <https://doi.org/10.1105/tpc.106.044107>.
- Li, Y.B., Suen, D.F., Huang, C.Y., Kung, S.Y., Huang, A.H.C., 2012a. The maize tapetum employs diverse mechanisms to synthesize and store proteins and flavonoids and transfer them to the pollen surface. *Plant Physiol.* 158, 1548-1561. <https://doi.org/10.1104/pp.111.189241>.
- Li, Z.Y., Li, B., Dong, A.W., 2012b. The *Arabidopsis* transcription factor AtTCP15 Regulates endoreduplication by modulating expression of key cell-cycle genes. *Mol. Plant* 5, 270-280. <https://doi.org/10.1093/mp/ssr086>.
- Lim, J., Moon, Y.H., An, G., Jang, S.K., 2000. Two rice MADS domain proteins interact with *OsMADS1*. *Plant Mol. Biol.* 44, 513-527. <https://doi.org/10.1023/A:1026517111843>.
- Liu, H.T., Cui, P., Zhan, K.H., Lin, Q., Zhuo, G.Y., Guo, X.L., Ding, F., Yang, W.L., Liu, D.C., Hu, S.N., Yu, J., Zhang, A.M., 2011. Comparative analysis of mitochondrial genomes between a wheat K-type cytoplasmic male sterility (CMS) line and its maintainer line. *Bmc Genomics* 12. <https://doi.org/10.1186/1471-2164-12-163>.
- Lo, S.-F., Yang, S.-Y., Chen, K.-T., Hsing, Y.-I., Zeevaart, J.A., Chen, L.-J., Yu, S.-M., 2008. A novel class of gibberellin 2-oxidases control semidwarfism, tillering, and root development in rice. *Plant Cell* 20, 2603-2618. <https://doi.org/10.1105/tpc.108.060913>.
- Lombardo, F., Yoshida, H., 2015. Interpreting lemma and palea homologies: a point of view from rice floral mutants. *Front. Plant Sci.* 6. <https://doi.org/10.3389/fpls.2015.00061>.
- Lu, Y., 2011. *Arabidopsis* pollen tube aniline blue staining. *Bio. Protoc.* 1, e88. <https://doi.org/10.21769/BioProtoc.88>.
- Lux, A., Luxova, M., Hattori, T., Inanaga, S., Sugimoto, Y., 2002. Silicification in sorghum (*Sorghum bicolor*) cultivars with different drought tolerance. *Physiol. Plantarum* 115, 87-92. <https://doi.org/10.1034/j.1399-3054.2002.1150110.x>.

- Makita, Y., Shimada, S., Kawashima, M., Kondou-Kuriyama, T., Toyoda, T., Matsui, M., 2014. MOROKOSHI: transcriptome database in *Sorghum bicolor*. Plant Cell Physiol. 56, e6-e6. <https://doi.org/10.1093/pcp/pcu187>.
- Malcomber, S.T., Kellogg, E.A., 2005. *SEPALLATA* gene diversification: brave new whorls. Trends Plant Sci. 10, 427-435. <https://doi.org/10.1016/j.tplants.2005.07.008>.
- Malcomber, S.T., Kellogg, E.A., 2006. Evolution of unisexual flowers in grasses (Poaceae) and the putative sex-determination gene, *TASSELSEED2* (*TS2*). New Phytol. 170, 885-899. <https://doi.org/10.1111/j.1469-8137.2006.01726.x>.
- Mandel, M.A., Gustafsonbrown, C., Savidge, B., Yanofsky, M.F., 1992. Molecular characterization of the *Arabidopsis* floral homeotic gene *APETALA1*. Nature 360, 273-277. <https://doi.org/10.1038/360273a0>.
- Mao, H.D., Wang, H.W., Liu, S.X., Li, Z., Yang, X.H., Yan, J.B., Li, J.S., Tran, L.S.P., Qin, F., 2015. A transposable element in a *NAC* gene is associated with drought tolerance in maize seedlings. Nat. Commun. 6. <https://doi.org/10.1038/ncomms9326>.
- Mara, C.D., Irish, V.F., 2008. Two GATA transcription factors are downstream effectors of floral homeotic gene action in Arabidopsis. Plant Physiol. 147, 707-718. <https://doi.org/10.1104/pp.107.115634>.
- Mariani, C., Debeuckeleer, M., Truettner, J., Leemans, J., Goldberg, R.B., 1990. Induction of male-sterility in plants by a chimeric ribonuclease gene. Nature 347, 737-741. <https://doi.org/10.1038/347737a0>.
- Martin-Trillo, M., Grandio, E.G., Serra, F., Marcel, F., Rodriguez-Buey, M.L., Schmitz, G., Theres, K., Bendahmane, A., Dopazo, H., Cubas, P., 2011. Role of tomato *BRANCHED1*-like genes in the control of shoot branching. Plant J. 67, 701-714. <https://doi.org/10.1111/j.1365-313X.2011.04629.x>.
- Mason, M.G., Ross, J.J., Babst, B.A., Wienclaw, B.N., Beveridge, C.A., 2014. Sugar demand, not auxin, is the initial regulator of apical dominance. Proc. Natl. Acad. Sci. U. S. A. 111, 6092-6097. <https://doi.org/10.1073/pnas.1322045111>.
- Matsui, T., Omasa, K., 2002. Rice (*Oryza sativa* L.) cultivars tolerant to high temperature at flowering: Anther characteristics. Ann. Bot. 89, 683-687. <https://doi.org/10.1093/aob/mcf112>.
- Matsui, T., Omasa, K., Horie, T., 2000. High temperature at flowering inhibits swelling of pollen grains, a driving force for thecae dehiscence in rice (*Oryza sativa* L.). Plant Prod. Sci. 3, 430-434. <https://doi.org/10.1626/pp.3.430>.
- Matzrafi, M., Shaar-Moshe, L., Rubin, B., Peleg, Z., 2017. Unraveling the transcriptional basis of temperature-dependent pinoxaden resistance in *Brachypodium hybridum*. Front. Plant Sci. 8, 1-11. <https://doi.org/10.3389/fpls.2017.01064>.
- McCormick, S., 1993. Male gametophyte development. Plant Cell 5, 1265-1275. <https://doi.org/10.1105/tpc.5.10.1265>.
- McDowell, E.M., Trump, B.F., 1976. Histologic fixatives suitable for diagnostic light and electron microscopy. Arch. Pathol. Lab. Med. 100, 405-414.
- McGinnis, K.M., Thomas, S.G., Soule, J.D., Strader, L.C., Zale, J.M., Sun, T.P., Steber, C.M., 2003. The *Arabidopsis* *SLEEPY1* gene encodes a putative F-box subunit of an SCF E3 ubiquitin ligase. Plant Cell 15, 1120-1130. <https://doi.org/10.1105/tpc010827>.
- Mena, M., Mandel, M.A., Lerner, D.R., Yanofsky, M.F., Schmidt, R.J., 1995. A characterization of the MADS-box gene family in maize. Plant J. 8, 845-854. <https://doi.org/10.1046/j.1365-313X.1995.8060845.x>.
- Micheva, K.D., Smith, S.J., 2007. Array tomography: A new tool for imaging the molecular architecture and ultrastructure of neural circuits. Neuron 55, 824-824. <https://doi.org/10.1016/j.neuron.2007.08.007>.
- Minakuchi, K., Kameoka, H., Yasuno, N., Umehara, M., Luo, L., Kobayashi, K., Hanada, A., Ueno, K., Asami, T., Yamaguchi, S., Kyozuka, J., 2010. *FINE CULM1* (*FC1*) works downstream of strigolactones to inhibit the outgrowth of axillary buds in rice. Plant Cell Physiol. 51, 1127-1135. <https://doi.org/10.1093/pcp/pcq083>.
- Mizzotti, C., Ezquer, I., Paolo, D., Rueda-Romero, P., Guerra, R.F., Battaglia, R., Rogachev, I., Aharoni, A., Kater, M.M., Caporali, E., Colombo, L., 2014. SEEDSTICK is a master regulator of development and metabolism in the Arabidopsis seed coat. Plos Genet. 10. <https://doi.org/10.1371/journal.pgen.1004856>.

- Moran, J.L., Rooney, W.L., 2003. Effect of cytoplasm on the agronomic performance of grain sorghum hybrids. *Crop Sci.* 43, 777-781. <https://doi.org/10.2135/cropsci2003.7770>.
- Moreno-Pachon, N.M., Mutimawurugo, M.C., Heynen, E., Sergeeva, L., Benders, A., Blilou, I., Hilhorst, H.W.M., Immink, R.G.H., 2018. Role of *Tulipa gesneriana* *TEOSINTE BRANCHED1* (*TgTB1*) in the control of axillary bud outgrowth in bulbs. *Plant Reprod.* 31, 145-157. <https://doi.org/10.1007/S00497-017-0316-z>.
- Morris, G.P., Ramu, P., Deshpande, S.P., Hash, C.T., Shah, T., Upadhyaya, H.D., Riera-Lizarazu, O., Brown, P.J., Acharya, C.B., Mitchell, S.E., Harriman, J., Glaubitz, J.C., Buckler, E.S., Kresovich, S., 2013. Population genomic and genome-wide association studies of agroclimatic traits in sorghum. *Proc. Natl. Acad. Sci. U. S. A.* 110, 453-458. <https://doi.org/10.1073/pnas.1215985110>.
- Munster, T., Wingen, L.U., Faigl, W., Werth, S., Saedler, H., Theissen, G., 2001. Characterization of three *GLOBOSA*-like *MADS*-box genes from maize: evidence for ancient paralogy in one class of floral homeotic B-function genes of grasses. *Gene* 262, 1-13. [https://doi.org/10.1016/s0378-1119\(00\)00556-4](https://doi.org/10.1016/s0378-1119(00)00556-4).
- Murase, K., Hirano, Y., Sun, T.-p., Hakoshima, T., 2008. Gibberellin-induced DELLA recognition by the gibberellin receptor GID1. *Nature* 456, 459. <https://doi.org/10.1038/nature07519>.
- Nagasawa, N., Miyoshi, M., Sano, Y., Satoh, H., Hirano, H., Sakai, H., Nagato, Y., 2003. *SUPERWOMAN1* and *DROOPING LEAF* genes control floral organ identity in rice. *Development* 130, 705-718. <https://doi.org/10.1242/dev.00294>.
- Napoli, C., 1996. Highly branched phenotype of the petunia *dad1-1* mutant is reversed by grafting. *Plant. Physiol.* 111, 27-37. <https://doi.org/10.1104/pp.111.1.27>.
- Nguyen, C.T., Singh, V., van Oosterom, E.J., Chapman, S.C., Jordan, D.R., Hammer, G.L., 2013. Genetic variability in high temperature effects on seed-set in sorghum. *Funct. Plant Biol.* 40, 439-448. <https://doi.org/10.1071/Fp12264>.
- Nicolas, M., Cubas, P., 2016. TCP factors: new kids on the signaling block. *Curr. Opin. Plant Biol.* 33, 33-41. <https://doi.org/10.1016/j.pbi.2016.05.006>.
- Nicolas, M., Rodriguez-Buey, M.L., Franco-Zorrilla, J.M., Cubas, P., 2015. A recently evolved alternative splice site in the *BRANCHED1a* gene controls potato plant architecture. *Curr. Biol.* 25, 1799-1809. <https://doi.org/10.1016/j.cub.2015.05.053>.
- Niu, B.X., He, F.R., He, M., Ren, D., Chen, L.T., Liu, Y.G., 2013a. The ATP-binding cassette transporter OsABCG15 is required for anther development and pollen fertility in rice. *J. Integr. Plant Biol.* 55, 710-720. <https://doi.org/10.1111/jipb.12053>.
- Niu, N.N., Liang, W.Q., Yang, X.J., Jin, W.L., Wilson, Z.A., Hu, J.P., Zhang, D.B., 2013b. EAT1 promotes tapetal cell death by regulating aspartic proteases during male reproductive development in rice. *Nat. Commun.* 4. <https://doi.org/10.1038/ncomms2396>.
- Oliver, A.L., Grant, R.J., Pedersen, J.F., O'Rear, J., 2004. Comparison of brown midrib-6 and-18 forage sorghum with conventional sorghum and corn silage in diets of lactating dairy cows. *J. Dairy Sci.* 87, 637-644. [https://doi.org/10.3168/jds.S0022-0302\(04\)73206-3](https://doi.org/10.3168/jds.S0022-0302(04)73206-3).
- Omidi, M., Siahpoosh, M.R., Mamghani, R., Modarresi, M., 2014. The influence of terminal heat stress on meiosis abnormalities in pollen mother cells of wheat. *Cytologia* 79, 49-58. <https://doi.org/10.1508/cytologia.79.49>.
- Ono, S., Liu, H., Tsuda, K., Fukai, E., Tanaka, K., Sasaki, T., Nonomura, K.-I., 2018. EAT1 transcription factor, a non-cell-autonomous regulator of pollen production, activates meiotic small RNA biogenesis in rice anther tapetum. *PLoS genet.* 14, e1007238. <https://doi.org/10.1371/journal.pgen.1007238>.
- Ordonio, R.L., Ito, Y., Hatakeyama, A., Ohmae-Shinohara, K., Kasuga, S., Tokunaga, T., Mizuno, H., Kitano, H., Matsuoka, M., Sazuka, T., 2014. Gibberellin deficiency pleiotropically induces culm bending in sorghum: An insight into sorghum semi-dwarf breeding. *Sci. Rep.* 4. <https://doi.org/10.1038/srep05287>.
- Oshino, T., Abiko, M., Saito, R., Ichiishi, E., Endo, M., Kawagishi-Kobayashi, M., Higashitani, A., 2007. Premature progression of anther early developmental programs accompanied by comprehensive alterations in transcription during high-temperature injury in barley plants. *Mol. Genet. Genomics* 278, 31-42. <https://doi.org/10.1007/s00438-007-0229-x>.
- Palmer, G.H., 1992. Sorghum—food, beverage and brewing potentials. 27, 145-153. [http://dx.doi.org/10.1016/0032-9592\(92\)87002-X](http://dx.doi.org/10.1016/0032-9592(92)87002-X).

- Parenicova, L., de Folter, S., Kieffer, M., Horner, D.S., Favalli, C., Busscher, J., Cook, H.E., Ingram, R.M., Kater, M.M., Davies, B., Angenent, G.C., Colombo, L., 2003. Molecular and phylogenetic analyses of the complete MADS-box transcription factor family in Arabidopsis: New openings to the MADS world. *Plant Cell* 15, 1538-1551. <https://doi.org/10.1105/tpc.011544>.
- Parish, R.W., Li, S.F., 2010. Death of a tapetum: A programme of developmental altruism. *Plant Sci.* 178, 73-89. <https://doi.org/10.1016/j.plantsci.2009.11.001>.
- Parish, R.W., Phan, H.A., Iacuone, S., Li, S.F., 2012. Tapetal development and abiotic stress: A centre of vulnerability. *Funct. Plant Biol.* 39, 553-559. <https://doi.org/10.1071/fp12090>.
- Park, J.H., Halitschke, R., Kim, H.B., Baldwin, I.T., Feldmann, K.A., Feyereisen, R., 2002. A knock-out mutation in allene oxide synthase results in male sterility and defective wound signal transduction in *Arabidopsis* due to a block in jasmonic acid biosynthesis. *Plant J.* 31, 1-12. <https://doi.org/10.1046/j.1365-313X.2002.01328.x>.
- Pasuquin, E., Lafarge, T., Tubana, B., 2008. Transplanting young seedlings in irrigated rice fields: Early and high tiller production enhanced grain yield. *Field Crop Res.* 105, 141-155. <https://doi.org/10.1016/j.fcr.2007.09.001>.
- Paterson, A.H., Bowers, J.E., Bruggmann, R., Dubchak, I., Grimwood, J., Gundlach, H., Haberer, G., Hellsten, U., Mitros, T., Poliakov, A., Schmutz, J., Spannagl, M., Tang, H.B., Wang, X.Y., Wicker, T., Bharti, A.K., Chapman, J., Feltus, F.A., Gowik, U., Grigoriev, I.V., Lyons, E., Maher, C.A., Martis, M., Narechania, A., Ollilar, R.P., Penning, B.W., Salamov, A.A., Wang, Y., Zhang, L.F., Carpita, N.C., Freeling, M., Gingle, A.R., Hash, C.T., Keller, B., Klein, P., Kresovich, S., McCann, M.C., Ming, R., Peterson, D.G., Mehboob-ur-Rahman, Ware, D., Westhoff, P., Mayer, K.F.X., Messing, J., Rokhsar, D.S., 2009. The *Sorghum bicolor* genome and the diversification of grasses. *Nature* 457, 551-556. <https://doi.org/10.1038/nature07723>.
- Pelaz, S., Ditta, G.S., Baumann, E., Wisman, E., Yanofsky, M.F., 2000. B and C floral organ identity functions require *SEPALLATA* MADS-box genes. *Nature* 405, 200-203. <https://doi.org/10.1038/35012103>.
- Peng, J.R., Richards, D.E., Hartley, N.M., Murphy, G.P., Devos, K.M., Flintham, J.E., Beales, J., Fish, L.J., Worland, A.J., Pelica, F., Sudhakar, D., Christou, P., Snape, J.W., Gale, M.D., Harberd, N.P., 1999. 'Green revolution' genes encode mutant gibberellin response modulators. *Nature* 400, 256-261. <https://doi.org/10.1038/22307>.
- Perez, D.E., Hoyer, J.S., Johnson, A.I., Moody, Z.R., Lopez, J., Kaplinsky, N.J., 2009. *BOBBER1* is a noncanonical Arabidopsis small heat shock protein required for both development and thermotolerance. *Plant Physiol.* 151, 241-252. <https://doi.org/10.1104/pp.109.142125>.
- Pertea, M., Kim, D., Pertea, G.M., Leek, J.T., Salzberg, S.L., 2016. Transcript-level expression analysis of RNA-seq experiments with HISAT, StringTie and Ballgown. *Nat. Protoc.* 11, 1650-1667. <https://doi.org/10.1038/nprot.2016.095>.
- Prasad, K., Sriram, P., Kumar, C.S., Kushalappa, K., Vijayraghavan, U., 2001. Ectopic expression of rice *OsMADS1* reveals a role in specifying the lemma and palea, grass floral organs analogous to sepals. *Dev. Genes Evol.* 211, 281-290. <https://doi.org/10.1007/s004270100153>.
- Prasad, P.V.V., Boote, K.J., Allen, L.H., 2006a. Adverse high temperature effects on pollen viability, seed-set, seed yield and harvest index of grain-sorghum [*Sorghum bicolor* (L.) Moench] are more severe at elevated carbon dioxide due to higher tissue temperatures. *Agr. Forest Meteorol.* 139, 237-251. <https://doi.org/10.1016/j.agrformet.2006.07.003>.
- Prasad, P.V.V., Boote, K.J., Allen, L.H., Sheehy, J.E., Thomas, J.M.G., 2006b. Species, ecotype and cultivar differences in spikelet fertility and harvest index of rice in response to high temperature stress. *Field Crops Res.* 95, 398-411. <https://doi.org/10.1016/j.fcr.2005.04.008>.
- Prasad, P.V.V., Djanaguiraman, M., Perumal, R., Ciampitti, I.A., 2015. Impact of high temperature stress on floret fertility and individual grain weight of grain sorghum: sensitive stages and thresholds for temperature and duration. *Front. Plant Sci.* 6. <https://doi.org/10.3389/fpls.2015.00820>.
- Prasad, P.V.V., Pisipati, S.R., Mutava, R.N., Tuinstra, M.R., 2008. Sensitivity of grain sorghum to high temperature stress during reproductive development. *Crop Sci.* 48, 1911-1917. <https://doi.org/10.2135/cropsci2008.01.0036>.
- Praveen, M., Anurag Uttam, G., Suneetha, N., Umakanth, A., Patil, J.V., Madhusudhana, R., 2015. Inheritance and molecular mapping of *Rf6* locus with pollen fertility restoration ability on A1 and A2 cytoplasm in sorghum. *Plant Sci.* 238, 73-80. <https://doi.org/10.1016/j.plantsci.2015.05.020>.

- Premachandra, G.S., Hahn, D.T., Axtell, J.D., Joly, R.J., 1994. Epicuticular wax load and water-use efficiency in bloomless and sparse-bloom mutants of *Sorghum bicolor* L. *Environ. Exp. Bot.* 34, 293-301. [https://doi.org/10.1016/0098-8472\(94\)90050-7](https://doi.org/10.1016/0098-8472(94)90050-7).
- Premachandra, G.S., Saneoka, H., Fujita, K., Ogata, S., 1992. Leaf water relations, osmotic adjustment, cell membrane stability, epicuticular wax load and growth as affected by increasing water deficits in sorghum. *J. Exp. Bot.* 43, 1569-1576. <https://doi.org/10.1093/jxb/43.12.1569>.
- Raghavan, V., 1988. Anther and pollen development in rice (*Oryza sativa*). *Am. J. Bot.* 75, 183-196. <https://doi.org/10.2307/2443885>.
- Ramsay, L., Comadran, J., Druka, A., Marshall, D.F., Thomas, W.T.B., Macaulay, M., MacKenzie, K., Simpson, C., Fuller, J., Bonar, N., Hayes, P.M., Lundqvist, U., Franckowiak, J.D., Close, T.J., Muehlbauer, G.J., Waugh, R., 2011. *INTERMEDIUM-C*, a modifier of lateral spikelet fertility in barley, is an ortholog of the maize domestication gene *TEOSINTE BRANCHED 1*. *Nat. Genet.* 43, 169-U125. <https://doi.org/10.1038/ng.745>.
- Rawson, H., Evans, L., 1970. The pattern of grain growth within the ear of wheat. *Aust. J. Biol. Sci.* 23, 753-764. <https://doi.org/10.1071/BI9700753>.
- Reddy, B.V., Ramesh, S., Reddy, P.S., Ramaiah, B., Salimath, M., Kachapur, R., 2005. Sweet sorghum-a potential alternate raw material for bio-ethanol and bio-energy. *Int. Sorghum Millets Newslett.* 46, 79-86. <https://doi.org/10.1016/j.rser.2017.10.066>.
- Reddy, N., Yang, Y.Q., 2007. Structure and properties of natural cellulose fibers obtained from sorghum leaves and stems. *J. Agr. Food Chem.* 55, 5569-5574. <https://doi.org/10.1021/jf0707379>.
- Regassa, T.H., Wortmann, C.S., 2014. Sweet sorghum as a bioenergy crop: Literature review. *Biomass Bioenerg.* 64, 348-355. <https://doi.org/10.1016/j.biombioe.2014.03.052>.
- Rocateli, A.C., Raper, R.L., Balkcom, K.S., Arriaga, F.J., Bransby, D.I., 2012. Biomass sorghum production and components under different irrigation/tillage systems for the southeastern US. *Ind. Crop Prod.* 36, 589-598. <https://doi.org/10.1016/j.indcrop.2011.11.007>.
- Rooney, W.L., Blumenthal, J., Bean, B., Mullet, J.E., 2007. Designing sorghum as a dedicated bioenergy feedstock. *Biofuel. Bioprod. Biorefin.* 1, 147-157. <https://doi.org/10.1002/bbb.15>.
- Rosenzweig, C., Parry, M.L., 1994. Potential impact of climate-change on world food-supply. *Nature* 367, 133-138. <https://doi.org/10.1038/367133a0>.
- Rounsley, S.D., Ditta, G.S., Yanofsky, M.F., 1995. Diverse roles for MADS box genes in Arabidopsis development. *Plant Cell* 7, 1259-1269. <https://doi.org/10.1105/tpc.7.8.1259>.
- Sablowski, R.W.M., Meyerowitz, E.M., 1998. A homolog of NO APICAL MERISTEM is an immediate target of the floral homeotic genes APETALA3/PISTILLATA. *Cell* 92, 93-103. [https://doi.org/10.1016/S0092-8674\(00\)80902-2](https://doi.org/10.1016/S0092-8674(00)80902-2).
- Saini, H.S., Aspinall, D., 1982. Abnormal sporogenesis in wheat (*Triticum aestivum* L.) induced by short periods of high temperature. *Ann. Bot.* 49, 835-846. <https://doi.org/10.1093/oxfordjournals.aob.a086310>.
- Saini, H.S., Sedgley, M., Aspinall, D., 1984. Development anatomy in wheat of male sterility induced by heat stress, water deficit or abscisic acid. *Plant Physiol.* 11, 243-253. <https://doi.org/10.1071/PP9840243>.
- Sakamoto, T., Matsuoka, M., 2004. Generating high-yielding varieties by genetic manipulation of plant architecture. *Curr. Opin. Biotech.* 15, 144-147. <https://doi.org/10.1016/j.copbio.2004.02.003>.
- Sakata, T., Oda, S., Tsunaga, Y., Shomura, H., Kawagishi-Kobayashi, M., Aya, K., Saeki, K., Endo, T., Nagano, K., Kojima, M., Sakakibara, H., Watanabe, M., Matsuoka, M., Higashitani, A., 2014. Reduction of gibberellin by low temperature disrupts pollen development in rice. *Plant Physio.* 164, 2011-2019. <https://doi.org/10.1104/pp.113.234401>.
- Sakata, T., Oshino, T., Miura, S., Tomabechei, M., Tsunaga, Y., Higashitani, N., Miyazawa, Y., Takahashi, H., Watanabe, M., Higashitani, A., 2010. Auxins reverse plant male sterility caused by high temperatures. *Proc. Natl. Acad. Sci. U. S. A.* 107, 8569-8574. <https://doi.org/10.1073/pnas.1000869107>.
- Sakata, T., Takahashi, H., Nishiyama, I., Higashitani, A., 2000. Effects of high temperature on the development of pollen mother cells and microspores in barley *Hordeum vulgare* L. *J. Plant Res.* 113, 395-402. <https://doi.org/10.1007/PI00013947>.
- Sakuma, S., Golan, G., Guo, Z., Ogawa, T., Tagiri, A., Sugimoto, K., Bernhardt, N., Brassac, J., Mascher, M., Hensel, G., 2019. Unleashing floret fertility in wheat through the mutation of a homeobox gene. *Proc. Natl. Acad. Sci. U. S. A.*, 201815465. <https://doi.org/10.1101/434985>

- Salih, A.A., Ali, I.A., Lux, A., Luxova, M., Cohen, Y., Sugimoto, Y., Inanaga, S., 1999. Rooting, water uptake, and xylem structure adaptation to drought of two sorghum cultivars. *Crop Sci* 39, 168-173. <https://doi.org/10.2135/cropsci1999.0011183X003900010027x>.
- Sanders, P.M., Bui, A.Q., Weterings, K., McIntire, K.N., Hsu, Y.C., Lee, P.Y., Truong, M.T., Beals, T.P., Goldberg, R.B., 1999. Anther developmental defects in *Arabidopsis thaliana* male-sterile mutants. *Sex. Plant Reprod.* 11, 297-322. <https://doi.org/10.1007/s004970050158>.
- Sang, X.C., Li, Y.F., Luo, Z.K., Ren, D.Y., Fang, L.K., Wang, N., Zhao, F.M., Ling, Y.H., Yang, Z.L., Liu, Y.S., He, G.H., 2012. *CHIMERIC FLORAL ORGANS1*, Encoding a monocot-specific MADS box protein, regulates floral organ identity in rice. *Plant Physiol.* 160, 788-807. <https://doi.org/10.1104/pp.112.200980>.
- Satake, T., Yoshida, S., 1978. High temperature-induced sterility in indica rices at flowering. *Jpn. J. Crop. Sci.* 47, 6-17. <https://doi.org/10.1626/jcs.47.6>.
- Sato, K., Inaba, K., Tozawa, M., 1973. High temperature injury of ripening in rice plant: I. The effects of high temperature treatments as different stages of panicle development on the ripening. *Jpn. J. Crop. Sci.* 42, 207-213. <https://doi.org/10.1626/jcs.42.207>.
- Schaller, F., Biesgen, C., Müssig, C., Altmann, T., Weiler, E.W., 2000. 12-Oxophytodienoate reductase 3 (OPR3) is the isoenzyme involved in jasmonate biosynthesis. *Planta* 210, 979-984. <https://doi.org/10.1007/s004250050706>.
- Schertz, K.F., Dalton, L.G., 1980. Sorghum, in: Fehr, W.R., Hadley, H.H. (Eds.), *Hybridization of Crop Plants*. American Society of Agronomy, Crop Science Society of America, Madison, WI, pp 577-588.
- Schieffhale, U., Balasubramanian, S., Sieber, P., Chevalier, D., Wisman, E., Schneitz, K., 1999. Molecular analysis of *NOZZLE*, a gene involved in pattern formation and early sporogenesis during sex organ development in *Arabidopsis thaliana*. *Proc. Natl. Acad. Sci. U. S. A.* 96, 11664-11669. <https://doi.org/10.1073/pnas.96.20.11664>
- Schmidt, R.J., Ambrose, B.A., 1998. The blooming of grass flower development. *Curr. Opin. Plant Biol.* 1, 60-67. [https://doi.org/10.1016/S1369-5266\(98\)80129-5](https://doi.org/10.1016/S1369-5266(98)80129-5).
- Schomburg, F.M., Bizzell, C.M., Lee, D.J., Zeevaart, J.A.D., Amasino, R.M., 2003. Overexpression of a novel class of gibberellin 2-oxidases decreases gibberellin levels and creates dwarf plants. *Plant Cell* 15, 151-163. <https://doi.org/10.1105/tpc.005975>.
- Schoper, J.B., Lambert, R.J., Vasila, B., 1987a. Pollen viability, pollen shedding, and combining ability for tassel heat tolerance in maize. *Crop Sci.* 27, 27-31. <https://doi.org/10.2135/cropsci1987.0011183X002700010007x>.
- Schoper, J.B., Lambert, R.J., Vasila, B.L., 1986. Maize pollen viability and ear receptivity under water and high temperature stress. *Crop Sci.* 26, 1029-1033. <https://doi.org/10.2135/cropsci1986.0011183X002600050038x>.
- Schoper, J.B., Lambert, R.J., Vasilas, B.L., Westgate, M.E., 1987b. Plant factors controlling seed set in maize: The influence of silk, pollen, and ear-leaf water status and tassel heat treatment at pollination. *Plant. Physiol.* 83, 121-125. <https://doi.org/10.1104/pp.83.1.121>.
- Seager, R., Ting, M.F., Held, I., Kushnir, Y., Lu, J., Vecchi, G., Huang, H.P., Harnik, N., Leetmaa, A., Lau, N.C., Li, C.H., Velez, J., Naik, N., 2007. Model projections of an imminent transition to a more arid climate in southwestern North America. *Science* 316, 1181-1184. <https://doi.org/10.1126/science.1139601>.
- Seale, M., Bennett, T., Leyser, O., 2017. *BRC1* expression regulates bud activation potential but is not necessary or sufficient for bud growth inhibition in *Arabidopsis*. *Development* 144, 1661-1673. <https://doi.org/10.1242/dev.145649>.
- Shimizu-Sato, S., Tanaka, M., Mori, H., 2009. Auxin-cytokinin interactions in the control of shoot branching. *Plant Mol. Biol.* 69, 429-435. <https://doi.org/10.1007/s11103-008-9416-3>.
- Smith, A.R., Zhao, D.Z., 2016. Sterility caused by floral organ degeneration and abiotic stresses in *Arabidopsis* and cereal grains. *Front. Plant Sci.* 7. <https://doi.org/10.3389/fpls.2016.01503>.
- Smyth, D.R., Bowman, J.L., Meyerowitz, E.M., 1990. Early Flower Development in *Arabidopsis*. *Plant Cell* 2, 755-767. <https://doi.org/10.1105/tpc.2.8.755>.
- Sommer, H., Beltran, J.P., Huijser, P., Pape, H., Lonngig, W.E., Saedler, H., Schwarzsommer, Z., 1990. *Deficiens*, a homeotic gene involved in the control of flower morphogenesis in *Antirrhinum majus*: The protein shows homology to transcription factors. *EMBO J.* 9, 605-613. <https://doi.org/10.1002/j.1460-2075.1990.tb08152.x>.

- Stieglitz, H., Stern, H., 1973. Regulation of beta-1,3-glucanase activity in developing anthers of *Lilium*. Dev. Biol. 34, 169-173. [https://doi.org/10.1016/0012-1606\(73\)90347-3](https://doi.org/10.1016/0012-1606(73)90347-3).
- Stintzi, A., Browse, J., 2000. The *Arabidopsis* male-sterile mutant, *opr3*, lacks the 12-oxophytodienoic acid reductase required for jasmonate synthesis. P. Natl. Acad. Sci. U.S.A. 97, 10625-10630. <https://doi.org/10.1073/pnas.190264497>.
- Studer, A.J., Wang, H., Doebley, J.F., 2017. Selection during maize domestication targeted a gene network controlling plant and inflorescence architecture. Genetics 207, 755-765. <https://doi.org/10.1534/genetics.117.300071>.
- Takeda, T., Suwa, Y., Suzuki, M., Kitano, H., Ueguchi-Tanaka, M., Ashikari, M., Matsuoka, M., Ueguchi, C., 2003. The *OsTB1* gene negatively regulates lateral branching in rice. Plant J. 33, 513-520. <https://doi.org/10.1046/j.1365-313X.2003.01648.x>.
- Tang, H.V., Pring, D.R., Shaw, L.C., Salazar, R.A., Muza, F.R., Yan, B., Schertz, K.F., 1996. Transcript processing internal to a mitochondrial open reading frame is correlated with fertility restoration in male-sterile sorghum. Plant J. 10, 123-133. <https://doi.org/10.1046/j.1365-313X.1996.10010123.x>.
- Tashiro, T., Wardlaw, I.F., 1990. The response to high temperature shock and humidity changes prior to and during the early stages of grain development in wheat. Aust. J. Plant. Physiol. 17, 551-561. <https://doi.org/10.1071/PP9900551>.
- Taylor, J.R.N., Schober, T.J., Bean, S.R., 2006. Novel food and non-food uses for sorghum and millets. J. Cereal Sci. 44, 252-271. <https://doi.org/10.1016/j.jcs.2006.06.009>.
- Thakur, P., Kumar, S., Malik, J.A., Berger, J.D., Nayyar, H., 2010. Cold stress effects on reproductive development in grain crops: An overview. Environ. Exper. Bot. 67, 429-443. <https://doi.org/10.1016/j.envexpbot.2009.09.004>.
- Thimann, K.V., Skoog, F., William, G., 1934. On the inhibition of bud development and other functions of growth substance in *Vicia faba*. Proc. R. Soc. Lond. B 114, 317-339. <https://doi.org/10.1098/rspb.1934.0010>.
- Thompson, B.E., Bartling, L., Whipple, C., Hall, D.H., Sakai, H., Schmidt, R., Hake, S., 2009. *bearded-ear* encodes a MADS Box transcription factor critical for maize floral development. Plant Cell 21, 2578-2590. <https://doi.org/10.1105/tpc.109.067751>.
- Tie, S.G., Xia, J.H., Qiu, F.Z., Zheng, Y.L., 2006. Genome-wide analysis of maize cytoplasmic male sterility-S based on QTL mapping. Plant Mol. Biol. Rep. 24, 71-80. <https://doi.org/10.1007/Bf02914047>.
- Trobner, W., Ramirez, L., Motte, P., Hue, I., Huijser, P., Lonig, W.E., Saedler, H., Sommer, H., Schwarzsommer, Z., 1992. *GLOBOSA*: A homeotic gene which interacts with *DEFICIENS* in the control of *Antirrhinum* floral organogenesis. EMBO J. 11, 4693-4704. <https://doi.org/10.1002/j.1460-2075.1992.tb05574.x>.
- Tsou, C.H., Cheng, P.C., Tseng, C.M., Yen, H.J., Fu, Y.L., You, T.R., Walden, D.B., 2015. Anther development of maize (*Zea mays*) and longstamen rice (*Oryza longistaminata*) revealed by cryo-SEM, with foci on locular dehydration and pollen arrangement. Plant Reprod. 28, 47-60. <https://doi.org/10.1007/s00497-015-0257-3>.
- Ullstrup, A., 1972. The impacts of the southern corn leaf blight epidemics of 1970-1971. Annu. Rev. Phytopathol. 10, 37-50. <https://doi.org/10.1146/annurev.py.10.090172.000345>.
- USDOE, 2016. Bioenergy technologies office multi-year program plan: March 2016. US Department of Energy.
- Uttam, G.A., Praveen, M., Rao, Y.V., Tonapi, V.A., Madhusudhana, R., 2017. Molecular mapping and candidate gene analysis of a new epicuticular wax locus in sorghum (*Sorghum bicolor* L. Moench). Theor. Appl. Genet. 130, 2109-2125. <https://doi.org/10.1007/s00122-017-2945-x>.
- Vermerris, W., 2011. Survey of genomics approaches to improve bioenergy traits in maize, sorghum and sugarcane. J. Integr. Plant. Biol. 53, 105-119. <https://doi.org/10.1111/j.1744-7909.2010.01020.x>.
- Vizcay-Barrena, G., Wilson, Z.A., 2006. Altered tapetal PCD and pollen wall development in the *Arabidopsis* *ms1* mutant. J. Exp. Bot. 57, 2709-2717. <https://doi.org/10.1093/jxb/erl032>.
- Wang, H.H., Zhang, L., Cai, Q., Hu, Y., Jin, Z.M., Zhao, X.X., Fan, W., Huang, Q.M., Luo, Z.J., Chen, M.J., Zhang, D.B., Yuan, Z., 2015. *OsMADS32* interacts with PI-like proteins and regulates rice flower development. J. Integr. Plant. Biol. 57, 504-513. <https://doi.org/10.1111/jipb.12248>.

- Wang, S.K., Bai, Y.H., Shen, C.J., Wu, Y.R., Zhang, S.N., Jiang, D.A., Guilfoyle, T.J., Chen, M., Qi, Y.H., 2010. Auxin-related gene families in abiotic stress response in *Sorghum bicolor*. *Funct. Integr. Genomic.* 10, 533-546. <https://doi.org/10.1007/s10142-010-0174-3>.
- Worrall, D., Hird, D.L., Hodge, R., Paul, W., Draper, J., Scott, R., 1992. Premature dissolution of the microsporocyte callose wall causes male-sterility in transgenic Tobacco. *Plant Cell* 4, 759-771. <https://doi.org/10.1105/tpc.4.7.759>.
- Wu, H.M., Cheung, A.Y., 2000. Programmed cell death in plant reproduction. *Plant Mol. Biol.* 44, 267-281. <https://doi.org/10.1023/a:1026536324081>.
- Xie, D.X., Feys, B.F., James, S., Nieto-Rostro, M., Turner, J.G., 1998. *COI1*: An *Arabidopsis* gene required for jasmonate-regulated defense and fertility. *Science* 280, 1091-1094. <https://doi.org/10.1126/science.280.5366.1091>.
- Xin, Z.G., Chen, J.P., 2012. A high throughput DNA extraction method with high yield and quality. *Plant Methods* 8. <https://doi.org/10.1186/1746-4811-8-26>.
- Xin, Z.G., Huang, J., Smith, A.R., Chen, J.P., Burke, J., Sattler, S.E., Zhao, D.Z., 2017. Morphological characterization of a new and easily recognizable nuclear male sterile mutant of *Sorghum* (*Sorghum bicolor*). *PLoS One* 12. <https://doi.org/10.1371/journal.pone.0165195>.
- Xu, W.W., Subudhi, P.K., Crasta, O.R., Rosenow, D.T., Mullet, J.E., Nguyen, H.T., 2000. Molecular mapping of QTLs conferring stay-green in grain sorghum (*Sorghum bicolor* L. Moench). *Genome* 43, 461-469. <https://doi.org/10.1139/g00-003>.
- Xu, Z.Y., Gongbuzhaxi, Wang, C.Y., Xue, F., Zhang, H., Ji, W.Q., 2015. Wheat NAC transcription factor TaNAC29 is involved in response to salt stress. *Plant Physiol. Bioch.* 96, 356-363. <https://doi.org/10.1016/j.plaphy.2015.08.013>.
- Yamaguchi, T., Lee, D.Y., Miyao, A., Hirochika, H., An, G.H., Hirano, H.Y., 2006. Functional diversification of the two C-class MADS box genes *OSMADS3* and *OSMADS58* in *Oryza sativa*. *Plant Cell* 18, 15-28. <https://doi.org/10.1105/tpc.105.037200>.
- Yang, K.Z., Xia, C., Liu, X.L., Dou, X.Y., Wang, W., Chen, L.Q., Zhang, X.Q., Xie, L.F., He, L., Ma, X., Ye, D., 2009. A mutation in *THERMOSENSITIVE MALE STERILE 1*, encoding a heat shock protein with DnaJ and PDI domains, leads to thermosensitive gametophytic male sterility in *Arabidopsis*. *Plant J.* 57, 870-882. <https://doi.org/10.1111/j.1365-313X.2008.03732.x>.
- Yang, W.C., Ye, D., Xu, J., Sundaresan, V., 1999. The *SPOROCTELESS* gene of *Arabidopsis* is required for initiation of sporogenesis and encodes a novel nuclear protein. *Genes Dev.* 13, 2108-2117. <https://doi.org/10.1101/gad.13.16.2108>.
- Yang, Y., Varbanova, M., Ross, J., Wang, G., Cortes, D., Fridman, E., Shulaev, V., Noel, J.P., Pichersky, E., 2006. Methylation and demethylation of plant signaling molecules, *Recent Advances in Phytochemistry*. Elsevier, Oxford, UK, pp 253-270.
- Yao, F.Y., Xu, C.G., Yu, S.B., Li, J.X., Gao, Y.J., Li, X.H., Zhang, Q.F., 1997. Mapping and genetic analysis of two fertility restorer loci in the wild-abortive cytoplasmic male sterility system of rice (*Oryza sativa* L.). *Euphytica* 98, 183-187. <https://doi.org/10.1023/A:1003165116059>.
- Yoshida, A., Suzaki, T., Tanaka, W., Hirano, H.Y., 2009. The homeotic gene *long sterile lemma* (*G1*) specifies sterile lemma identity in the rice spikelet. *Proc. Natl. Acad. Sci. U. S. A.* 106, 20103-20108. <https://doi.org/10.1073/pnas.0907896106>.
- Yoshida, H., 2012. Is the lodicule a petal: Molecular evidence? *Plant Sci.* 184, 121-128. <https://doi.org/10.1016/j.plantsci.2011.12.016>.
- Yoshida, H., Nagato, Y., 2011. Flower development in rice. *J. Exp. Bot.* 62, 4719-4730. <https://doi.org/10.1093/jxb/err272>.
- Young, T.E., Ling, J., Geisler-Lee, C.J., Tanguay, R.L., Caldwell, C., Gallie, D.R., 2001. Developmental and thermal regulation of the maize heat shock protein, HSP101. *Plant Physiol.* 127, 777-791. <https://doi.org/10.1104/pp.010160>.
- Youssef, H.M., Eggert, K., Kopplu, R., Alqudah, A.M., Poursarebani, N., Fazeli, A., Sakuma, S., Tagiri, A., Rutten, T., Govind, G., Lundqvist, U., Graner, A., Komatsuda, T., Sreenivasulu, N., Schnurbusch, T., 2017. *VRS2* regulates hormone-mediated inflorescence patterning in barley. *Nat. Genet.* 49, 157-161. <https://doi.org/10.1038/ng.3717>.
- Youssef, H.M., Koppolu, R., Rutten, T., Korzun, V., Schweizer, P., Schnurbusch, T., 2014. Genetic mapping of the *labile* (*lab*) gene: a recessive locus causing irregular spikelet fertility in *labile*-barley (*Hordeum vulgare* convar. *labile*). *Theor. Appl. Genet.* 127, 1123-1131. <https://doi.org/10.1007/s00122-014-2284-0>.

- Yuan, L.P., 1990. Progress of two-line system hybrid rice breeding. *Sci. Agr. Sin.* 23, 1-6.
- Zhang, D.B., Luo, X., Zhu, L., 2011. Cytological analysis and genetic control of rice anther development. *J. Genet. Genomics* 38, 379-390. <https://doi.org/10.1016/j.jgg.2011.08.001>.
- Zhang, D.B., Yuan, Z., 2014. Molecular control of grass inflorescence development. *Annu. Rev. Plant Biol.* 65, 553-578. <https://doi.org/10.1146/annurev-arplant-050213-040104>.
- Zhang, D.F., Wu, S.W., An, X.L., Xie, K., Dong, Z.Y., Zhou, Y., Xu, L.W., Fang, W., Liu, S.S., Liu, S.S., Zhu, T.T., Li, J.P., Rao, L.Q., Zhao, J.R., Wan, X.Y., 2018a. Construction of a multicontrol sterility system for a maize male-sterile line and hybrid seed production based on the *ZmMs7* gene encoding a PHD-finger transcription factor. *Plant Biotechnol. J.* 16, 459-471. <https://doi.org/10.1111/pbi.12786>.
- Zhang, N., Wang, Z.X., Bao, Z.L., Yang, L.Y., Wu, D.X., Shu, X.L., Hua, J., 2018b. MOS1 functions closely with TCP transcription factors to modulate immunity and cell cycle in *Arabidopsis*. *Plant J.* 93, 66-78. <https://doi.org/10.1111/tpj.13757>.
- Zhao, C.Z., Huang, J., Gyaneshwar, P., Zhao, D.Z., 2018. *Rhizobium* sp IRBG74 alters *Arabidopsis* root development by affecting auxin signaling. *Front. Microbiol.* 8. <https://doi.org/10.3389/fmicb.2017.02556>.
- Zhao, D.Z., Wang, G.F., Speal, B., Ma, H., 2002. The *EXCESS MICROSPOROCYTES1* gene encodes a putative leucine-rich repeat receptor protein kinase that controls somatic and reproductive cell fates in the *Arabidopsis* anther *Genes Dev.* 16, 2021-2031. <https://doi.org/10.1101/gad.997902>.
- Zhao, Y., Li, X.Y., Chen, W.J., Peng, X.J., Cheng, X.A., Zhu, S.W., Cheng, B.J., 2011. Whole-genome survey and characterization of MADS-box gene family in maize and sorghum. *Plant Cell Tiss. Org.* 105, 159-173. <https://doi.org/10.1007/s11240-010-9848-8>.
- Zhou, H., Zhou, M., Yang, Y.Z., Li, J., Zhu, L.Y., Jiang, D.G., Dong, J.F., Liu, Q.J., Gu, L.F., Zhou, L.Y., Feng, M.J., Qin, P., Hu, X.C., Song, C.L., Shi, J.F., Song, X.W., Ni, E.D., Wu, X.J., Deng, Q.Y., Liu, Z.L., Chen, M.S., Liu, Y.G., Cao, X.F., Zhuang, C.X., 2014. RNase Z(S1) processes Ub(L40) mRNAs and controls thermosensitive genic male sterility in rice. *Nat. Commun.* 5. <https://doi.org/10.1038/ncomms5884>.
- Ziemann, M., 2010. Glutaredoxin family genes in plant development. PhD. <https://www.researchgate.net/publication/302247203>
- Zinn, K.E., Tunc-Ozdemir, M., Harper, J.F., 2010. Temperature stress and plant sexual reproduction: Uncovering the weakest links. *J. Exp. Bot.* 61, 1959-1968. <https://doi.org/10.1093/jxb/erq053>.
- Zwirek, M., Waugh, R., McKim, S.M., 2018. Interaction between row-type genes in barley controls meristem determinacy and reveals novel routes to improved grain. *New Phytol.* <https://doi.org/10.1111/nph.15548>.

Curriculum Vitae

Ashley R. Smith

EDUCATION

- 2013-Pres PhD, Biological Sciences: Plant Molecular Genetics, University of Wisconsin-Milwaukee, Milwaukee, WI, USA. Dissertation Working Title: Dissection of Floral Organ Development and the genetic basis of sterility in *Sorghum bicolor*.
- 2011-2013 Master of Science, Biology, University of Wisconsin-La Crosse, La Crosse, WI, USA. Thesis Title: Biological Control of *Cryphonectria parasitica* with *Streptomyces* and an Analysis of Vegetative Compatibility Diversity in Wisconsin, USA
- 2006-2011 Bachelor of Science, Biology; 2nd Major: Archaeology, University of Wisconsin- La Crosse, La Crosse, WI, USA

TEACHING EXPERIENCE AND AWARDS

- 2014-Pres Foundations of Biological Sciences II TA at UW-Milwaukee, Approximately 500 students, average evaluation score 4.6/5.0 over 24 sections
- 2013-Pres Undergraduate and High School Mentor. Independently mentoring of 6 undergraduates for university credit and 3 high school students via summer workshops at UW-Milwaukee.
- 2013-2017 Anatomy and Physiology I TA at UW-Milwaukee fall and summer sessions. Approximately 80 students, average evaluation score 4.62/5.0 over 4 sections.
- 2015 Student Success Award for continuous dedication to the academic success of UW-Milwaukee students.
- 2012-2013 Biology 103/105 introductory biology lab Instructor at the University of Wisconsin-La Crosse
- 2011-2012 Biology tutor for University of Wisconsin-La Crosse at the University sponsored tutoring center.

RESEARCH EXPERIENCE

- 2013-Pres Characterization of floral development in *Sorghum bicolor*. Research under Dr. Dave Zhao, UW-Milwaukee. Research employs advanced microscopy: Scanning electron microscopy, transmission electron microscopy, and confocal microscopy. Additional techniques: DNA and RNA extraction, PCR (RT, qRT), RNA sequencing / RNA-seq data analysis, TUNEL assay, sectioning work, in-situ hybridization, and plant transformation.
- 2011-2013 Generating a novel *Streptomyces* based biocontrol to control *Cryphonectria parasitica* dispersal. Wide variety of techniques from RNA extraction, fungal and bacterial work, single sporing, vegetative compatibility testing, PCR, and employing a large field study. Research under Dr. Anita Baines at UW-La Crosse.
- 2009-2013 Hypovirus mediated recovery of *Castanea dentata* employing the fungus *Cryphonectria parasitica*. Research at UW-La Crosse under Dr. Anita Baines.
- 2010-2011 Gauging Oneota seasonal movement through the examination of floral remains (identifying seed types and determining seasonal habitation at Oneota period sites). Research was monitored by Dr. Constance Arzigian at UW-La Crosse

GRANTS AND AWARDS

- 2013-2018 UW-Milwaukee Chancellor's Award (Varies Annually)
- 2018 Louise Neitge Scholarship (\$1500)
- 2017 Ruth Walker Grant-in-Aid Award (\$1500).
- 2016 Cold Spring Harbor Cereal Genomics Scholarship (\$1000)
- 2016 Ruth Walker Travel Grant (\$200) and Graduate School Travel Grant (\$450) for Characterization of Floral Development in *Sorghum bicolor*. Poster Presented at the International Plant Reproduction conference in Tucson Arizona.
- 2015 Conference fees (\$450) for Characterization of Floral Development in *Sorghum bicolor*. Poster Presented at the International Plant Reproduction conference in Tucson Arizona. Awarded by Pollen RCN.
- 2012 Conference fees waived for Dispersal of *Cryphonectria parasitica* and dsRNA. Poster Presented at the International Chestnut Symposium in Shepherdstown, WV.
- 2010 University of Wisconsin-La Crosse Undergraduate Research Grant: Tracking the Spread: A Look at Hypovirus Mediated Recovery in West Salem, WI (\$1350.00).

- 2010 University of Wisconsin-La Crosse Undergraduate Research Grant: An Analysis of Floral Remains and their Correlations to Seasonal Movement at the Sand Lake Site (\$650.00).
- 2009 University of Wisconsin-La Crosse Undergraduate Research Grant: Analysis of the Paleoethnobotanical Remains at the Pirque Alto Site in the Cochabamba Valley of Bolivia: A Comparison to Primary and Secondary Centers (\$2100.00).

PUBLICATIONS

- 2016 Smith, A. R., and Zhao, D. Floral organ degeneration and abiotic stress caused sterility in *Arabidopsis* and cereal grains.
- 2016 Zhanquo, X., Huang, J., Smith, A., Chen, J., Burke, J., Sattler, S., and Zhao, D. Characterization of a New and Easily Recognizable Nuclear Male Sterile Mutant of Sorghum (*Sorghum bicolor*).
- 2016 Huang, J., Smith, A. R., Zhang, T., and Zhao, D. 2016. Creating Completely Both Male and Female Sterile Plants by Specifically Ablating Microspore and Megaspore Mother Cells *Frontiers in Plant Science: Plant Biotechnology*, 7(30).
- 2010 Schultz, A. (2010). Analysis of the Paleoethnobotanical Remains at the Pirque Alto Site in the Cochabamba Valley of Bolivia: A Comparison to Primary and Secondary Centers. *UW-La Crosse Journal of Undergraduate Research*, (XIII).

PRESENTATIONS

- 2018 Uncovering the Genetic Basis of Sterility in *Sorghum bicolor*. Oral Presentation at the UW-Milwaukee research symposium. Winner Best talk.
- 2018 Heat Stress Resistance in *Sorghum bicolor*. Poster Presented at the UW-Milwaukee research symposium.
- 2016 Characterization of Floral Development in *Sorghum bicolor*. Oral Presentation at the UW-Milwaukee research symposium. Winner Best talk.
- 2016 Characterization of Floral Development in *Sorghum bicolor*. Poster Presented at the International Plant Reproduction conference in Tucson Arizona.
- 2015 Floral Development in *Sorghum bicolor*. Poster Presented at UW-Milwaukee research symposium.
- 2012 Dispersal of *Cryphonectria parasitica* and dsRNA. Poster Presented at the International Chestnut Symposium in Shepherdstown, WV.
- 2012 Tracking the spread: A look at hypovirus mediated recovery in West Salem, WI. Poster Presented at the spring Celebration of Student Research & Creativity at the University of Wisconsin-La Crosse.

- 2011 at the An Analysis of Floral Remains from the Sand Lake Site. Poster Presented spring Celebration of Student Research & Creativity at the University of Wisconsin-La Crosse.
- 2010 Analysis of the Paleoethnobotanical Remains at the Pirque Alto Site in the Cochabamba Valley of Bolivia: A Comparison to Primary and Secondary Centers. Poster Presented at the spring Celebration of Student Research & Creativity at the University of Wisconsin-La Crosse.

AFFILIATIONS

- 2015-Pres International Association of Sexual Plant Reproduction Research (IASPRR)
- 2014-Pres Graduate Organization of Biological Sciences member
- 2017-2018 Graduate Organization of Biological Sciences president
- 2017 Coordinator for Graduate Biology Symposium at UW-Milwaukee. Organized conference for 50 Presenters.
- 2006-Pres Alpha Xi Delta member and now alumnae member
- 2010-2011 UW-La Crosse archaeology club president
- 2008-2011 UW-La Crosse archaeology club member
- 2006-2011 UW-La Crosse biology club
- 2009-2010 UW-La Crosse women's studies student association vice president
- 2008-2010 UW-La Crosse women's studies student association member

TRAININGS

- 2013-2019 UW-Milwaukee Chemical hygiene and Lab Safety, Hazardous waste generator
- 2017 Title IX Training
- 2017 Active Shooter Training
- 2015 Radioactive Safety Training
- 2015 Veterans on campus

VOLUNTEER EXPERIENCE

- 2015-2018 Barack Obama School of Career and Technological Education FIRST Robotics Mentor
- 2016-2017 Hosted a series of high school biology workshops for Barack Obama School of Career and Technological Education students.